International Atomic Energy Agency

INDC(CCP)-387
Distrib.: G

INDC INTERNATIONAL NUCLEAR DATA COMMITTEE

ATLAS OF ENERGY-ANGULAR DISTRIBUTIONS OF GAMMA RAYS PRODUCED IN NEUTRON REACTIONS

A.I. Blokhin, V.V. Vozyakov, M.V. Mikhailyukova,
S.M. Nasyrova
Institute of Physics and Power Engineering, Obninsk, Russia

February 1996

IAEA NUCLEAR DATA SECTION, WAGRAMERSTRASSE 5, A-1400 VIENNA

INDC(CCP)-387
Distrib.: G

ATLAS OF ENERGY-ANGULAR DISTRIBUTIONS OF GAMMA RAYS PRODUCED IN NEUTRON REACTIONS

A.I. Blokhin, V.V. Vozyakov, M.V. Mikhailyukova,
S.M. Nasyrova
Institute of Physics and Power Engineering, Obninsk, Russia

February 1996

Translated by IAEA from a Russian original published in Voprosy Atomnoj Nauki i Tekhniki, Jadernye Konstanty, issue 2/1993.

Reproduced by the IAEA in Austria
February 1996

CONTENTS

95-10765 (28)
Translated from Russian

UDC 539.17

ATLAS OF ENERGY-ANGULAR DISTRIBUTIONS OF GAMMA RAYS PRODUCED IN NEUTRON REACTIONS

A.I. Blokhin, V.V. Vozyakov, M.V. Mikhailyukova,
S.M. Nasyrova
Power Physics Institute, Obninsk

ABSTRACT

ATLAS OF ENERGY ANGULAR DISTRIBUTIONS OF GAMMA RAYS PRODUCED IN NEUTRON REACTIONS. An atlas of energy angular differential gamma-ray production cross-sections was produced using EXFOR data for 52 elements and some of their isotopes. In some cases experimental and evaluation data from BROND-2 and ENDF/B-VI were compared.

One of the main steps towards the compilation of the BROND-2 library of recommended evaluated neutron data [1, 2] is the evaluation of nuclear data on processes responsible for the production of gamma rays in various neutron reactions. For a number of elements the BROND-2 library includes evaluated nuclear data on gamma-ray production, but there are many elements for which this work remains to be done. One of the preparatory stages of such work is the compilation and analysis of existing experimental information on the processes in question and its comparison with the available evaluated data.

We have compiled the information available on differential gamma-ray production cross-sections in the region of the continuum for the absorption and radiative capture of neutrons of different energies on the basis of the EXFOR international library of experimental data which was established as a result of the work of the network of international nuclear data centres [3]. The atlas, containing 353 graphs, was produced on the basis of this compilation. The available experimental data were compared with evaluated data from the BROND-2 and ENDF/B-VI libraries [4]. The atlas covers the following elements as well as many of their isotopes: N, O, F, Na, Mg, Al, Si, P, S, Ca, Sc, Ti, V, Cr, Mn, Fe, Co, Ni, Cu, Zn, Se, Br, Rb, Sr, Y, Zr, Nb, Mo, Ag, In, Sn, Sb, I, Cs, Ba, La, Ce, Pr, Gd, Tb, Ho, Lu, Ta, W, Re, Os, Pt, Au, Tl, Pb, Bi, ^{238}U.

The substance of the experimental information studied is presented in the table. The nuclides are listed in ascending order of atomic number, and the table gives for each nuclide the first author, the main bibliographical reference, and significant characteristics of the experiment: the value measured, the energy range of the neutrons and gamma radiation, the angle relative to the neutron beam axis at which the detector was placed for the gamma measure and some information on the experimental conditions. The step change in the neutron energy varied from experiment to experiment; for example, it was 2 MeV in the measurements at the ORELA facility. In the EXFOR library, $\frac{d^2\sigma_\gamma\ prod}{dE_\gamma d\Omega}(E_\gamma)$, spectra and cross-sections σ_γ prod (E_γ) are given for each neutron energy step. In our atlas graphs of the measured values are not given for all E_n , as the differences between neighbouring steps are small.

The bibliography contains references to the experimental work included in the table, giving a complete list of authors, the code and name of the laboratory where the work was carried out, and a full list of references in which the results obtained were published.

The atlas itself comprises two parts: Part 1 contains data on the energy angular distributions of gamma rays produced in neutron reactions; Part 2 includes work in which data on integral gamma-ray production cross-sections in specific energy intervals were obtained. The figures are given in ascending order of atomic number, and for each atomic number in ascending order of initial neutron energy.

The experimental material compiled, together with the comparison with available evaluated data, provide a basis for future evaluations of gamma-ray production cross-sections for neutron reactions.

REFERENCES

[1] BLOKHIN, A.I., IGNATYUK, A.V., KUZMINOV, B.D., et al., Proc. Int. Conf. on Nuclear Data for Science and Technology, Japan, Mito (1988) 611.

[2] BROND-2: Library of Recommended Evaluated Neutron Data. Documentation of Data Files. Editors: BLOKHIN, A.I., IGNATYUK, A.V., MANOKHIN, V.N., NIKOLAEV, M.N., PRONYAEV, V.G., Journal Yadernye Konstanty, v. 2 & 3 (1991).

[3] McLANE, V., NORDBORG, C., LEMMEL, H.D., MANOKHIN, V.N., Proc. Int. Conf. on Nuclear Data for Science and Technology, Japan, Mito (1988) 1157.

[4] ENDF/B-VI Summary Documentation, Compiled and Edited by P.F. Rose. Report ENDF-201, BNL (1991).

EXPERIMENTAL WORK ON γ-SPECTRA AND $\sigma_{\gamma\ production}$ IN NEUTRON REACTIONS INCLUDED IN ATLAS

Nuclide	Reference	Quantities measured	Neutron energy, MeV	Energy angular characteristics of γ-radiation, φ, degrees; Eγ, MeV	Measurement method, detectors	Remarks
^{0}N	J.K.Dickens et al. R, ORNL-4864, 1973 Exf. 10351002	$\frac{d^2\sigma_{\gamma prod}}{d\Omega\, dE_\gamma}$ in (n,xγ) reactions	2-20	90° 0.8-11.	ORELA n: Ta(γ,n), TOF; scintillation detectors γ: NaI, heavy shielding + LiH, paraffin	
^{16}O	G.L.Morgan et al. R, ORNL-5575, 1979 Exf. 10847002		6.5-20	125° 0.7-11.		
^{19}F	J.K.Dickens et al. NSE,62,515,1977 Exf. 10502002		1-20	125° 0.7-10.6		
^{23}Na	D.C.Larson et al. NSE,75,151,1980 Exf. 10926002		0.2-20	125° 0.4-10.6		
^{0}Mg	J.K.Dickens et al. NSE,62,515,1977 Exf. 10582002	$\frac{d^2\sigma_{prod}}{d\Omega\, dE_\gamma}$ in (n,xγ) reactions	0.76-20	90°,125° 0.7-10.6		
^{0}Mg	M.Budnar et al. NP/A,213,525,1973 Exf. 30532003	$\frac{d\,\sigma_{n\gamma}}{d\,E_\gamma}$ in (n,xγ) reactions	14.1 ±0.6	12-24	Cockcroft-Walton accelerator n: T(d,n)^{4}He, recoil proton method γ: anticoincidence, scintillation detector	Absolute measurements in 4π geometry
^{27}Al	M.Budnar NP/A,213,525,1973 Exf. 30532005					
^{27}Al	G.L.Morgan et al. NSE,62,515,1977 Exf. 10582002	$\frac{d^2\sigma_{prod}}{d\Omega\, dE_\gamma}$ in (n,xγ) reactions	0.85-20	90°,125° 0.7-10.6	ORELA n: Ta(γ,n), TOF, scintillation detectors γ: NaI, heavy shielding + LiH, paraffin	

Nuclide	Reference	Quantities measured	Neutron energy, MeV	Energy angular characteristics of γ-radiation, φ, degrees; Eγ, MeV	Measurement method, detectors	Remarks
^{0}Si	J.K.Dickens et al. NSE,62,515,1997 Exf. 10397002 10397003	$\frac{d^2\sigma_{prod}}{d\Omega\, dE_\gamma}$ in (n,xγ) reactions	1-20	90°,125° 0.7-10.6	ORELA n: Ta(γ,n), TOF, scintillation detectors γ: NaI, heavy shielding + LiH, paraffin	
^{0}Si	M.Budnar et al. NP/A,213,525,1973 Exf. 30532003	$\frac{d\,\sigma_{n\gamma}}{dE_\gamma}$ in (n,γ) reactions	14.1±0.6	12-24	Cockcroft-Walton accelerator n: T(d,n)^{4}He, recoil proton method γ: anticoincidence, scintillation pair spectrometer, scintillators - plastic and NE-102A	
^{0}Si	W.E.Tucker BAP,15,1667,1970 Exf. 10091002	$\frac{d\,\sigma_{\gamma prod}}{dE_\gamma}$ in (n,xγ) reactions	5,8,9,10,11	55° 0.4-9	Van de Graaf and tandem n: D(D,n)^{3}He, T(p,n)^{3}He TOF, recoil protons γ: GeLi, NaI(Tl), NaI(Gr)	
^{31}P	M.Budnar et al. NP/A,213,525,1973 Exf. 30532009	$\frac{d\,\sigma_{n\gamma}}{dE_\gamma}$ in (n,γ) reactions	14.1±0.6	12-24	Cockcroft-Walton accelerator n: T(d,n)^{4}He, recoil proton method γ: anticoincidence, scintillation pair spectrometer	Absolute measurements in 4π geometry
^{0}S	M.Budnar et al. NP/A,213,525,1973 Exf.30532011					
^{0}Ca	M.Budnar et al. NP/A,213,525,1973 Exf. 30532013					
^{0}Ca	J.K.Dickens et al. NSE,53,277,1974 Exf. 10350002	$\frac{d^2\sigma_{\gamma prod}}{d\Omega\, dE_\gamma}$ in (n,xγ) reactions	0.7-20	125° 0.7-10.6	ORELA n: Ta(γ,n), TOF, scintillation detectors γ: NaI, heavy shielding + LiH, paraffin	
^{45}Sc	M.Budnar et al. NP/A,13,525,1973 Exf. 30532015	$\frac{d\,\sigma_{n\gamma}}{dE_\gamma}$ in (n,γ) reactions	14.1±0.6	12-24	Cockcroft-Walton accelerator n: T(d,n)^{4}He, recoil proton method γ: anticoincidence, scintillation pair spectrometer	Absolute measurements in 4π geometry

Nuclide	Reference	Quantities measured	Neutron energy, MeV	Energy angular characteristics of γ-radiation, φ, degrees; Eγ, MeV	Measurement method, detectors	Remarks
^{45}Sc	J.Voignier et al. NSE,93,43,1986 Exf. 22006042	$\frac{d^2\sigma_{n\gamma}}{d\Omega\, dE_\gamma}$ and gamma-ray multiplicity	0.5-3	90° 0.7-9.2	Van de Graaf n: ^{7}Li(p,n)^{7}Be, ^{3}H(p,n)^{3}He, TOF, BF_3 counters γ: NaI annular, heavy shielding + paraffin + Li + B	Below E_γ = 1.5 MeV data taken from calculation
^{0}Ti	J.Voignier et al. NSE,93,43,1986 Exf. 22006043					
^{0}Ti	G.L.Morgan et al. R, ORNL-TM-6323,1978 Exf. 10790002	$\frac{d^2\sigma_{\gamma prod}}{d\Omega\, dE_\gamma}$ in (n,xγ) reactions	0.3-20	125° 0.3-10.6	ORELA n: Ta(γ,n), TOF, scintillation detectors γ: NaI, heavy shielding + LiH, paraffin	
^{51}V	E.Newman et al. NSE,62,515,1977 Exf. 10657002		0.2-20	125° 0.3-10.6		
^{51}V	M.Budnar et al. NP/A,213,525,1973 Exf. 30532017	$\frac{d\sigma_{n\gamma}}{dE_\gamma}$ in (n,γ) reactions	14.1±0.6	12-24	Cockcroft-Walton accelerator n: T(d,n)^{4}He, recoil proton method γ: anticoincidence, scintillation pair spectrometer	Absolute measurements in 4π geometry
^{0}Cr	M.Budnar et al. NP/A,213,525,1973 Exf. 30532019					
^{0}Cr	G.L.Morgan et al. R,ORNL-TM-5098,1976 Exf. 10581002	$\frac{d^2\sigma_{\gamma prod}}{d\Omega\, dE_\gamma}$ in (n,xγ) reactions	0.2-20	125° 0.3-10.6	ORELA n: Ta(γ,n), TOF, scintillation detectors γ: NaI, heavy shielding + LiH, paraffin	
^{55}Mn	G.L.Morgan et al. R,ORNL-TM-5416,1976 Exf. 10580002					
^{55}Mn	M.Budnar et al. NP/A,213,525,1973 Exf. 30532021	$\frac{d\sigma_{n\gamma}}{dE_\gamma}$ in (n,γ) reactions	14.1±0.6	12-24	Cockcroft-Walton accelerator n: T(d,n)^{4}He, recoil proton method γ: anticoincidence, scintillation pair spectrometer	Absolute measurements in 4π geometry
^{0}Fe	M.Budnar et al. NP/A,213,525,1975 Exf. 30532023					

Nuclide	Reference	Quantities measured	Neutron energy, MeV	Energy angular characteristics of γ-radiation, φ, degrees; Eγ, MeV	Measurement method, detectors	Remarks
^{0}Fe	G.T.Chapman et al. R,ORNL-TM-5416,1976 Exf. 10580002	$\frac{d^2\sigma_{\gamma prod}}{d\Omega\, dE_\gamma}$ in (n,xγ) reactions	0.85-20	125^0 0.7-10.6	ORELA n: Ta(γ,n), TOF, scintillation detectors γ: NaI, heavy shielding + LiH, paraffin	
^{59}Co	M.Budnar et al. NP/A,213,525,1973 Exf. 30532025	$\frac{d\,\sigma_{n\gamma}}{dE_\gamma}$ in (n,γ) reactions	14.1±0.6	12-24	Cockcroft-Walton accelerator n: T(d,n)^{4}He, recoil proton method γ: anticoincidence, scintillation pair spectrometer	Absolute measurements in 4π geometry
^{0}Ni	J.K.Dickens et al. R,ORNL-TM-4379,1973 Exf. 10402002	$\frac{d^2\sigma_{\gamma prod}}{d\Omega\, dE_\gamma}$ in (n,xγ) reactions	1-20	125^0 0.7-10.6	ORELA n: Ta(γ,n), TOF, scintillation detectors γ: NaI, heavy shielding + LiH, paraffin	
^{0}Cu	G.L.Morgan et al. R,ORNL-TM-5499,1979 Exf. 10977003		1-20	130^0 0.8-10.		
^{0}Cu	М.В.Савин С,80 Kiev,2,17,1980 Exf. 40518002	$\sigma_{\gamma prod}\,(E_n\,,\,E_\gamma)$ in (n,xγ) reactions	1-10	125^0 1-5	Linac n: TOF, stilbene detector γ: liquid scintillator detector	Absolute measurements
^{0}Cu	M.Budnar et al. NP/A,213,525,1973 Exf. 30532021	$\frac{d\,\sigma_{n\gamma}}{dE_\gamma}$ in (n,γ) reactions	14.1±0.6	12-24	Cockcroft-Walton accelerator n: T(d,n)^{4}He, recoil proton method γ: anticoincidence, scintillation pair spectrometer	Absolute measurements in 4π geometry
^{0}Cu	J.Voignier et al. NSE,93,43,1986 Exf. 22006044	$\frac{d^2\sigma_{n\gamma}}{d\Omega\, dE_\gamma}$ and gamma-ray multiplicity	0.5-3	90^0 0.7-8	Van de Graaf n: ^{7}Li(p,n)^{7}Be, ^{3}H(p,n)^{3}He, TOF, BF_3 counters γ: NaI + NaI annular, heavy shielding + paraffin + Li + B	Below E_γ = 1.5 MeV data taken from calculation
^{63}Cu	J.Voignier et al. NSE,93,43,1986 Exf. 22006045					
^{65}Cu	J.Voignier et al. NSE,93,43,1986 Exf. 22006046					

Nuclide	Reference	Quantities measured	Neutron energy, MeV	Energy angular characteristics of γ-radiation, φ, degrees; Eγ, MeV	Measurement method, detectors	Remarks
^{0}Zn	J.K.Dickens et al. R,ORNL-TM-4464,1974 Exf. 10398002	$\frac{d^2\sigma_{\gamma prod}}{d\Omega\, dE_\gamma}$ in (n,xγ) reactions	0.85-20	125° 0.7-10.6	ORELA n: Ta(γ,n), TOF, scintillation detectors γ: NaI, heavy shielding + LiH, paraffin	
^{0}Se	M.Budnar et al. NP/A,213,525,1973 Exf. 30532029	$\frac{d\sigma_{n\gamma}}{dE_\gamma}$ in (n,γ) reactions	14.1±0.6	12-24	Cockcroft-Walton accelerator n: T(d,n)^{4}He, recoil proton method γ: anticoincidence, scintillation pair spectrometer	Absolute measurements in 4π geometry
^{0}Br	M.Budnar et al. NP/A,213,525,1973 Exf. 30532031					
^{0}Rb	J.Voignier et al. NSE,93,43,1986 Exf. 22006047	$\frac{d^2\sigma_{n\gamma}}{d\Omega\, dE_\gamma}$ and gamma-ray multiplicity	0.5-3	90° 0.7-8	Van de Graaf n: ^{7}Li(p,n)^{7}Be, ^{3}H(p,n)^{3}He, TOF, BF_3 counters γ: NaI + NaI annular, heavy shielding + paraffin + Li + B	Below E_γ = 1.5 MeV data taken from calculation
^{0}Sr	M.Budnar et al. NP/A,213,525,1973 Exf. 30532033	$\frac{d\sigma_{n\gamma}}{dE_\gamma}$ in (n,γ) reactions	14.1±0.6	12-24	Cockcroft-Walton accelerator n: T(d,n)^{4}He, recoil proton method γ: anticoincidence, scintillation pair spectrometer	Absolute measurements in 4π geometry
^{89}Y	M.Budnar et al. NP/A,213,525,1973 Exf. 30532035					
^{88}Y	J.Voignier et al. NSE,93,43,1986 Exf. 22006048	$\frac{d^2\sigma_{n\gamma}}{d\Omega\, dE_\gamma}$ and gamma-ray multiplicity	0.5-3	90° 0.7-8	Van de Graaf n: ^{7}Li(p,n)^{7}Be, ^{3}H(p,n)^{3}He, TOF, BF_3 counters γ: NaI + NaI annular, heavy shielding + paraffin + Li + B	Below E_γ = 1.5 MeV data taken from calculation
^{0}Zr	J.Voignier et al. NSE,93,43,1986 Exf. 22006049					
^{93}Nb	J.Voignier et al. NSE,93,43,1986 Exf. 22006050					

Nuclide	Reference	Quantities measured	Neutron energy, MeV	Energy angular characteristics of γ-radiation, φ, degrees; Eγ, MeV	Measurement method, detectors	Remarks
^{93}Nb	J.K.Dickens et al. NSE,62,515,1977 Exf. 10553002	$\frac{d^2\sigma_{\gamma prod}}{d\Omega\, dE_\gamma}$ in (n,xγ) reactions	0.65-20	90° 0.7-10.6	ORELA n: Ta(γ,n), TOF, scintillation detectors γ: NaI, heavy shielding + LiH, paraffin	
^{0}Mo	G.L.Morgan et al. R,ORNL-TM-5097,1975 Exf. 10584002		0.2-20	125° 0.3-10.6		
^{0}Mo	М.В.Савин C, 80 Kiev,2,17,1980 Exf.40518007-40518013	$\sigma_{\gamma prod}(E_n, E_\gamma)$ in (n,xγ) reactions	1-10	125° 1-5	Linac n: TOF, stilbene detector γ: liquid scintillator detector	Absolute measurements
^{0}Mo	J.Voignier et al. NSE,93,43,1986 Exf. 22006051	$\frac{d^2\sigma_{n\gamma}}{d\Omega\, dE_\gamma}$ and gamma-ray multiplicity	0.5-3	90° 0.7-8	Van de Graaf n: ^{7}Li(p,n)^{7}Be, ^{3}H(p,n)^{3}He, TOF, BF_3 counters γ: NaI + NaI annular, heavy shielding + paraffin + Li + B	Below E_γ = 1.5 MeV data taken from calculation
^{0}Ag	J.K.Dickens et al. NSE,62,515,1977 Exf. 10400002	$\frac{d\,\sigma_{\gamma prod}}{d\Omega\, dE_\gamma}$ in (n,xγ) reactions	0.65-20	125° 0.3-10.6	ORELA n: Ta(γ,n), TOF, scintillation detectors γ: NaI, heavy shielding + LiH, paraffin	
^{0}In	M.Budnar et al. NP/A,213,525,1973 Exf. 30532037	$\frac{d\,\sigma_{n\gamma}}{dE_\gamma}$ in (n,γ) reactions	14.1±0.6	12-24	Cockcroft-Walton accelerator n: T(d,n)^{4}He, recoil proton method γ: anticoincidence, scintillation pair spectrometer	Absolute measurements in 4π geometry
^{0}Sn	J.K.Dickens et al. NSE,62,515,1977 Exf. 10351002	$\frac{d^2\sigma_{\gamma prod}}{d\Omega\, dE_\gamma}$ in (n,xγ) reactions	0.75-20	125°	ORELA n: Ta(γ,n), TOF, scintillation detectors γ: NaI, heavy shielding + LiH, paraffin	
^{0}Sb	M.Budnar et al. NP/A,213,525,1973 Exf. 30532039	$\frac{d\,\sigma_{n\gamma}}{dE_\gamma}$ in (n,γ) reactions	14.1±0.6	12-24	Cockcroft-Walton accelerator n: T(d,n)^{4}He, recoil proton method γ: anticoincidence, scintillation pair spectrometer	Absolute measurements in 4π geometry

Nuclide	Reference	Quantities measured	Neutron energy, MeV	Energy angular characteristics of γ-radiation, φ, degrees; Eγ, MeV	Measurement method, detectors	Remarks
^{127}I	M.Budnar et al. NP/A,213,525,1973 Exf. 30532041	$\frac{d\sigma_{n\gamma}}{dE_\gamma}$ in (n,γ) reactions	14.1±0.6	12-24	Cockcroft-Walton accelerator n: T(d,n)^{4}He, recoil proton method γ: anticoincidence, scintillation pair spectrometer	Absolute measurements in 4π geometry
^{127}I	J.Voignier et al. NSE,93,43,1986 Exf. 22006052	$\frac{d^2\sigma_{n\gamma}}{d\Omega\, dE_\gamma}$ and gamma-ray multiplicity	0.5-3	90° 0.7-8	Van de Graaf n: ^{7}Li(p,n)^{7}Be, ^{3}H(p,n)^{3}He, TOF, BF_3 counters γ: NaI + NaI annular, heavy shielding + paraffin + Li + B	Below E_γ = 1.5 MeV data taken from calculation
^{137}Cs	J.Voignier et al. NSE,93,43,1986 Exf. 22006053					
^{0}Ba	M.Budnar et al. NP/A,213,525,1973 Exf. 30532043	$\frac{d\sigma_{n\gamma}}{dE_\gamma}$ in (n,γ) reactions	14.1±0.6	12-24	Cockcroft-Walton accelerator n: T(d,n)^{4}He, recoil proton method γ: anticoincidence, scintillation pair spectrometer	Absolute measurements in 4π geometry
^{139}La	J.Voignier et al. NSE,93,43,1986 Exf. 22006054	$\frac{d^2\sigma_{n\gamma}}{d\Omega\, dE_\gamma}$ and gamma-ray multiplicity	0.5-3	90° 0.7-8	Van de Graaf n: ^{7}Li(p,n)^{7}Be, ^{3}H(p,n)^{3}He, TOF, BF_3 counters γ: NaI + NaI annular, heavy shielding + paraffin + Li + B	Below E_γ = 1.5 MeV data taken from calculation
^{0}Ce	J.Voignier et al. NSE,93,43,1986 Exf. 22006055					
^{141}Pr	J.Voignier et al. NSE,93,43,1986 Exf. 22006056					
^{141}Pr	M.Budnar et al. NP/A,213,525,1973 Exf. 30532045	$\frac{d\sigma_{n\gamma}}{dE_\gamma}$ in (n,γ) reactions	14.1±0.6	12-24	Cockcroft-Walton accelerator n: T(d,n)^{4}He, recoil proton method γ: anticoincidence, scintillation pair spectrometer	Absolute measurements in 4π geometry
^{0}Gd	J.Voignier et al. NSE,93,43,1986 Exf. 22006057	$\frac{d^2\sigma_{n\gamma}}{d\Omega\, dE_\gamma}$ and gamma-ray multiplicity	0.5-3	90° 0.7-8	Van de Graaf n: ^{7}Li(p,n)^{7}Be, ^{3}H(p,n)^{3}He, TOF, BF_3 counters γ: NaI + NaI annular, heavy shielding + paraffin + Li + B	Below E_γ = 1.5 MeV data taken from calculation

Nuclide	Reference	Quantities measured	Neutron energy, MeV	Energy angular characteristics of γ-radiation, φ, degrees; Eγ, MeV	Measurement method, detectors	Remarks
^{155}Gd	J.Voignier et al. NSE,93,43,1986 Exf. 22006058	$\frac{d^2\sigma_{n\gamma}}{d\Omega\, dE_\gamma}$ and gamma-ray multiplicity	0.5-3	90° 0.7-8	Van de Graaf n: ^{7}Li(p,n)^{7}Be, ^{3}H(p,n)^{3}He, TOF, BF_3 counters γ: NaI + NaI annular, heavy shielding + paraffin + Li + B	Below E_γ = 1.5 MeV data taken from calculation
^{156}Gd	J.Voignier et al. NSE,93,43,1986 Exf. 22006059					
^{157}Gd	J.Voignier et al. NSE,93,43,1986 Exf. 22006060					
^{158}Gd	J.Voignier et al. NSE,93,43,1986 Exf. 22006061					
^{160}Gd	J.Voignier et al. NSE,93,43,1986 Exf. 22006062					
^{159}Tb	J.Voignier et al. NSE,93,43,1986 Exf. 22006063					
^{165}Ho	J.Voignier et al. NSE,93,43,1986 Exf. 22006064					
^{165}Ho	M.Budnar et al. NP/A,213,525,1973 Exf. 30532047	$\frac{d\,\sigma_{n\gamma}}{dE_\gamma}$ in (n,γ) reactions	14.1±0.6	12-24	Cockcroft-Walton accelerator n: T(d,n)^{4}He, recoil proton method γ: anticoincidence, scintillation pair spectrometer	Absolute measurements in 4π geometry
^{0}Lu	J.Voignier et al. NSE,93,43,1986 Exf. 22006065	$\frac{d^2\sigma_{n\gamma}}{d\Omega\, dE_\gamma}$ and gamma-ray multiplicity	0.5-3	90° 0.7-8	Van de Graaf n: ^{7}Li(p,n)^{7}Be, ^{3}H(p,n)^{3}He, TOF, BF_3 counters γ: NaI + NaI annular, heavy shielding + paraffin + Li + B	Below E_γ = 1.5 MeV data taken from calculation

Nuclide	Reference	Quantities measured	Neutron energy, MeV	Energy angular characteristics of γ-radiation, φ, degrees; Eγ, MeV	Measurement method, detectors	Remarks
^{0}Ta	G.L.Morgan et al. ORNL-TM-3702,1972 Exf. 10399002	$\frac{d^2\sigma_{prod}}{d\Omega\, dE_\gamma}$ in (n,xγ) reactions	0.007-20	125° 0.7-10.6	ORELA n: Ta(γ,n), TOF, scintillation detectors γ: NaI, heavy shielding + LiH, paraffin	Fission chamber for neutrons
^{181}Ta	P.Ramakrishnan NSE,98,348,1988 Exf. 13168002		2-100	45°, 55°, 90°, 125°, 140° 0.8-25.	Meson physical facility in LANL n: TOF, fission chamber with ^{235}U γ: detectors with bismuth germanate crystals	
^{181}Ta	M.Budnar et al. NP/A, 213,525,1973 Exf. 30532049	$\frac{d\,\sigma_{n\gamma}}{dE_\gamma}$ in (n,γ) reactions	14.1±0.6	12-24	Cockcroft-Walton accelerator n: T(d,n)^{4}He, recoil proton method γ: anticoincidence, scintillation pair spectrometer	Absolute measurements in 4π geometry
^{181}Ta	J.Voignier et al. NSE,93,43,1986 Exf. 22006066	$\frac{d^2\sigma_{n\gamma}}{d\Omega\, dE_\gamma}$ and gamma-ray multiplicity	0.5-3	90° 0.7-8	Van de Graaf n: ^{7}Li(p,n)^{7}Be, ^{3}H(p,n)^{3}He, TOF, BF_3 counters γ: NaI + NaI annular, heavy shielding + paraffin + Li + B	Below E_γ = 1.5 MeV data taken from calculation
^{0}W	М.В.Савин R,YFI,27,5,1979 Exf. 40533002	$\sigma_{\gamma prod}(E_n, E_\gamma)$ in (n,xγ) reactions	1-10	125° 1-5	Linac n: TOF, stilbene detector γ: liquid scintillator detector	Absolute measurements
^{0}W	M.Budnar et al. NP/A, 213,525,1973 Exf. 30532051	$\frac{d\,\sigma_{n\gamma}}{dE_\gamma}$ in (n,γ) reactions	14.1±0.6	12-24	Cockcroft-Walton accelerator n: T(d,n)^{4}He, recoil proton method γ: anticoincidence, scintillation pair spectrometer	Absolute measurements in 4π geometry
^{0}W	J.K.Dickens et al. R,ORNL-4847,1973 Exf. 10353002	$\frac{d^2\sigma_{\gamma prod}}{d\Omega\, dE_\gamma}$ in (n,xγ) reactions	1-20	125° 0.7-10.6	ORELA n:Ta(γ,n), TOF, scintillation detectors γ:NaI, heavy shielding + LiH, paraffin	
^{0}W	W.E.Tucker BAP,15,1667,1970 Exf. 10091003	$\frac{d\sigma_{\gamma prod}}{dE_\gamma}$ in (n,xγ) reactions	8,9,10,11	55° 0.4-6.5	Van de Graaf, tandem n: D(D,n)^{3}He, T(p,n)^{3}He, TOF γ: NaI(Tl), NaI(Cr), GeLi	

Nuclide	Reference	Quantities measured	Neutron energy, MeV	Energy angular characteristics of γ-radiation, φ, degrees; Eγ, MeV	Measurement method, detectors	Remarks
^{0}W	J.Voignier et al. NSE,93,43,1986 Exf. 22006067	$\frac{d^2\sigma_{n\gamma}}{d\Omega\, dE_\gamma}$ and gamma-ray multiplicity	0.5-3	90° 0.7-8	Van de Graaf n: ^{7}Li(p,n)^{7}Be, ^{3}H(p,n)^{3}He, TOF, BF_3 counters γ: NaI + NaI annular, heavy shielding + paraffin + Li + B	Below E_γ = 1.5 MeV data taken from calculation
^{182}W	J.Voignier et al. NSE,93,43,1986 Exf. 22006068					
^{183}W	J.Voignier et al. NSE,93,43,1986 Exf. 22006069					
^{184}W	J.Voignier et al. NSE,93,43,1986 Exf. 22006070					
^{186}W	J.Voignier et al. NSE,93,43,1986 Exf. 22006071					
^{0}Re	J.Voignier et al. NSE,93,43,1986 Exf. 22006072					
^{190}Os	J.Voignier et al. NSE,93,43,1986 Exf. 22006073					
^{192}Os	J.Voignier et al. NSE,93,43,1986 Exf. 22006074					
^{194}Pr	J.Voignier et al. NSE,93,43,1986 Exf. 22006076					
^{197}Au	J.Voignier et al. NSE,93,43,1986 Exf. 22006077					

Nuclide	Reference	Quantities measured	Neutron energy, MeV	Energy angular characteristics of γ-radiation, φ, degrees; Eγ, MeV	Measurement method, detectors	Remarks
^{197}Au	G.L.Morgan et al. R,ORNL-1973,1975 Exf. 10551002	$\frac{d^2\sigma_{prod}}{d\Omega\, dE_\gamma}$ in (n,xγ) reactions	0.2-20	125° 0.3-10.6	ORELA n: Ta(γ,n), TOF, scintillation detectors γ: NaI, heavy shielding + LiH, paraffin	Fission chamber for neutrons
^{0}Tl	J.Voignier et al. NSE,93,43,1986 Exf.22006078	$\frac{d^2\sigma_{n\gamma}}{d\Omega\, dE_\gamma}$ and gamma-ray multiplicity	0.5-3	90° 0.7-8	Van de Graaf n: ^{7}Li(p,n)^{7}Be, ^{3}H(p,n)^{3}He, TOF, BF_3 counters γ: NaI + NaI annular, heavy shielding + paraffin + Li + B	Below E_γ = 1.5 MeV data taken from calculation
^{0}Tl	M.Budnar et al. NP/A,213,525,1973 Exf. 30532053	$\frac{d\,\sigma_{n\gamma}}{dE_\gamma}$ in (n,γ) reactions	14.1±0.6	12-24	Cockcroft-Walton accelerator n: T(d,n)^{4}He, recoil proton method γ: anticoincidence, scintillation pair spectrometer	Absolute measurements in 4π geometry
^{0}Pb	M.Budnar et al. NP/A,213,525,1973 Exf. 30532055					
^{0}Pb	C.T.Chapman et al. NSE,62,515,1977 Exf. 10586003	$\frac{d^2\sigma_{\gamma prod}}{d\Omega\, dE_\gamma}$ in (n,xγ) reactions	0.6-20	125° 0.3-10.6	ORELA n: Ta(γ,n), TOF, scintillation detectors γ: NaI, heavy shielding + LiH, paraffin	
^{208}Pb	J.K.Dickens et al. NSE,63,101,1997 Exf. 10692003	$\sigma_{\gamma prod}$ in (n,xγ) reactions	5.4-8	55° 0.55-4.8	Pulsed Van de Graaf accelerator n: d(d,n)^{1}H, TOF γ, GeLi	
^{209}Bi	J.K.Dickens et al. NSE,63,101,1997 Exf. 10692002					
^{209}Bi	B.Joensson et al. AF,39,295,1969 Exf. 20164039	$\sigma_{\gamma prod}$	14.7-15.5	80o 0.9-2.7	Van de Graaf n: T(d,n)^{4}He, BF_3 counters γ: Ge(Li) spectrometer	
^{209}Bi	M.Budnar et al. NP/A,213,525,1973 Exf. 30532057	$\frac{d\,\sigma_{n\gamma}}{dE_\gamma}$ in (n,γ) reactions	14.1±0.6	12-24	Cockcroft-Walton accelerator n: T(d,n)^{4}He, recoil proton method γ: anticoincidence, scintillation pair spectrometer	Absolute measurements in 4π geometry

Nuclide	Reference	Quantities measured	Neutron energy, MeV	Energy angular characteristics of γ-radiation, φ, degrees; Eγ, MeV	Measurement method, detectors	Remarks
^{209}Bi	J.Voignier et al. NSE,93,43,1986 Exf.22006079	$\frac{d^2\sigma_{n\gamma}}{d\Omega\, dE_\gamma}$ and gamma-ray multiplicity	0.5-3	90° 0.7-8	Van de Graaf n: ^{7}Li(p,n)^{7}Be, ^{3}H(p,n)^{3}He, TOF, BF_3 counters γ: NaI + NaI annular, heavy shielding + paraffin + Li + B	Below E_γ = 1.5 MeV data taken from calculation
^{238}U	J.Voignier et al. NSE,93,43,1986 Exf.22006080					

BIBLIOGRAPHY OF EXPERIMENTAL WORK ON
NUCLEI COVERED

1. W.E.TUCKER, P.S.BUCHANAN, T.C.MARTIN, D.O.NELLIS, G.H.WILLIAMS
NEUTRON INDUCED GAMMA-RAY PRODUCTION CROSS SECTIONS FOR SILICON AND TUNGSTEN.
R,DASA-2333,6907; J,BAP,15,1667,7012

2. J.K.DICKENS, T.A.LOVE, G.L.MORGAN
NEUTRON-INDUCED GAMMA-RAY PRODUCTION IN CALCIUM IN THE ENERGY RANGE 0.7 TO 20 MEV.
J,NSE,53,277,7403; J,NSE,62,515,7703; R,ORNL-TM-4252,7307

3. J.K.DICKENS, T.A.LOVE, G.L.MORGAN
GAMMA-RAY PRODUCTION DUE TO NEUTRON INTERACTIONS WITH NITROGEN FOR INCIDENT NEUTRON ENERGIES BETWEEN 2.0 AND 20 MEV-TABULATED DIFFERENTIAL CROSS SECTIONS.
R,ORNL-4864,7304; J,NSE,62,515,7703

4. J.K.DICKENS, T.A.LOVE, G.L.MORGAN
GAMMA-RAY PRODUCTION DUE TO NEUTRON INTERACTIONS WITH TUNGSTEN FOR INCIDENT NEUTRON ENERGIES BETWEEN 1.0 AND 20 MEV-TABULATED DIFFERENTIAL CROSS SECTIONS.
R,ORNL-4847,7301; J,NSE,62,515,7703

5. J.K.DICKENS, T.A.LOVE, G.L.MORGAN
GAMMA-RAY PRODUCTION DUE TO NEUTRON INTERACTIONS WITH TIN FOR INCIDENT NEUTRON ENERGIES BETWEEN 0.75 AND 20 MEV-TABULATED DIFFERENTIAL CROSS SECTIONS.
R,ORNL-TM-4406,7311; J,NSE,62,515,7703

6. J.K.DICKENS, T.A.LOVE, G.L.MORGAN
GAMMA-RAY PRODUCTION FROM NEUTRON INTERACTIONS WITH SILICON FOR INCIDENT NEUTRON ENERGIES BETWEEN 1.0 AND 20 MEV-TABULATED DIFFERENTIAL CROSS SECTIONS.
J,PR/C,10,958,7408; R,ORNL-TM-4389,7312

7. J.K.DICKENS, T.A.LOVE, G.L.MORGAN
GAMMA-RAY PRODUCTION DUE TO NEUTRON INTERACTIONS WITH ZINC FOR INCIDENT NEUTRON ENERGIES BETWEEN 0.85 AND 20 MEV-TABULATED DIFFERENTIAL CROSS SECTIONS.
R,ORNL-TM-4464,7402; J,NSE,62,515,7703,REVIEW

8. G.L.MORGAN, T.A.LOVE, J.K.DICKENS, F.G.PEREY
GAMMA-RAY PRODUCTION CROSS SECTIONS OF TANTALUM AND CARBON FOR INCIDENT NEUTRON ENERGIES BETWEEN 0.007 AND 20.0 MEV
R,ORNL-TM-3702,7202; J,NSE,62,515,7703

9. J.K.DICKENS, T.A.LOVE, G.L.MORGAN
GAMMA-RAY PRODUCTION DUE TO NEUTRON INTERACTIONS WITH SILVER FOR INCIDENT NEUTRON ENERGIES BETWEEN 0.3 AND 20 MEV-TABULATED DIFF. CROSS SECTIONS.
R,ORNL-TM-5081,7511; J,NSE,62,515,7703

10. J.K.DICKENS, T.A.LOVE, G.L.MORGAN
GAMMA-RAY PRODUCTION FROM NEUTRON INTERACTIONS WITH NICKEL FOR INCIDENT NEUTRON ENERGIES BETWEEN 1.0 AND 20-MEV -TABULATED DIFF. CROSS SECTIONS.
R,ORNL-TM-4379,7311; J,NSE,62.515.7703
W,DICKENS,7412; W,PURSER,7312

11. J.K.DICKENS, T.A.LOVE, G.L.MORGAN
GAMMA-RAY PRODUCTION DUE TO NEUTRON INTERACTIONS WITH FLUORINE AND LITHIUM FOR INCIDENT NEUTRON ENERGIES BETWEEN 0.55 AND 20 MEV-TAB:DIF.CROSS SECTIONS.
R,ORNL-TM-4538,7404; J,NSE,62.515,7703,REVIEW

12. G.L.MORGAN, E.NEWMAN
THE AU(N,X GAMMA) REACTION CROSS SECTION FOR INCIDENT NEUTRON ENERGIES BETWEEN 0.2 AND 20.0 MEV.
R,ORNL-TM-4973,7508; J,NSE,62,515,7703,REVIEW

13. J.K.DICKENS, G.L.MORGAN, E.NEWMAN
THE NB(N,X GAMMA) REACTION CROSS SECTION FOR INCIDENT NEUTRON ENERGIES BETWEEN 0.65 AND 20.0 MEV.
R,ORNL-TM-4972,7509; J,NSE,62,515,7703,REVIEW

14. G.T.CHAPMAN, G.L.MORGAN, F.G.PEREY
A RE-MEASUREMENT OF THE NEUTRON-INDUCED GAMMA-RAY PRODUCTION CROSS-SECTIONS FOR IRONIN THE ENERGY RANGE FROM 850 KEV TO 20.0 MEV.
R,ORNL-TM-5416,7607

15. G.L.MORGAN, E.NEWMAN
THE CR(N,X GAMMA) REACTION CROSS SECTION FOR INCIDENT NEUTRON ENERGIES BETWEEN 0.2 AND 20.0 MEV.
R,ORNL-TM-5098,7601; J,NSE,62,515,7703,REVIEW

16. J.K.DICKENS, T.A.LOVE, G.L.MORGAN
GAMMA-RAY PRODUCTION DUE TO NEUTRON INTERACTIONS WITH MAGNESIUM FOR INCIDENT NEUTRON ENERGIES BETWEEN 0.8 AND 20 MEV-TABULATED DIF.CROSS SECTIONS.
J,NSE,62,515,7703; R,ORNL-TM-4544,7405

17. G.L.MORGAN, E.NEWMAN
THE MO(N,X GAMMA) REACTION CROSS SECTION FOR INCIDENT NEUTRON ENERGIES BETWEEN 0.2 AND 20.0 MEV.
J,NSE,62.515,7703; R,ORNL-TM-5097,7512

18. G.T.CHAPMAN, G.L.MORGAN
THE PB(N,X GAMMA) REACTION CROSS SECTION FOR INCIDENT NEUTRON ENERGIES BETWEEN 0.6 AND 20.0 MEV.
R,ORNL-TM-4822,7502; J,NSE,62,515,7703

19. G.L.MORGAN
THE MN(N,X GAMMA) REACTION CROSS SECTION FOR INCIDENT NEUTRON ENERGIES BETWEEN 0.2 AND 20.0 MEV.
R,ORNL-TM-5531,7608

20. E.NEWMAN, G.L.MORGAN
THE V (N,X GAMMA) REACTION CROSS SECTION FOR INCIDENT NEUTRON ENERGIES BETWEEN 0.2 AND 20.0 MEV.
R,ORNL-TM-5299,7604; J,NSE,62,515,7703

21. J.K.DICKENS
NEUTRON-INDUCED GAMMA-RAY PRODUCTION IN LEAD-208 FOR INCIDENT-NEUTRON ENERGIES BETWEEN 4.9 AND 8.0 MEV AND IN BISMUTH-209 FOR AN INCIDENT-NEUTRON ENERGY OF 5.4 MEV.
J,NSE,63,101,7705

22. G.L.MORGAN, D.C.LARSON
THE TI(N,XG) REACTION CROSS SECTION FOR INCIDENT NEUTRON ENERGIES BETWEEN 0.3 AND 20.0 MEV.
R,ORNL-TM-6323,7806

23. G.L.MORGAN, G.T.CHAPMAN
THE O-16(N,X)GAMMA REACTION CROSS SECTION FOR INCIDENT NEUTRON ENERGIES BETWEEN 6.5 AND 20.0 MEV.
R,ORNL-5575,7909

24. D.C.LARSON, G.L.MORGAN
MEASUREMENT AND ANALYSIS OF THE NA-23(N,X-GAMMA) REACTION CROSS SECTION FOR NEUTRON ENERGIES BETWEEN 0.2 AND 20 MEV.
J,NSE,75,151,8008; R,ORNL-TM-6281,7805

25. G.L.MORGAN, F.G.PEREY
CROSS SECTIONS FOR THE AL(N,XN) AND AL(N,X-GAMMA) REACTIONS BETWEEN 1 AND 20 MEV.
J,NSE,61,337,7611; R,ORNL-TM-5241,7602

26. G.L.MORGAN
CROSS SECTIONS FOR THE CU(N,XN) AN CU(N,X-GAMMA) REACTIONS BETWEEN 1 AND 20 MEV.
R,ORNL,5499,7902

27. P.RAMAKRISHNAN, G.E.MITCHELL, C.R.GOULD, S.A.WENDER, G.F.AUCHAMPAUGH
PHOTON PRODUCTION CROSS SECTION FOR 181TA.
J,NSE,98,348,88

28. B.JOENSSON, K.NYBERG, I.BERGQVIST
HIGH RESOLUTION MEASUREMENTS OF GAMMA RAYS PRODUCED BY 15 MEV NEUTRONS.
J,AF,39,295,6904

29. J.VOIGNIER, S.JOLY, G.GRENIER
CAPTURE CROSS SECTIONS AND GAMMA-RAY SPECTRA FROM THE INTERACTION OF 0.5 TO 3.0 MEV NEUTRON WITH NUCLEI IN THE MASS RANGE A=63 TO 209
J,NSE,93,43,86

30. M.BUDNAR, F.CVELBAR, E.HODGSON, A.HUDOKLIN, V.IVKOVIC, A.LIKAR, M.V.MIHAILOVIC, R.MARTINCIC, M.NAJZER, A.PERDAN, M.POTOKAR, V.RAMSAK
PROMPT GAMMA-RAY SPECTRA AND INTEGRATED CROSS SECTIONS FOR THE RADIATIVE CAPTURE OF 14 MEV NEUTRONS FOR 28 NATURAL TARGETS IN THE MASS REGION FROM 12 TO 208
R,INDC(YUG)-6,7912 SUMMARY AND REVISED NUMERICAL VALUES FOR ALL MEASURED NUCLEI
R,INDC(YUG)-5,7701 DETAILED DESCRIPTION OF METHOD. NUMERICAL VALUES FOR SC,Y,PR,HO SUPERSEDED
J,NIM,44,292,6610 SPECTROMETER DESCRIBED
R,NIJS-R-470,6511 SAME AS NUCL.INSTR.44,292
J,NP/A,213,525,7310 SUPERSEDED
J,FIZ,5,37,73 SUPERSEDED
J,FIZ/S,4,53,7212 SUPERSEDED
J,FIZ/S,4,55,7212 SUPERSEDED
C,72BUD,,(D-21),7208 SUPERSEDED
J,NP/A,158,251,7012 SUPERSEDED
J,FIZ,2,41,70 SUPERSEDED
J,NP/A,138,412,6911 SUPERSEDED
J,NP/A,130,401,6903 SUPERSEDED
J,IZV,32,1972,6812 SUPERSEDED
J,BAS,32(12),1816,69 ENGL.TRANSL.OF IZV.32,1972
R,NIJS-R-545,6810 SUPERSEDED

31. M.V.SAVIN, JU.A.KHOKHLOV, I.N.PARAMONOVA, V.A.CHIRKIN, V.N.LUDIN, N.N.ZALJALOV
GAMMA-QUANTA PRODUCTION CROSS-SECTION AT THE INTERACTION OF THE FAST NEUTRONS ON THE NUCLEI OF THE CARBON, LEAD AND RHENIUM
J,AE,49,(4),236,8010 GRAPHS ARE GIVEN
C,75KIEV,4,191,7506 PRELIMINARY RESULTS

32. M.V.SAVIN, I.N.PARAMONOVA, V.A.CHIRKIN, V.N.LUDIN, N.N.ZALJALOV
TOTAL GAMMA-EMISSION CROSS-SECTIONS AT THE FAST NEUTRONS INTERACTION WITH THE COPPER AND MOLYBDENUM NUCLEI.
R,YK-4(39),17,8011 NUMERICAL DATA; C,80KIEV,2,17,8009 GRAPHS ONLY

33. M.V.SAVIN, JU.A.KHOKHLOV, I.N.PARAMONOVA, V.A.CHIRKIN, V.N.LUDIN, N.N.ZALJALOV
TOTAL GAMMA-PRODUCTION CROSS-SECTION IN THE (N,X-GAMMA) REACTION ON THE TUNGSTEN IN THE NEUTRON ENERGY RANGE 1-10 MEV
R,YFI-27,5,7911 DATA ARE GIVEN

PART 1.

ENERGY-ANGULAR GAMMA RAY DISTRIBUTIONS

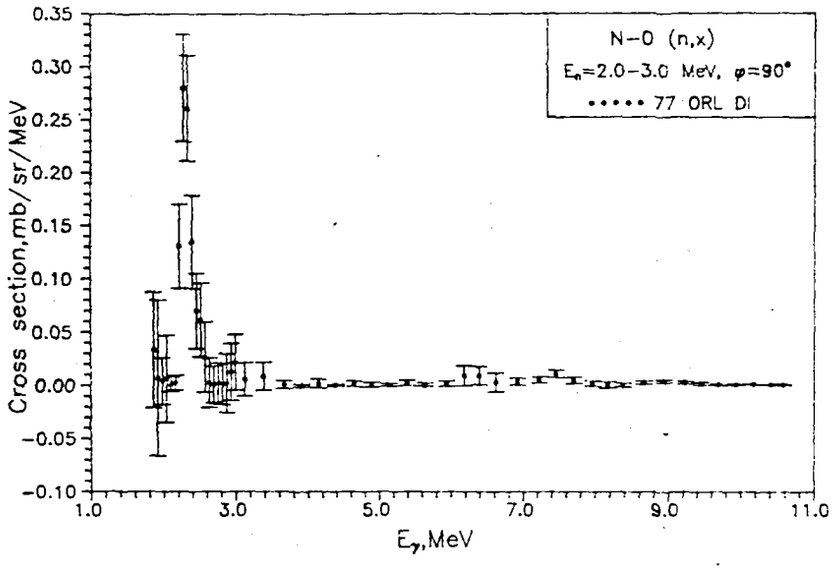
N–O (n,x)
E_n=2.0–3.0 MeV, φ=90°
77 ORL DI
Cross section,mb/sr/MeV
E_γ,MeV

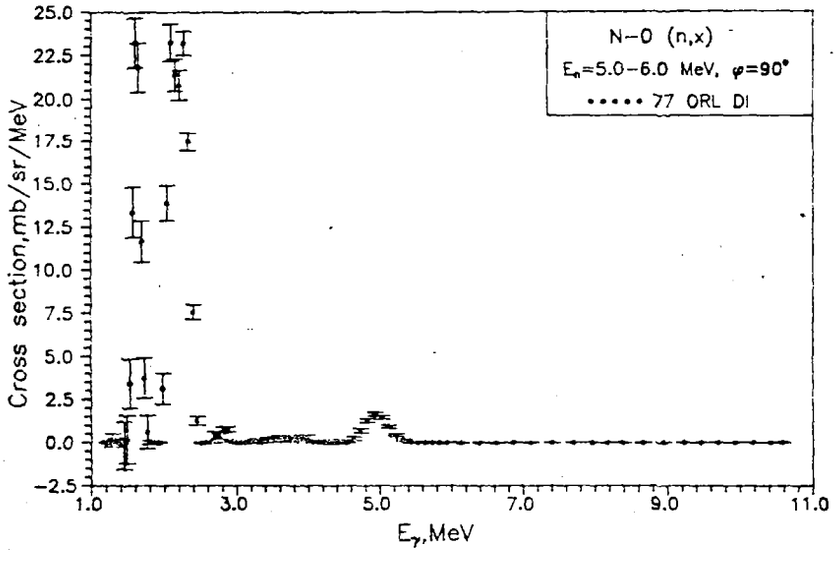
N–O (n,x)
E_n=5.0–6.0 MeV, φ=90°
77 ORL DI
Cross section,mb/sr/MeV
E_γ,MeV

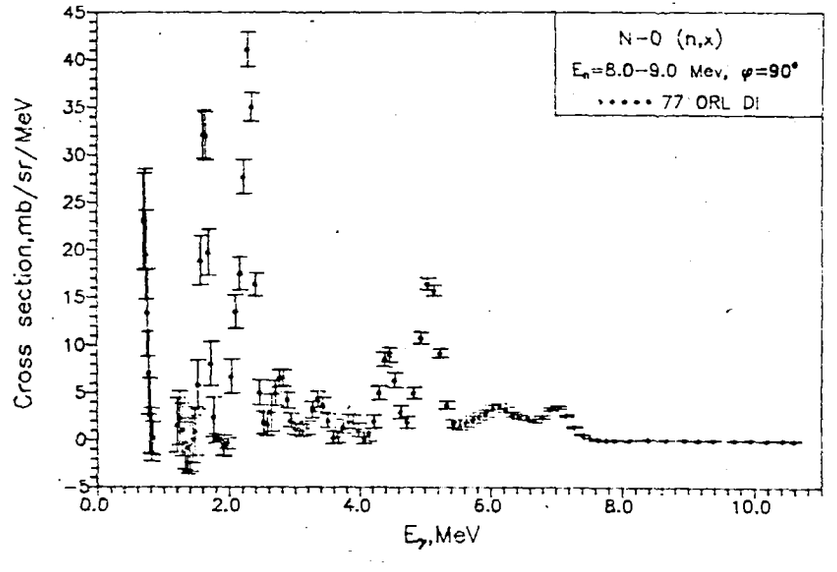
N–O (n,x)
E_n=8.0–9.0 MeV, φ=90°
77 ORL DI
Cross section,mb/sr/MeV
E_γ,MeV

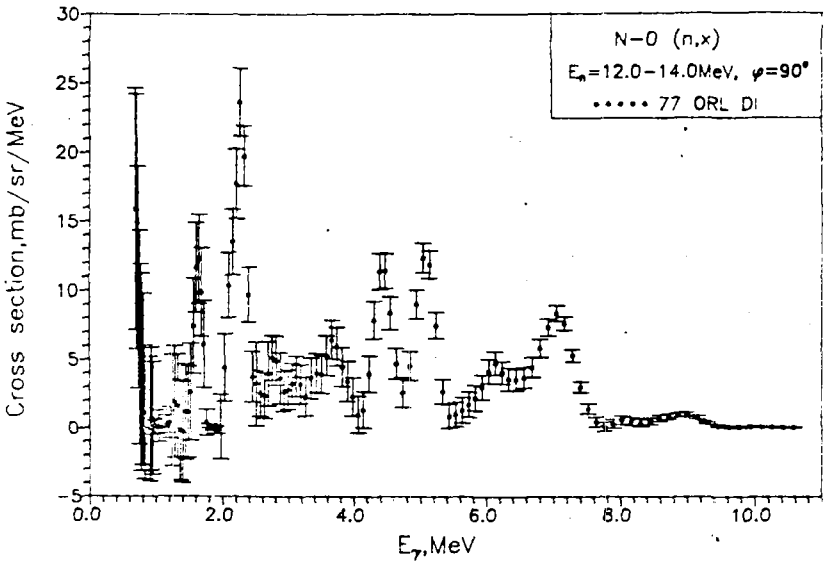
N-O (n,x)
E_n=12.0-14.0MeV, φ=90°
••••• 77 ORL DI
Cross section,mb/sr/MeV
E_γ,MeV

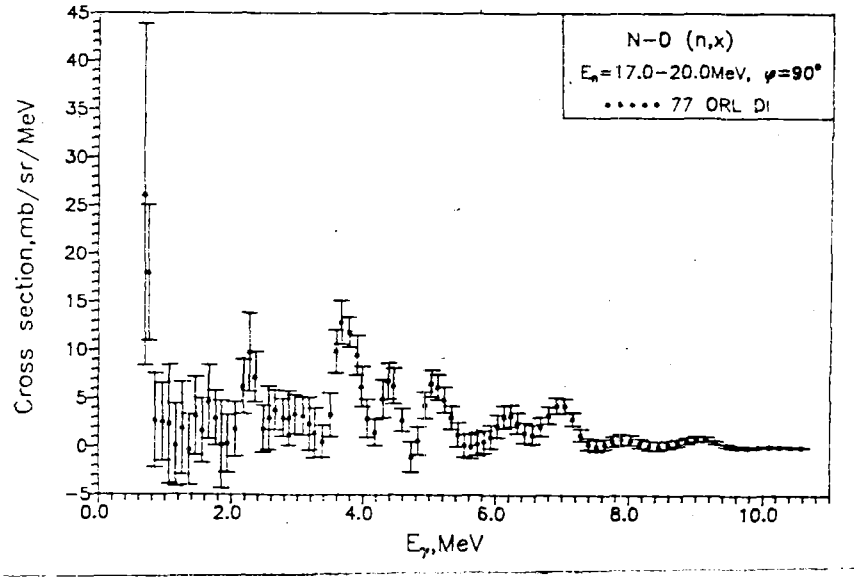
N-O (n,x)
E_n=17.0-20.0MeV, φ=90°
••••• 77 ORL DI
Cross section,mb/sr/MeV
E_γ,MeV

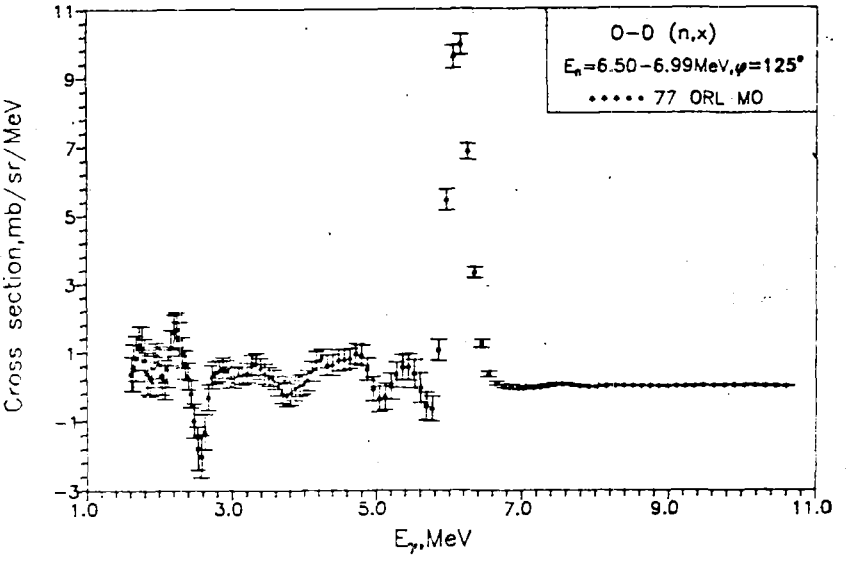
O-O (n,x)
E_n=6.50-6.99MeV,φ=125°
••••• 77 ORL MO
Cross section,mb/sr/MeV
E_γ,MeV

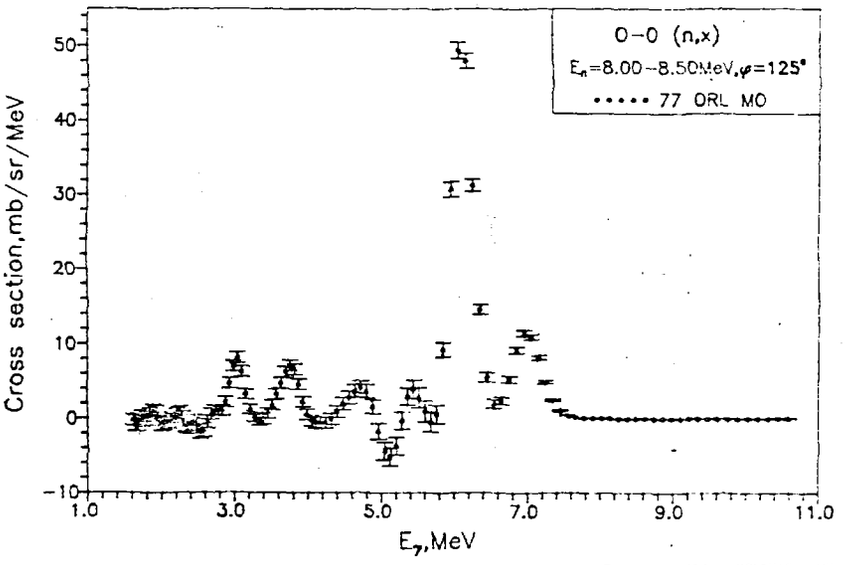
0-0 (n,x)
E_n=8.00-8.50MeV,φ=125°
77 ORL MO
Cross section,mb/sr/MeV
E_γ,MeV

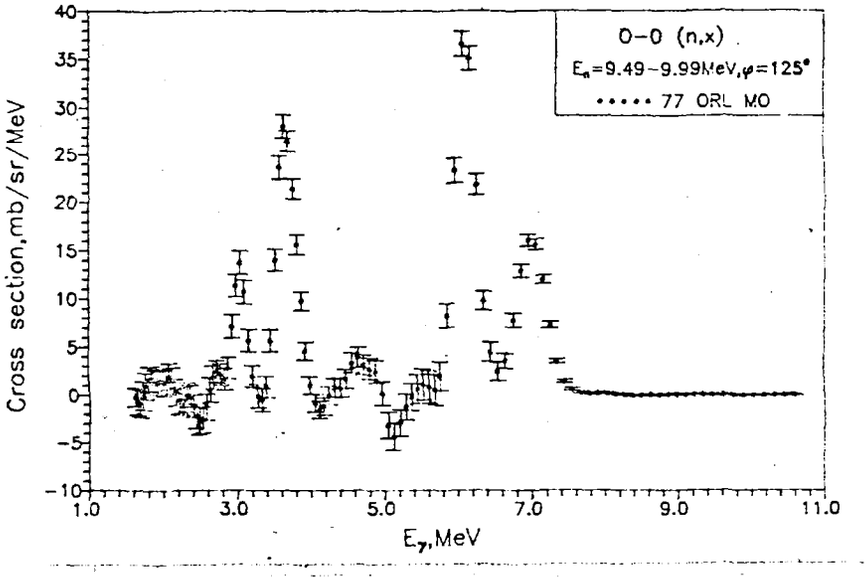
0-0 (n,x)
E_n=9.49-9.99MeV,φ=125°
77 ORL MO
Cross section,mb/sr/MeV
E_γ,MeV

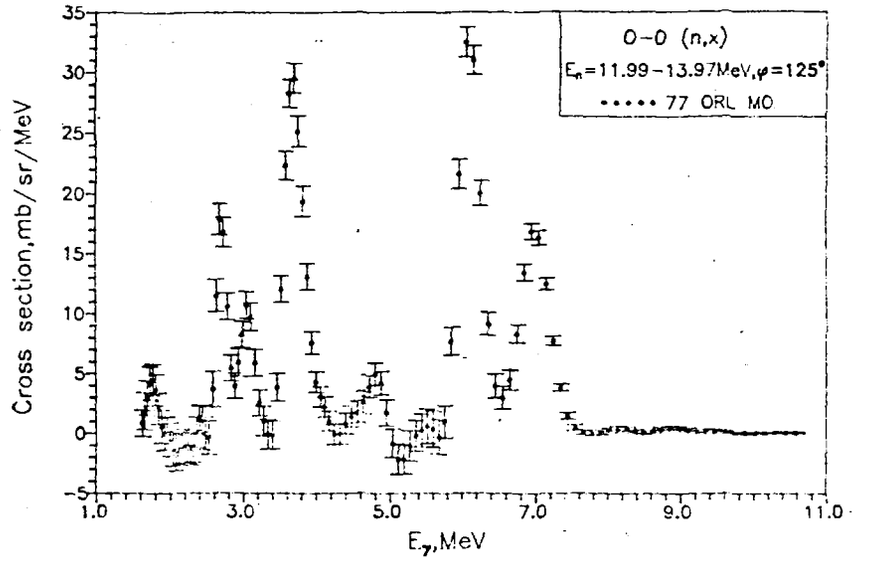
0-0 (n,x)
E_n=11.99-13.97MeV,φ=125°
77 ORL MO
Cross section,mb/sr/MeV
E_γ,MeV

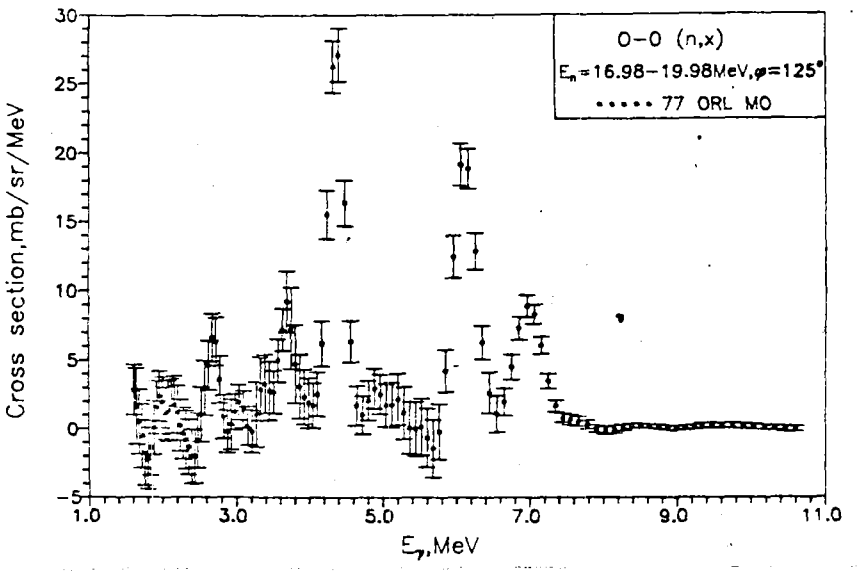
0-0 (n,x)
E_n=16.98-19.98MeV,φ=125°
77 ORL MO
Cross section,mb/sr/MeV
E_γ,MeV

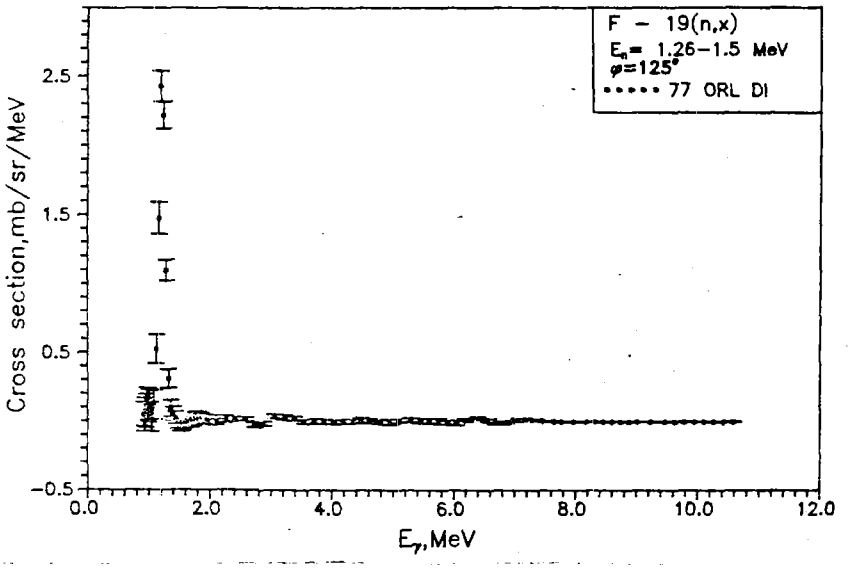
F - 19(n,x)
E_n= 1.26-1.5 MeV
φ=125°
77 ORL DI
Cross section,mb/sr/MeV
E_γ,MeV

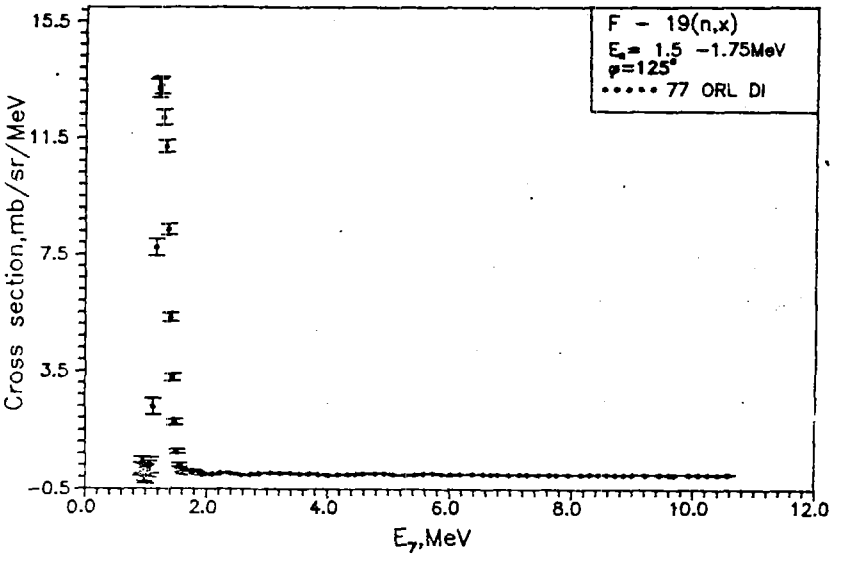
F - 19(n,x)
E_n= 1.5 -1.75MeV
φ=125°
77 ORL DI
Cross section,mb/sr/MeV
E_γ,MeV

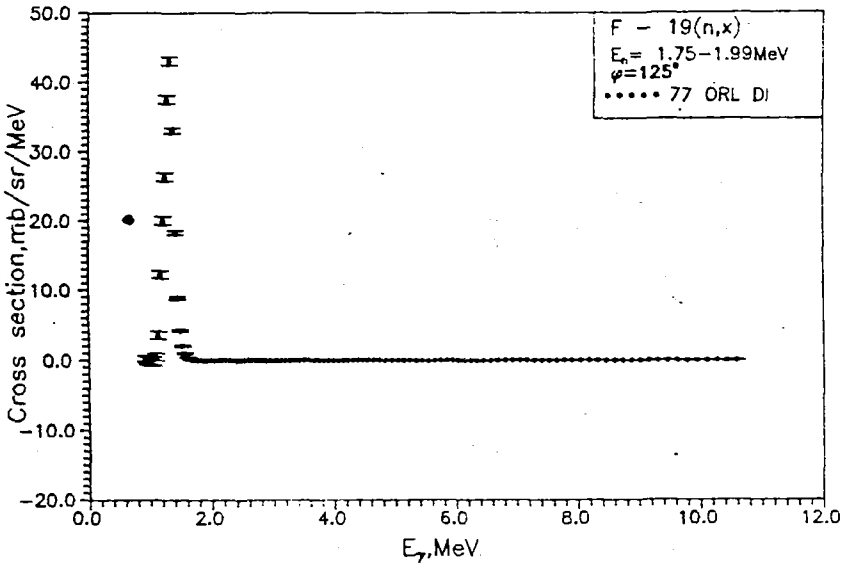
F – 19(n,x)
E_n= 1.75–1.99MeV
φ=125°
••••• 77 ORL DI
Cross section,mb/sr/MeV
E_γ,MeV

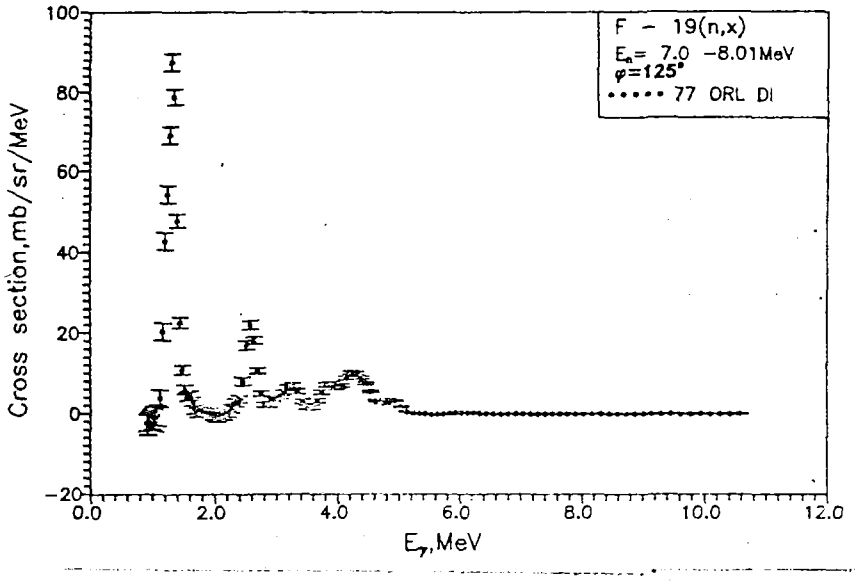
F – 19(n,x)
E_n= 7.0 –8.01MeV
φ=125°
••••• 77 ORL DI
Cross section,mb/sr/MeV
E_γ,MeV

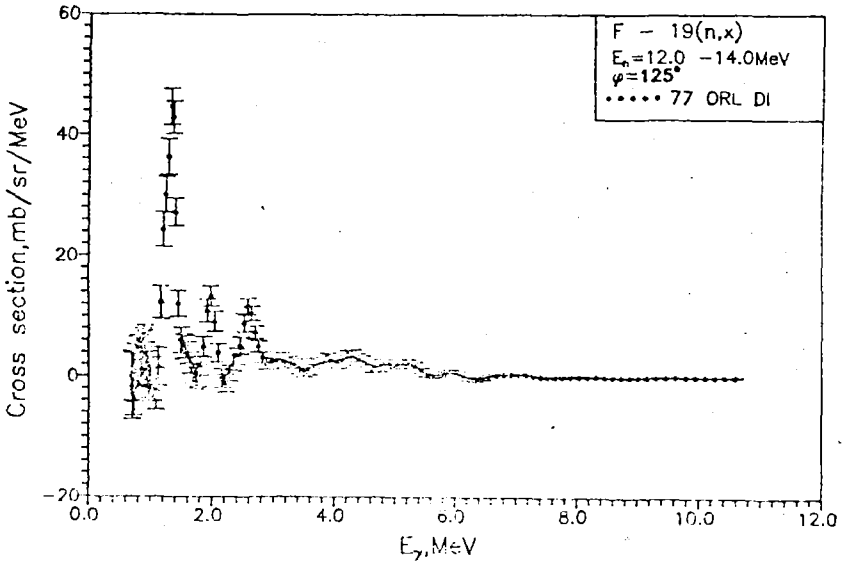
F – 19(n,x)
E_n=12.0 –14.0MeV
φ=125°
••••• 77 ORL DI
Cross section,mb/sr/MeV
E_γ,MeV

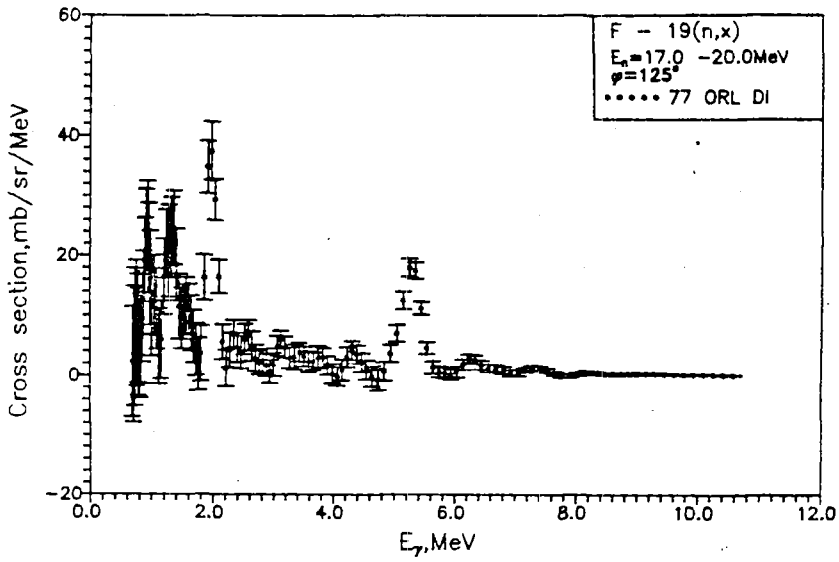
F - 19(n,x)
E_n=17.0 -20.0MeV
φ=125°
77 ORL DI
Cross section,mb/sr/MeV
E_γ,MeV

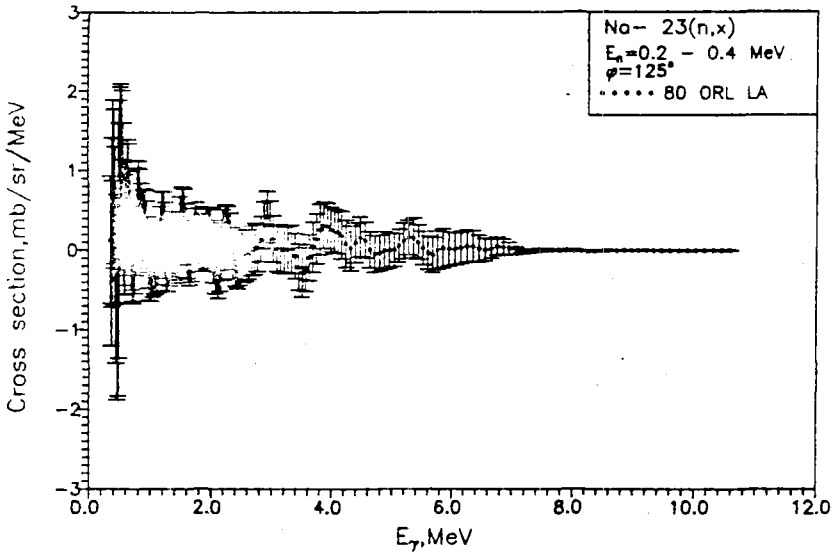
Na- 23(n,x)
E_n=0.2 - 0.4 MeV
φ=125°
80 ORL LA
Cross section,mb/sr/MeV
E_γ,MeV

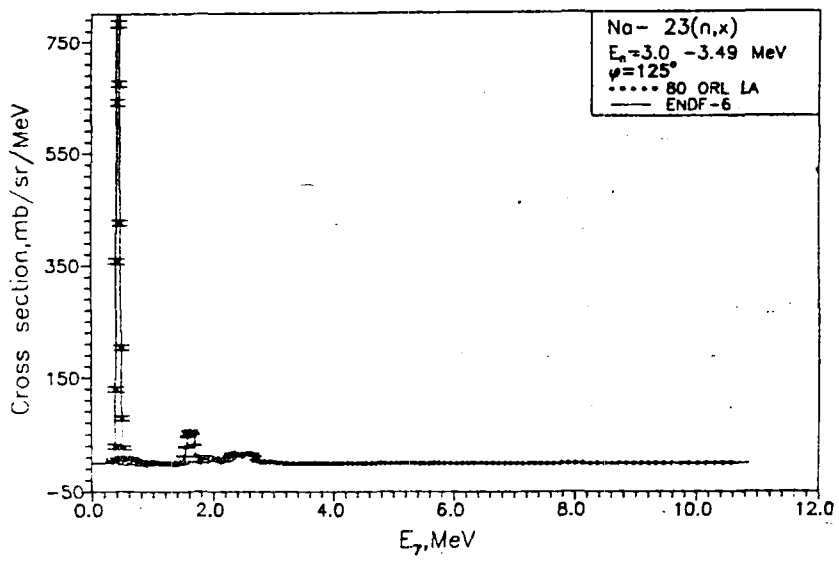
Na- 23(n,x)
E_n=3.0 -3.49 MeV
φ=125°
80 ORL LA
ENDF-6
Cross section,mb/sr/MeV
E_γ,MeV

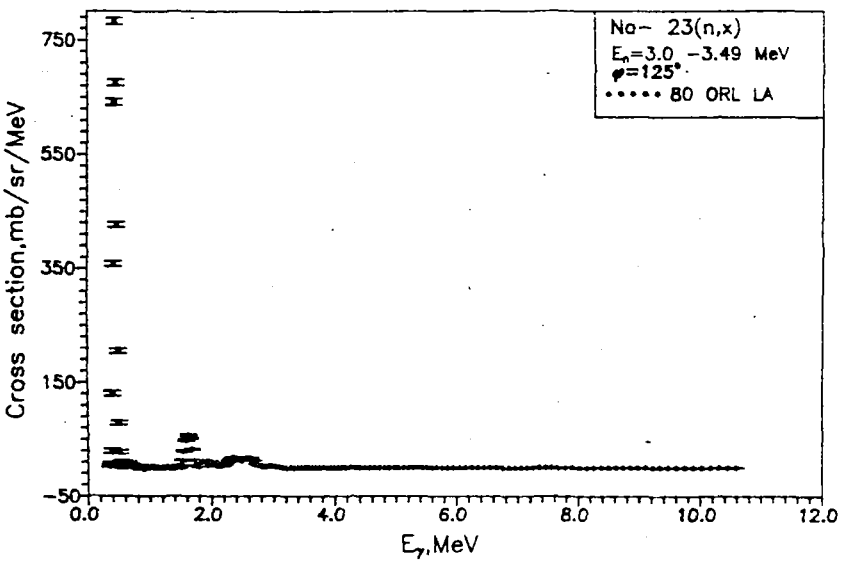
Na- 23(n,x)
E_n=3.0 -3.49 MeV
φ=125°
80 ORL LA
Cross section,mb/sr/MeV
E_γ,MeV

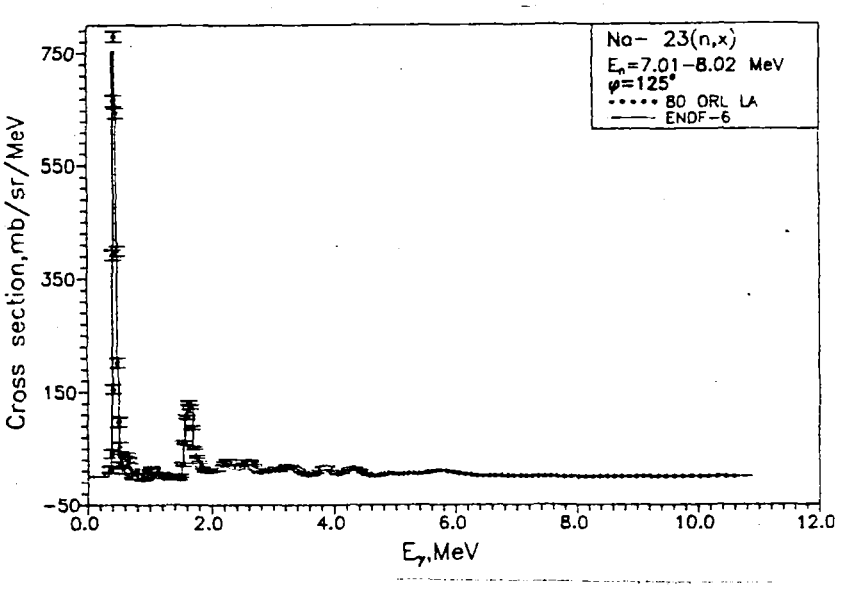
Na- 23(n,x)
E_n=7.01-8.02 MeV
φ=125°
80 ORL LA
ENDF-6
Cross section,mb/sr/MeV
E_γ,MeV

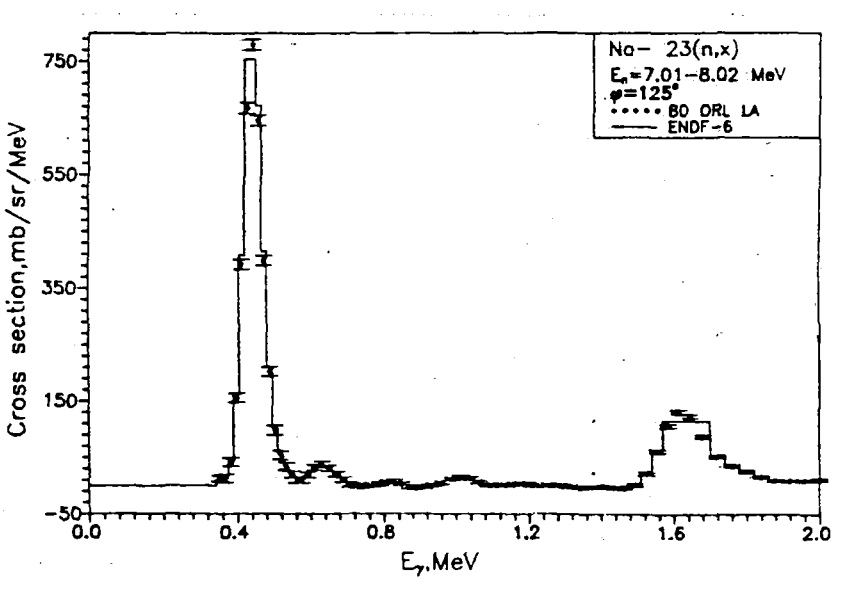
Na- 23(n,x)
E_n=7.01-8.02 MeV
φ=125°
80 ORL LA
ENDF-6
Cross section,mb/sr/MeV
E_γ,MeV

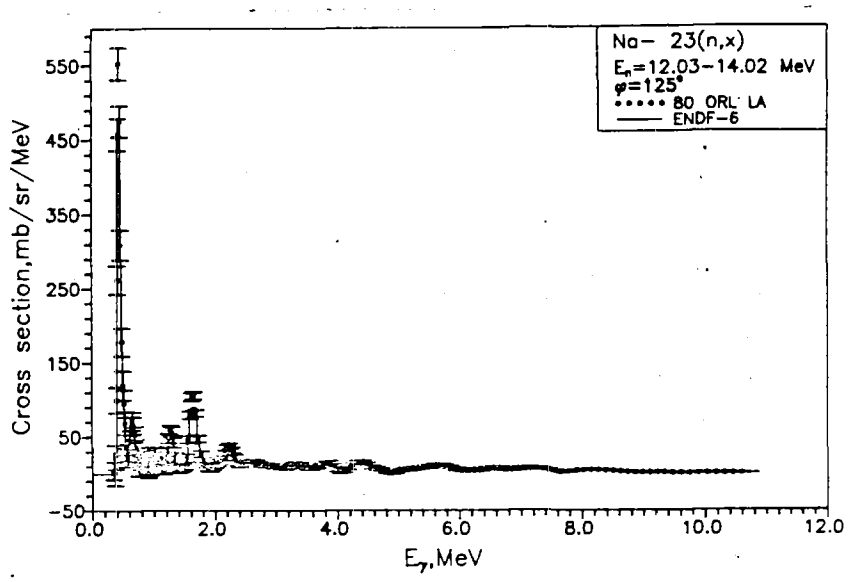
Na- 23(n,x)
E_n=12.03-14.02 MeV
φ=125°
80 ORL LA
ENDF-6
Cross section,mb/sr/MeV
E_γ,MeV

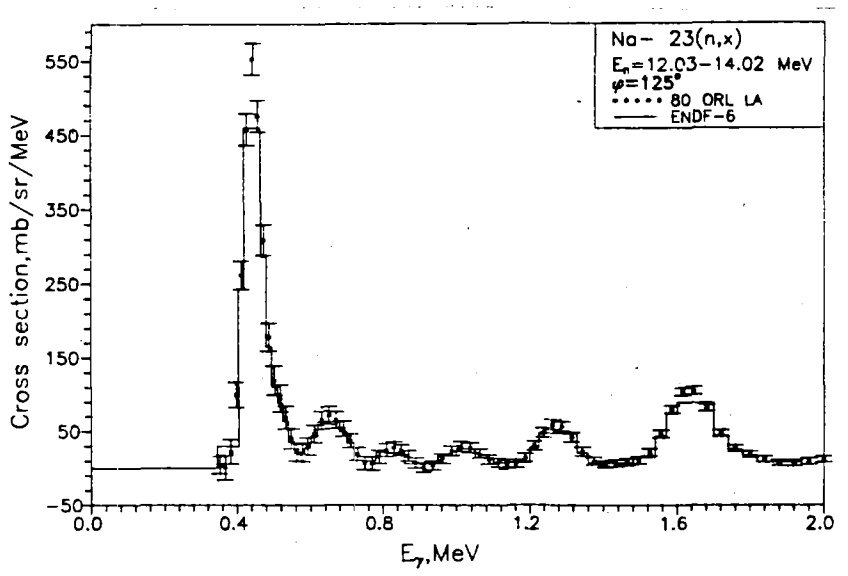
Na- 23(n,x)
E_n=12.03-14.02 MeV
φ=125°
80 ORL LA
ENDF-6
Cross section,mb/sr/MeV
E_γ,MeV

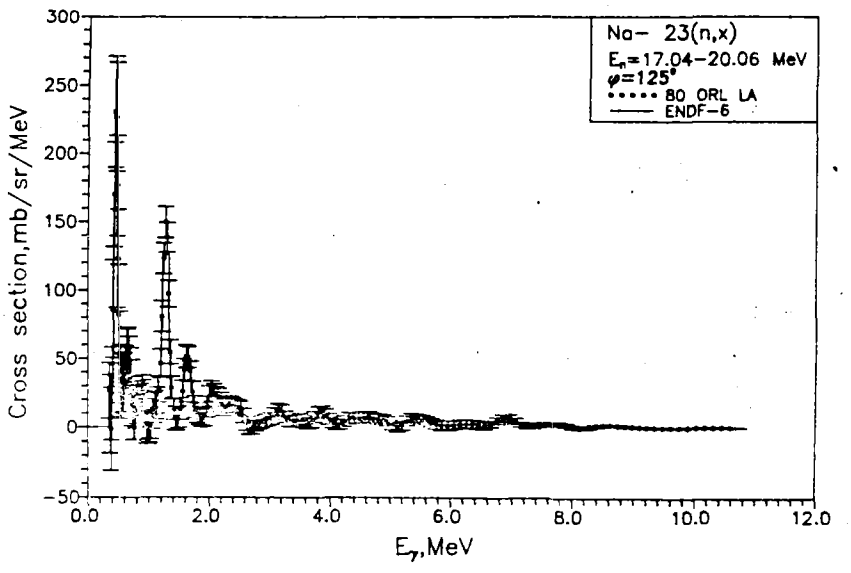
Na- 23(n,x)
E_n=17.04-20.06 MeV
φ=125°
80 ORL LA
ENDF-6
Cross section,mb/sr/MeV
E_γ,MeV

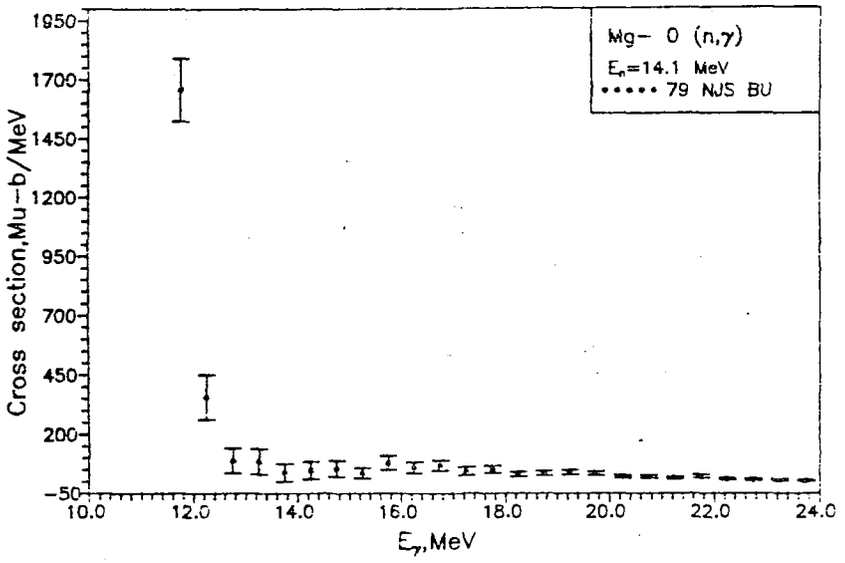
Mg- 0 (n,γ)
E_n=14.1 MeV
79 NJS BU
Cross section,Mu-b/MeV
E_γ,MeV

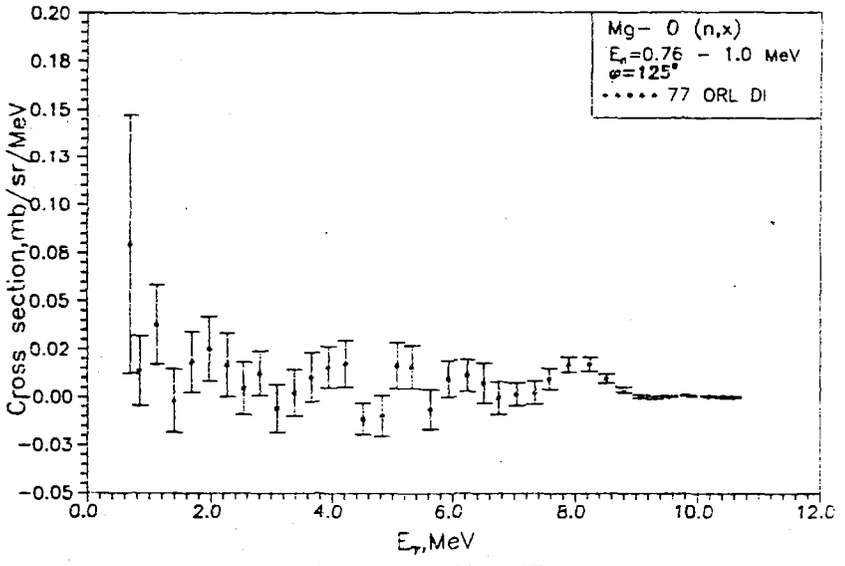
Mg- 0 (n,x)
E_n=0.76 - 1.0 MeV
φ=125°
77 ORL DI
Cross section,mb/sr/MeV
E_γ,MeV

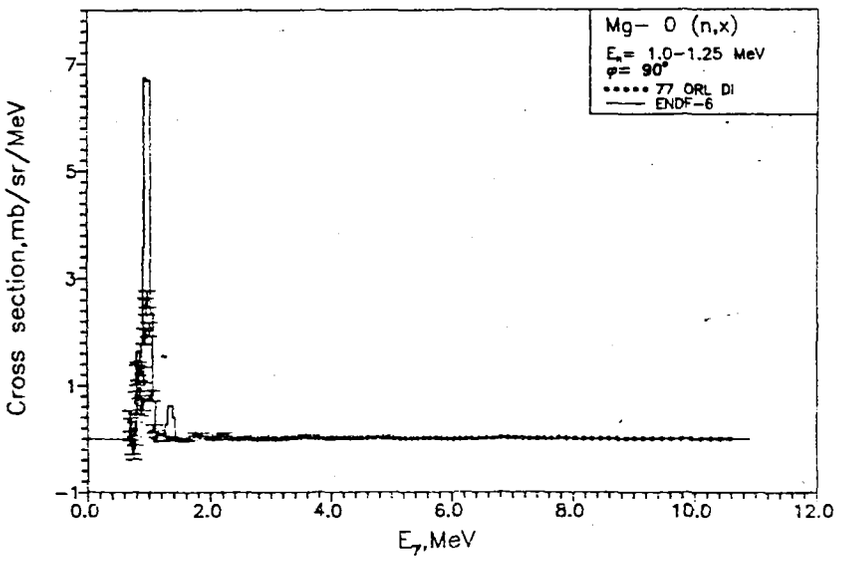
Mg- 0 (n,x)
E_n= 1.0-1.25 MeV
φ= 90°
77 ORL DI
ENDF-6
Cross section,mb/sr/MeV
E_γ,MeV

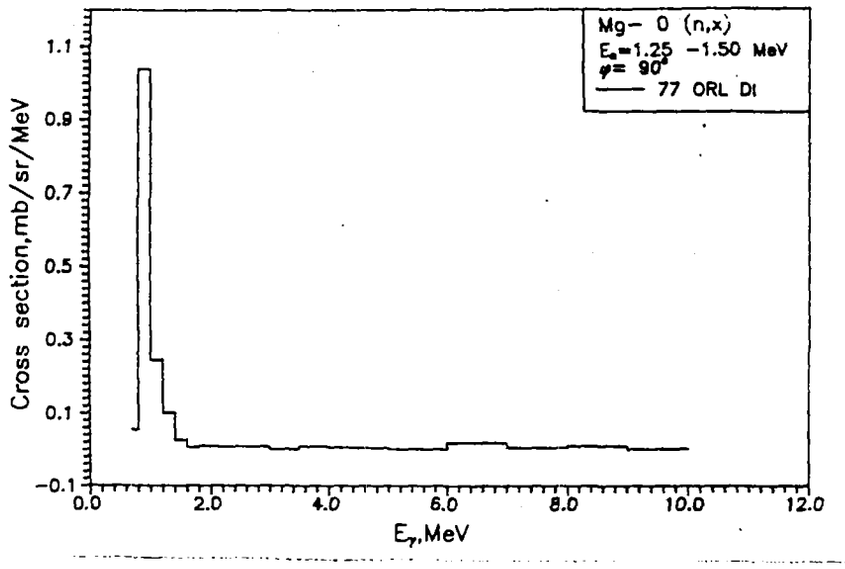
Mg– 0 (n,x)
E_n=1.25 –1.50 MeV
φ= 90°
77 ORL DI
Cross section,mb/sr/MeV
E_γ,MeV

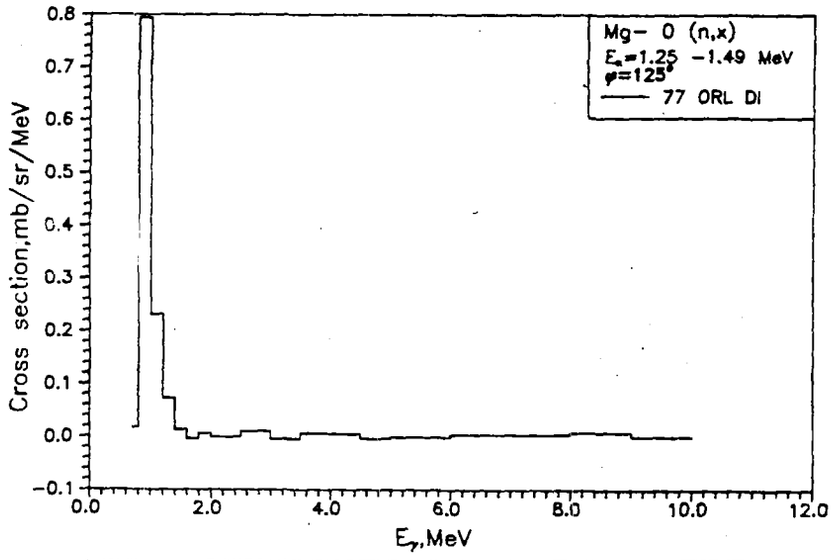
Mg– 0 (n,x)
E_n=1.25 –1.49 MeV
φ=125°
77 ORL DI
Cross section,mb/sr/MeV
E_γ,MeV

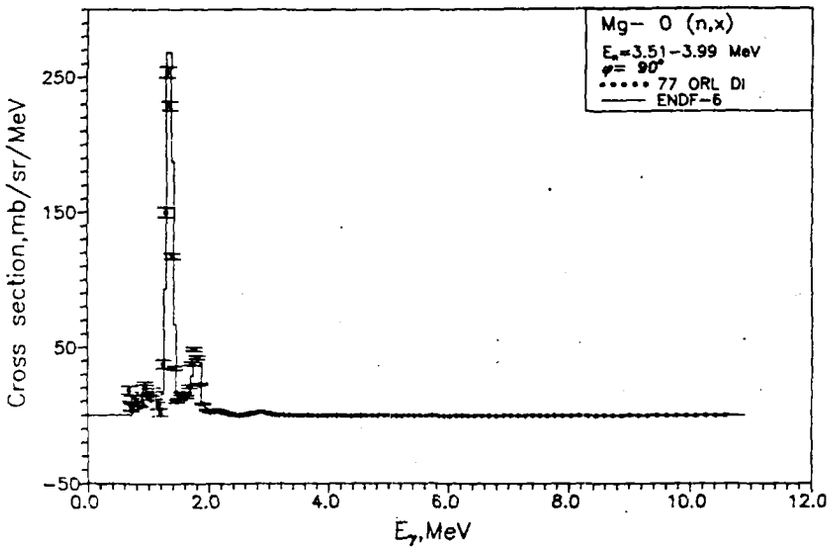
Mg– 0 (n,x)
E_n=3.51–3.99 MeV
φ= 90°
77 ORL DI
ENDF–6
Cross section,mb/sr/MeV
E_γ,MeV

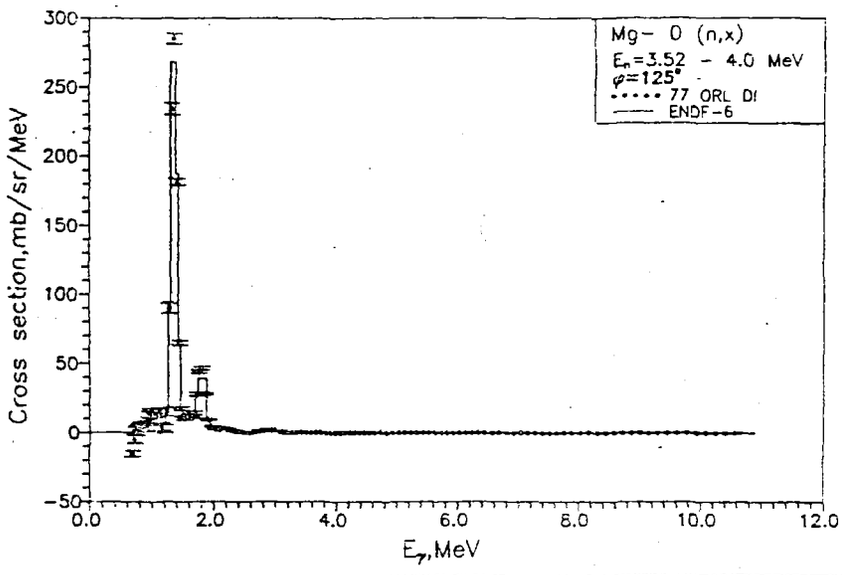
Mg- 0 (n,x)
E_n=3.52 - 4.0 MeV
φ=125°
77 ORL DI
ENDF-6
Cross section,mb/sr/MeV
E_γ,MeV

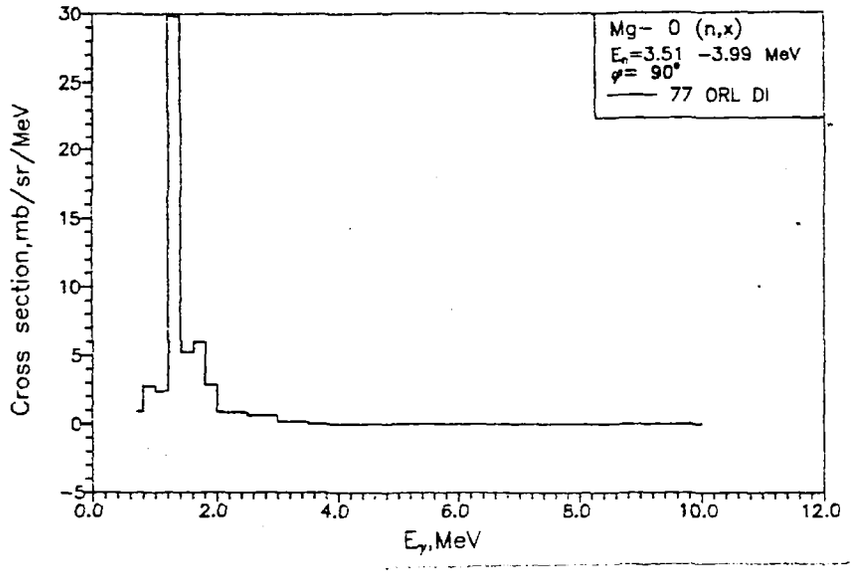
Mg- 0 (n,x)
E_n=3.51 -3.99 MeV
φ= 90°
77 ORL DI
Cross section,mb/sr/MeV
E_γ,MeV

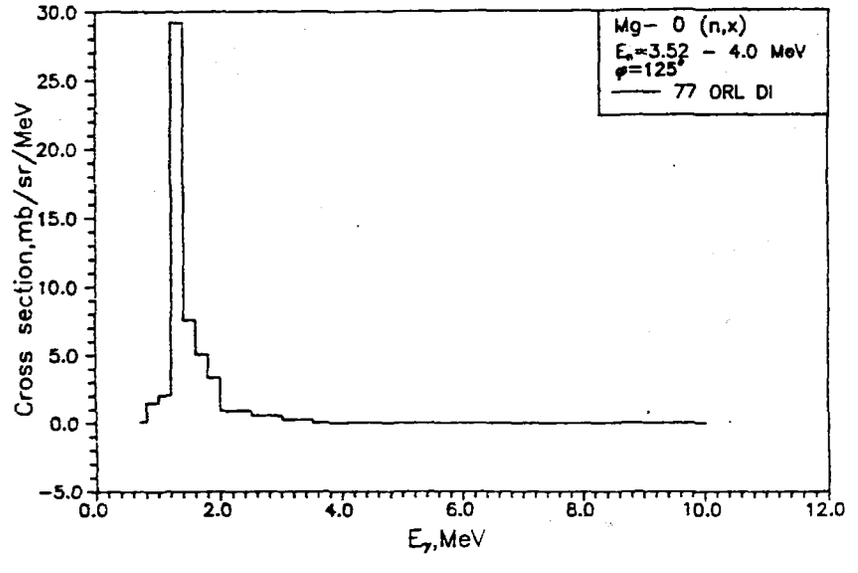
Mg- 0 (n,x)
E_n=3.52 - 4.0 MeV
φ=125°
77 ORL DI
Cross section,mb/sr/MeV
E_γ,MeV

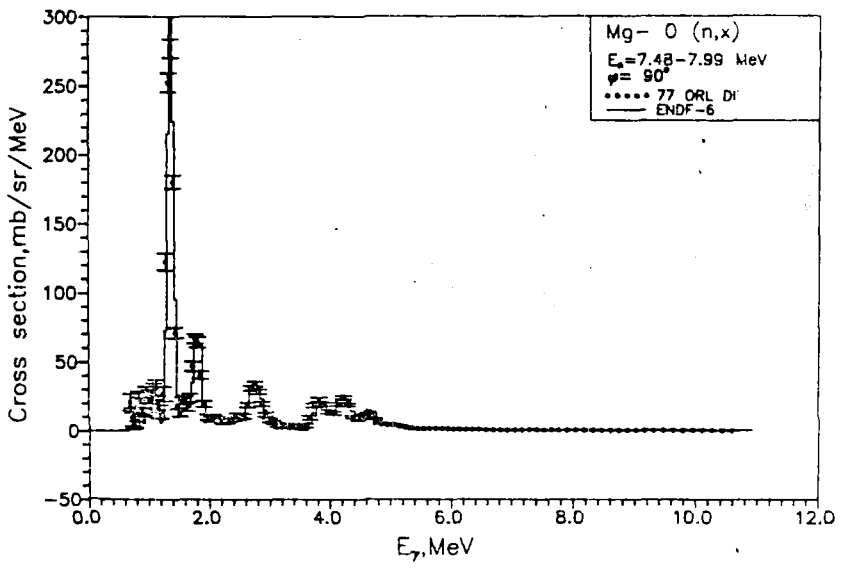
Mg- 0 (n,x)
E_n=7.48-7.99 MeV
φ= 90°
77 ORL DI
ENDF-6
Cross section,mb/sr/MeV
E_γ,MeV

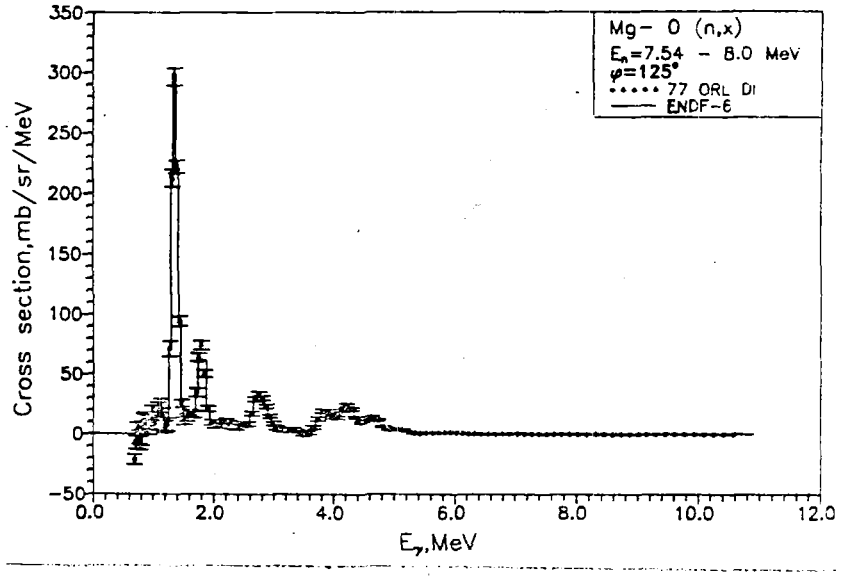
Mg- 0 (n,x)
E_n=7.54 - 8.0 MeV
φ=125°
77 ORL DI
ENDF-6
Cross section,mb/sr/MeV
E_γ,MeV

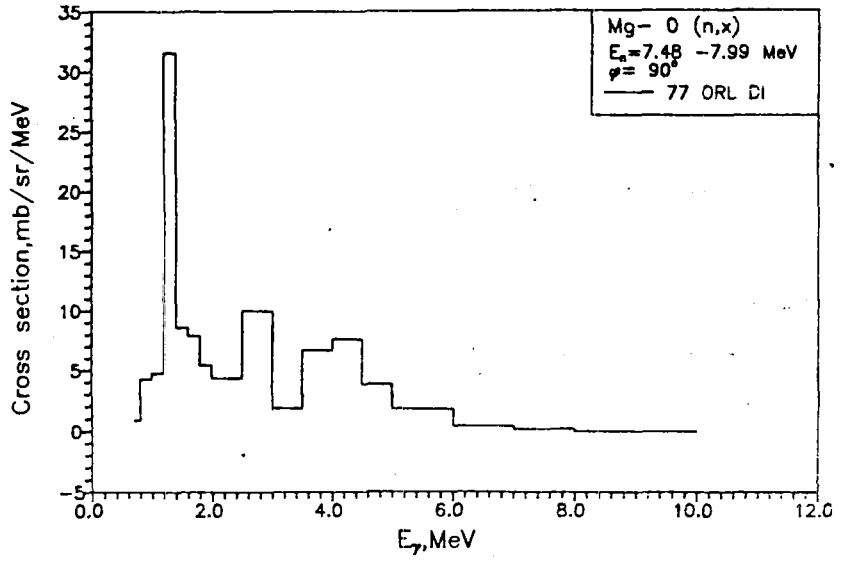
Mg- 0 (n,x)
E_n=7.48 -7.99 MeV
φ= 90°
77 ORL DI
Cross section,mb/sr/MeV
E_γ,MeV

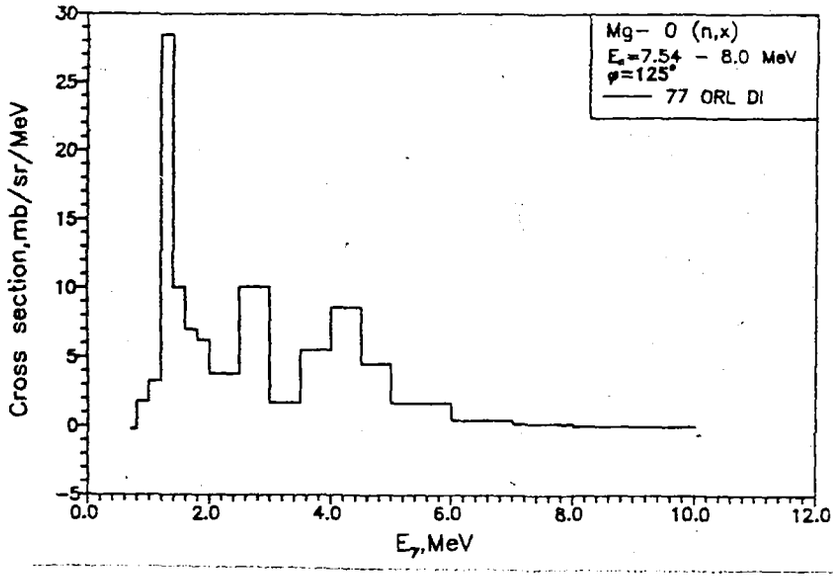
Mg– 0 (n,x)
E_n=7.54 – 8.0 MeV
φ=125°
77 ORL DI
Cross section,mb/sr/MeV
E_γ,MeV

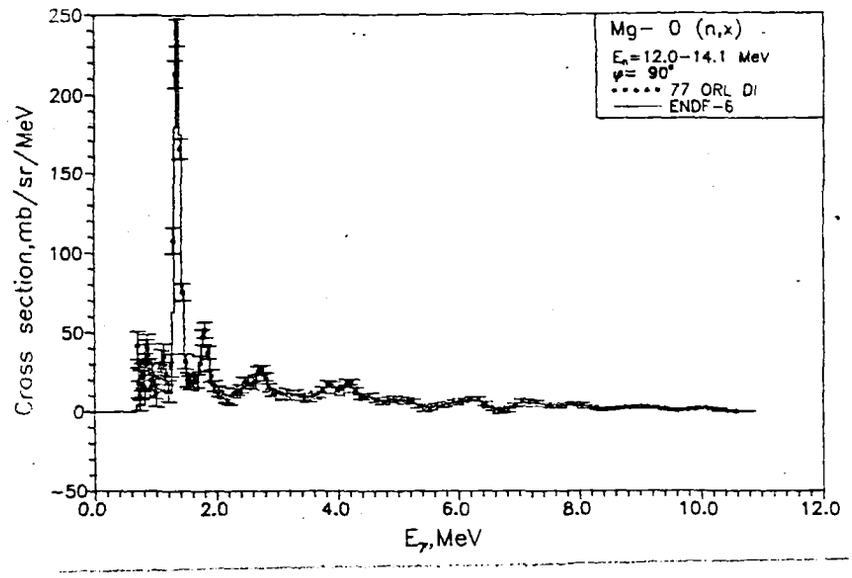
Mg– 0 (n,x)
E_n=12.0–14.1 MeV
φ= 90°
77 ORL DI
ENDF–6
Cross section,mb/sr/MeV
E_γ,MeV

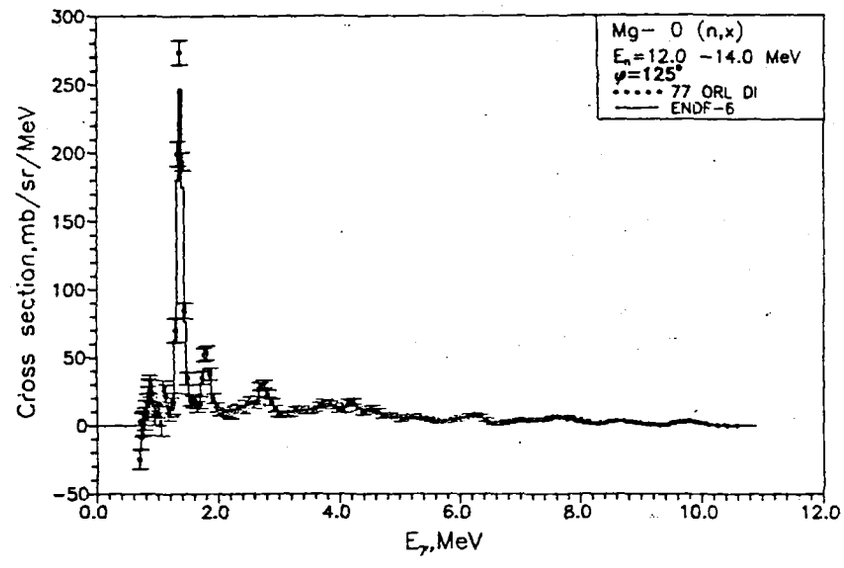
Mg– 0 (n,x)
E_n=12.0 –14.0 MeV
φ=125°
77 ORL DI
ENDF–6
Cross section,mb/sr/MeV
E_γ,MeV

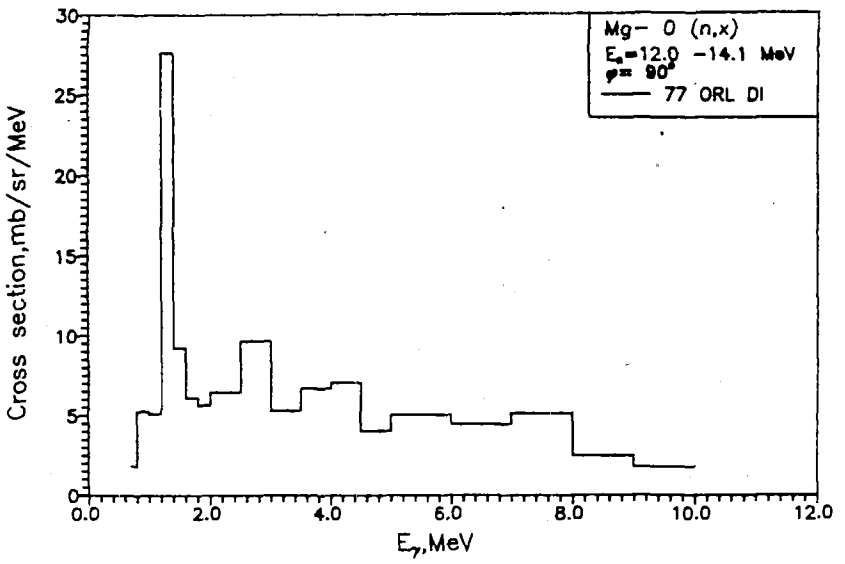
Mg- 0 (n,x)
E_n=12.0 -14.1 MeV
φ= 90°
77 ORL DI
Cross section,mb/sr/MeV
E_γ,MeV

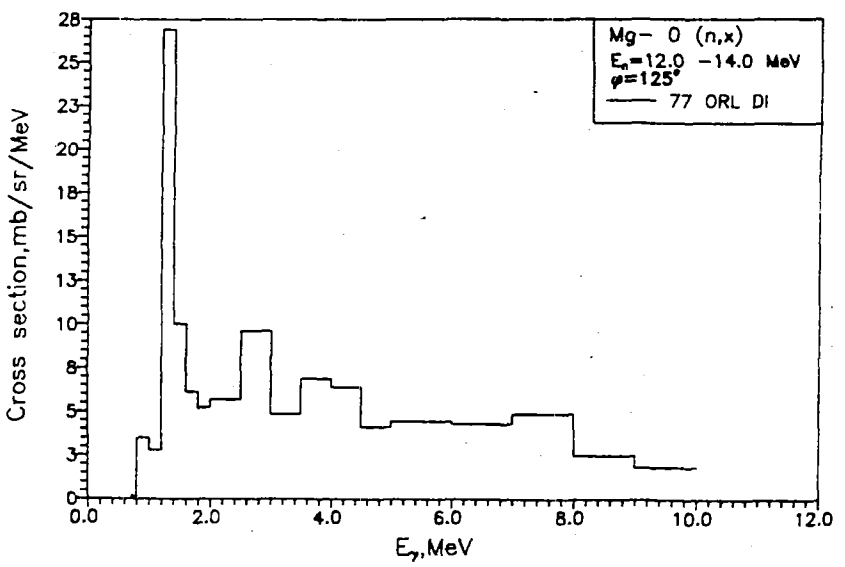
Mg- 0 (n,x)
E_n=12.0 -14.0 MeV
φ=125°
77 ORL DI
Cross section,mb/sr/MeV
E_γ,MeV

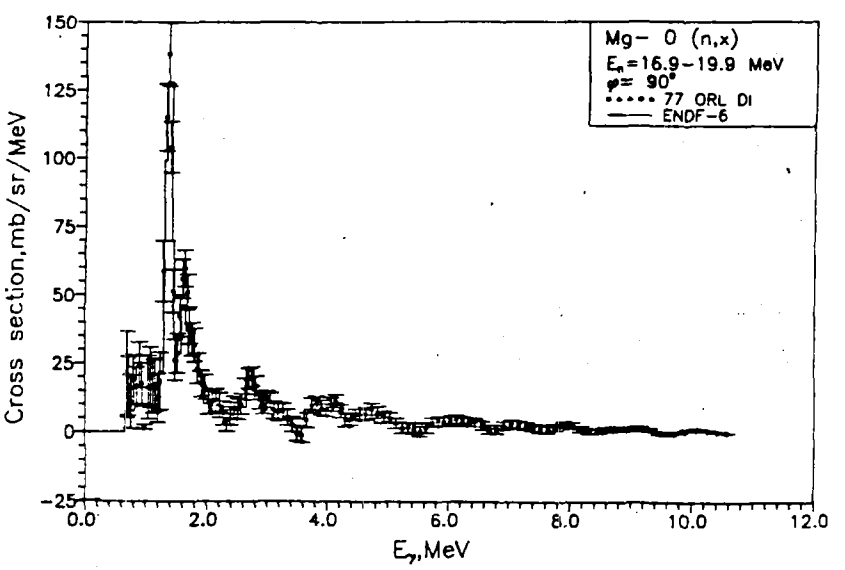
Mg- 0 (n,x)
E_n=16.9-19.9 MeV
φ= 90°
77 ORL DI
ENDF-6
Cross section,mb/sr/MeV
E_γ,MeV

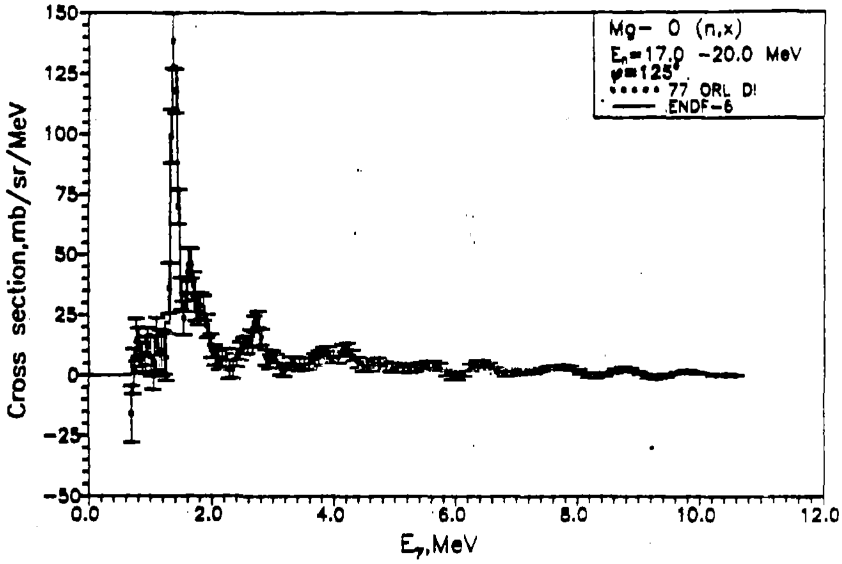
Mg- 0 (n,x)
E_n=17.0 -20.0 MeV
φ=125°
77 ORL DI
ENDF-6
Cross section,mb/sr/MeV
E_γ,MeV

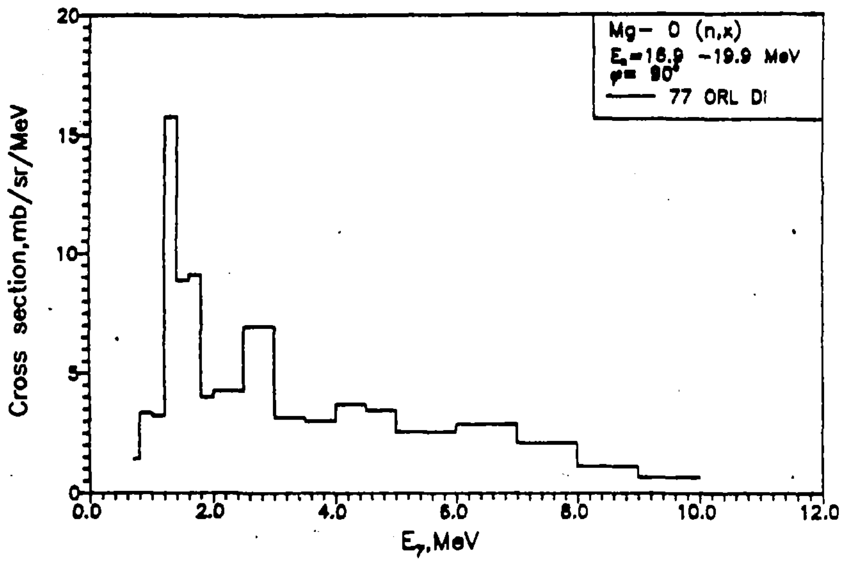
Mg- 0 (n,x)
E_n=16.9 -19.9 MeV
φ= 90°
77 ORL DI
Cross section,mb/sr/MeV
E_γ,MeV

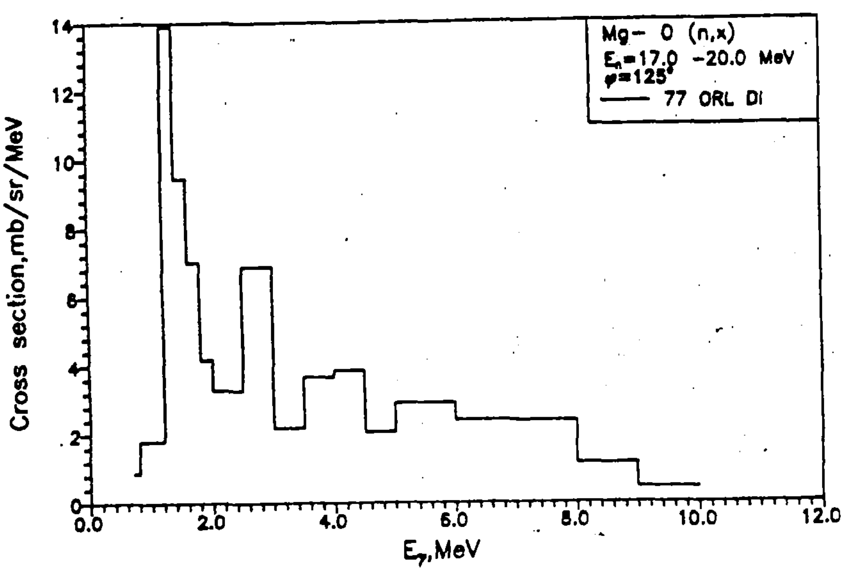
Mg- 0 (n,x)
E_n=17.0 -20.0 MeV
φ=125°
77 ORL DI
Cross section,mb/sr/MeV
E_γ,MeV

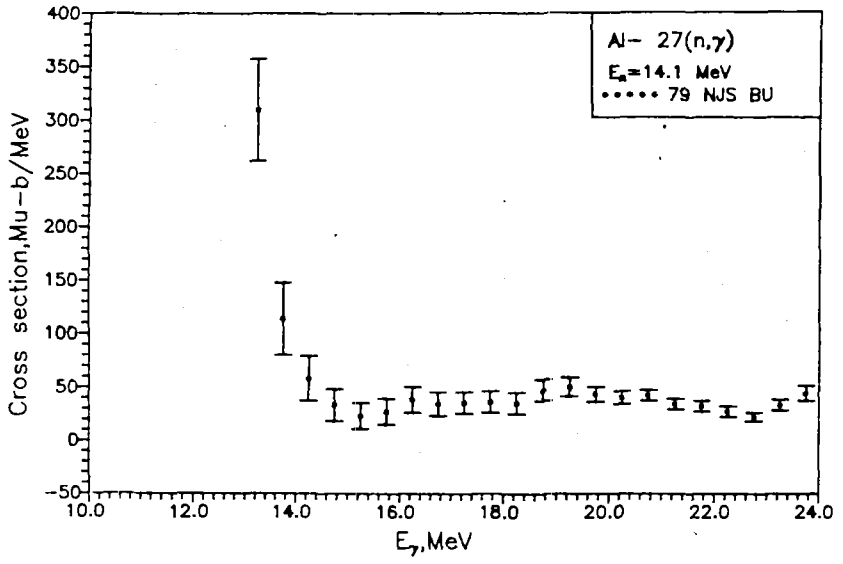
Al- 27(n,γ)
E_n=14.1 MeV
79 NJS BU
Cross section,Mu-b/MeV
E_γ,MeV

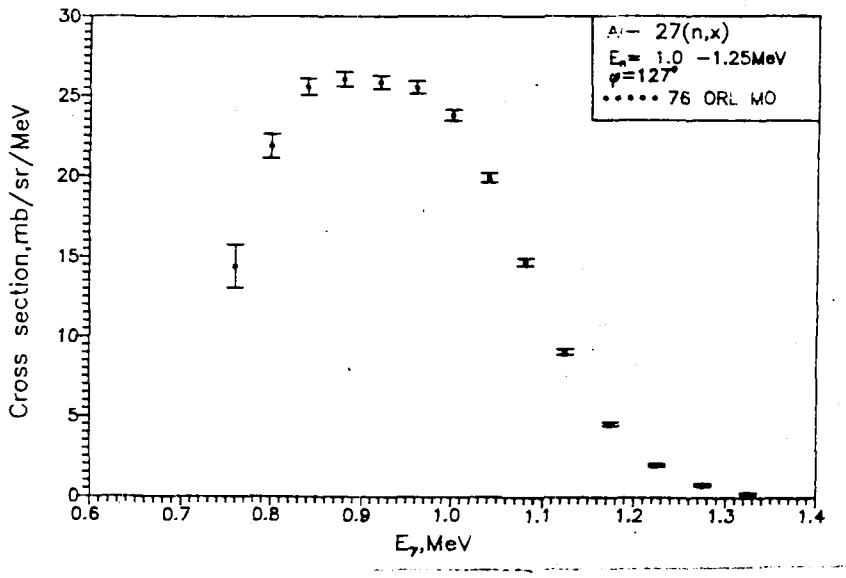
Al- 27(n,x)
E_n= 1.0 -1.25MeV
φ=127°
76 ORL MO
Cross section,mb/sr/MeV
E_γ,MeV

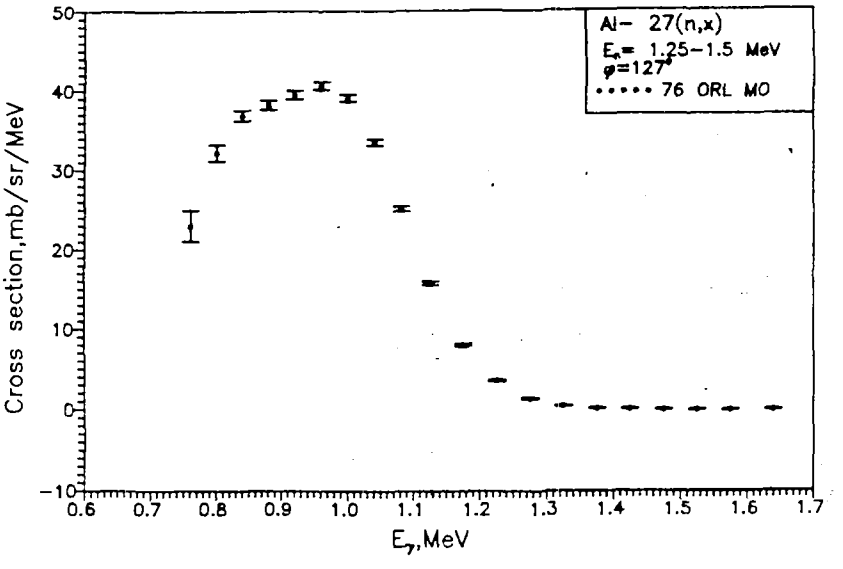
Al- 27(n,x)
E_n= 1.25-1.5 MeV
φ=127°
76 ORL MO
Cross section,mb/sr/MeV
E_γ,MeV

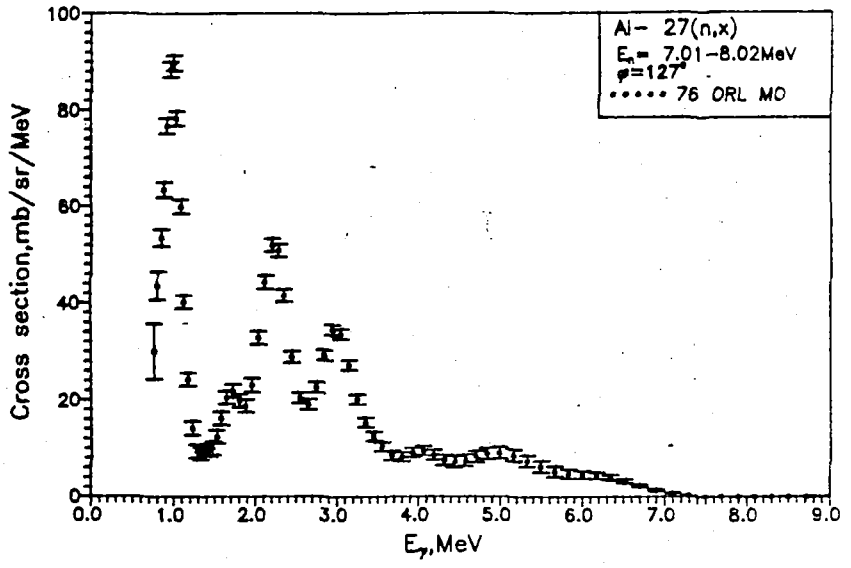
Al- 27(n,x)
E_n= 7.01-8.02MeV
φ=127°
••••• 76 ORL MO
Cross section,mb/sr/MeV
E_γ,MeV

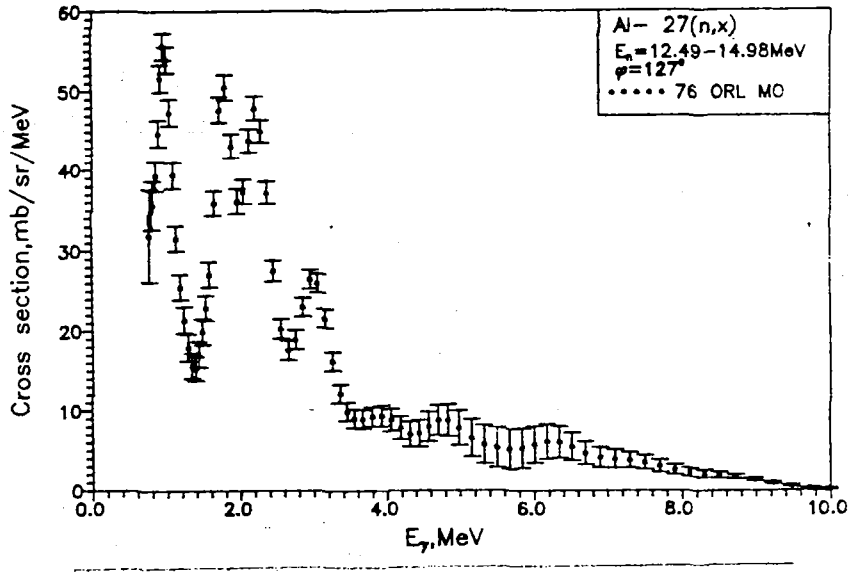
Al- 27(n,x)
E_n=12.49-14.98MeV
φ=127°
••••• 76 ORL MO
Cross section,mb/sr/MeV
E_γ,MeV

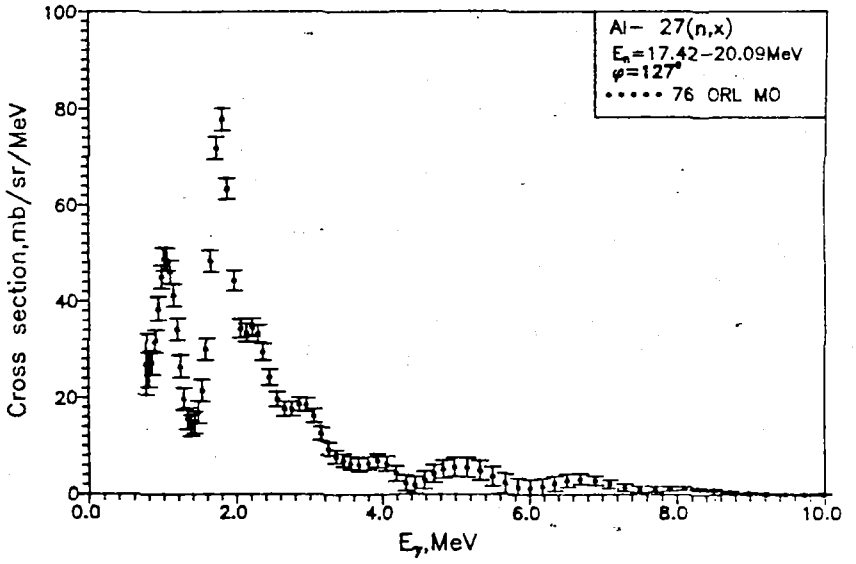
Al- 27(n,x)
E_n=17.42-20.09MeV
φ=127°
••••• 76 ORL MO
Cross section,mb/sr/MeV
E_γ,MeV

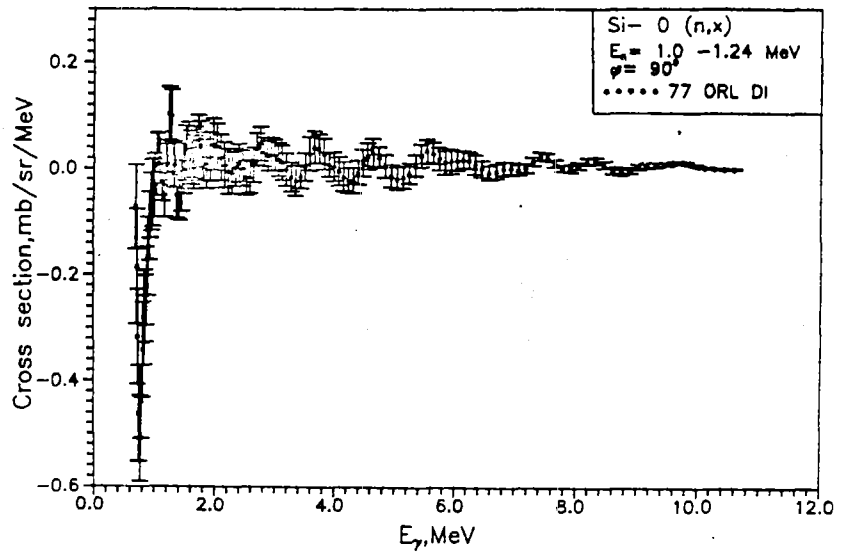
Si- 0 (n,x)
E_n= 1.0 -1.24 MeV
φ= 90°
••••• 77 ORL DI
Cross section,mb/sr/MeV
E_γ,MeV

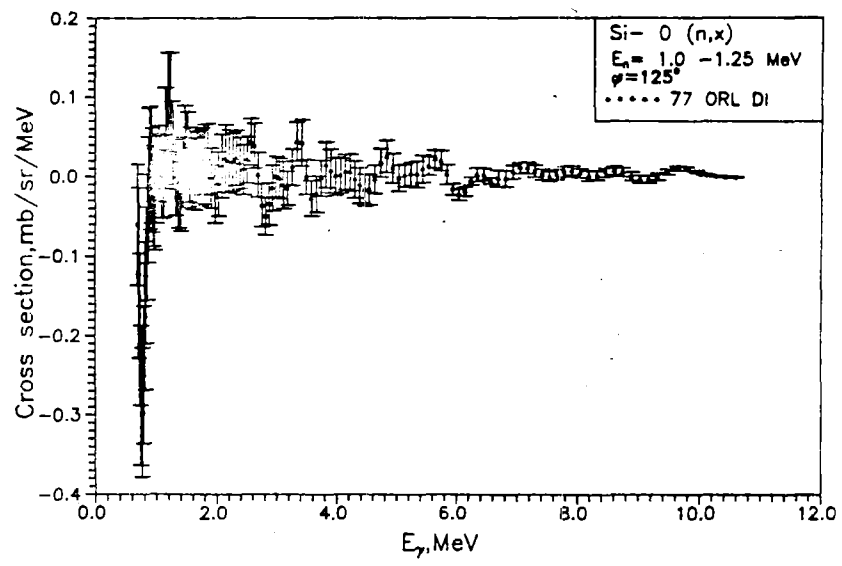
Si- 0 (n,x)
E_n= 1.0 -1.25 MeV
φ=125°
••••• 77 ORL DI
Cross section,mb/sr/MeV
E_γ,MeV

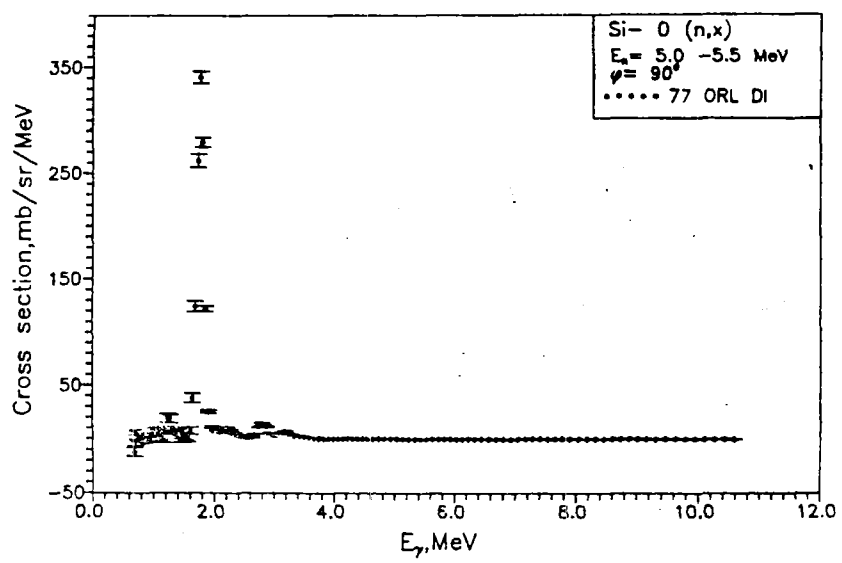
Si- 0 (n,x)
E_n= 5.0 -5.5 MeV
φ= 90°
••••• 77 ORL DI
Cross section,mb/sr/MeV
E_γ,MeV

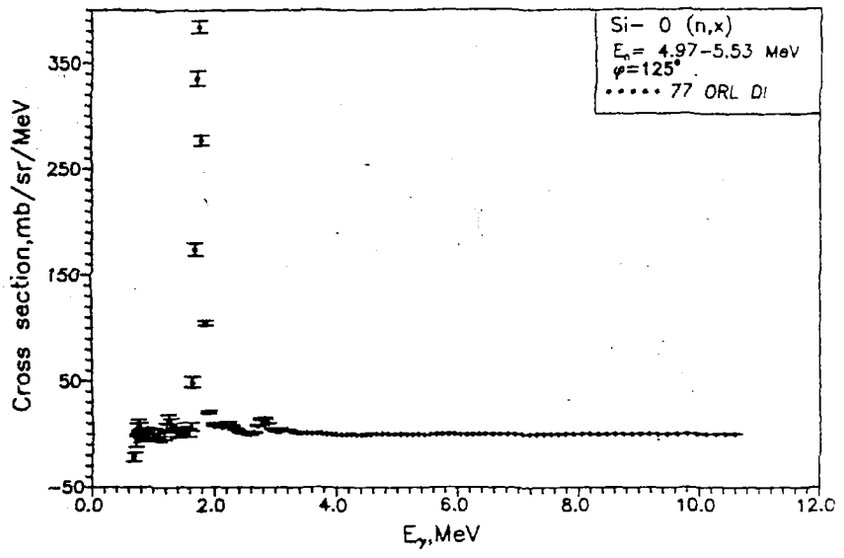
Si- O (n,x)
E_n= 4.97-5.53 MeV
φ=125°
77 ORL DI
Cross section,mb/sr/MeV
E_γ,MeV

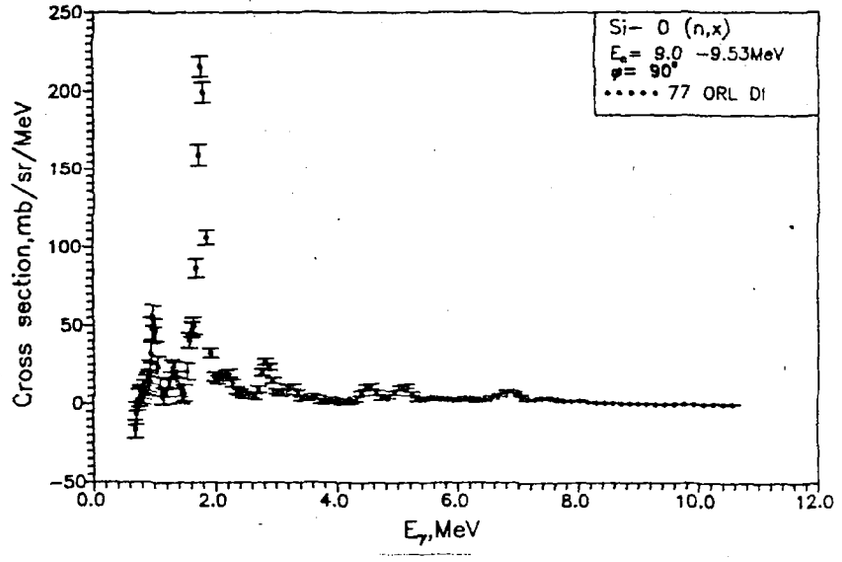
Si- O (n,x)
E_n= 9.0 -9.53MeV
φ= 90°
77 ORL DI
Cross section,mb/sr/MeV
E_γ,MeV

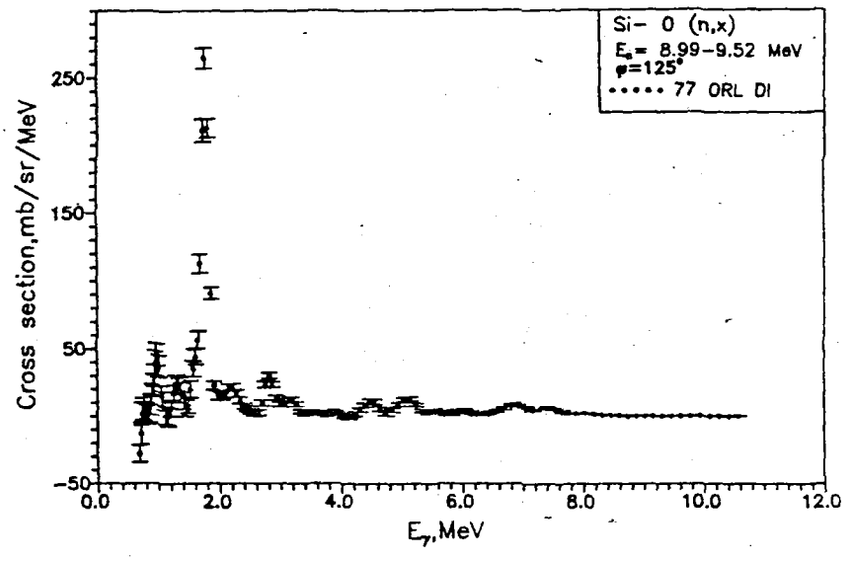
Si- O (n,x)
E_n= 8.99-9.52 MeV
φ=125°
77 ORL DI
Cross section,mb/sr/MeV
E_γ,MeV

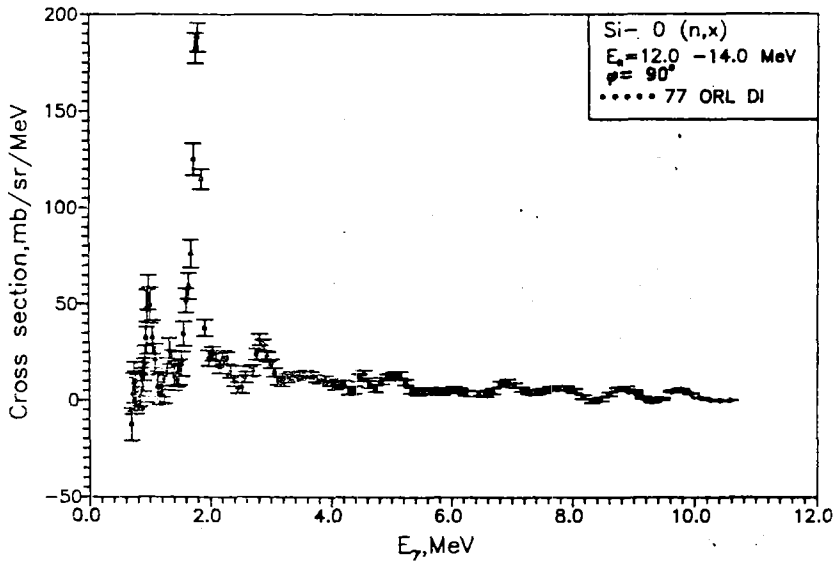
Si- 0 (n,x)
E_n=12.0 -14.0 MeV
φ= 90°
••••• 77 ORL DI
Cross section,mb/sr/MeV
E_γ,MeV

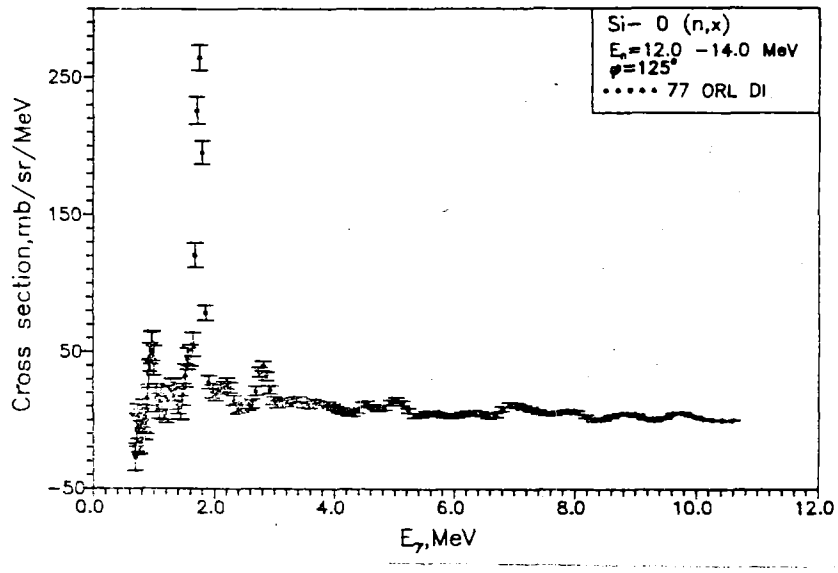
Si- 0 (n,x)
E_n=12.0 -14.0 MeV
φ=125°
••••• 77 ORL DI
Cross section,mb/sr/MeV
E_γ,MeV

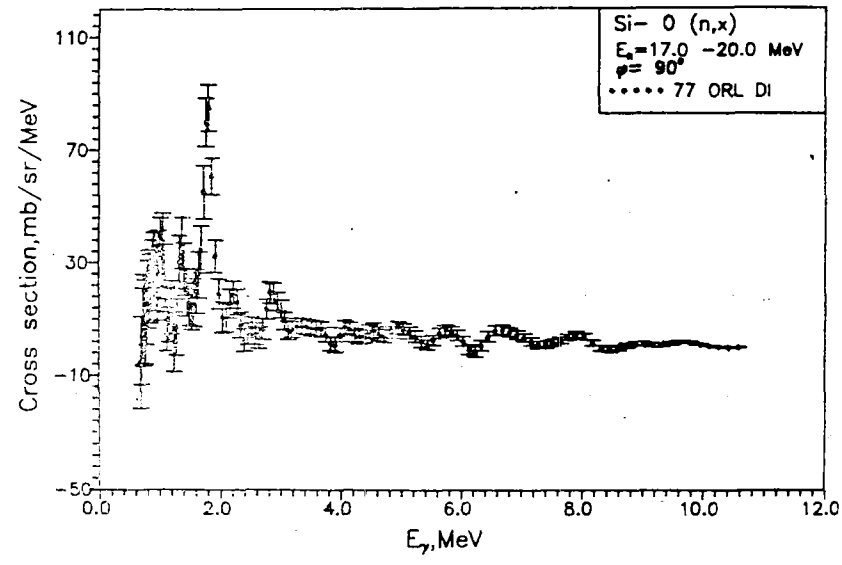
Si- 0 (n,x)
E_n=17.0 -20.0 MeV
φ= 90°
••••• 77 ORL DI
Cross section,mb/sr/MeV
E_γ,MeV

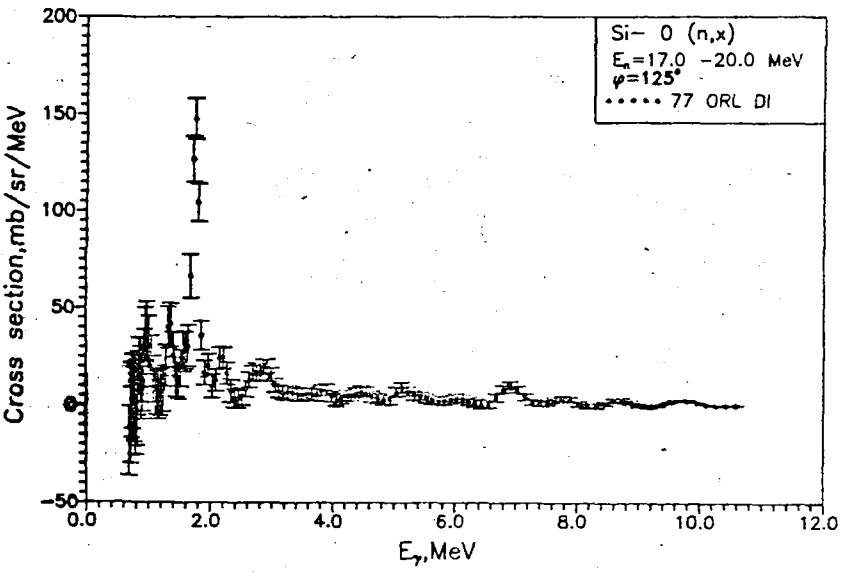
Si- 0 (n,x)
E_n=17.0 -20.0 MeV
φ=125°
77 ORL DI
Cross section,mb/sr/MeV
E_γ,MeV

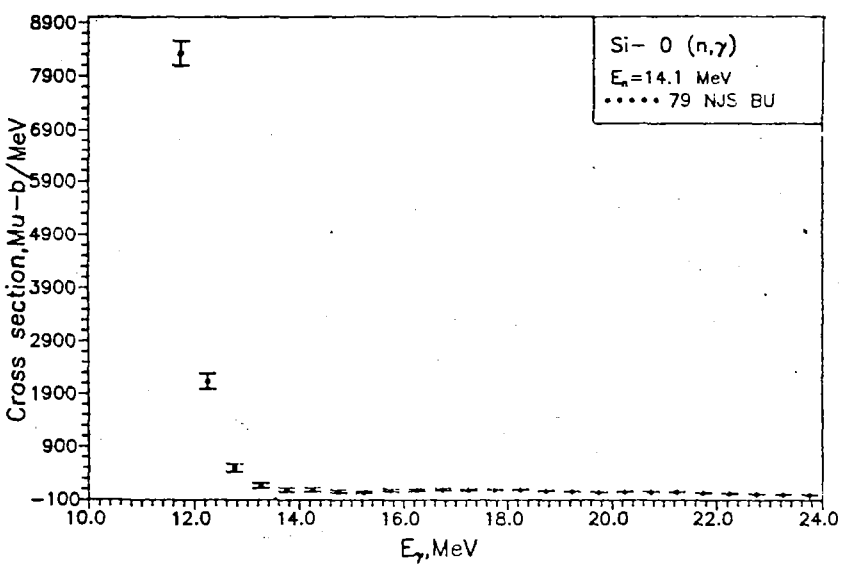
Si- 0 (n,γ)
E_n=14.1 MeV
79 NJS BU
Cross section,Mu-b/MeV
E_γ,MeV

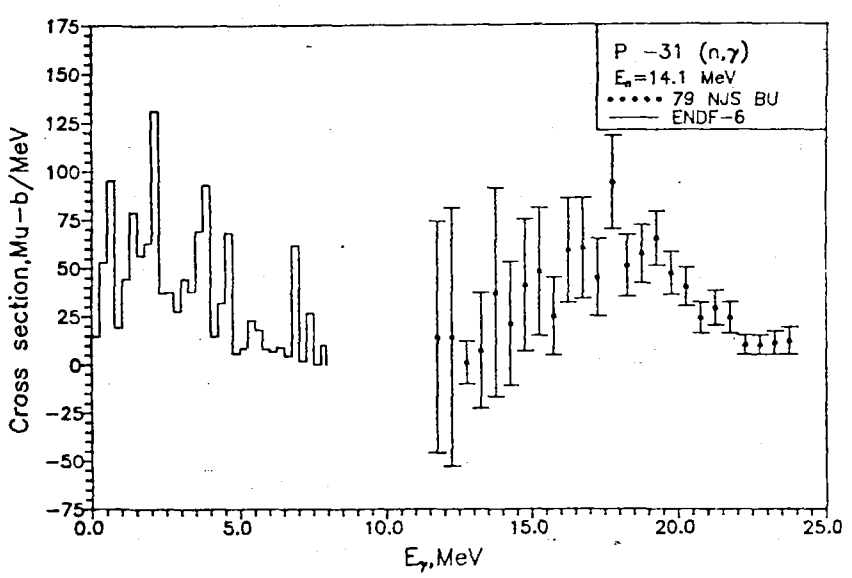
P -31 (n,γ)
E_n=14.1 MeV
79 NJS BU
ENDF-6
Cross section,Mu-b/MeV
E_γ,MeV

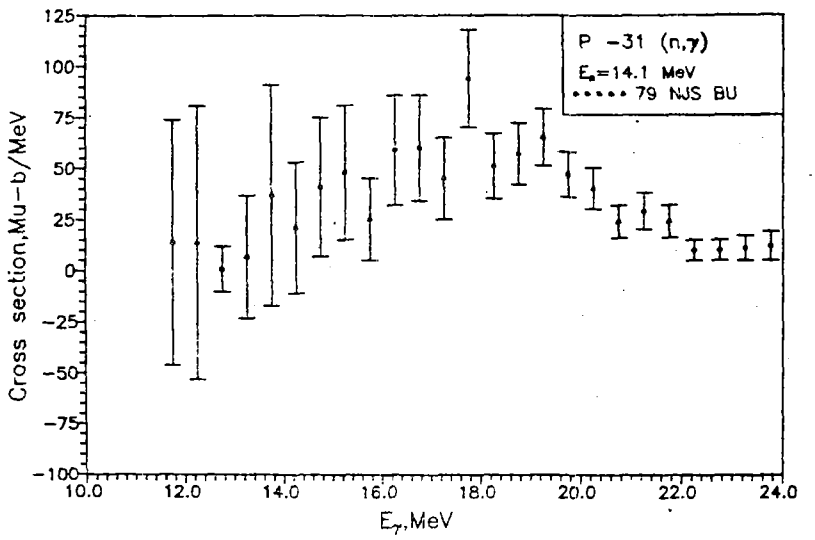
P -31 (n,γ)
E_n=14.1 MeV
79 NJS BU
Cross section,Mu-b/MeV
E_γ,MeV

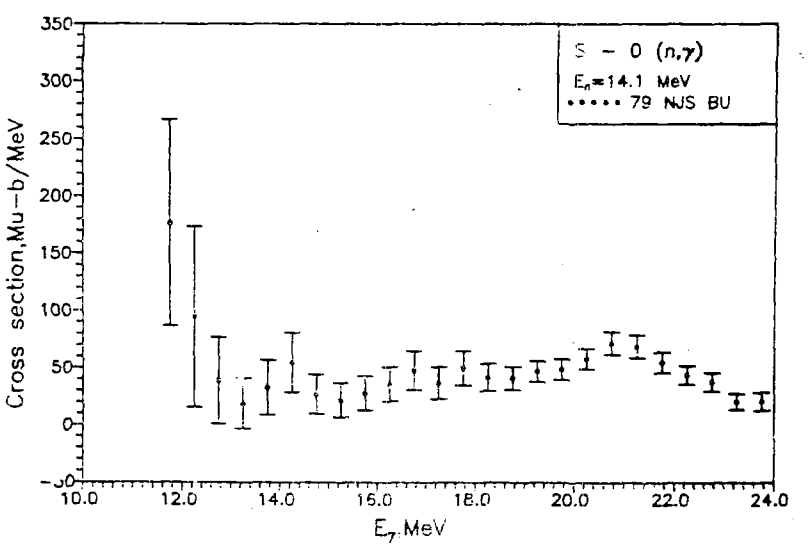
S - 0 (n,γ)
E_n=14.1 MeV
79 NJS BU
Cross section,Mu-b/MeV
E_γ,MeV

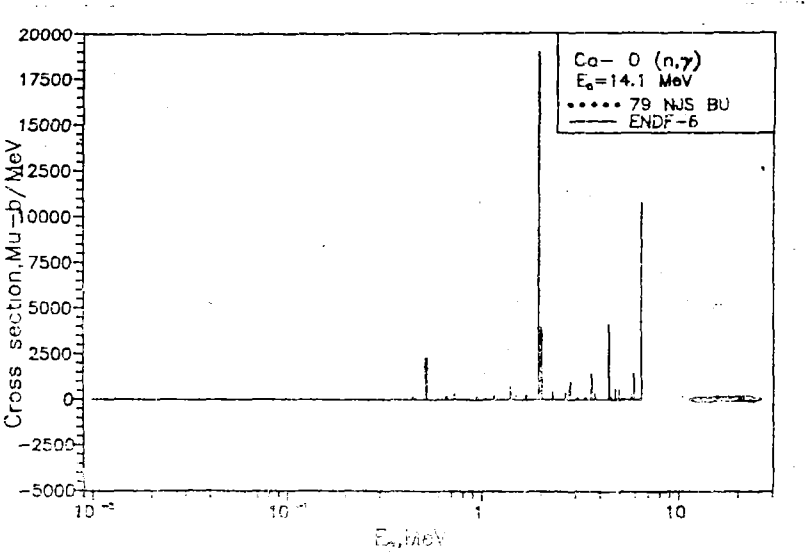
Co- 0 (n,γ)
E_n=14.1 MeV
79 NJS BU
ENDF-6
Cross section,Mu-b/MeV
E_γ,MeV

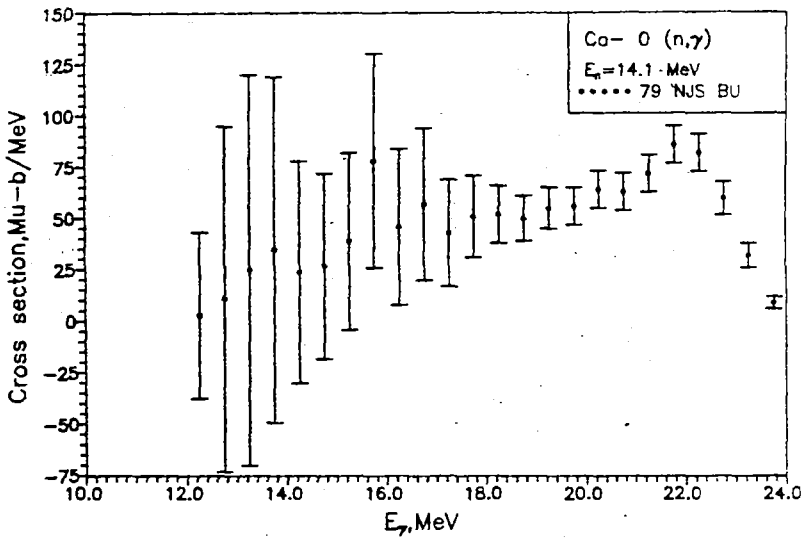
Ca- O (n,γ)
E_n=14.1 MeV
79 NJS BU
Cross section,Mu-b/MeV
E_γ,MeV

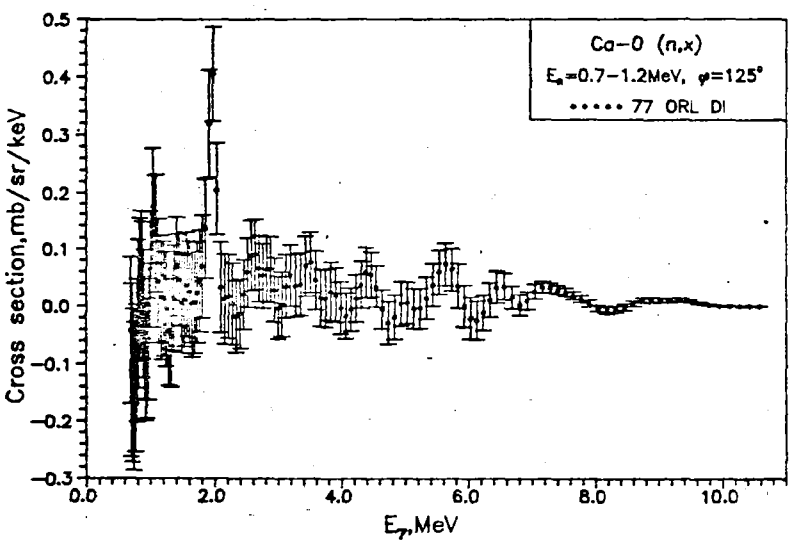
Ca-O (n,x)
E_n=0.7-1.2MeV, φ=125°
77 ORL DI
Cross section,mb/sr/keV
E_γ,MeV

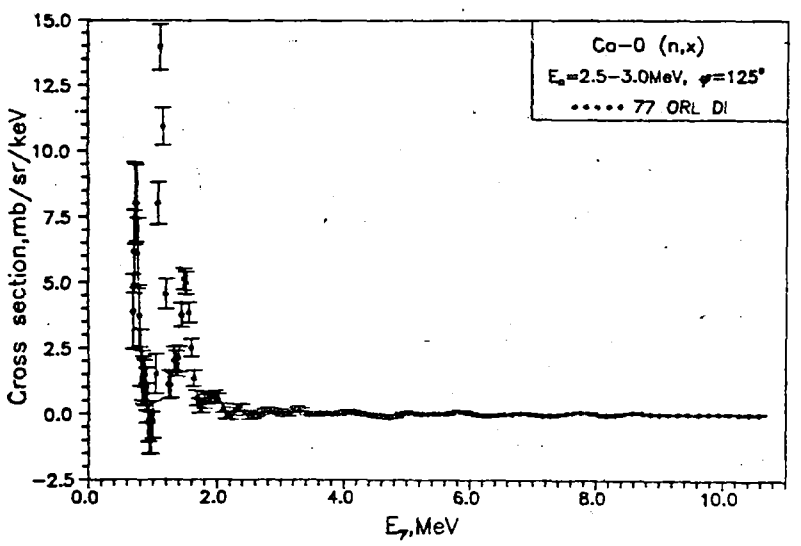
Ca-O (n,x)
E_n=2.5-3.0MeV, φ=125°
77 ORL DI
Cross section,mb/sr/keV
E_γ,MeV

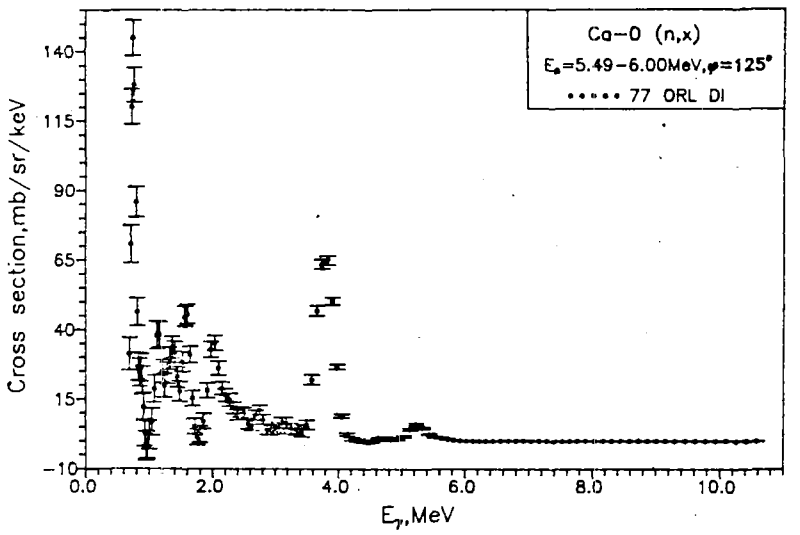
Ca-O (n,x)
E_n=5.49-6.00MeV,φ=125°
••••• 77 ORL DI
Cross section,mb/sr/keV
E_γ,MeV

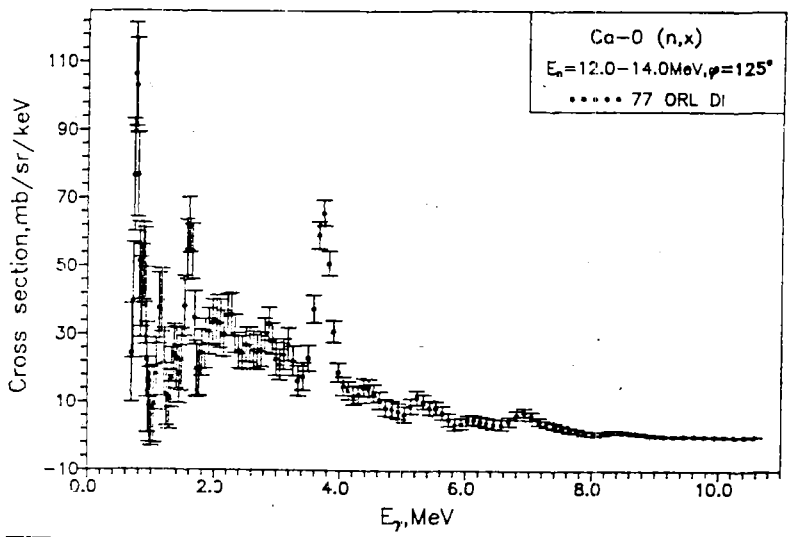
Ca-O (n,x)
E_n=12.0-14.0MeV,φ=125°
••••• 77 ORL DI
Cross section,mb/sr/keV
E_γ,MeV

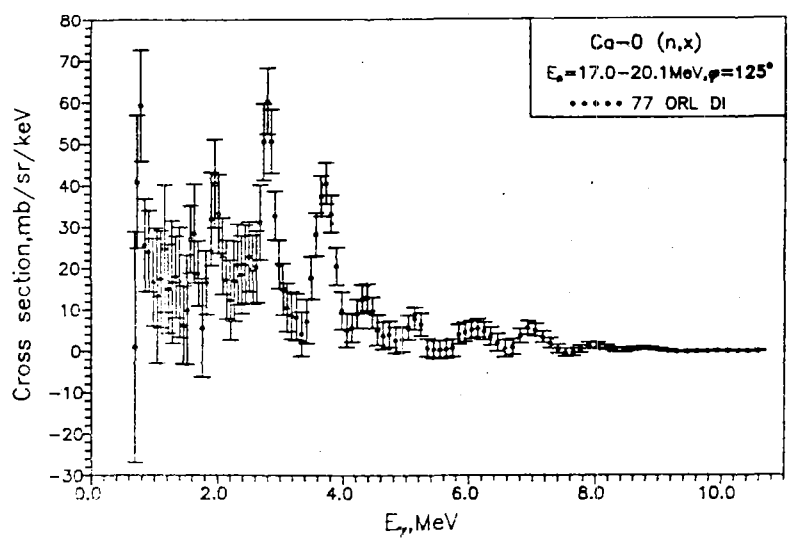
Ca-O (n,x)
E_n=17.0-20.1MeV,φ=125°
••••• 77 ORL DI
Cross section,mb/sr/keV
E_γ,MeV

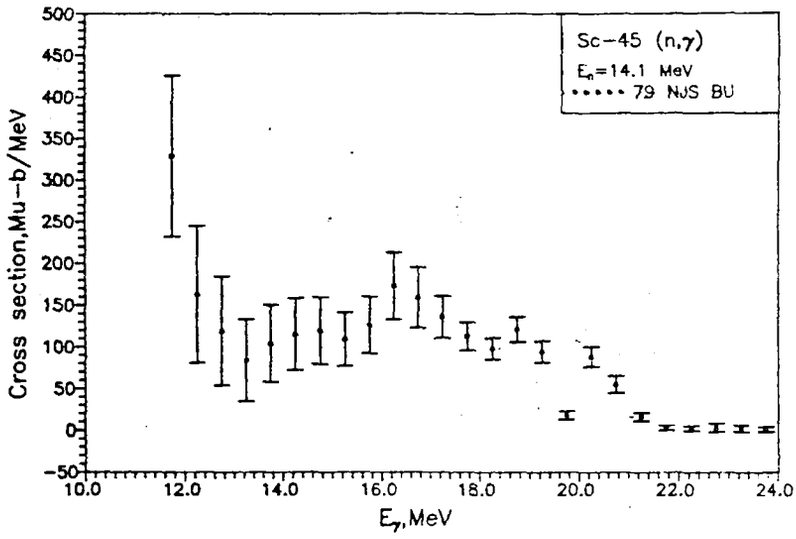
Sc-45 (n,γ)
E_n=14.1 MeV
79 NJS BU
Cross section,Mu-b/MeV
E_γ,MeV

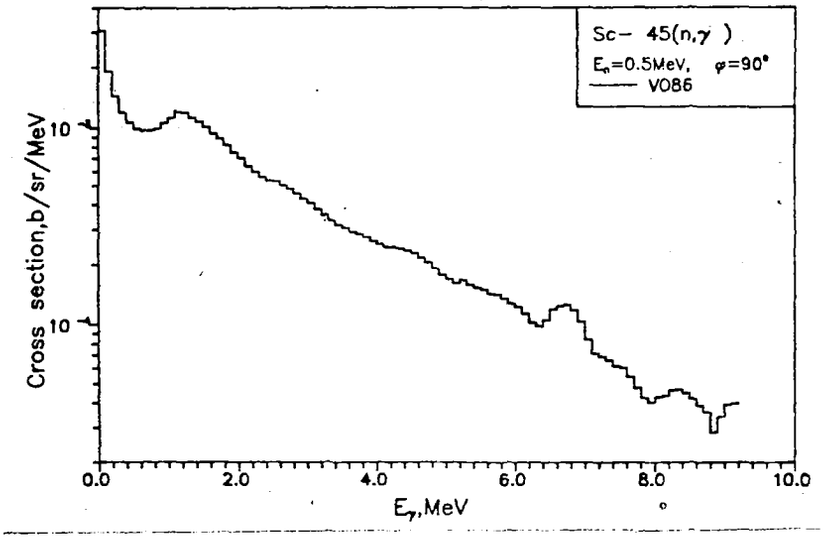
Sc- 45(n,γ)
E_n=0.5MeV, φ=90°
V086
Cross section,b/sr/MeV
E_γ,MeV

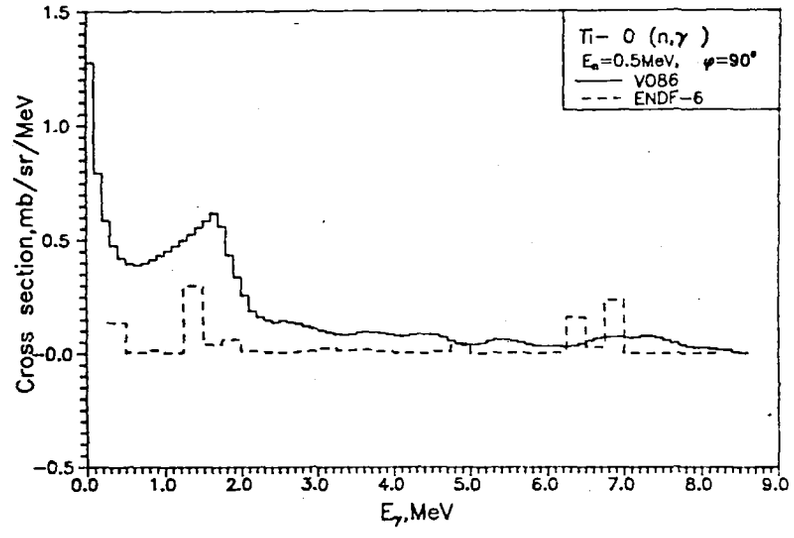
Ti- 0 (n,γ)
E_n=0.5MeV, φ=90°
V086
ENDF-6
Cross section,mb/sr/MeV
E_γ,MeV

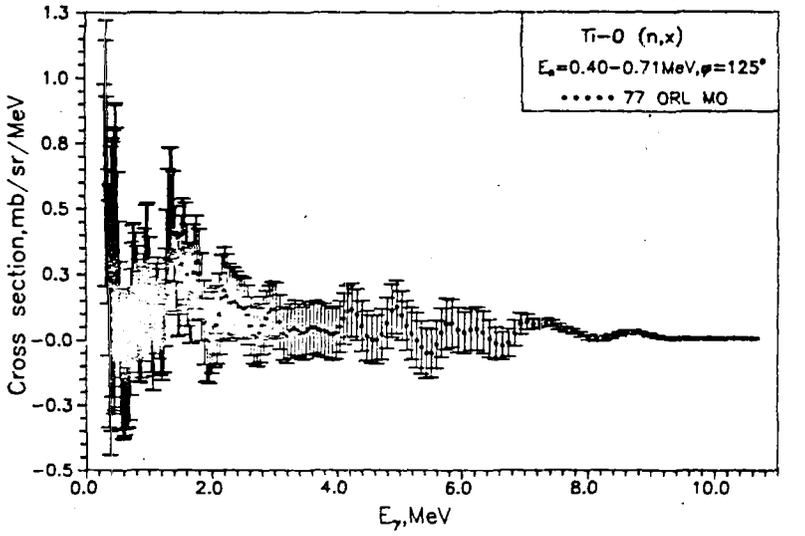
Ti-0 (n,x)
E_n=0.40-0.71MeV,φ=125°
77 ORL MO
Cross section,mb/sr/MeV
E_γ,MeV

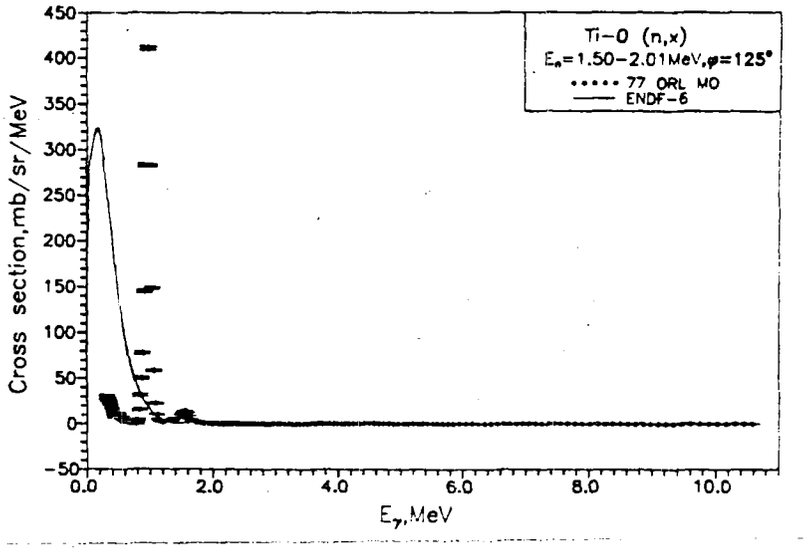
Ti-0 (n,x)
E_n=1.50-2.01MeV,φ=125°
77 ORL MO
ENDF-6
Cross section,mb/sr/MeV
E_γ,MeV

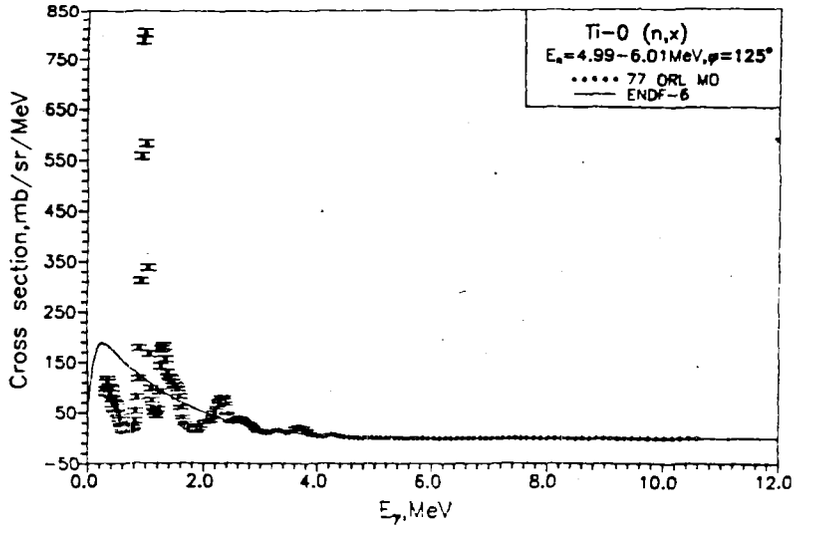
Ti-0 (n,x)
E_n=4.99-6.01MeV,φ=125°
77 ORL MO
ENDF-6
Cross section,mb/sr/MeV
E_γ,MeV

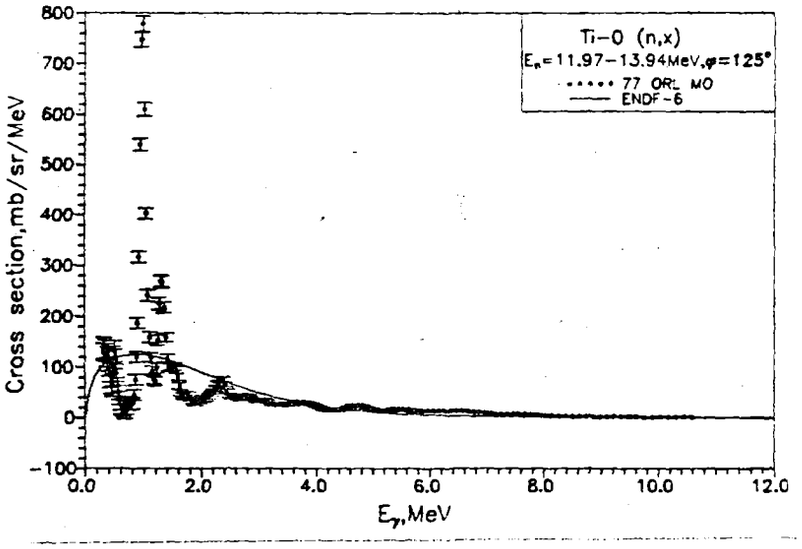
Ti-0 (n,x)
E_n=11.97-13.94MeV,φ=125°
77 ORL MO
ENDF-6
Cross section,mb/sr/MeV
E_γ,MeV

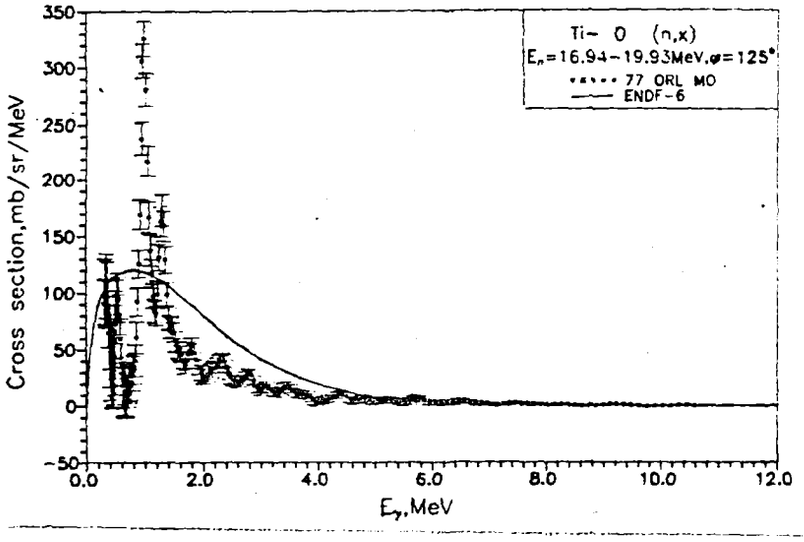
Ti- 0 (n,x)
E_n=16.94-19.93MeV,φ=125°
77 ORL MO
ENDF-6
Cross section,mb/sr/MeV
E_γ,MeV

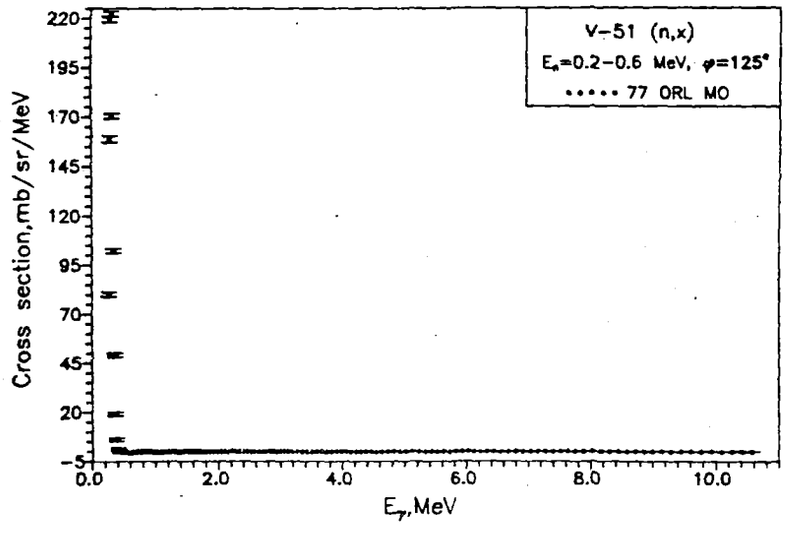
V-51 (n,x)
E_n=0.2-0.6 MeV, φ=125°
77 ORL MO
Cross section,mb/sr/MeV
E_γ,MeV

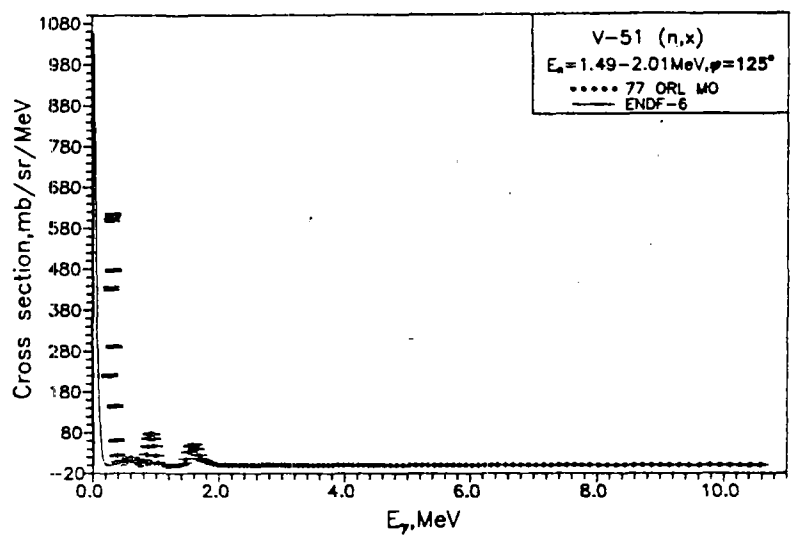
V-51 (n,x)
E_n=1.49-2.01MeV,φ=125°
77 ORL MO
ENDF-6
Cross section,mb/sr/MeV
E_γ,MeV

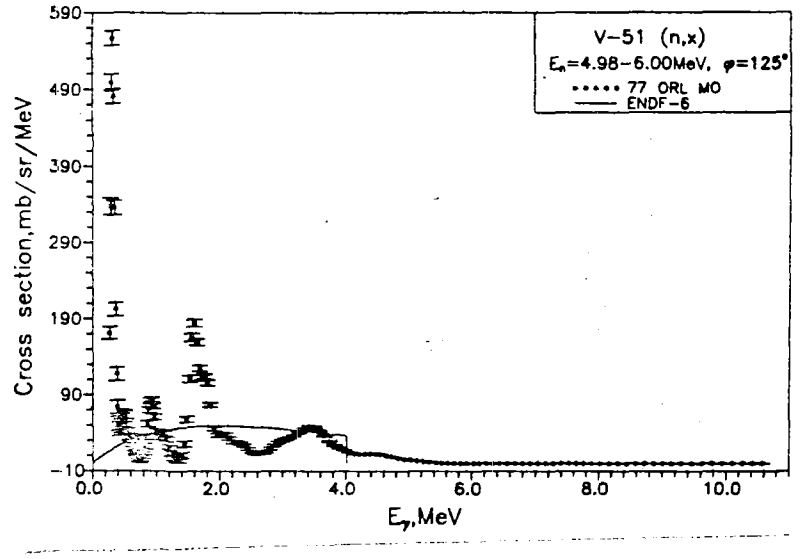
V-51 (n,x)
E_n=4.98-6.00MeV, φ=125°
77 ORL MO
ENDF-6
Cross section,mb/sr/MeV
E_γ,MeV

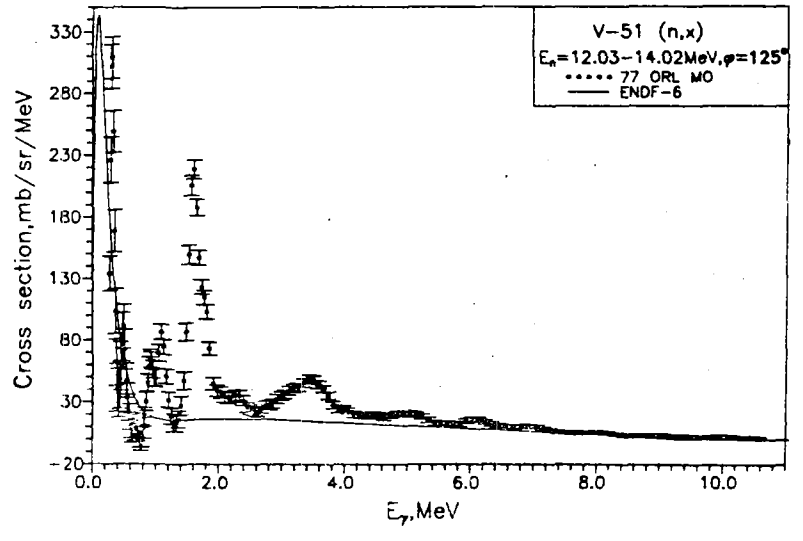
V-51 (n,x)
E_n=12.03-14.02MeV,φ=125°
77 ORL MO
ENDF-6
Cross section,mb/sr/MeV
E_γ,MeV

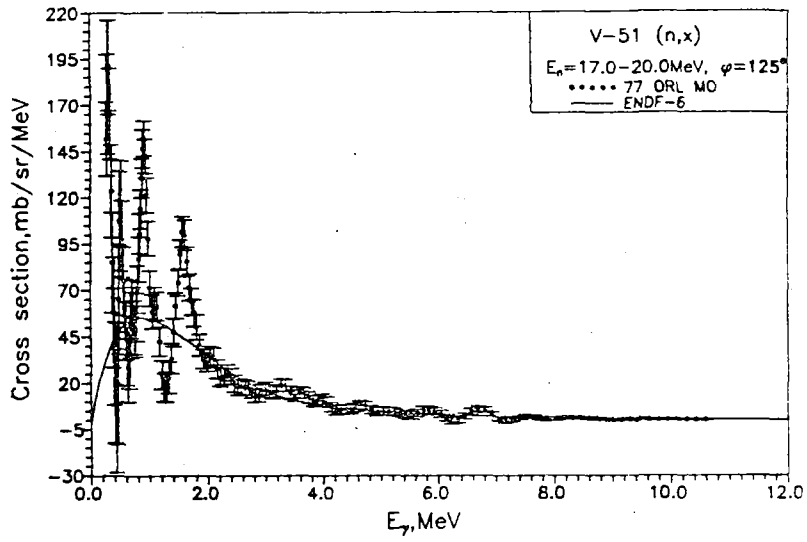
V-51 (n,x)
E_n=17.0-20.0MeV, φ=125°
77 ORL MO
ENDF-6
Cross section,mb/sr/MeV
E_γ,MeV

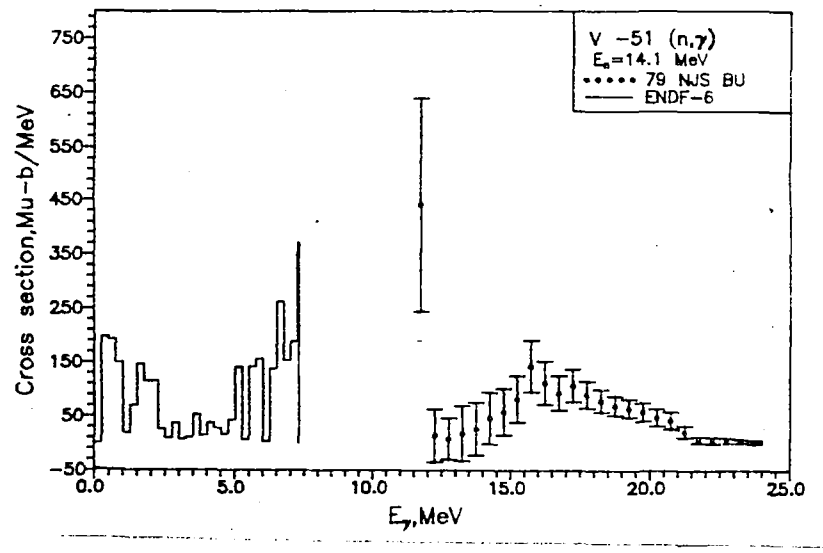
V -51 (n,γ)
E_n=14.1 MeV
79 NJS BU
ENDF-6
Cross section,Mu-b/MeV
E_γ,MeV

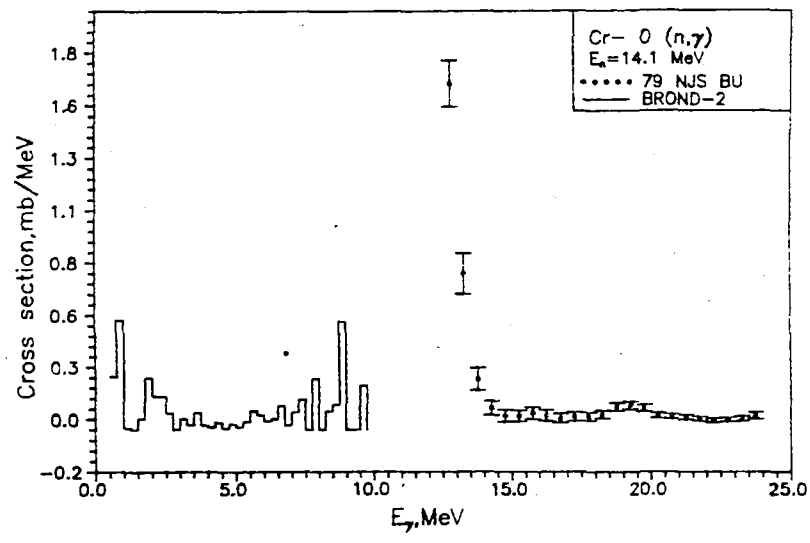
Cr- 0 (n,γ)
E_n=14.1 MeV
79 NJS BU
BROND-2
Cross section,mb/MeV
E_γ,MeV

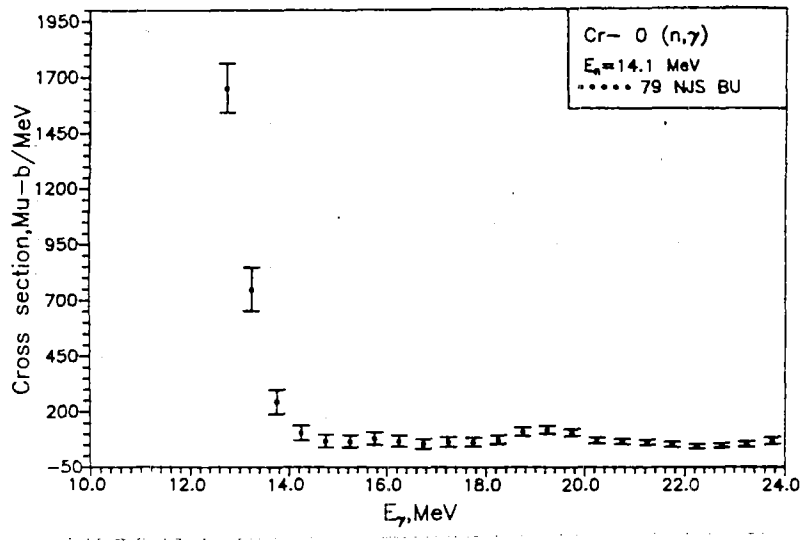
Cr- 0 (n,γ)
E_n=14.1 MeV
79 NJS BU
Cross section,Mu-b/MeV
E_γ,MeV

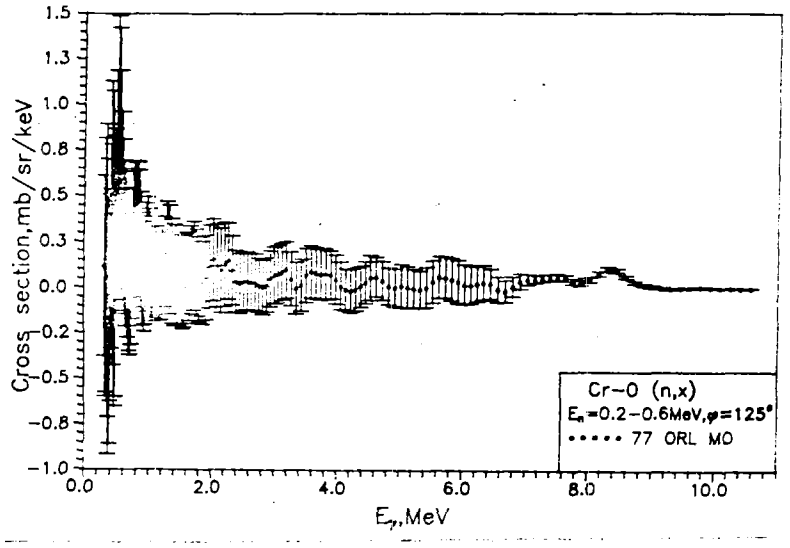
Cr-0 (n,x)
E_n=0.2-0.6MeV,φ=125°
77 ORL MO
Cross section,mb/sr/keV
E_γ,MeV

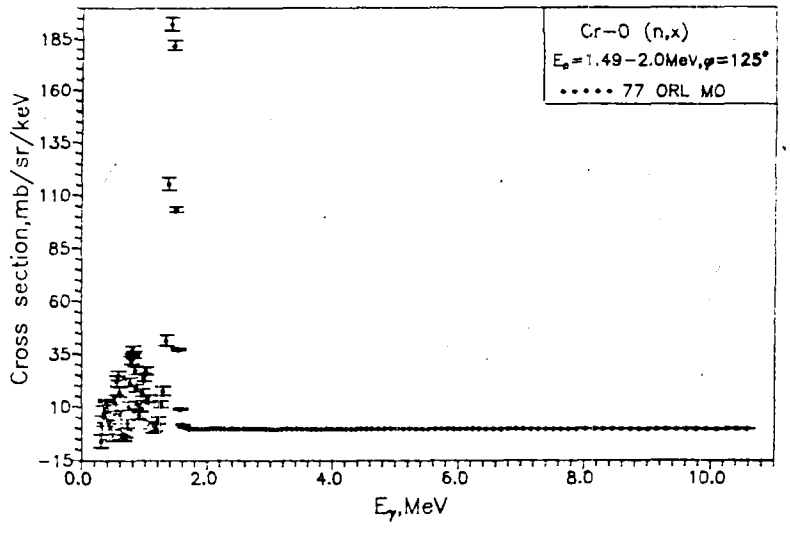
Cr-0 (n,x)
E_n=1.49-2.0MeV,φ=125°
77 ORL MO
Cross section,mb/sr/keV
E_γ,MeV

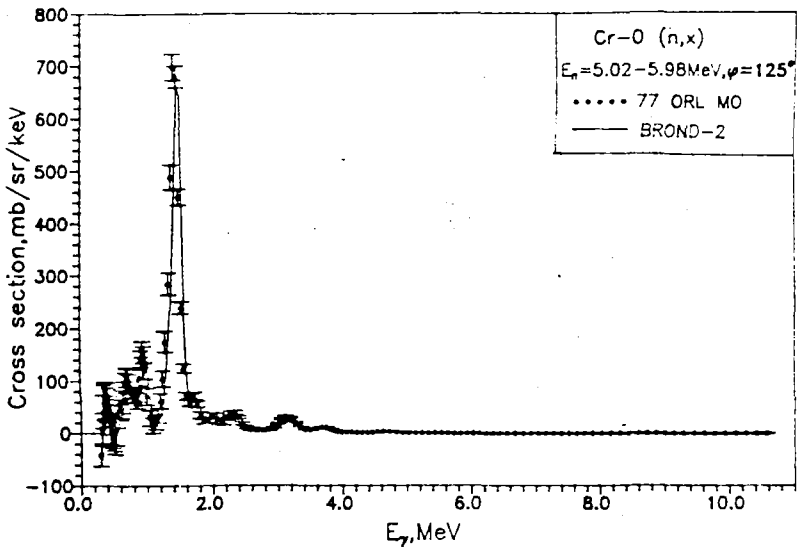
Cr–0 (n,x)
E_n=5.02–5.98MeV,φ=125°
77 ORL MO
BROND–2
Cross section,mb/sr/keV
E_γ,MeV

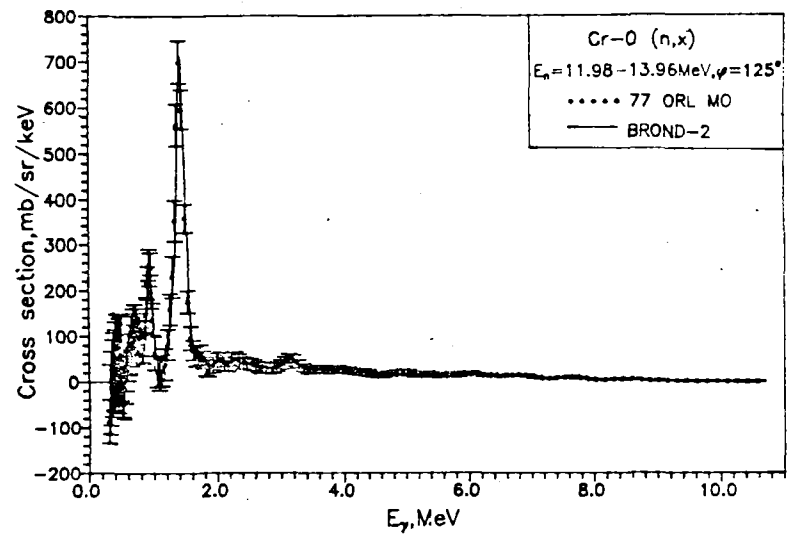
Cr–0 (n,x)
E_n=11.98–13.96MeV,φ=125°
77 ORL MO
BROND–2
Cross section,mb/sr/keV
E_γ,MeV

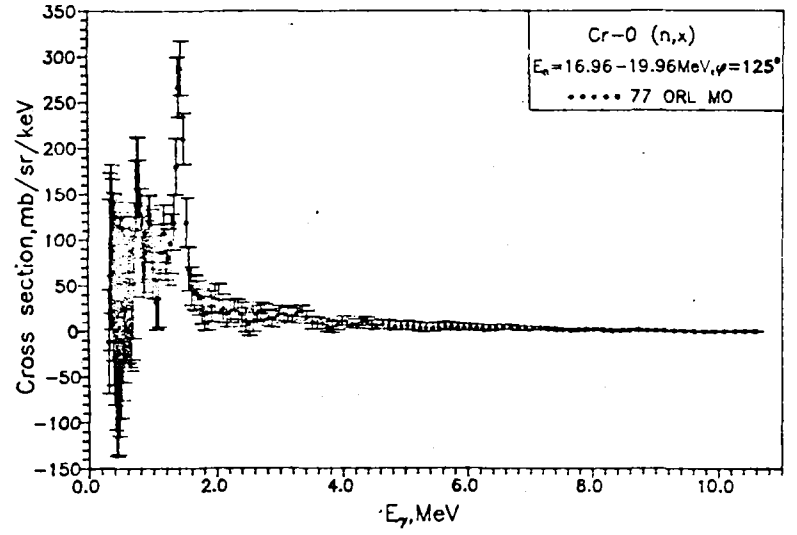
Cr–0 (n,x)
E_n=16.96–19.96MeV,φ=125°
77 ORL MO
Cross section,mb/sr/keV
E_γ,MeV

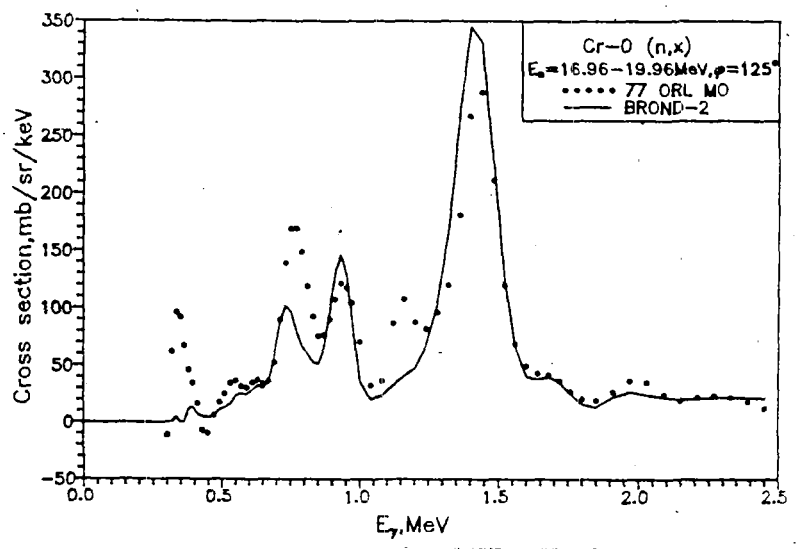
Cr–0 (n,x)
E_n=16.96–19.96MeV, φ=125°
77 ORL MO
BROND–2
Cross section,mb/sr/keV
E_γ,MeV

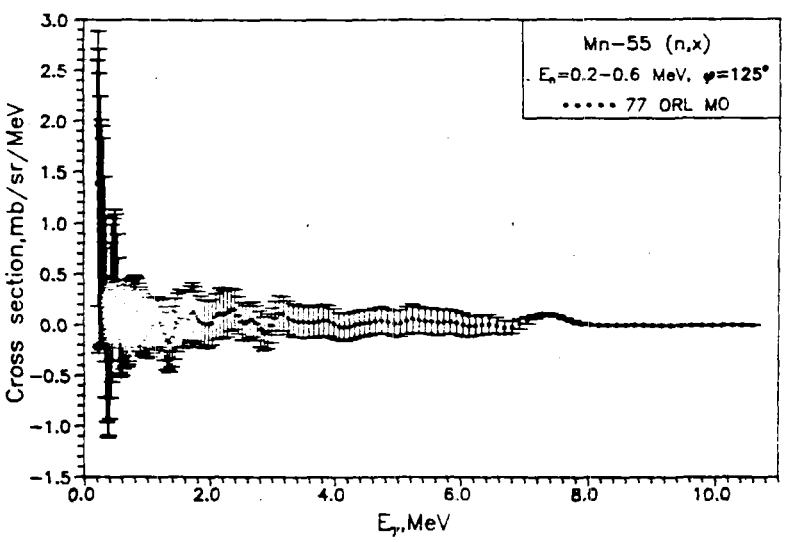
Mn–55 (n,x)
E_n=0.2–0.6 MeV, φ=125°
77 ORL MO
Cross section,mb/sr/MeV
E_γ,MeV

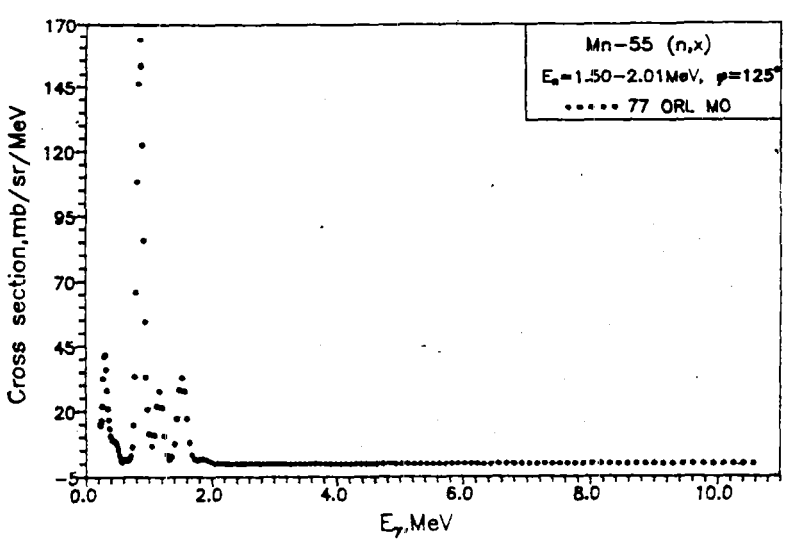
Mn–55 (n,x)
E_n=1.50–2.01MeV, φ=125°
77 ORL MO
Cross section,mb/sr/MeV
E_γ,MeV

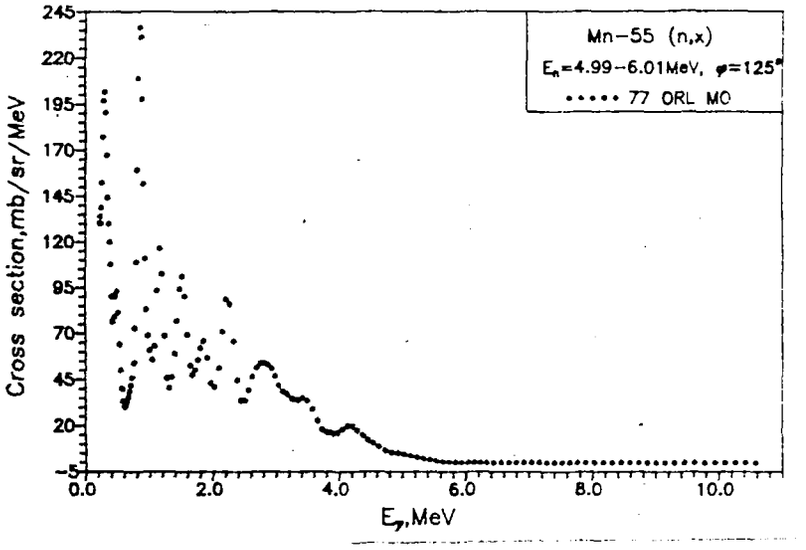
Mn-55 (n,x)
E_n=4.99-6.01MeV, φ=125°
77 ORL MO
Cross section,mb/sr/MeV
E_γ,MeV

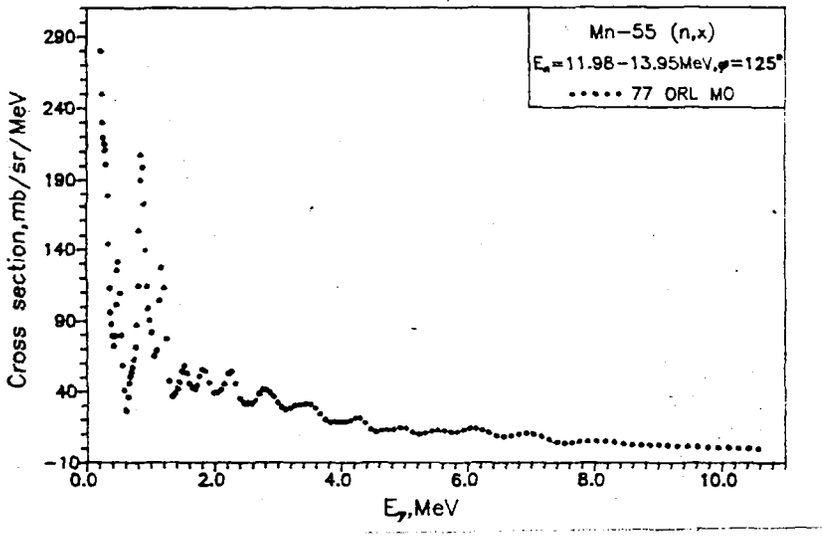
Mn-55 (n,x)
E_n=11.98-13.95MeV,φ=125°
77 ORL MO
Cross section,mb/sr/MeV
E_γ,MeV

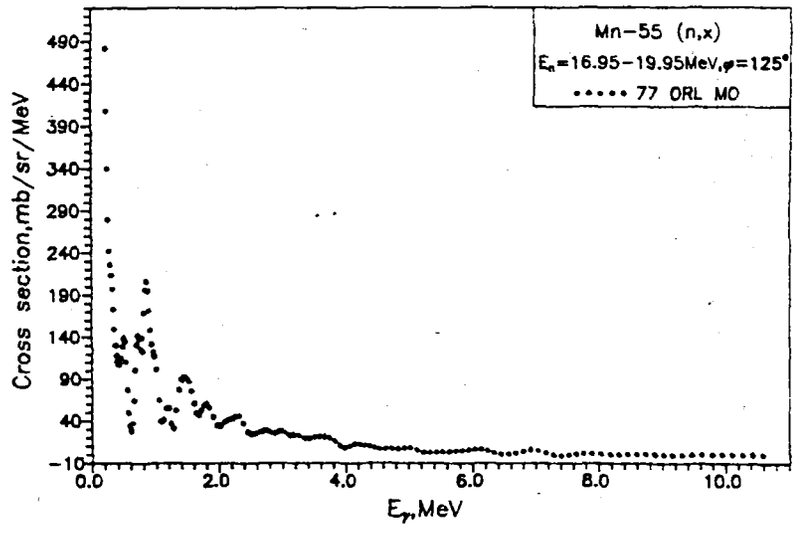
Mn-55 (n,x)
E_n=16.95-19.95MeV,φ=125°
77 ORL MO
Cross section,mb/sr/MeV
E_γ,MeV

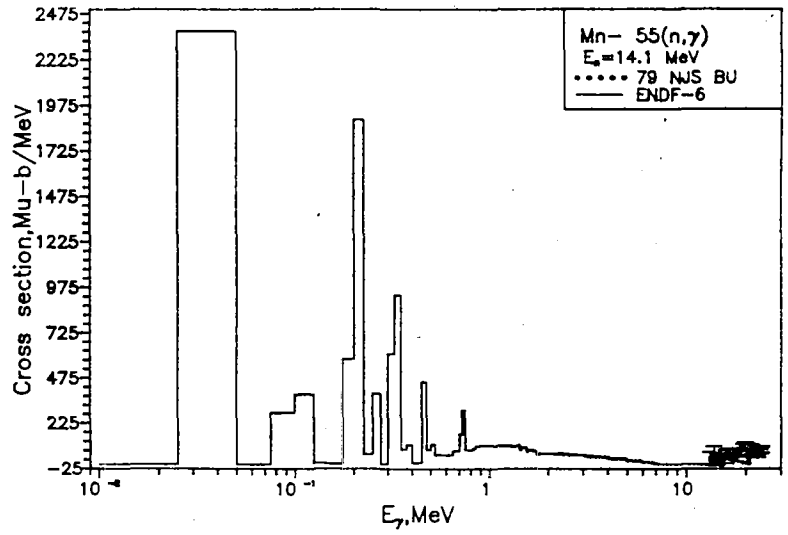
Mn- 55(n,γ)
E=14.1 MeV
79 NJS BU
ENDF-6
Cross section,Mu-b/MeV
E,MeV

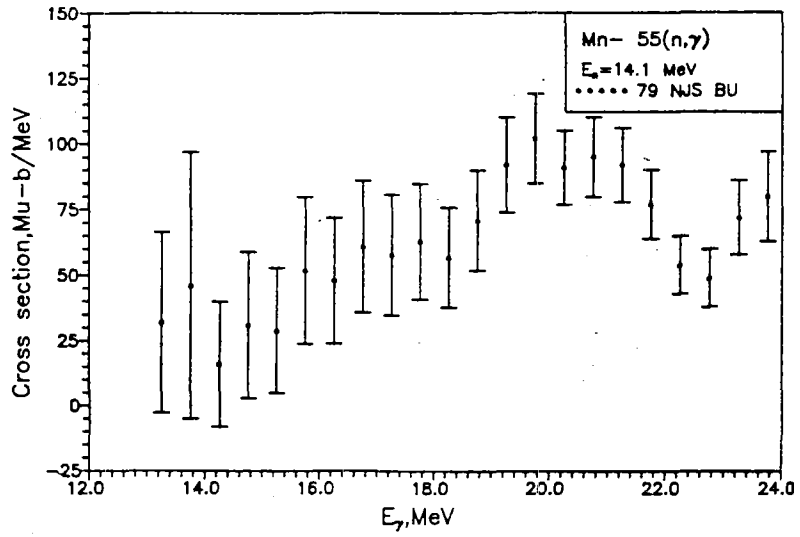
Mn- 55(n,γ)
E=14.1 MeV
79 NJS BU
Cross section,Mu-b/MeV
E,MeV

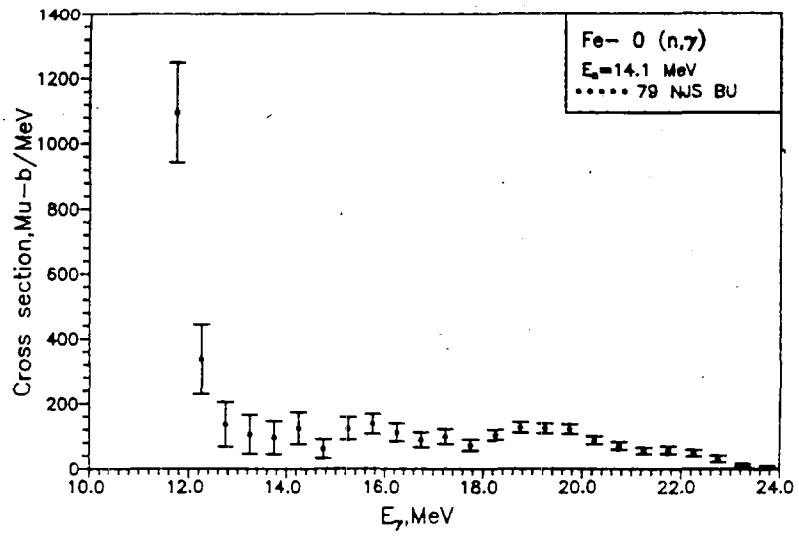
Fe- 0 (n,γ)
E=14.1 MeV
79 NJS BU
Cross section,Mu-b/MeV
E,MeV

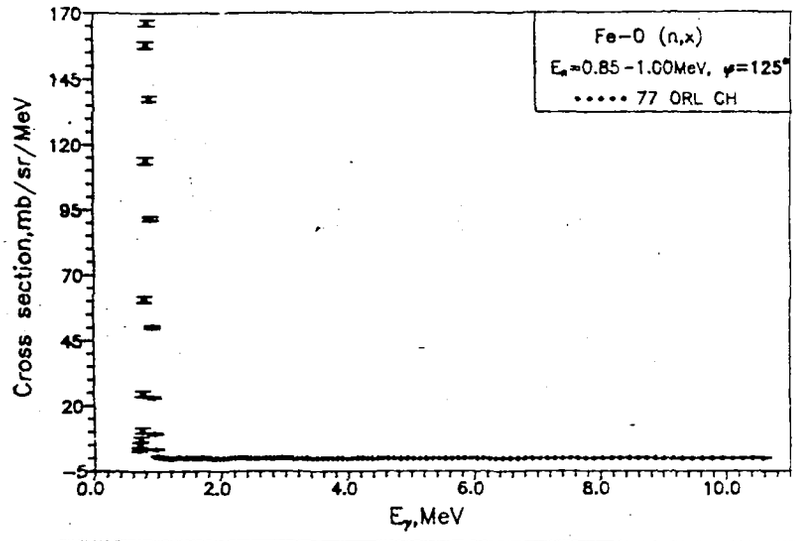
Fe-0 (n,x)
E_n=0.85-1.00MeV, φ=125°
77 ORL CH
Cross section,mb/sr/MeV
E_γ,MeV

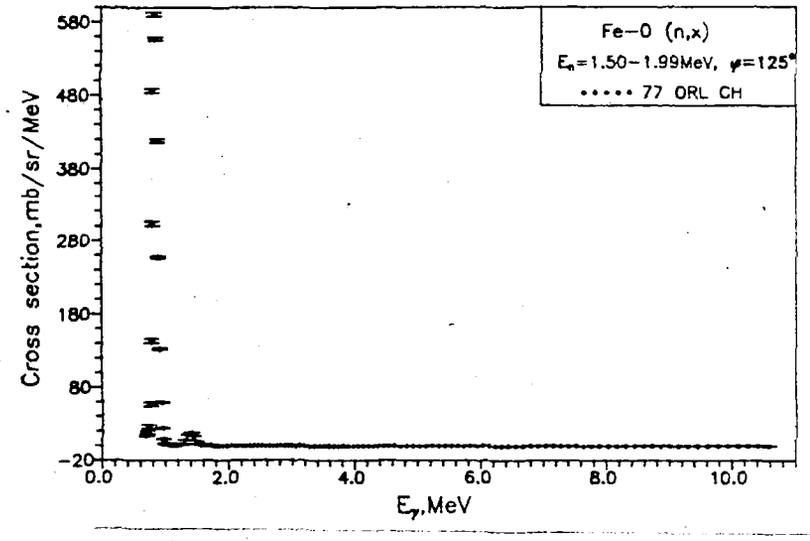
Fe-0 (n,x)
E_n=1.50-1.99MeV, φ=125°
77 ORL CH
Cross section,mb/sr/MeV
E_γ,MeV

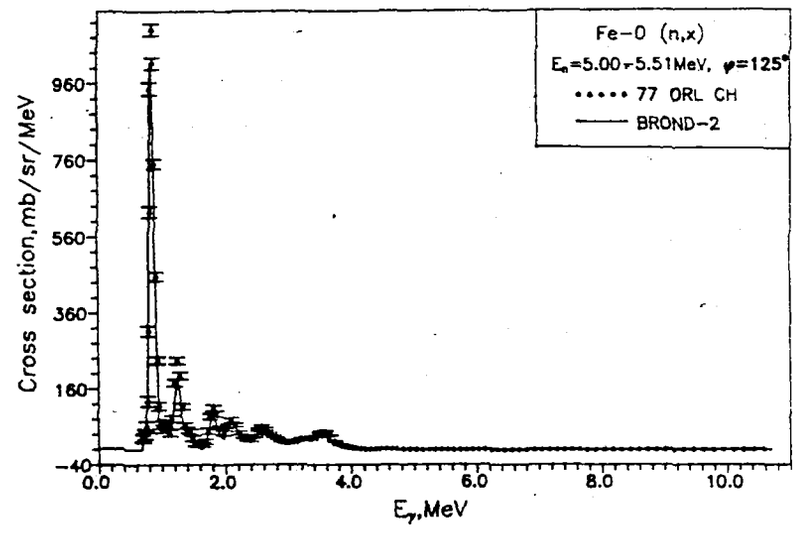
Fe-0 (n,x)
E_n=5.00-5.51MeV, φ=125°
77 ORL CH
BROND-2
Cross section,mb/sr/MeV
E_γ,MeV

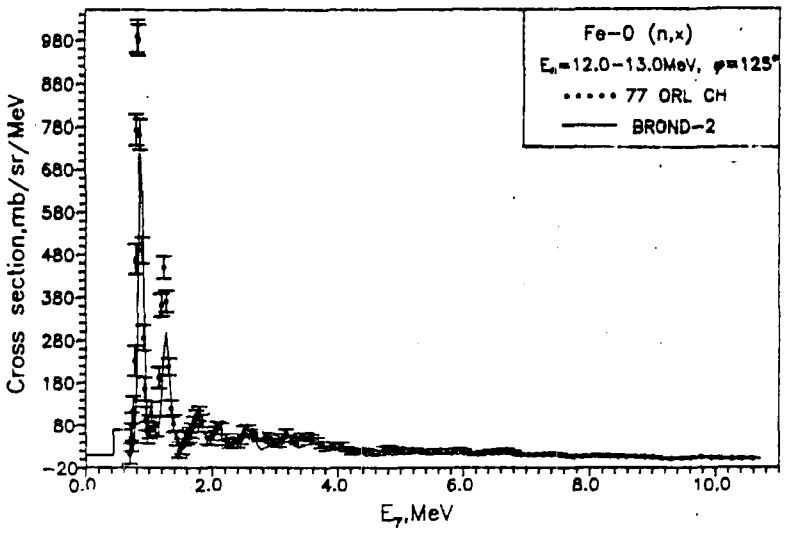
Fe-0 (n,x)
E_n=12.0-13.0MeV, φ=125°
77 ORL CH
BROND-2
Cross section,mb/sr/MeV
E_γ,MeV

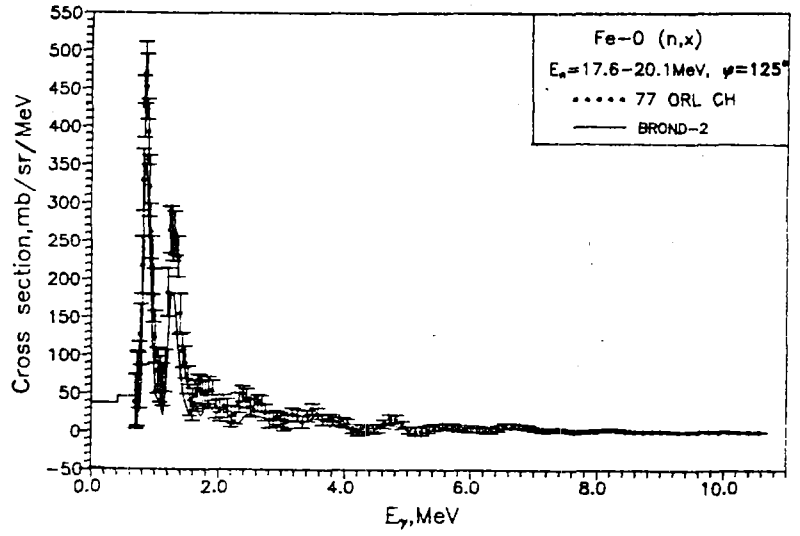
Fe-0 (n,x)
E_n=17.6-20.1MeV, φ=125°
77 ORL CH
BROND-2
Cross section,mb/sr/MeV
E_γ,MeV

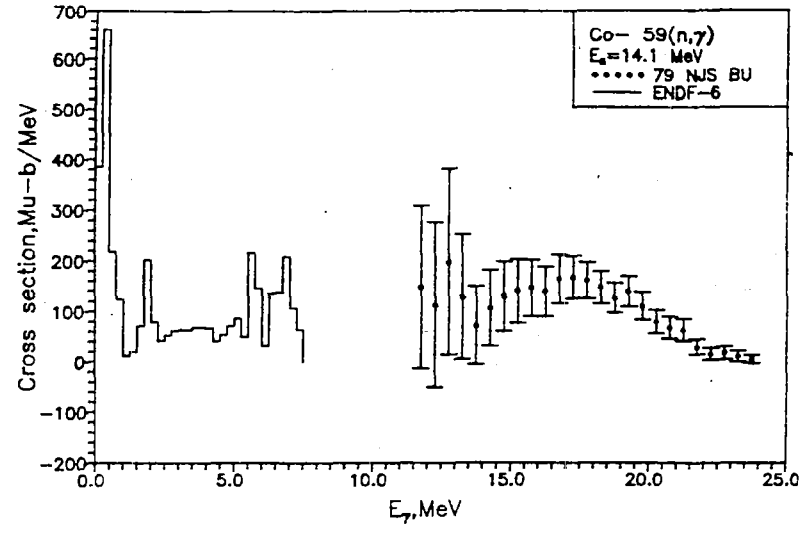
Co- 59(n,γ)
E_n=14.1 MeV
79 NJS BU
ENDF-6
Cross section,Mu-b/MeV
E_γ,MeV

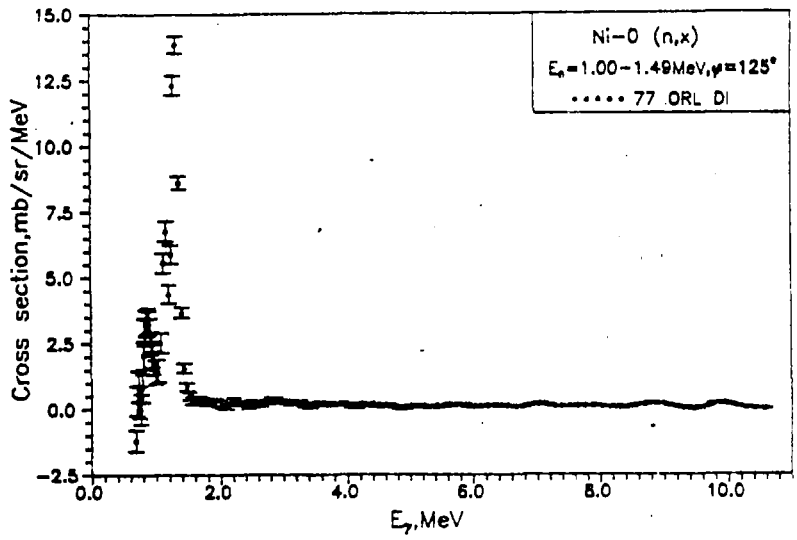
Ni-0 (n,x)
E_n=1.00-1.49MeV,φ=125°
77 ORL DI
Cross section,mb/sr/MeV
E_γ,MeV

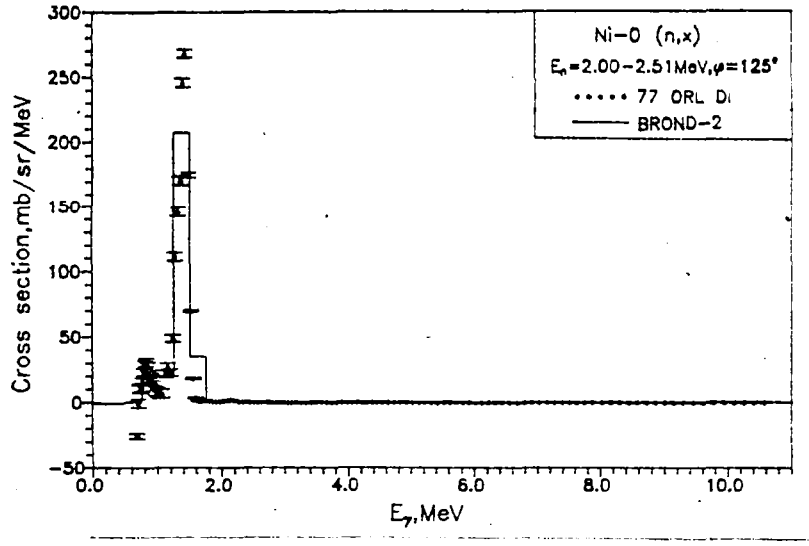
Ni-0 (n,x)
E_n=2.00-2.51MeV,φ=125°
77 ORL DI
BROND-2
Cross section,mb/sr/MeV
E_γ,MeV

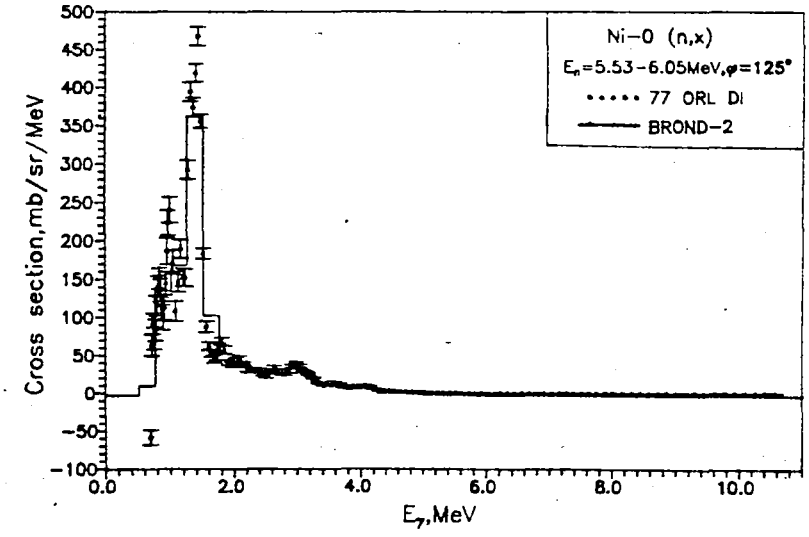
Ni-0 (n,x)
E_n=5.53-6.05MeV,φ=125°
77 ORL DI
BROND-2
Cross section,mb/sr/MeV
E_γ,MeV

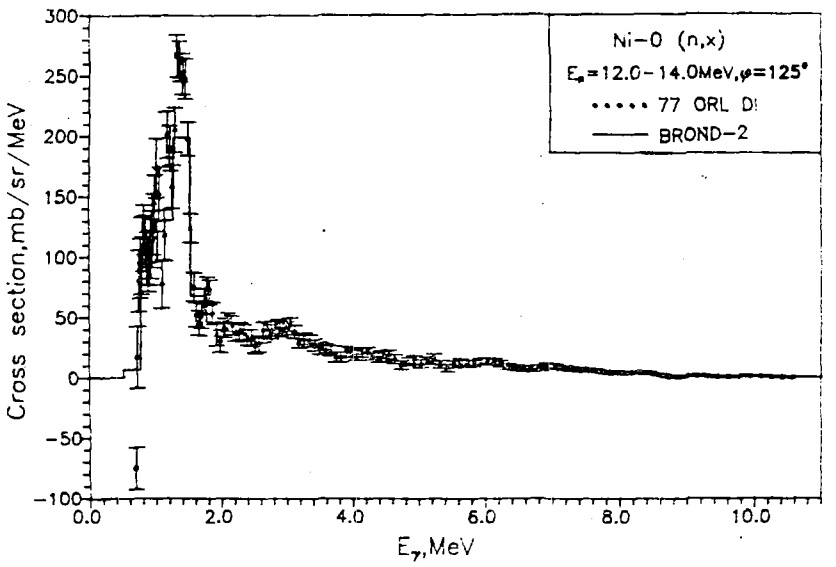
Ni-0 (n,x)
E_n=12.0-14.0MeV,φ=125°
77 ORL D
BROND-2
Cross section,mb/sr/MeV
E_γ,MeV

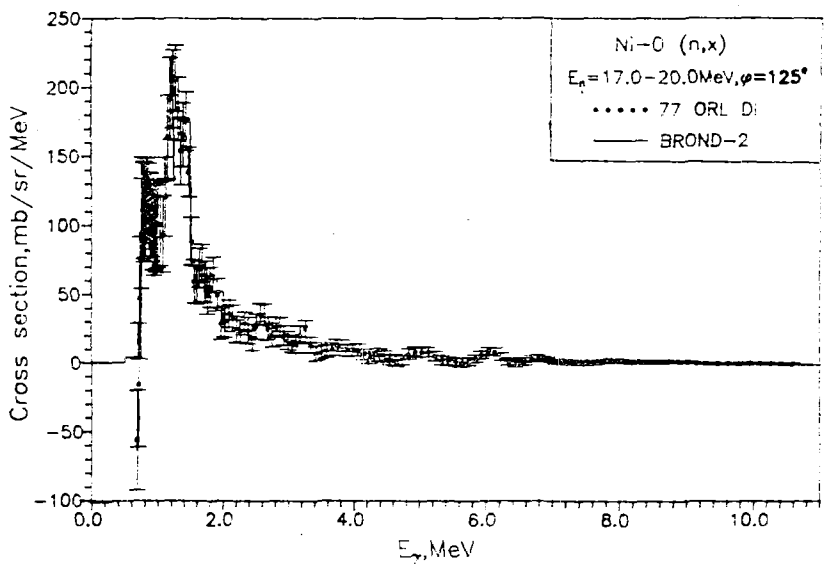
Ni-0 (n,x)
E_n=17.0-20.0MeV,φ=125°
77 ORL D
BROND-2
Cross section,mb/sr/MeV
E_γ,MeV

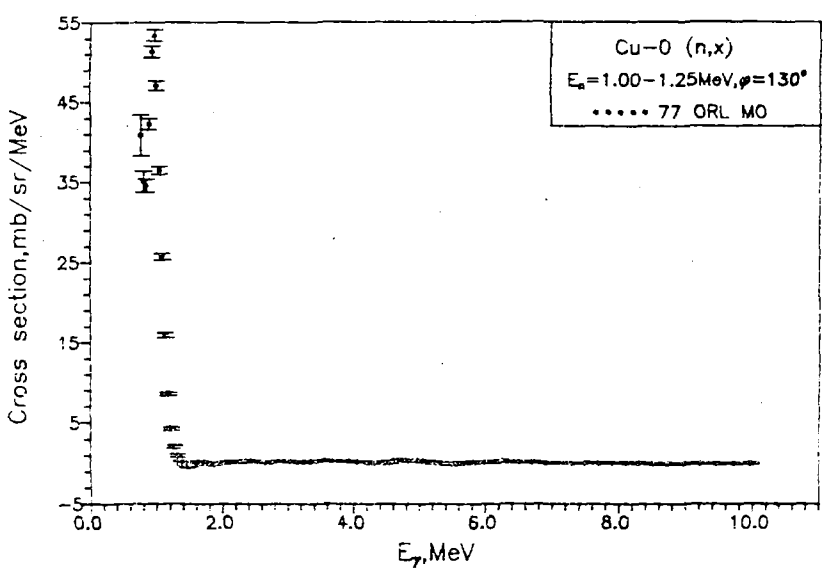
Cu-0 (n,x)
E_n=1.00-1.25MeV,φ=130°
77 ORL MO
Cross section,mb/sr/MeV
E_γ,MeV

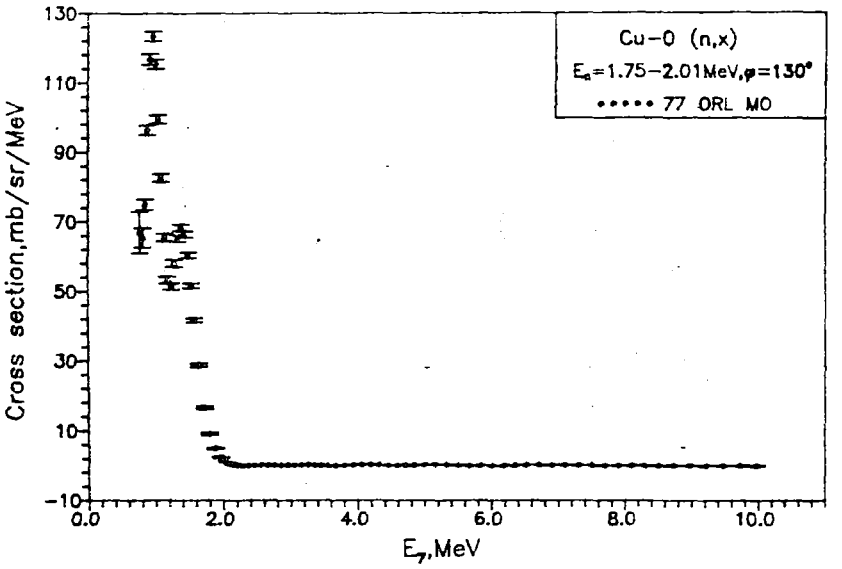
Cu-0 (n,x)
E_n=1.75-2.01MeV,φ=130°
77 ORL MO
Cross section,mb/sr/MeV
E_γ,MeV

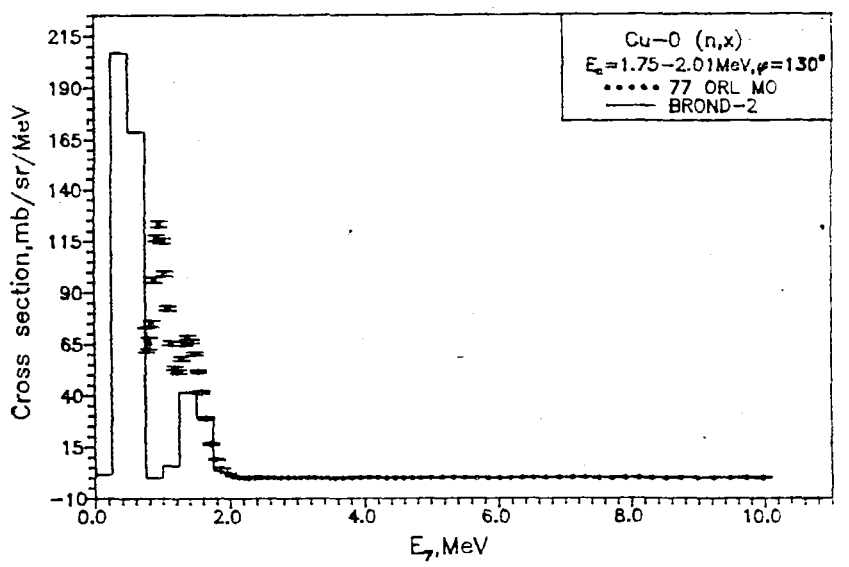
Cu-0 (n,x)
E_n=1.75-2.01MeV,φ=130°
77 ORL MO
BROND-2
Cross section,mb/sr/MeV
E_γ,MeV

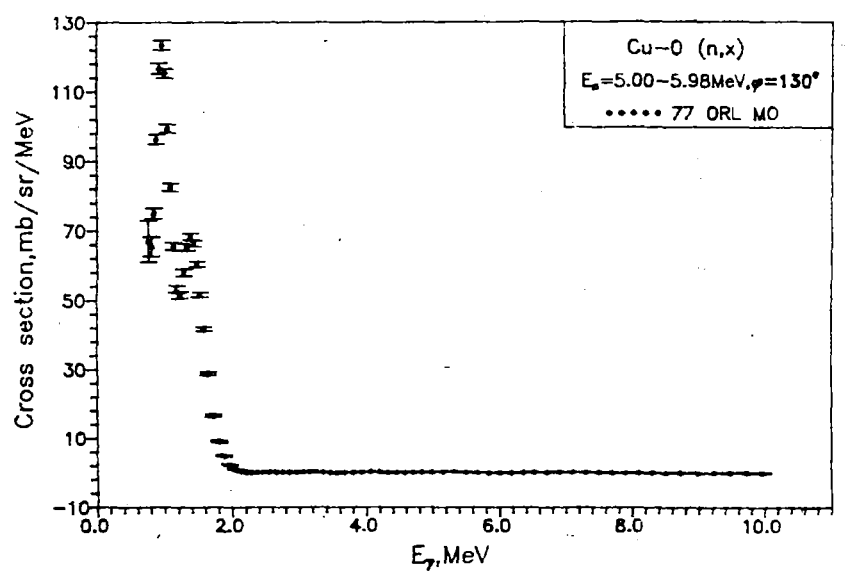
Cu-0 (n,x)
E_n=5.00-5.98MeV,φ=130°
77 ORL MO
Cross section,mb/sr/MeV
E_γ,MeV

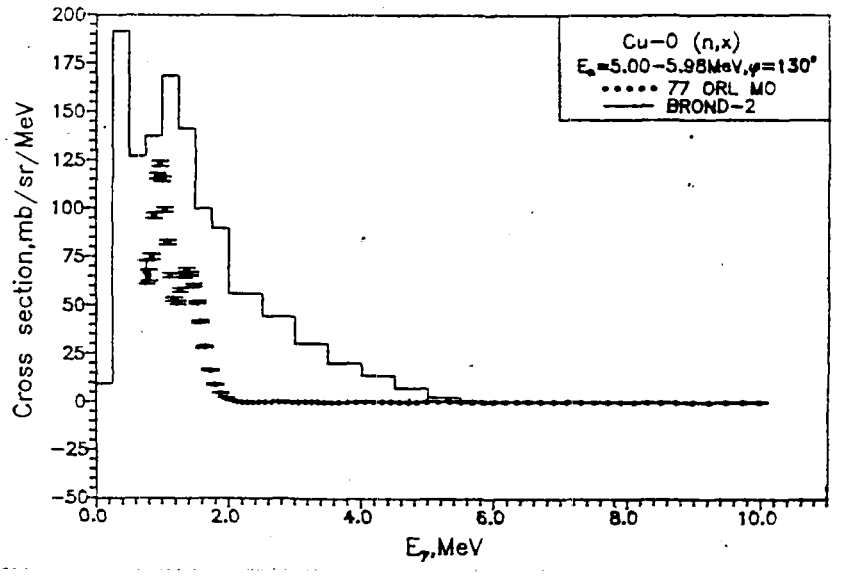
Cu-0 (n,x)
E_n=5.00-5.98MeV,φ=130°
77 ORL MO
BROND-2
Cross section,mb/sr/MeV
E_γ,MeV

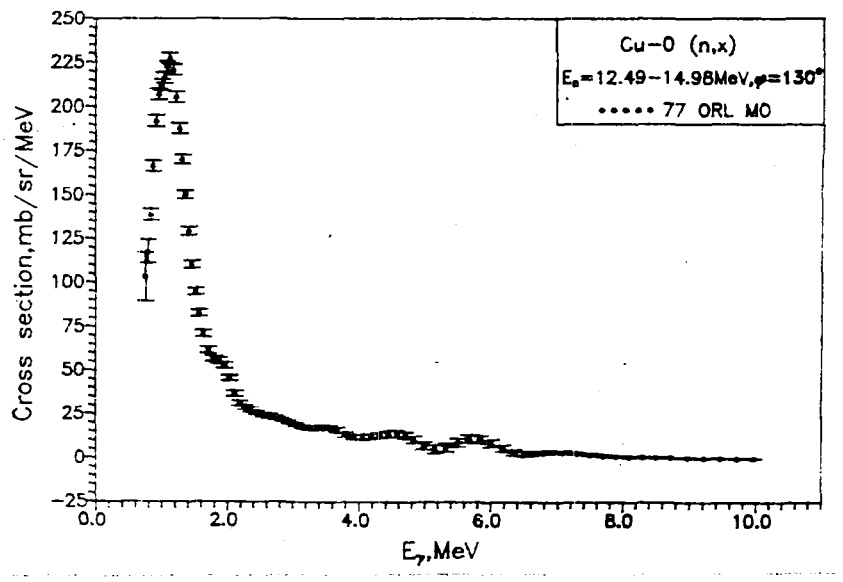
Cu-0 (n,x)
E_n=12.49-14.98MeV,φ=130°
77 ORL MO
Cross section,mb/sr/MeV
E_γ,MeV

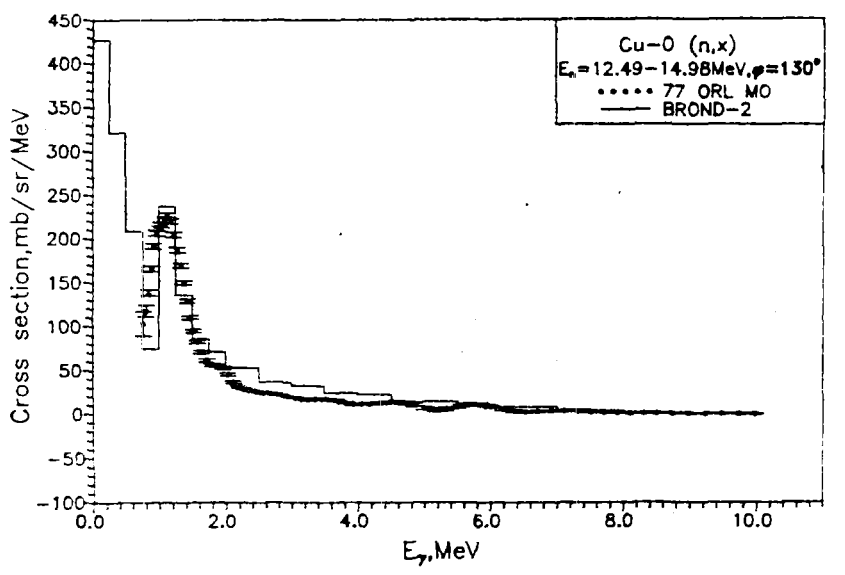
Cu-0 (n,x)
E_n=12.49-14.98MeV,φ=130°
77 ORL MO
BROND-2
Cross section,mb/sr/MeV
E_γ,MeV

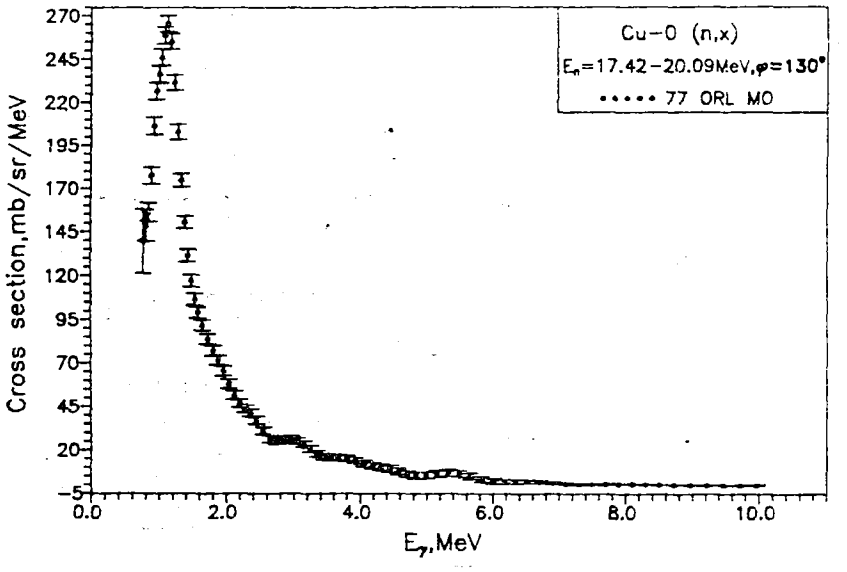
Cu–0 (n,x)
E_n=17.42–20.09MeV,φ=130°
••••• 77 ORL MO
Cross section,mb/sr/MeV
E_γ,MeV

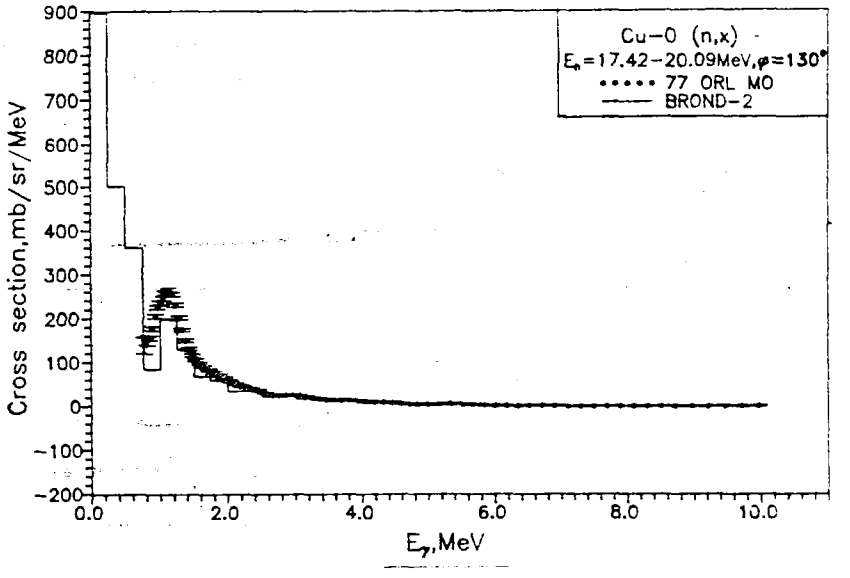
Cu–0 (n,x)
E_n=17.42–20.09MeV,φ=130°
••••• 77 ORL MO
—— BROND–2
Cross section,mb/sr/MeV
E_γ,MeV

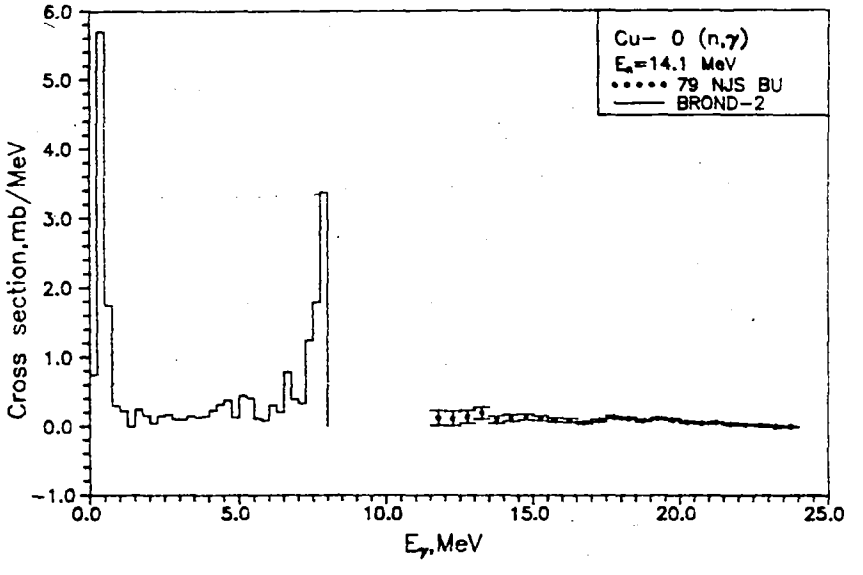
Cu– 0 (n,γ)
E_n=14.1 MeV
••••• 79 NJS BU
—— BROND–2
Cross section,mb/MeV
E_γ,MeV

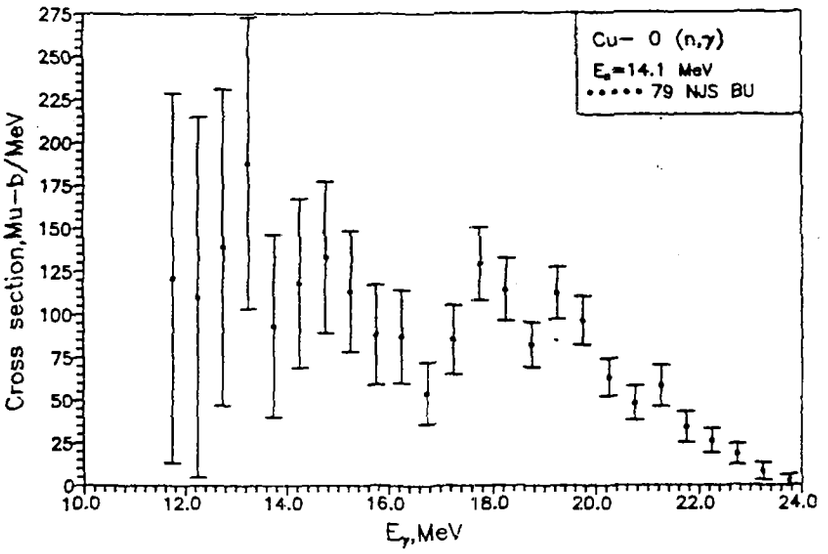
Cu- 0 (n,γ)
E_n=14.1 MeV
79 NJS BU
Cross section,Mu-b/MeV
E_γ,MeV

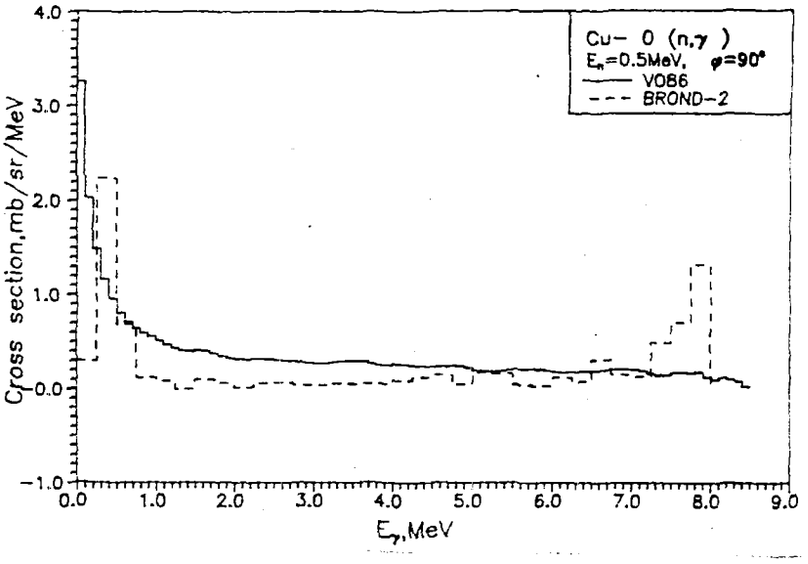
Cu- 0 (n,γ)
E_n=0.5MeV, φ=90°
V086
BROND-2
Cross section,mb/sr/MeV
E_γ,MeV

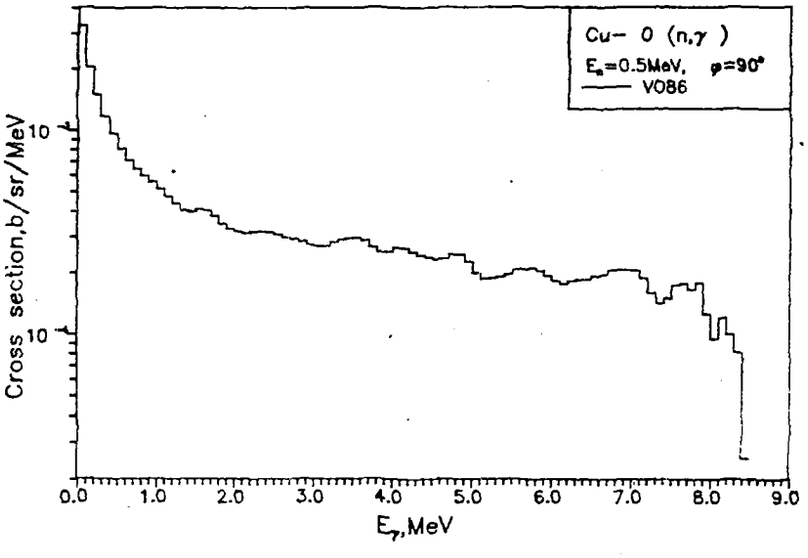
Cu- 0 (n,γ)
E_n=0.5MeV, φ=90°
V086
Cross section,b/sr/MeV
E_γ,MeV

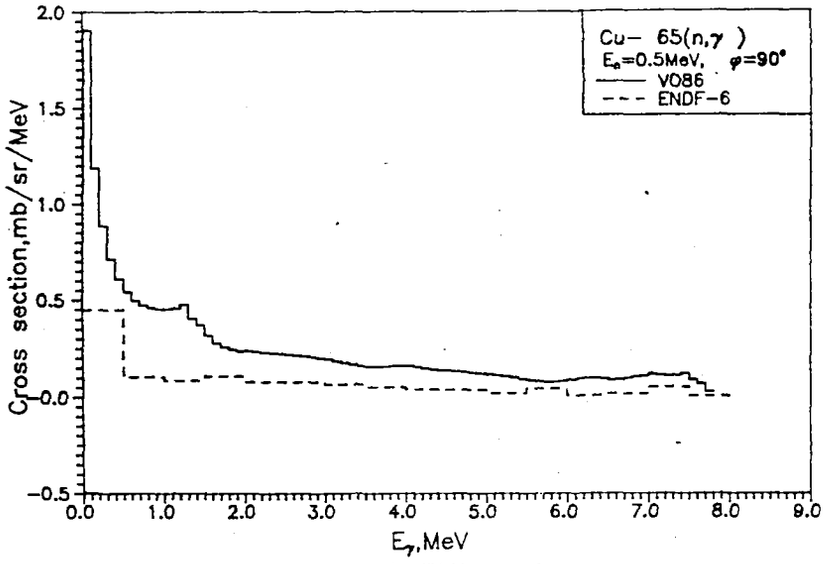
Cu– 65(n,γ)
E_n=0.5MeV, φ=90°
V086
ENDF–6
Cross section,mb/sr/MeV
E_γ,MeV

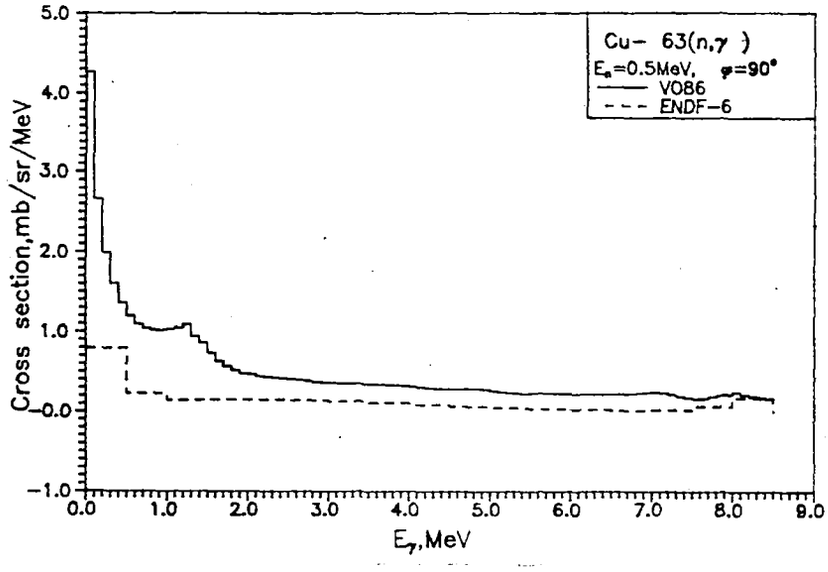
Cu– 63(n,γ)
E_n=0.5MeV, φ=90°
V086
ENDF–6
Cross section,mb/sr/MeV
E_γ,MeV

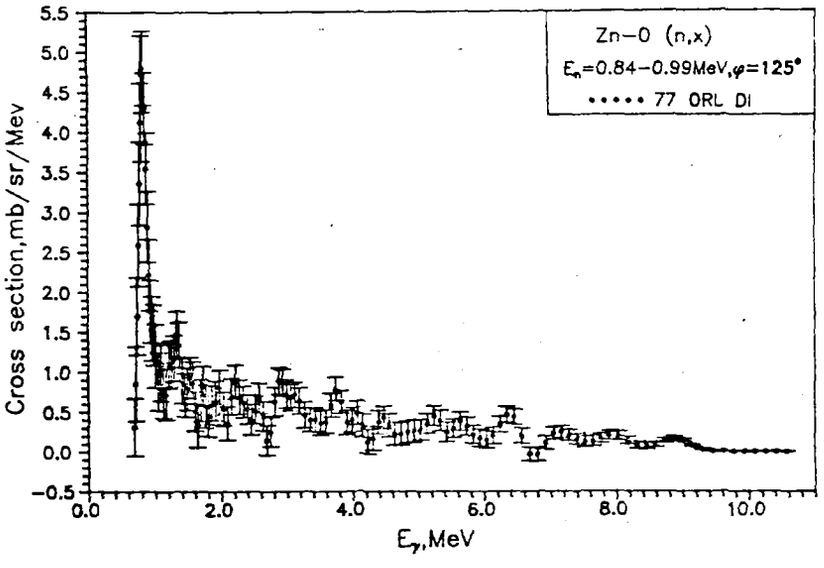
Zn–0 (n,x)
E_n=0.84–0.99MeV,φ=125°
77 ORL DI
Cross section,mb/sr/Mev
E_γ,MeV

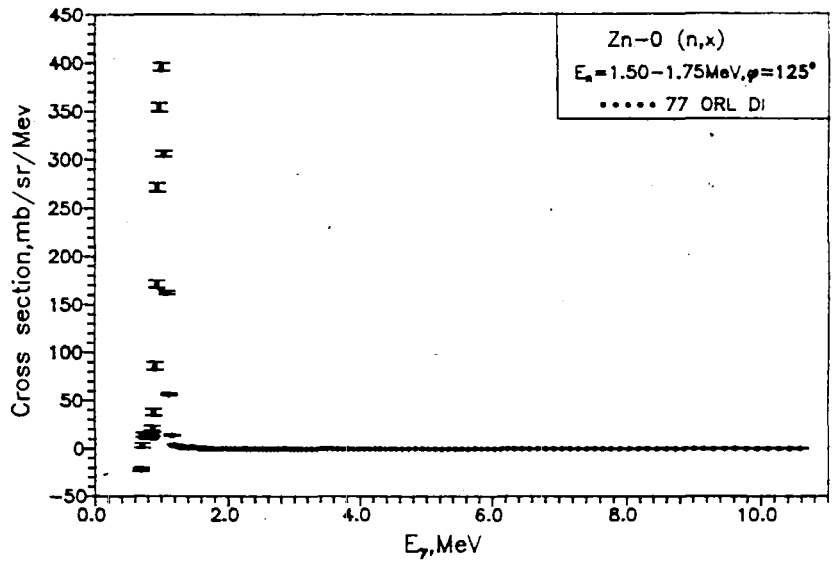
Zn-0 (n,x)
E_n=1.50-1.75MeV,φ=125°
77 ORL DI
Cross section,mb/sr/Mev
E_γ,MeV

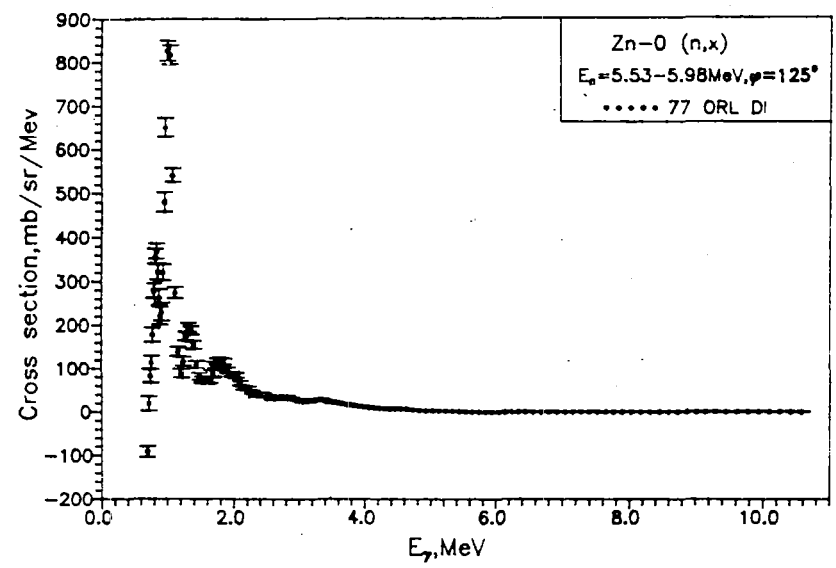
Zn-0 (n,x)
E_n=5.53-5.98MeV,φ=125°
77 ORL DI
Cross section,mb/sr/Mev
E_γ,MeV

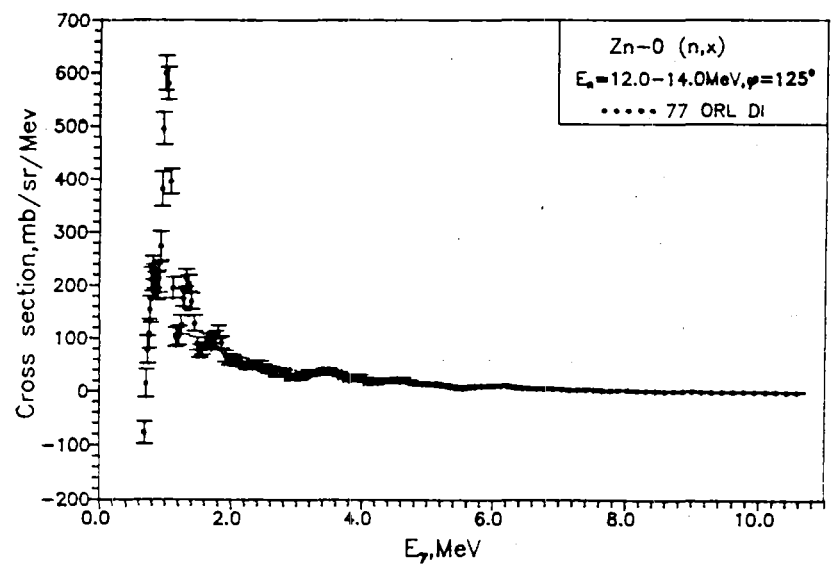
Zn-0 (n,x)
E_n=12.0-14.0MeV,φ=125°
77 ORL DI
Cross section,mb/sr/Mev
E_γ,MeV

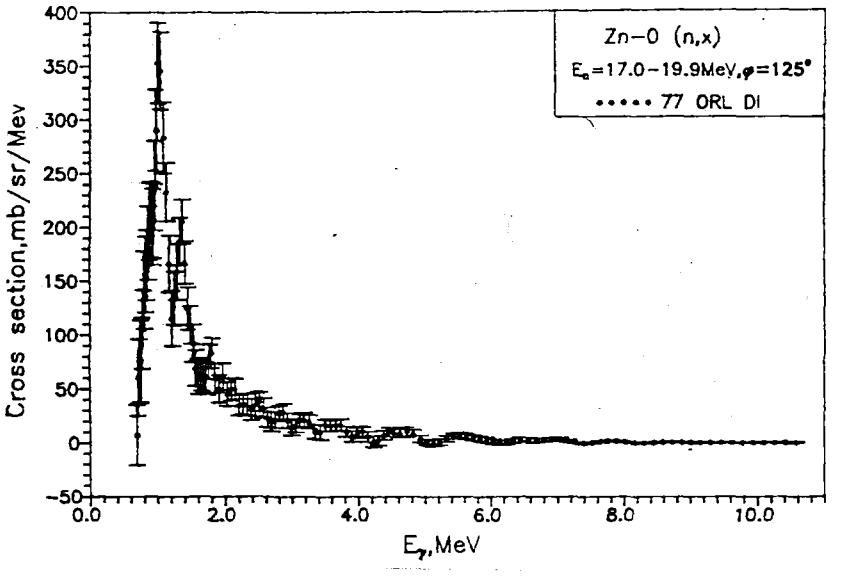
Zn–0 (n,x)
E_n=17.0–19.9MeV,φ=125°
77 ORL DI
Cross section,mb/sr/Mev
E_γ,MeV

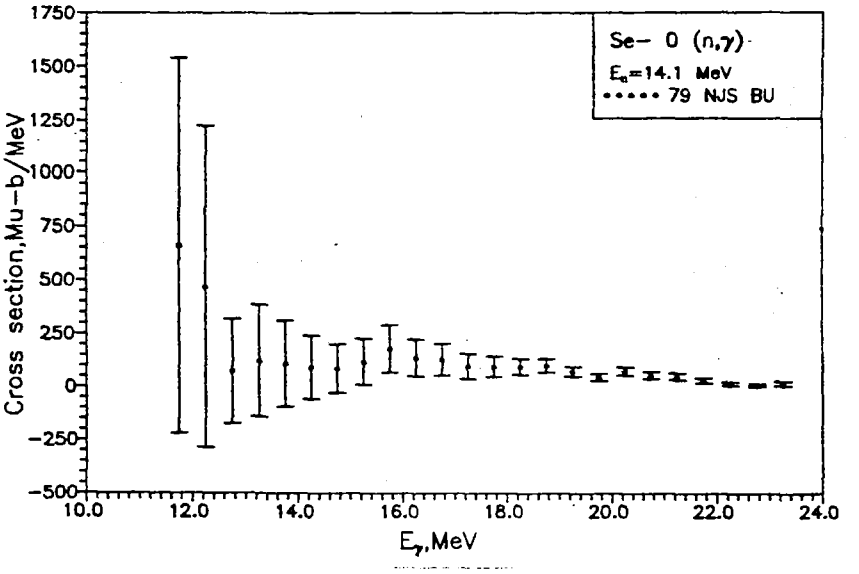
Se– 0 (n,γ)
E_n=14.1 MeV
79 NJS BU
Cross section,Mu–b/MeV
E_γ,MeV

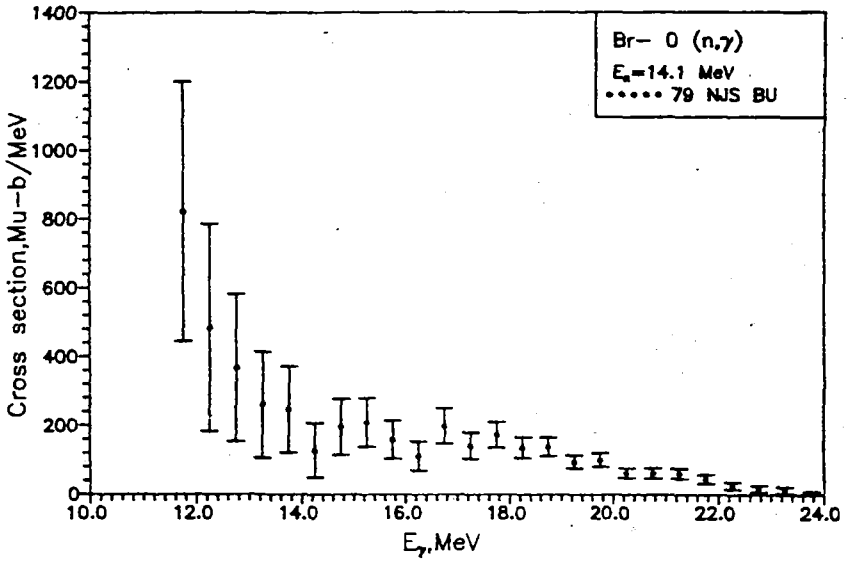
Br– 0 (n,γ)
E_n=14.1 MeV
79 NJS BU
Cross section,Mu–b/MeV
E_γ,MeV

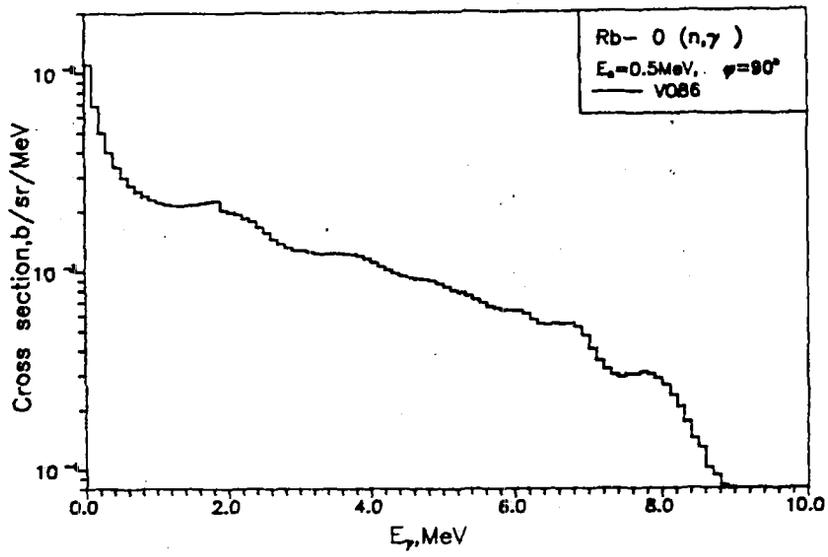
Rb– 0 (n,γ)
E_n=0.5MeV, φ=90°
V086
Cross section,b/sr/MeV
E_γ,MeV

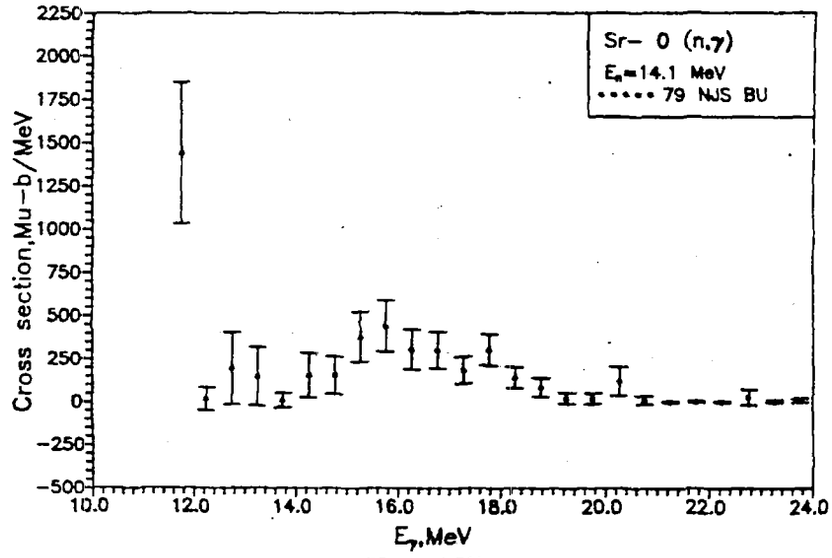
Sr– 0 (n,γ)
E_n=14.1 MeV
79 NJS BU
Cross section,Mu–b/MeV
E_γ,MeV

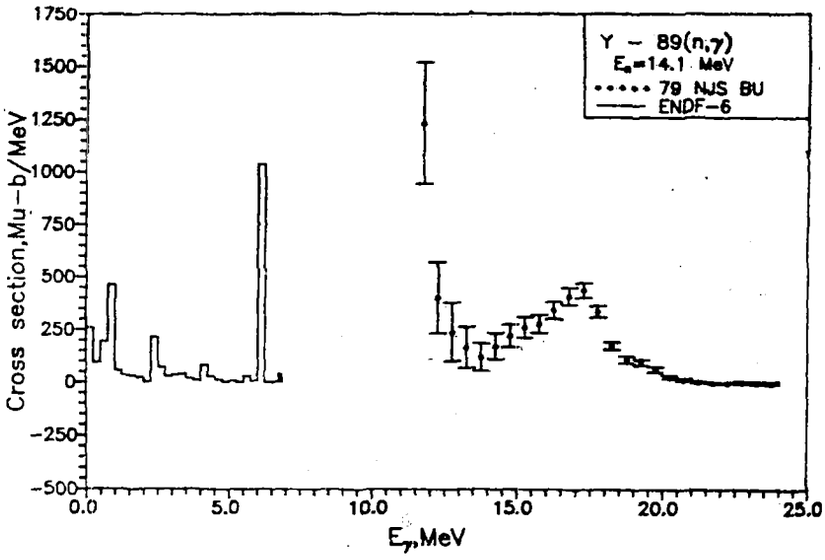
Y – 89(n,γ)
E_n=14.1 MeV
79 NJS BU
ENDF–6
Cross section,Mu–b/MeV
E_γ,MeV

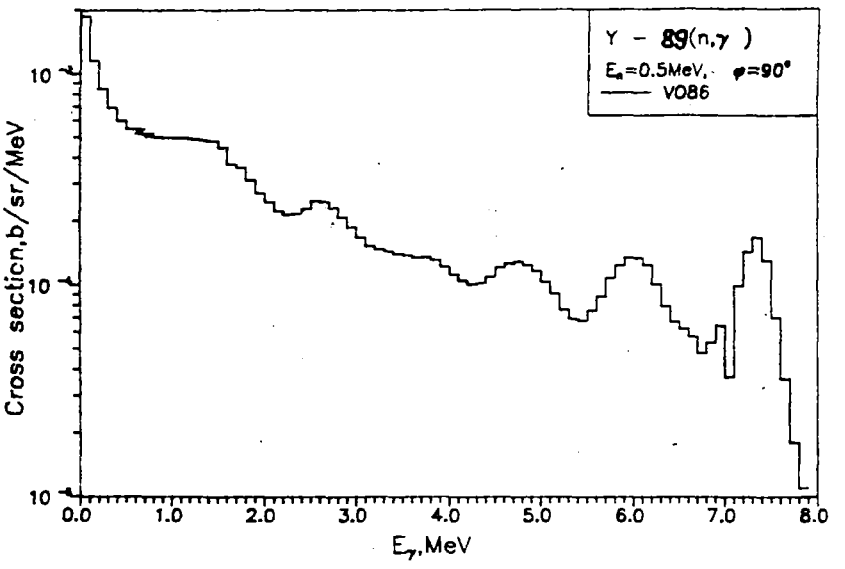
Y - 89(n,γ)
E_n=0.5MeV, φ=90°
V086
Cross section,b/sr/MeV
E_γ,MeV

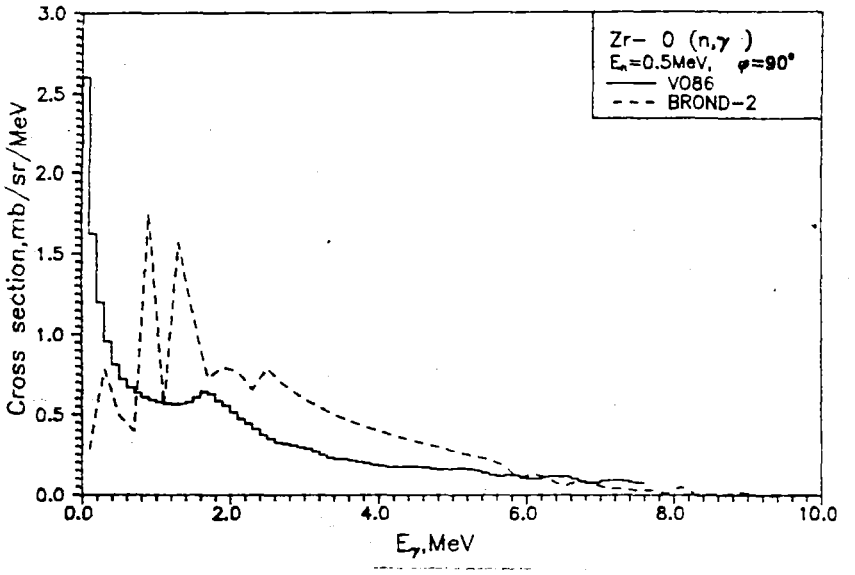
Zr- 0 (n,γ)
E_n=0.5MeV, φ=90°
V086
BROND-2
Cross section,mb/sr/MeV
E_γ,MeV

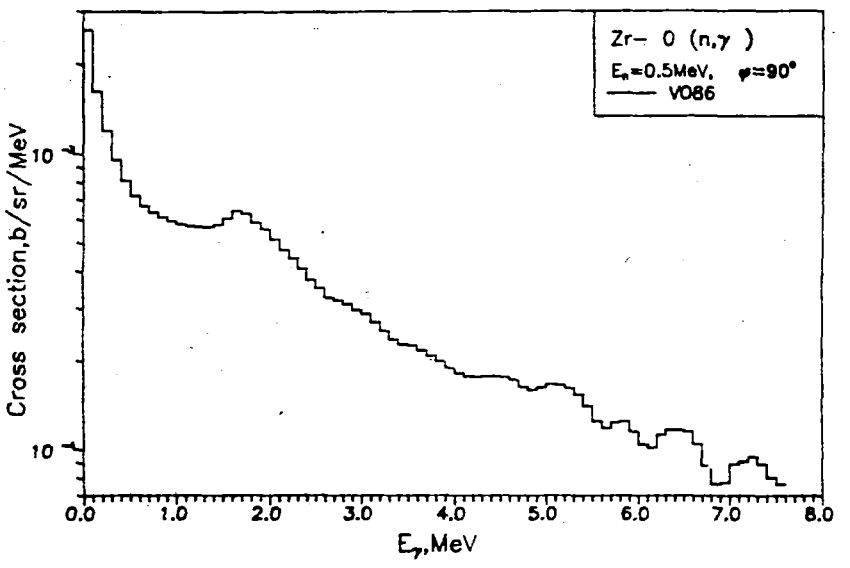
Zr- 0 (n,γ)
E_n=0.5MeV, φ=90°
V086
Cross section,b/sr/MeV
E_γ,MeV

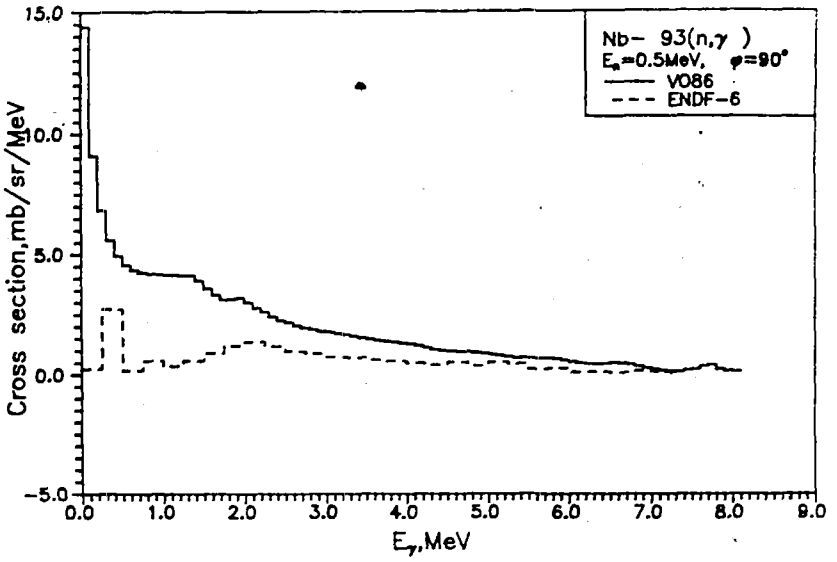
Nb- 93(n,γ)
E_n=0.5MeV, φ=90°
V086
ENDF-6
Cross section,mb/sr/MeV
E_γ,MeV

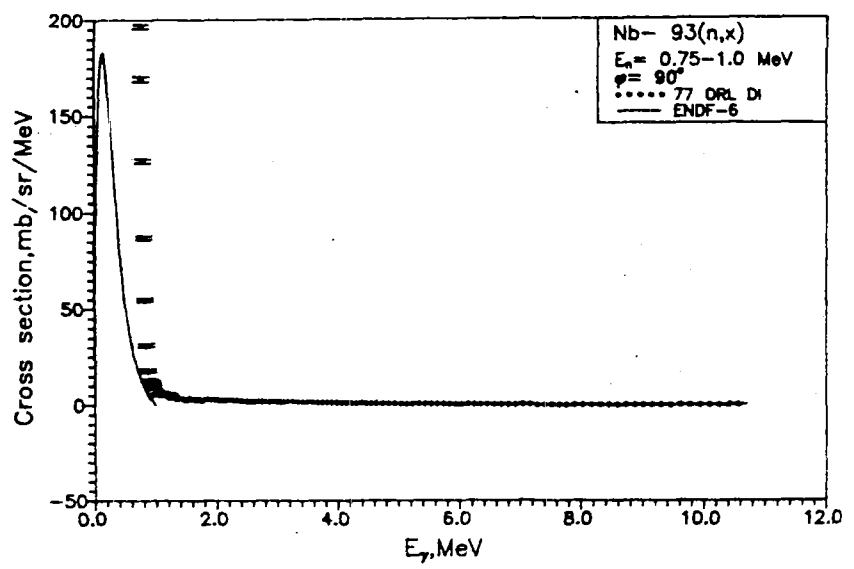
Nb- 93(n,x)
E_n= 0.75-1.0 MeV
φ= 90°
77 ORL DI
ENDF-6
Cross section,mb/sr/MeV
E_γ,MeV

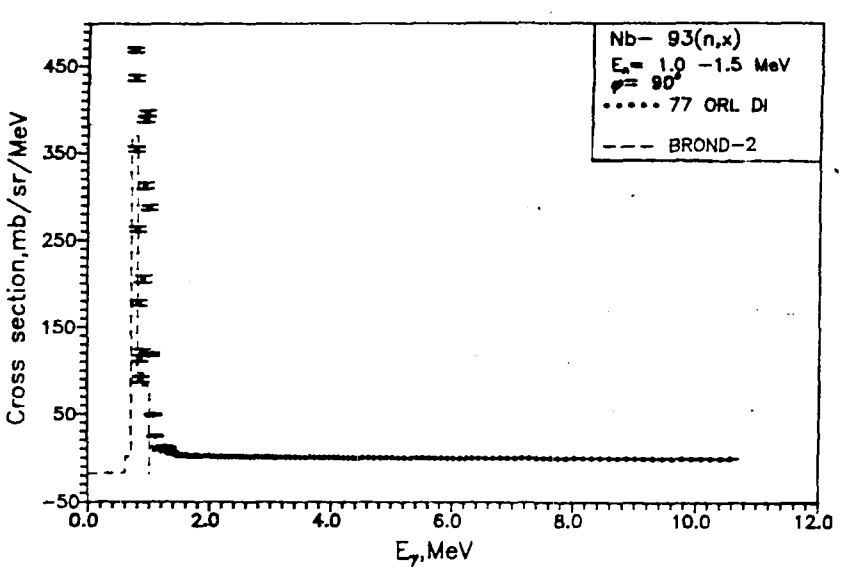
Nb- 93(n,x)
E_n= 1.0 -1.5 MeV
φ= 90°
77 ORL DI
BROND-2
Cross section,mb/sr/MeV
E_γ,MeV

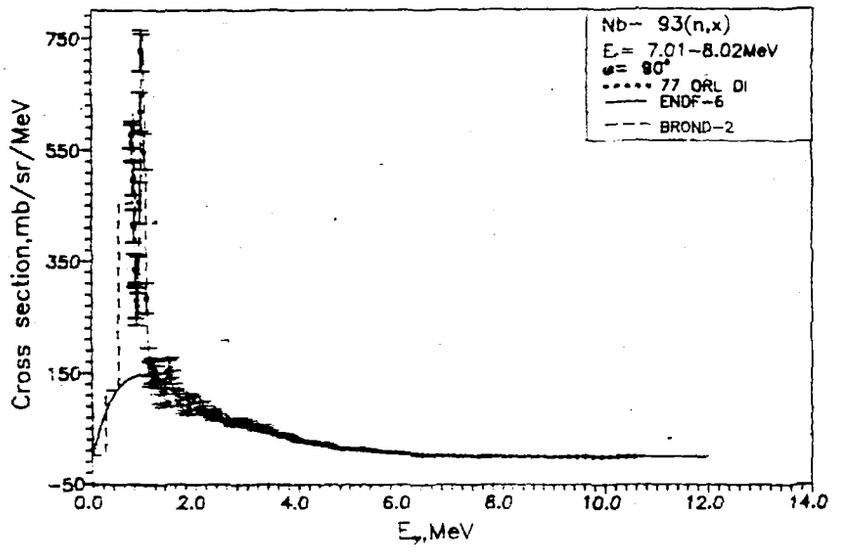
Nb- 93(n,x)
E_n= 7.01-8.02MeV
φ= 90°
77 ORL DI
ENDF-6
BROND-2
Cross section,mb/sr/MeV
E_γ,MeV

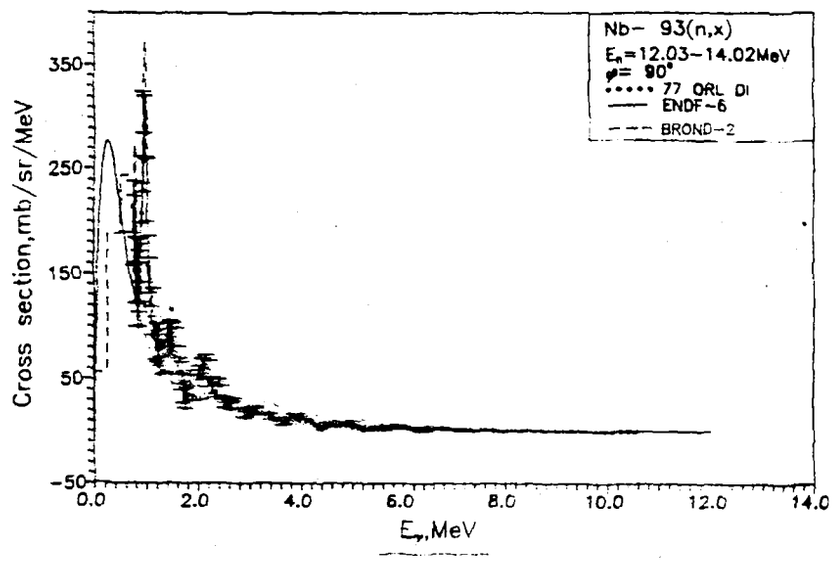
Nb- 93(n,x)
E_n=12.03-14.02MeV
φ= 90°
77 ORL DI
ENDF-6
BROND-2
Cross section,mb/sr/MeV
E_γ,MeV

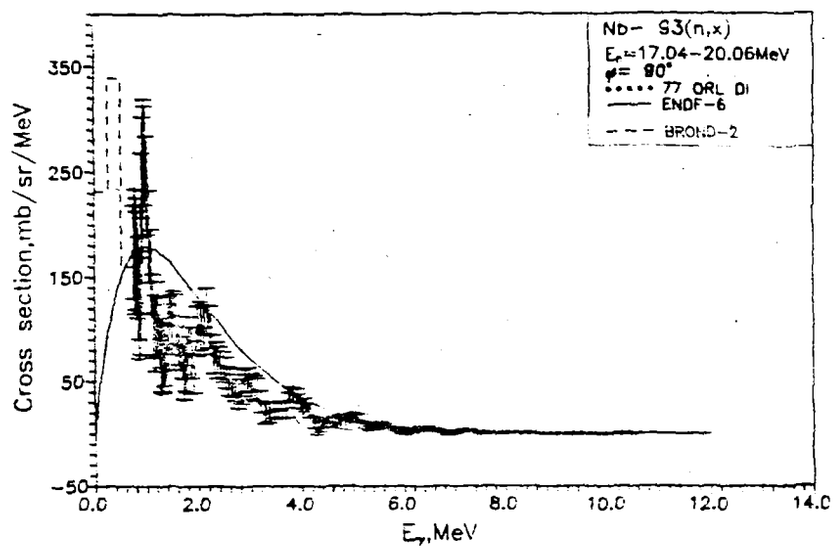
Nb- 93(n,x)
E_n=17.04-20.06MeV
φ= 90°
77 ORL DI
ENDF-6
BROND-2
Cross section,mb/sr/MeV
E_γ,MeV

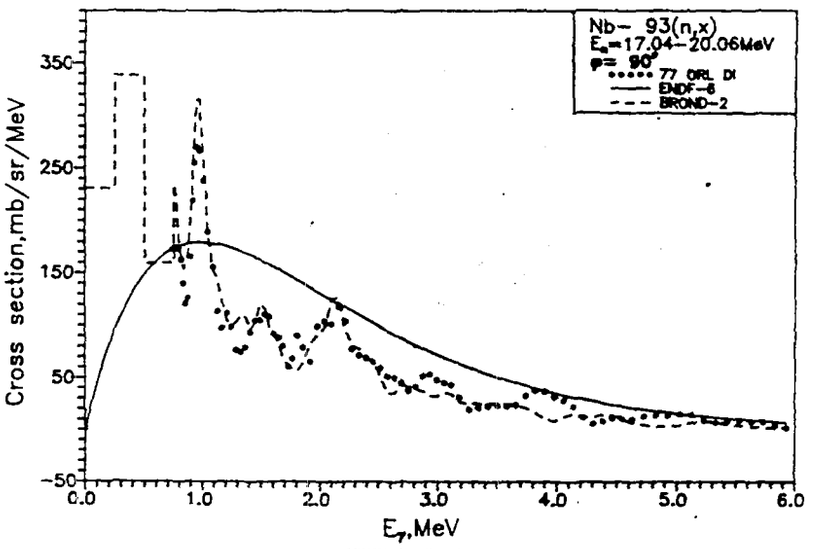
Nb- 93(n,x)
E_n=17.04-20.06MeV
φ= 90°
77 ORL DI
ENDF-6
BROND-2
Cross section,mb/sr/MeV
E_γ,MeV

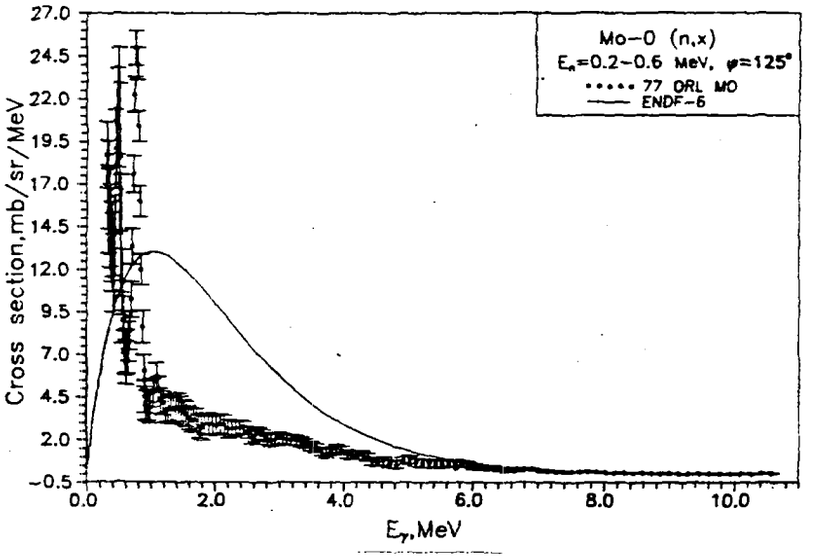
Mo-0 (n,x)
E_n=0.2-0.6 MeV, φ=125°
77 ORL MO
ENDF-6
Cross section,mb/sr/MeV
E_γ,MeV

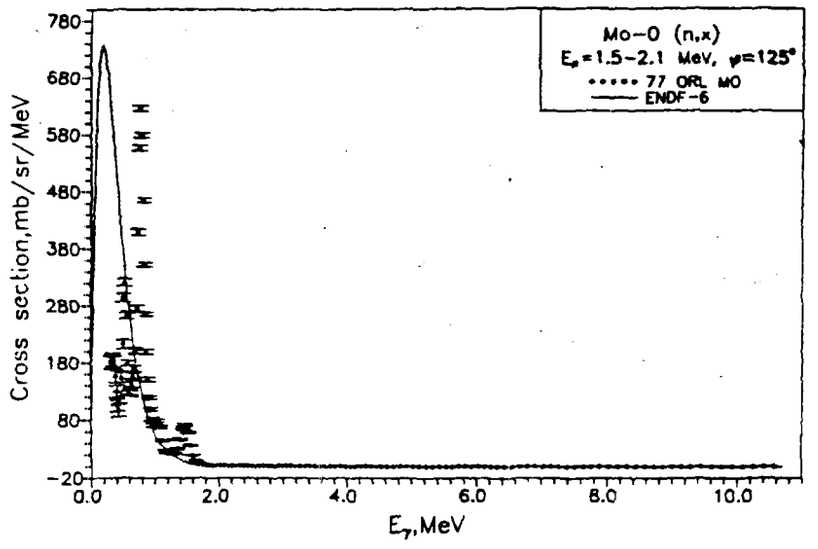
Mo-0 (n,x)
E_n=1.5-2.1 MeV, φ=125°
77 ORL MO
ENDF-6
Cross section,mb/sr/MeV
E_γ,MeV

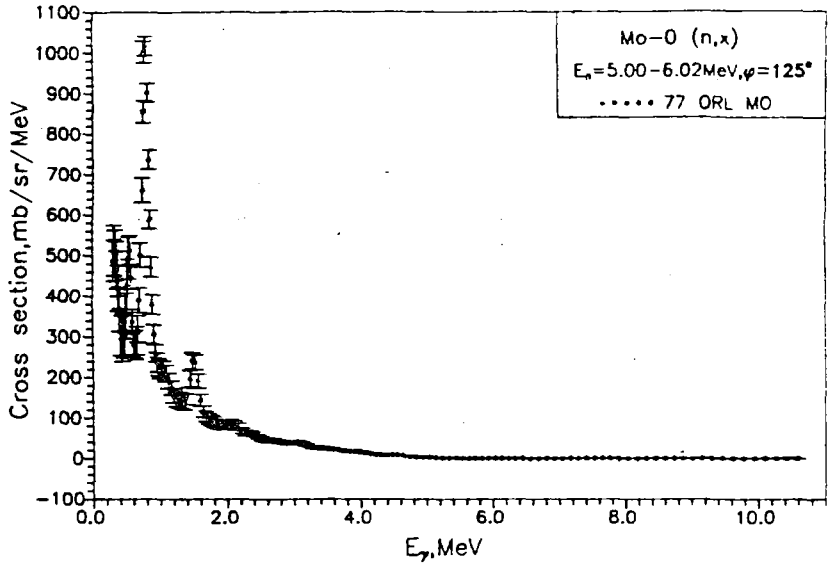
Mo-0 (n,x)
E_n=5.00-6.02MeV,φ=125°
77 ORL MO
Cross section,mb/sr/MeV
E_γ,MeV

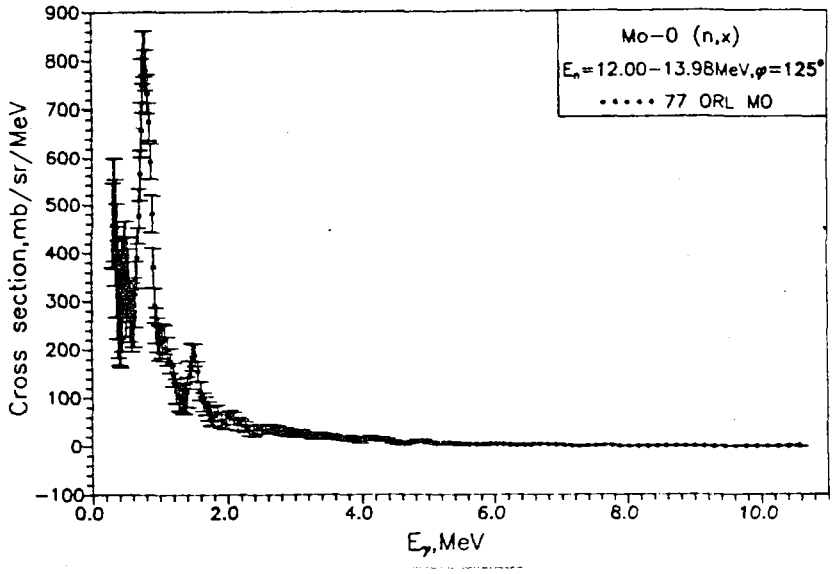
Mo-0 (n,x)
E_n=12.00-13.98MeV,φ=125°
77 ORL MO
Cross section,mb/sr/MeV
E_γ,MeV

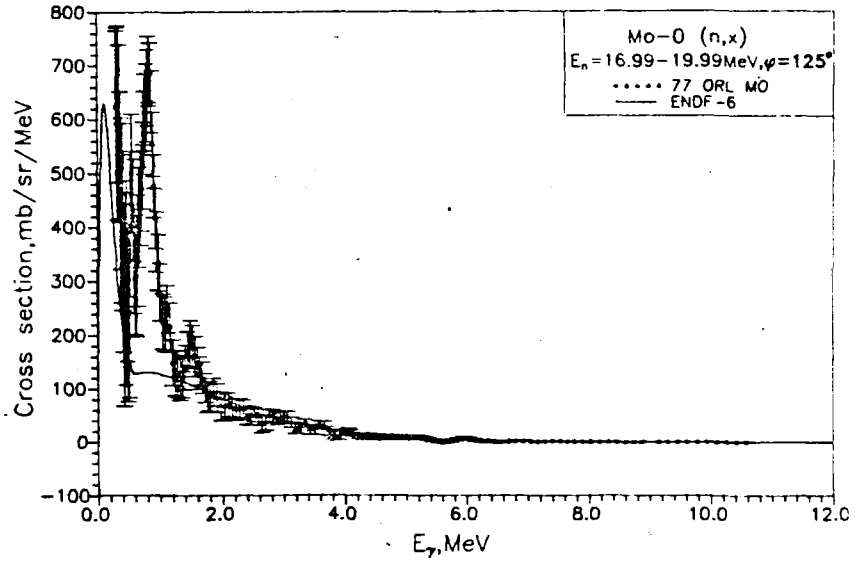
Mo-0 (n,x)
E_n=16.99-19.99MeV,φ=125°
77 ORL MO
ENDF-6
Cross section,mb/sr/MeV
E_γ,MeV

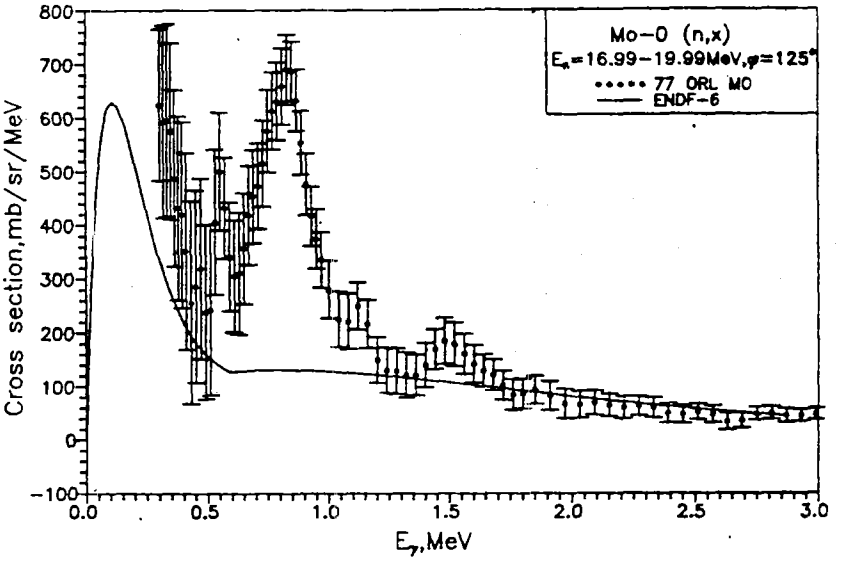
Mo-0 (n,x)
E_n=16.99-19.99MeV,φ=125°
77 ORL MO
ENDF-6
Cross section,mb/sr/MeV
E_γ,MeV

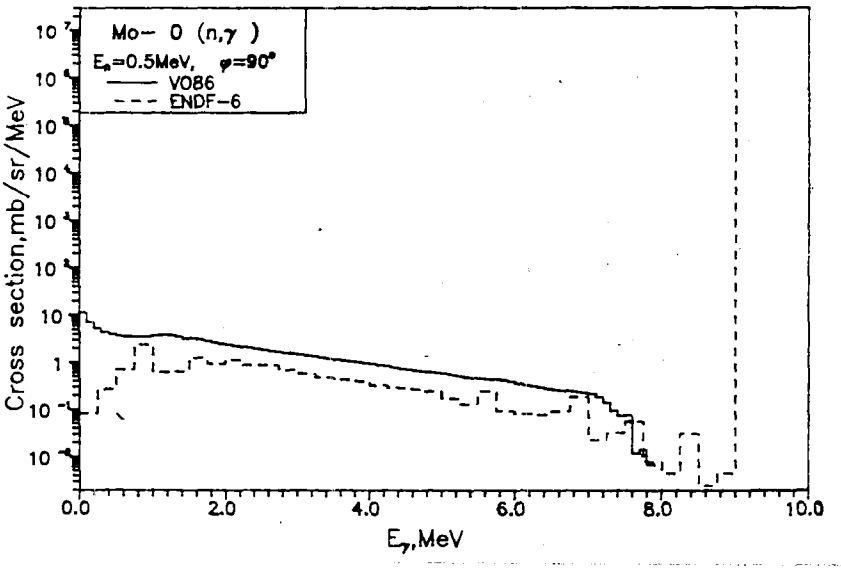
Mo- 0 (n,γ)
E_n=0.5MeV, φ=90°
V086
ENDF-6
Cross section,mb/sr/MeV
E_γ,MeV

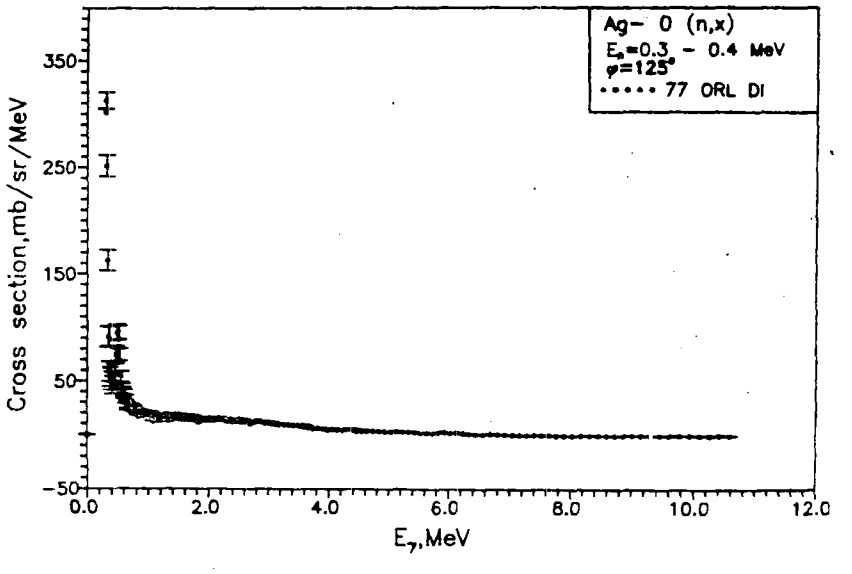
Ag- 0 (n,x)
E_n=0.3 - 0.4 MeV
φ=125°
77 ORL DI
Cross section,mb/sr/MeV
E_γ,MeV

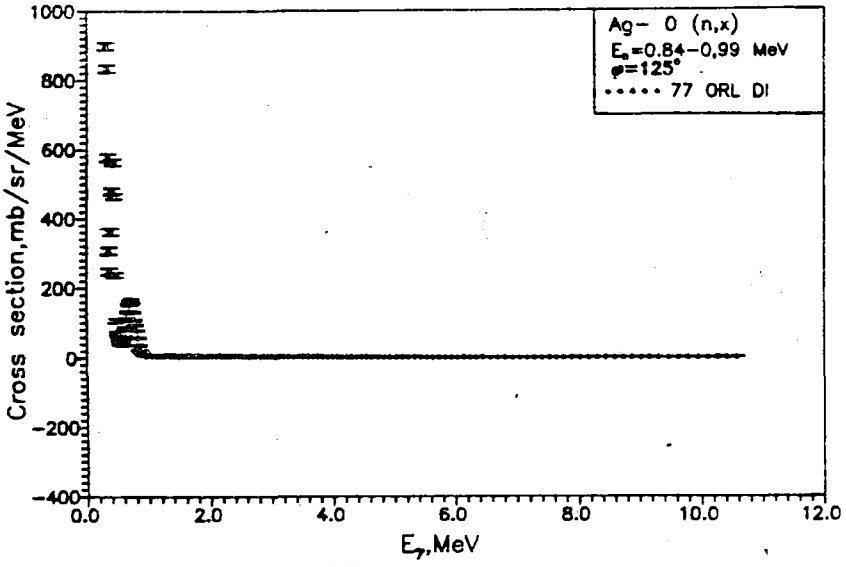
Ag- 0 (n,x)
E=0.84-0.99 MeV
φ=125°
77 ORL DI
Cross section,mb/sr/MeV
E,MeV

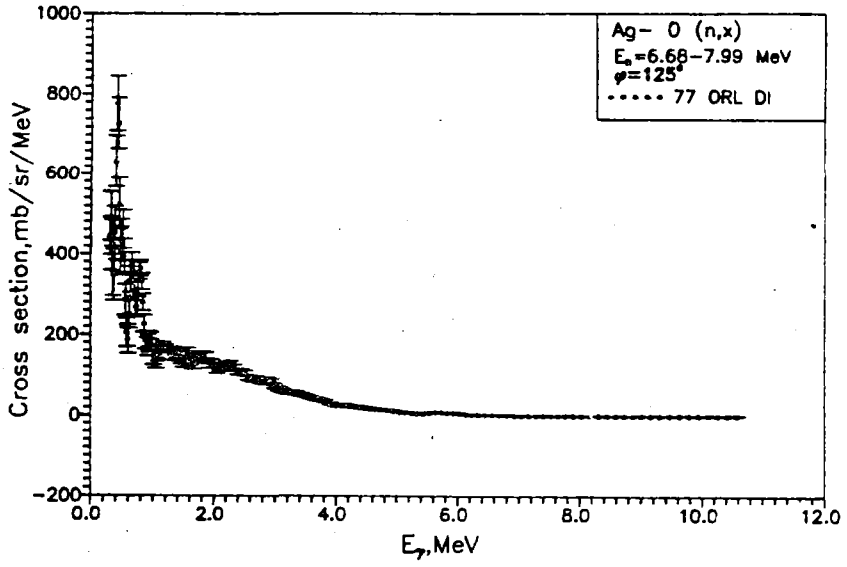
Ag- 0 (n,x)
E=6.68-7.99 MeV
φ=125°
77 ORL DI
Cross section,mb/sr/MeV
E,MeV

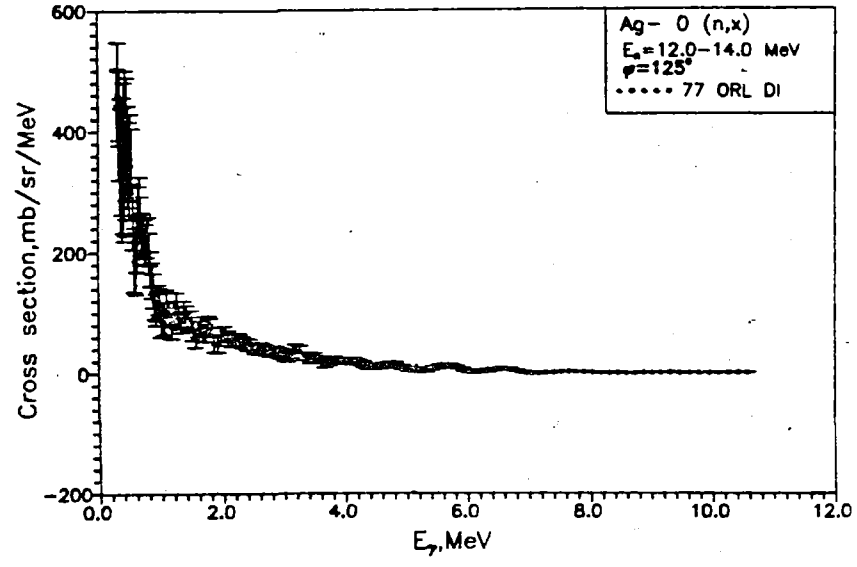
Ag- 0 (n,x)
E=12.0-14.0 MeV
φ=125°
77 ORL DI
Cross section,mb/sr/MeV
E,MeV

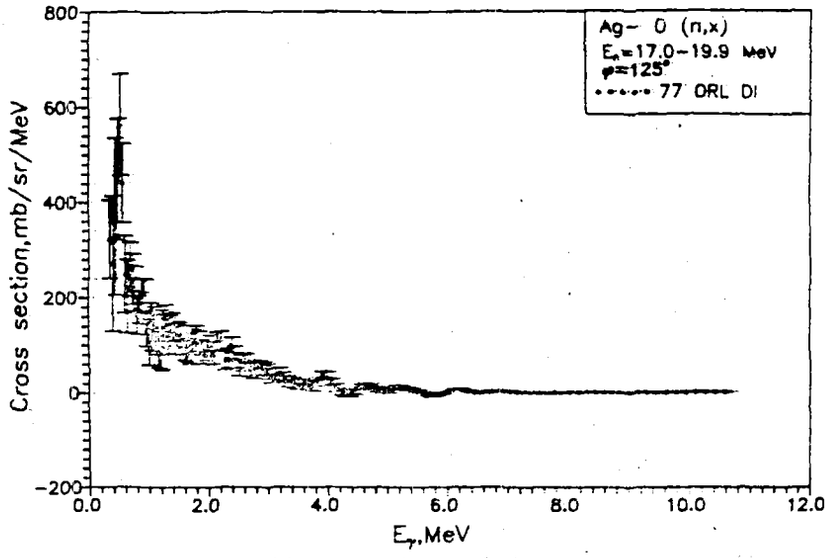
Ag- 0 (n,x)
E_n=17.0-19.9 MeV
φ=125°
77 ORL DI
Cross section,mb/sr/MeV
E_γ,MeV

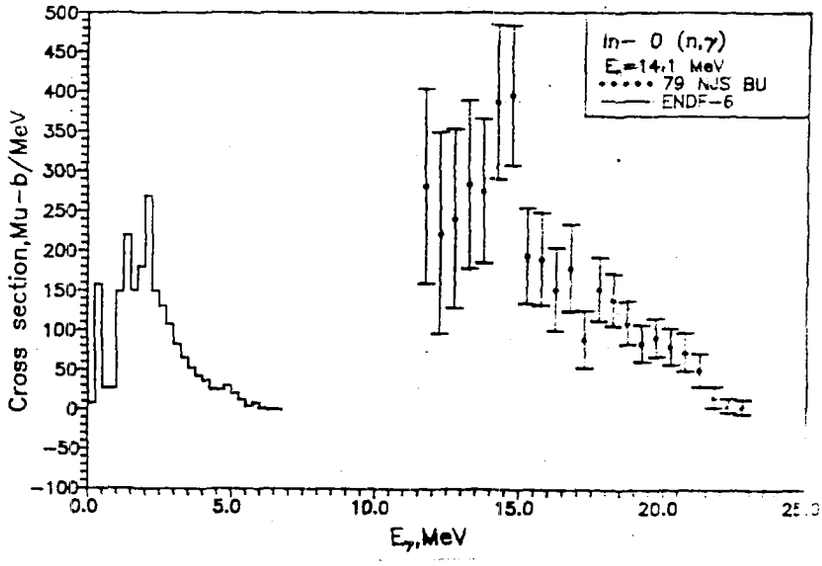
In- 0 (n,γ)
E_n=14.1 MeV
79 NJS BU
ENDF-6
Cross section,Mu-b/MeV
E_γ,MeV

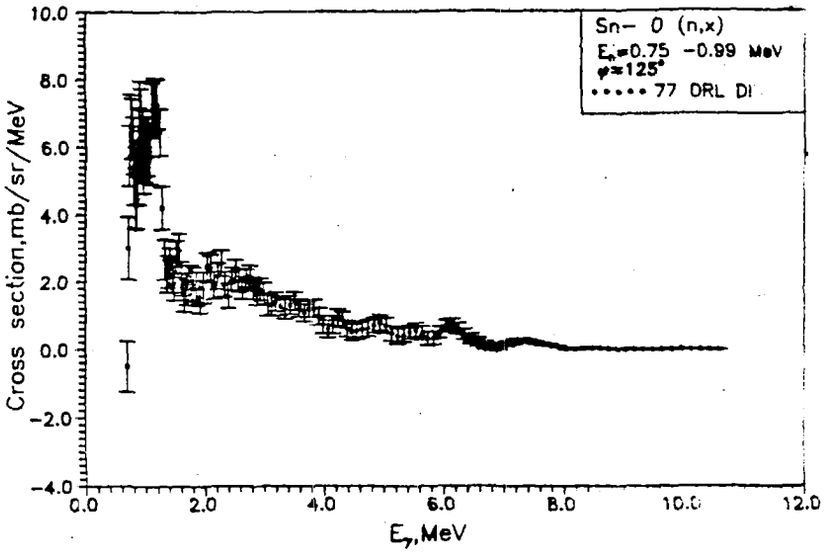
Sn- 0 (n,x)
E_n=0.75 -0.99 MeV
φ=125°
77 ORL DI
Cross section,mb/sr/MeV
E_γ,MeV

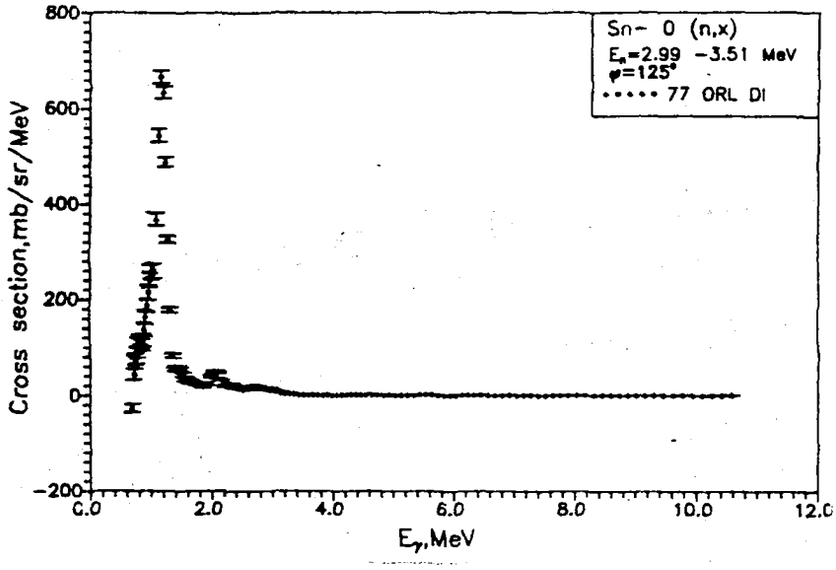
Sn- 0 (n,x)
E_n=2.99 -3.51 MeV
φ=125°
••••• 77 ORL DI
Cross section,mb/sr/MeV
E_γ,MeV

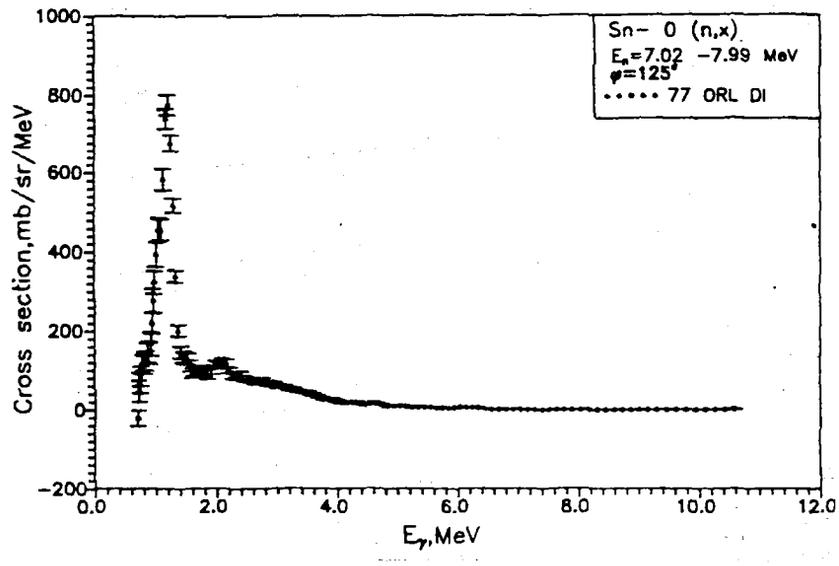
Sn- 0 (n,x)
E_n=7.02 -7.99 MeV
φ=125°
••••• 77 ORL DI
Cross section,mb/sr/MeV
E_γ,MeV

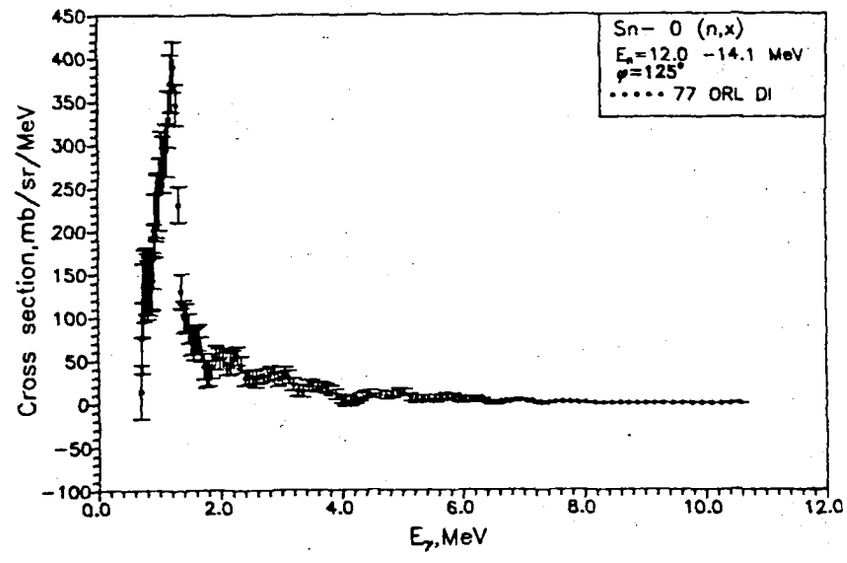
Sn- 0 (n,x)
E_n=12.0 -14.1 MeV
φ=125°
••••• 77 ORL DI
Cross section,mb/sr/MeV
E_γ,MeV

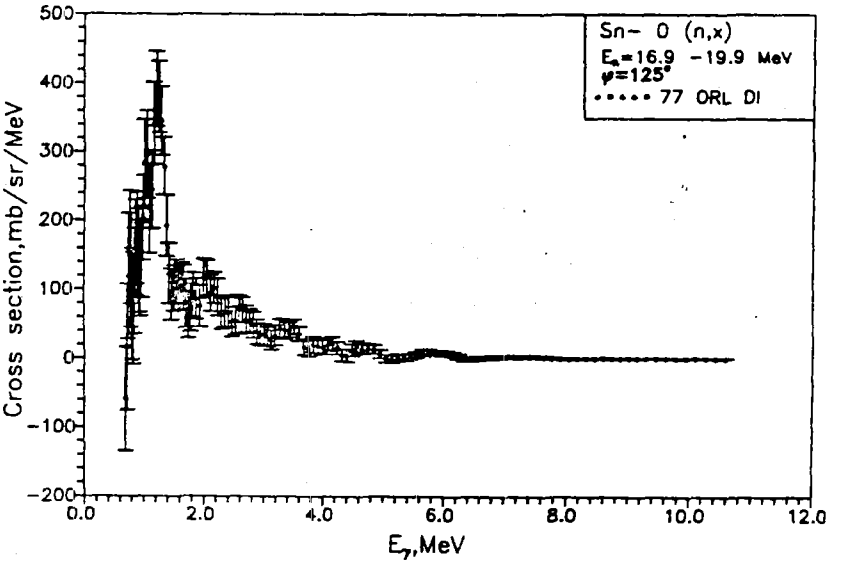
Sn- 0 (n,x)
E_n=16.9 -19.9 MeV
φ=125°
77 ORL DI
Cross section,mb/sr/MeV
E_γ,MeV

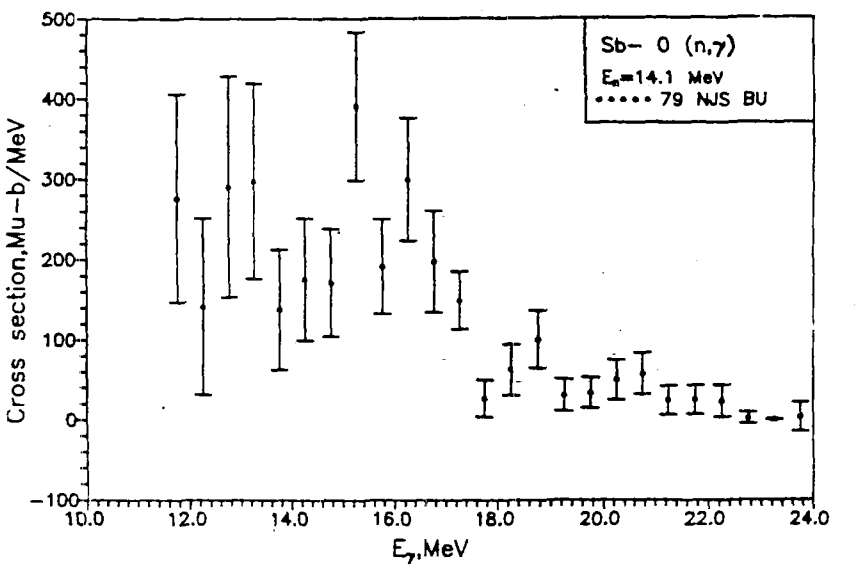
Sb- 0 (n,γ)
E_n=14.1 MeV
79 NJS BU
Cross section,Mu-b/MeV
E_γ,MeV

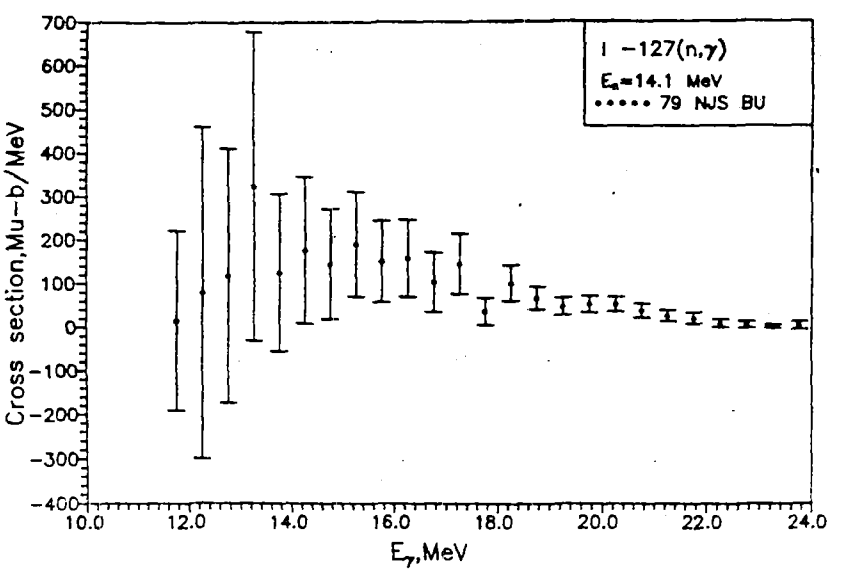
I -127(n,γ)
E_n=14.1 MeV
79 NJS BU
Cross section,Mu-b/MeV
E_γ,MeV

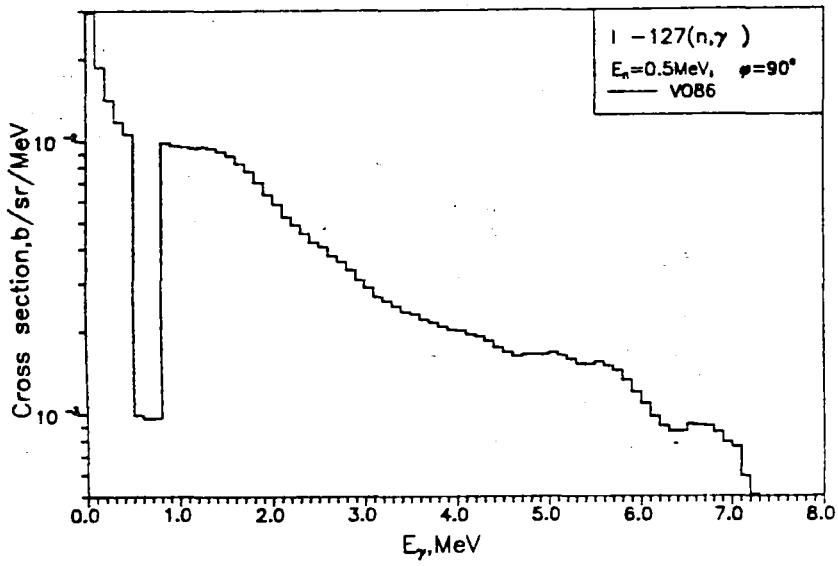
I −127(n,γ)
E_n=0.5MeV, φ=90°
V086
Cross section,b/sr/MeV
E_γ,MeV

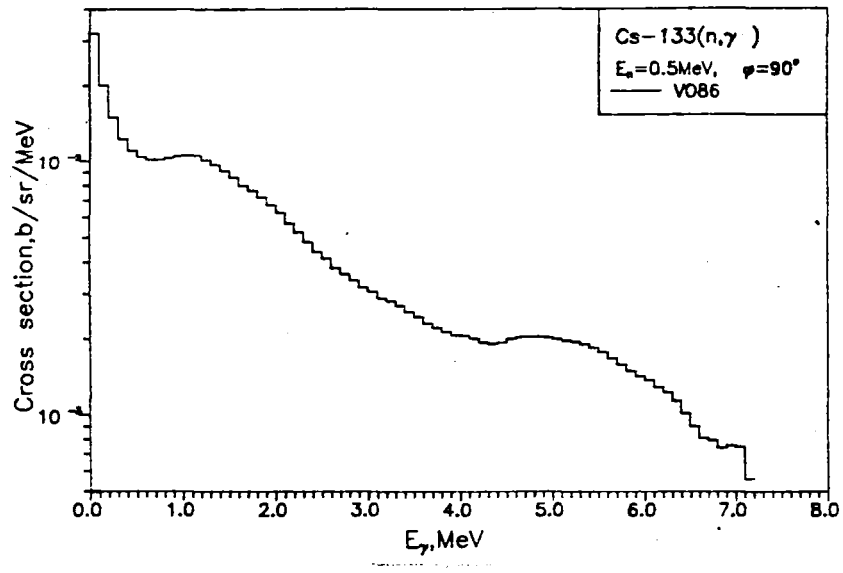
Cs−133(n,γ)
E_n=0.5MeV, φ=90°
V086
Cross section,b/sr/MeV
E_γ,MeV

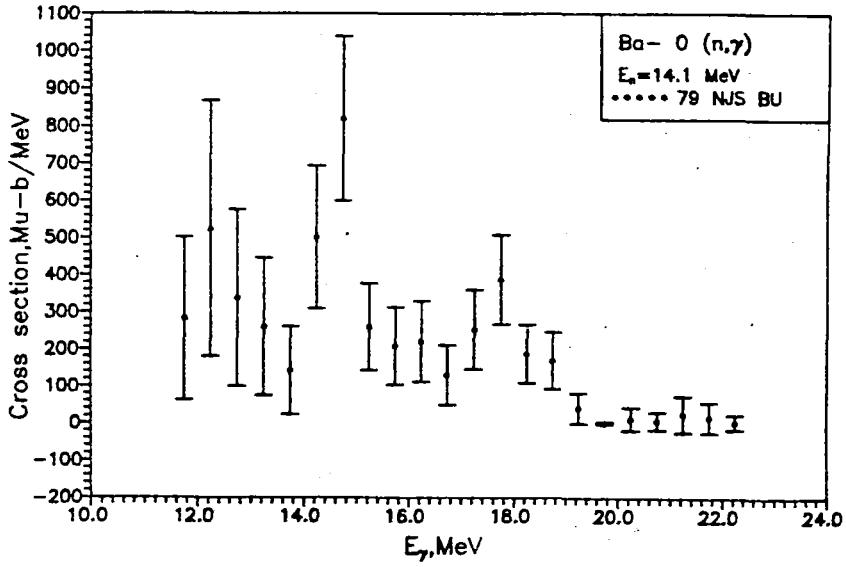
Ba− 0 (n,γ)
E_n=14.1 MeV
79 NJS BU
Cross section,Mu−b/MeV
E_γ,MeV

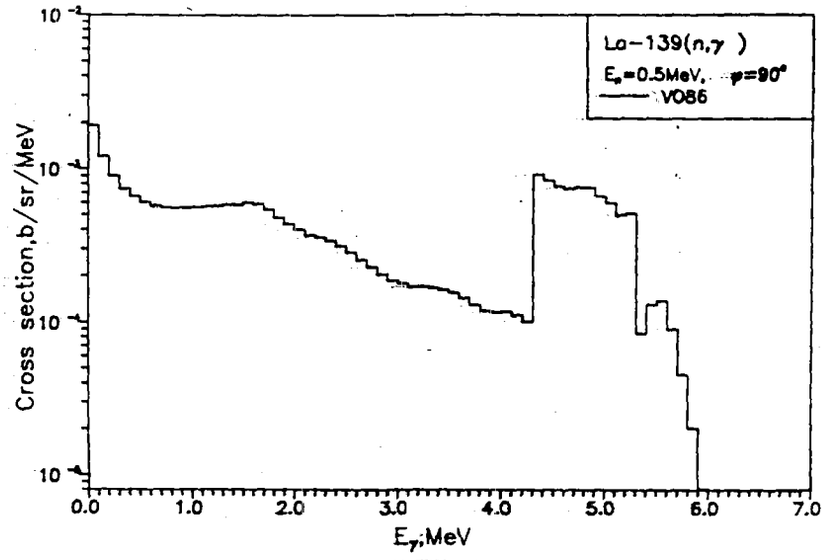
La-139(n,γ)
E=0.5MeV, φ=90°
V086
Cross section,b/sr/MeV
E_γ,MeV

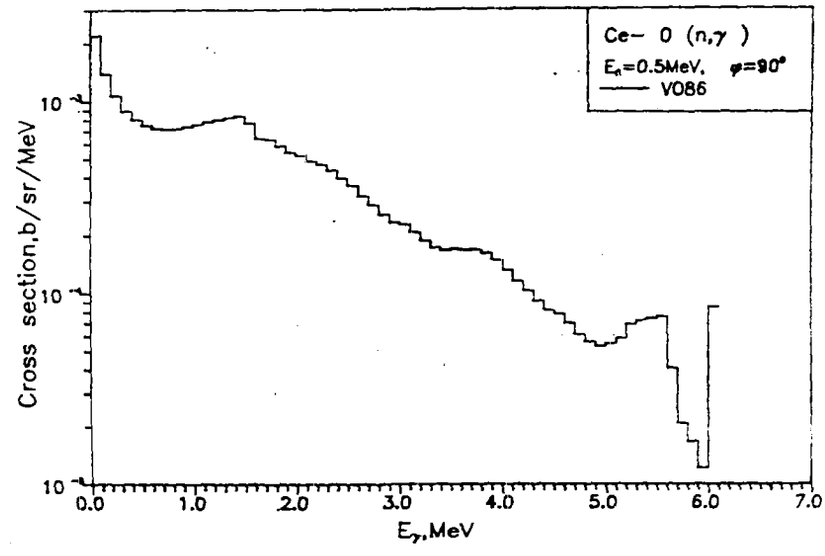
Ce- 0 (n,γ)
E=0.5MeV, φ=90°
V086
Cross section,b/sr/MeV
E_γ,MeV

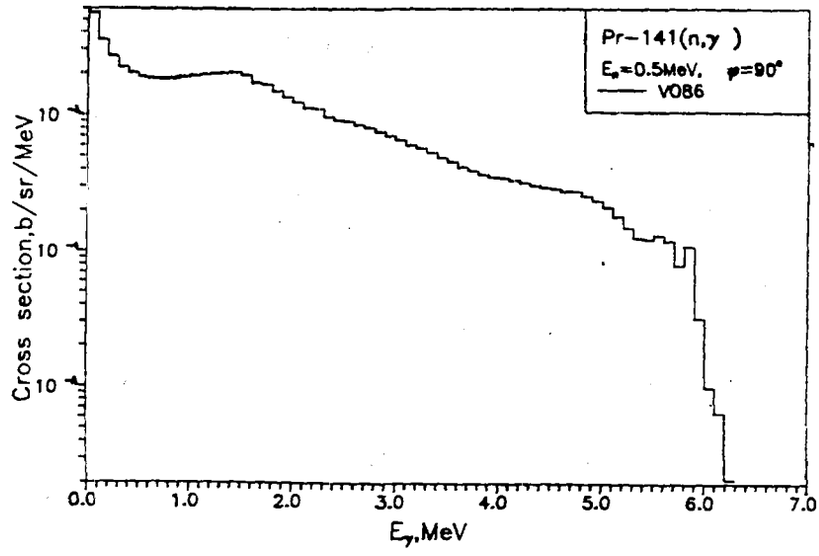
Pr-141(n,γ)
E=0.5MeV, φ=90°
V086
Cross section,b/sr/MeV
E_γ,MeV

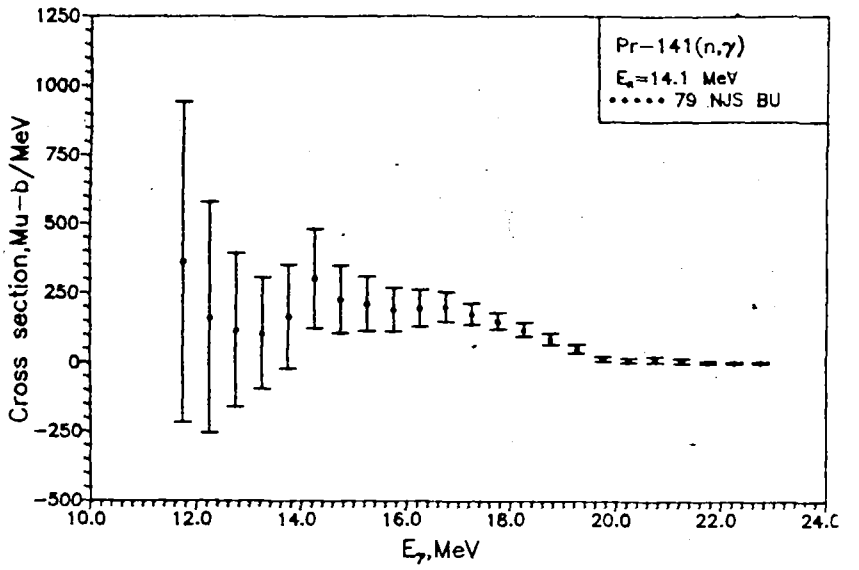
Pr-141(n,γ)
E_n=14.1 MeV
79 NJS BU
Cross section,Mu-b/MeV
E_γ,MeV

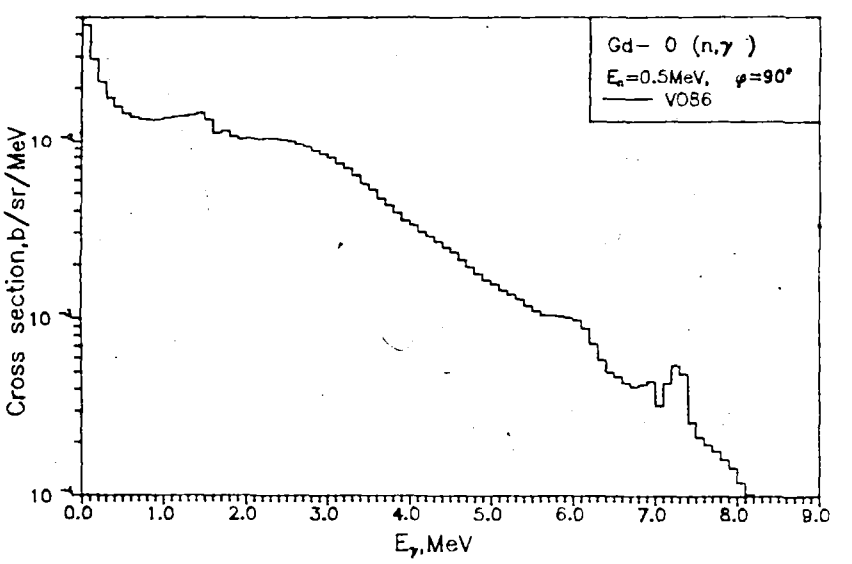
Gd- 0 (n,γ)
E_n=0.5MeV, φ=90°
V086
Cross section,b/sr/MeV
E_γ,MeV

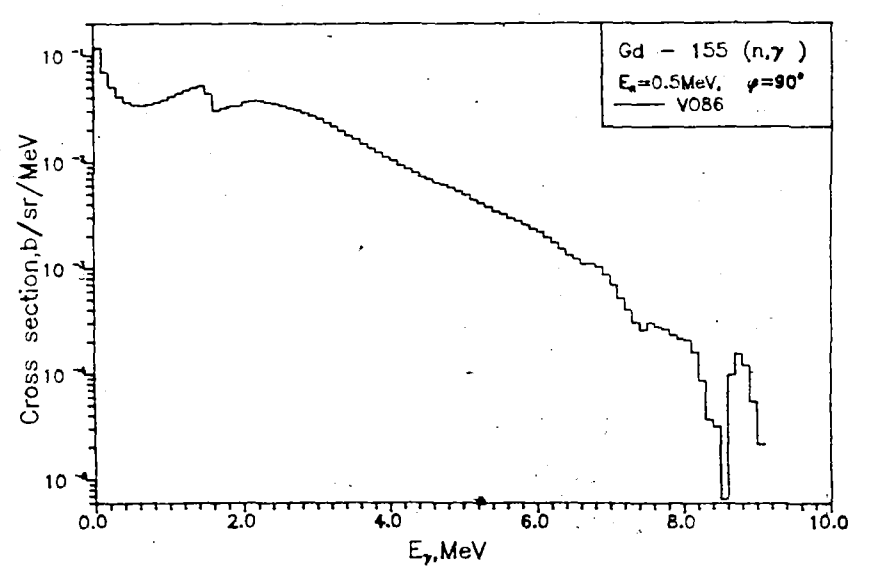
Gd - 155 (n,γ)
E_n=0.5MeV, φ=90°
V086
Cross section,b/sr/MeV
E_γ,MeV

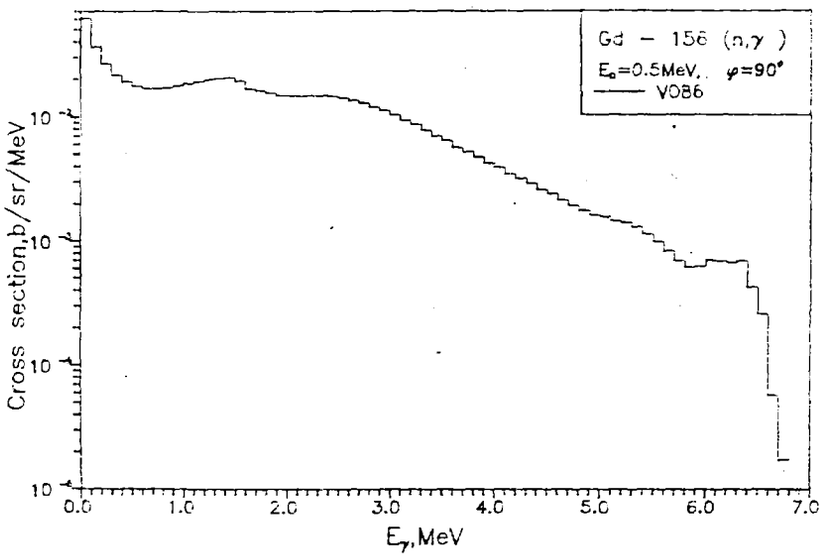
Gd – 156 (n,γ)
E₀=0.5MeV, φ=90°
V086
Cross section,b/sr/MeV
Eγ,MeV

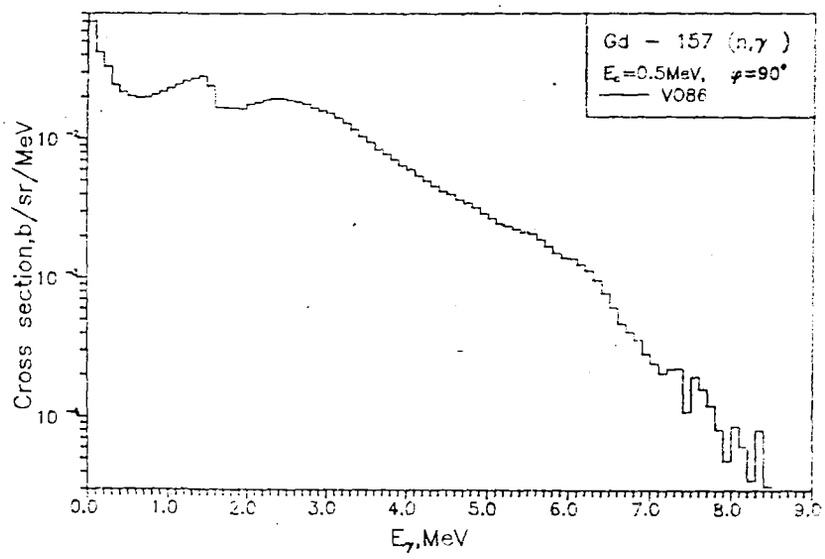
Gd – 157 (n,γ)
E₀=0.5MeV, φ=90°
V086
Cross section,b/sr/MeV
Eγ,MeV

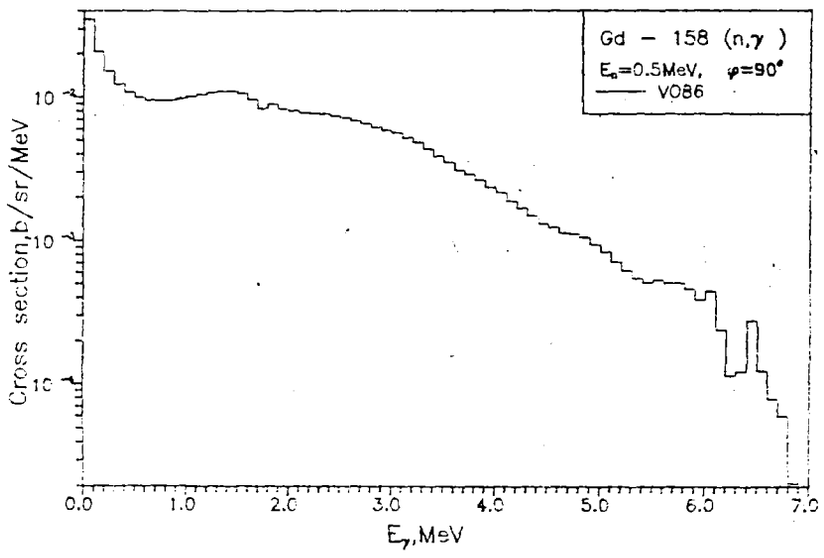
Gd – 158 (n,γ)
E₀=0.5MeV, φ=90°
V086
Cross section,b/sr/MeV
Eγ,MeV

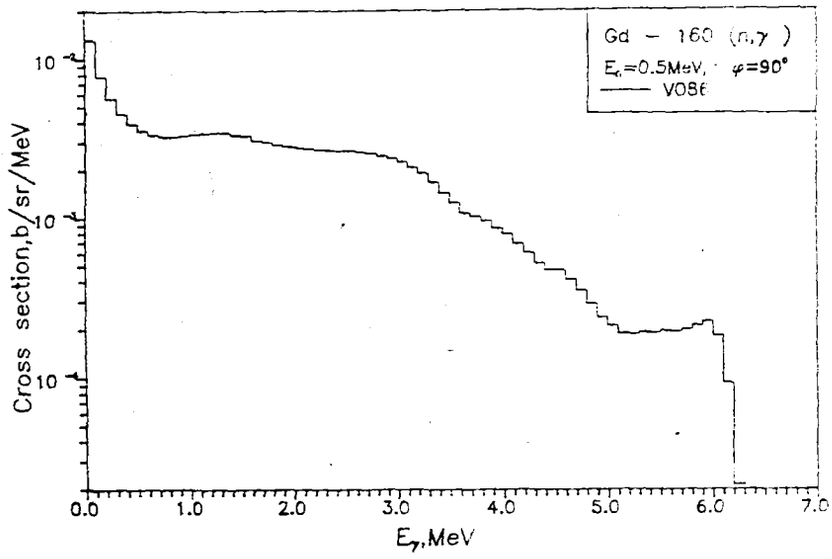
Gd – 160 (n,γ)
E_n=0.5MeV, φ=90°
V086
Cross section,b/sr/MeV
E_γ,MeV

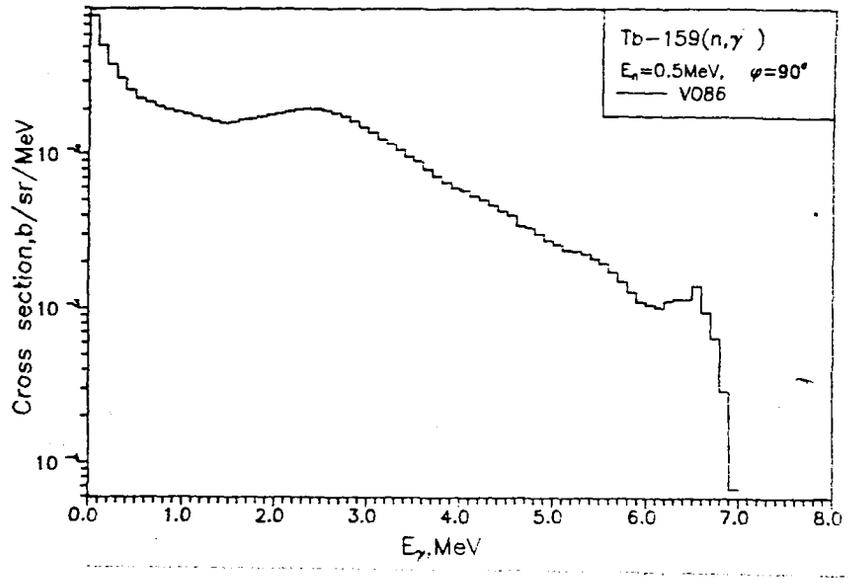
Tb–159(n,γ)
E_n=0.5MeV, φ=90°
V086
Cross section,b/sr/MeV
E_γ,MeV

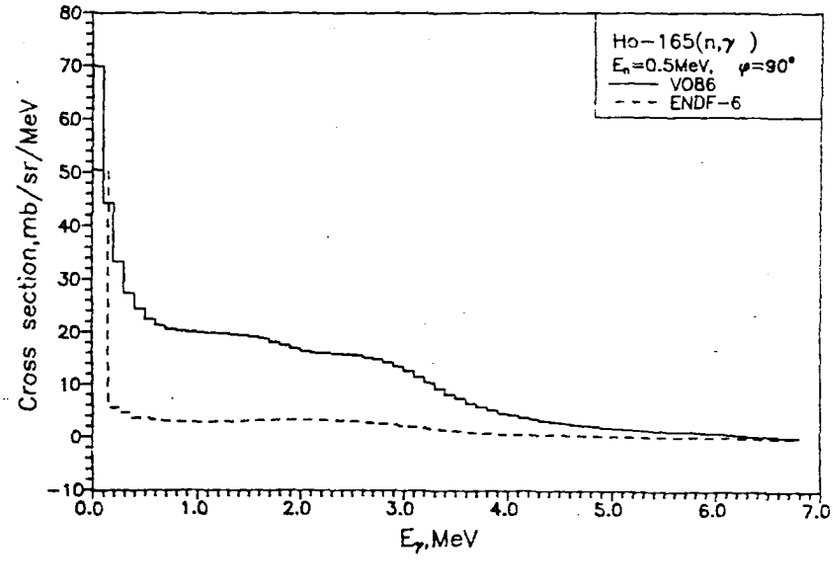
Ho–165(n,γ)
E_n=0.5MeV, φ=90°
V086
ENDF–6
Cross section,mb/sr/MeV
E_γ,MeV

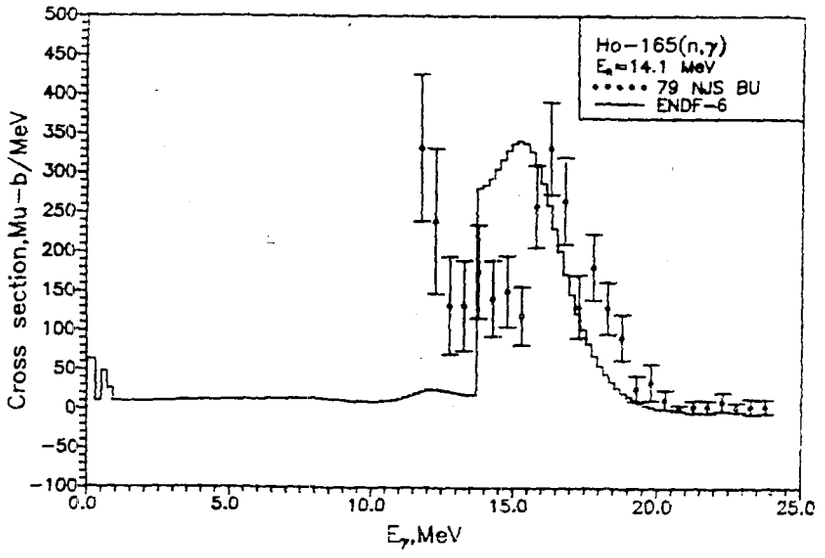
Ho-165(n,γ)
E_n=14.1 MeV
79 NJS BU
ENDF-6
Cross section,Mu-b/MeV
E_γ,MeV

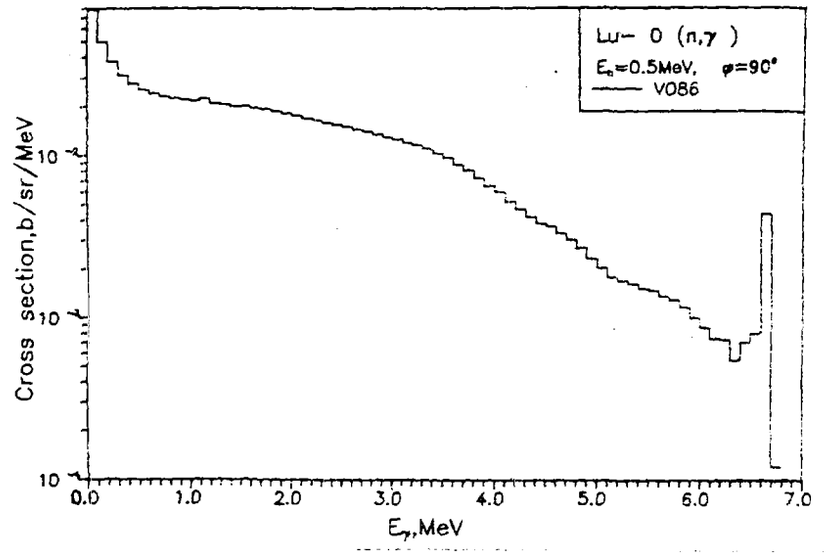
Lu- 0 (n,γ)
E_n=0.5MeV, φ=90°
V086
Cross section,b/sr/MeV
E_γ,MeV

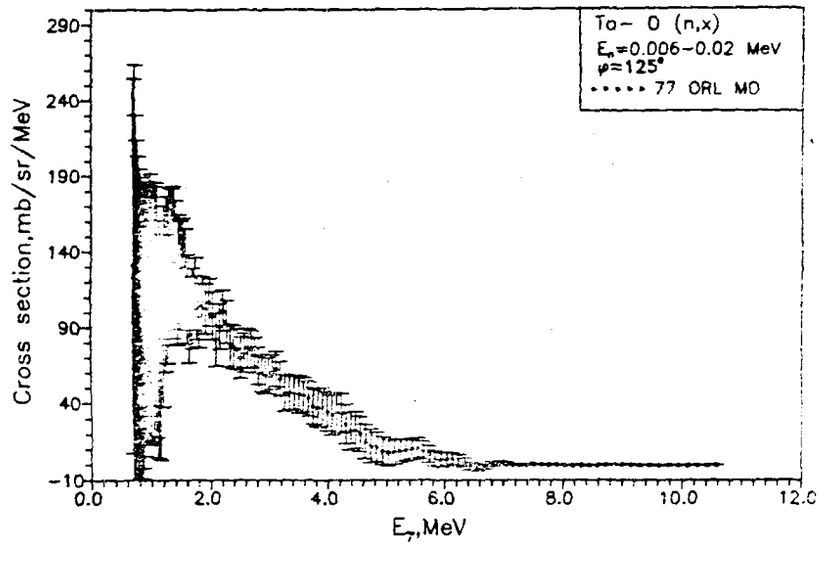
To- 0 (n,x)
E_n=0.006-0.02 MeV
φ=125°
77 ORL MO
Cross section,mb/sr/MeV
E_γ,MeV

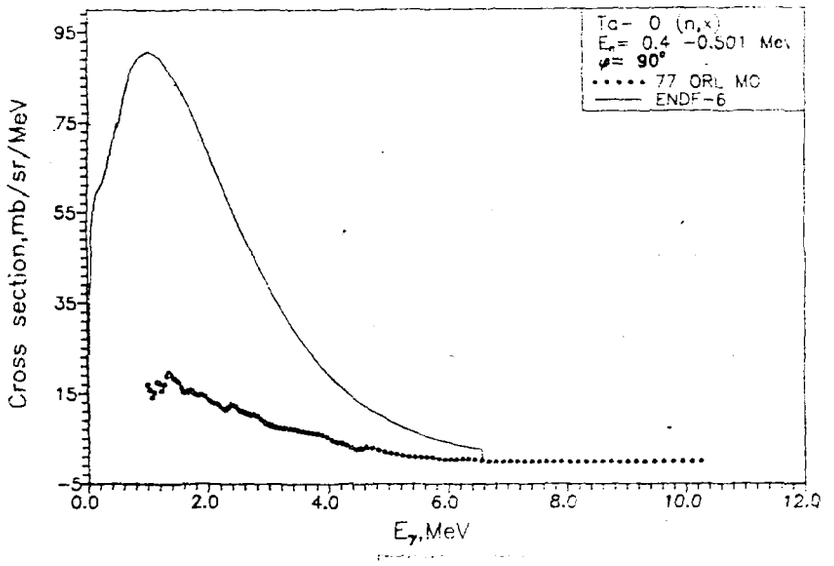
Ta- 0 (n,x)
E_n= 0.4 -0.501 MeV
φ= 90°
77 ORL MO
ENDF-6
Cross section,mb/sr/MeV
E_γ,MeV

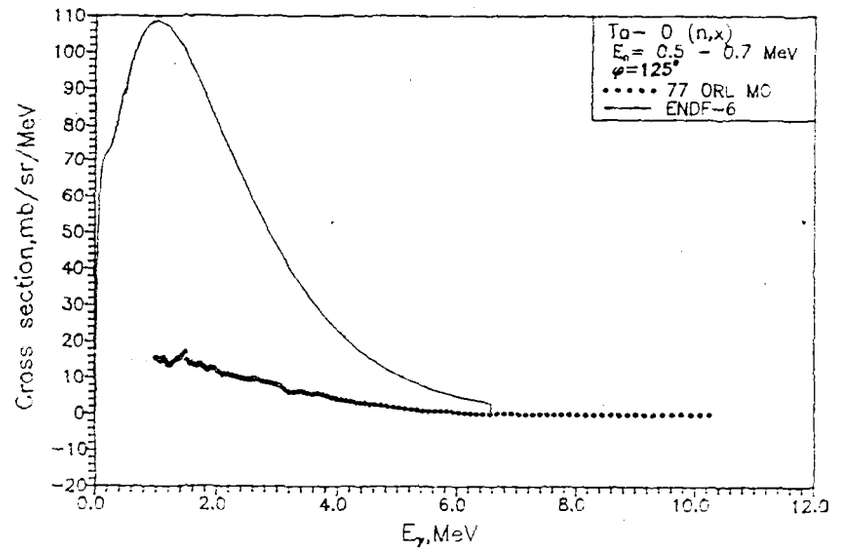
Ta- 0 (n,x)
E_n= 0.5 - 0.7 MeV
φ=125°
77 ORL MO
ENDF-6
Cross section,mb/sr/MeV
E_γ,MeV

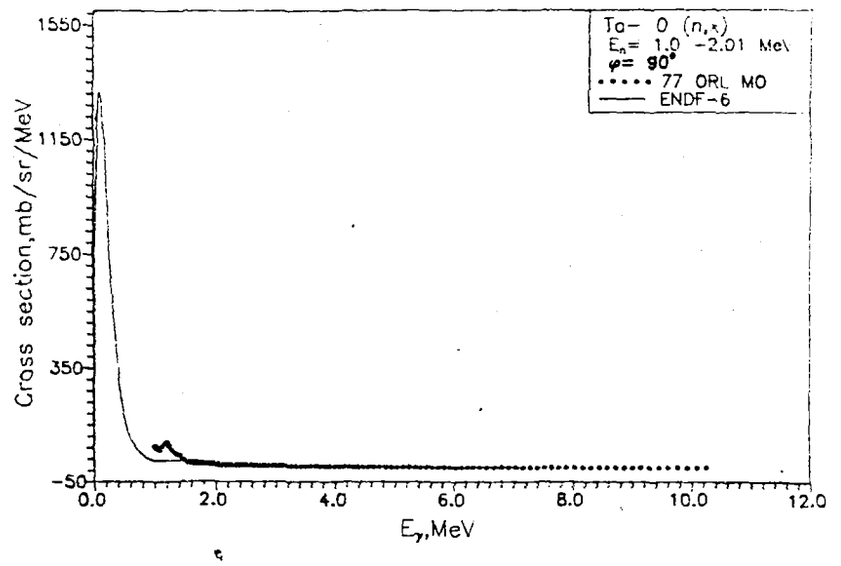
Ta- 0 (n,x)
E_n= 1.0 -2.01 MeV
φ= 90°
77 ORL MO
ENDF-6
Cross section,mb/sr/MeV
E_γ,MeV

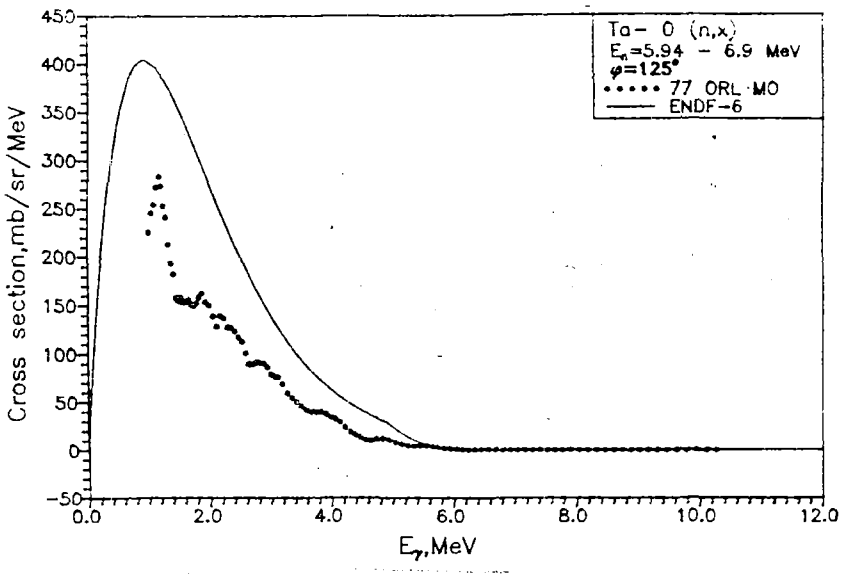
Ta- 0 (n,x)
E_n=5.94 - 6.9 MeV
φ=125°
77 ORL MO
ENDF-6
Cross section,mb/sr/MeV
E_γ,MeV

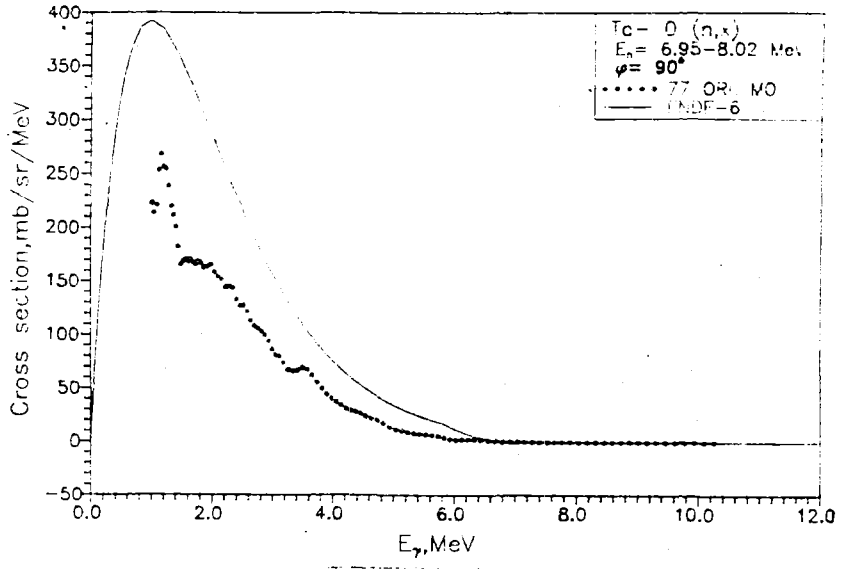
Tc- 0 (n,x)
E_n= 6.95-8.02 MeV
φ= 90°
77 ORL MO
ENDF-6
Cross section,mb/sr/MeV
E_γ,MeV

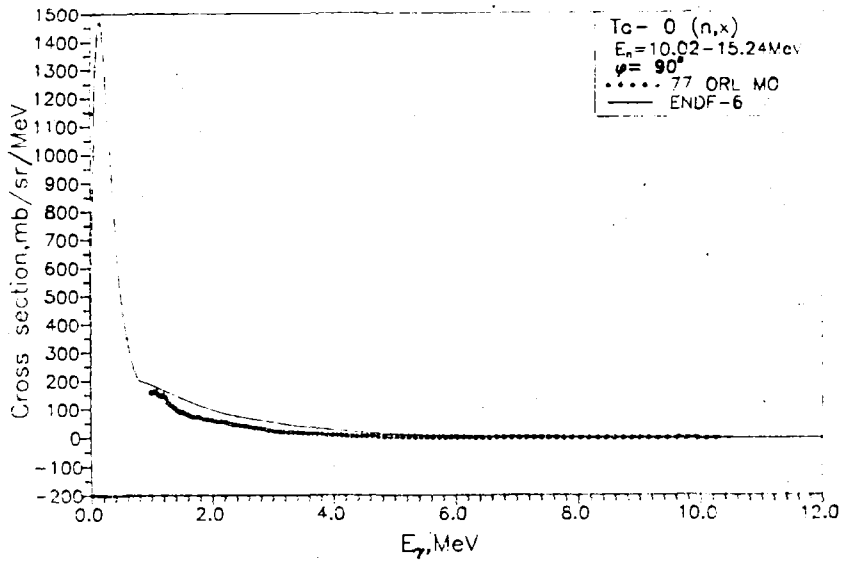
Tc- 0 (n,x)
E_n=10.02-15.24MeV
φ= 90°
77 ORL MO
ENDF-6
Cross section,mb/sr/MeV
E_γ,MeV

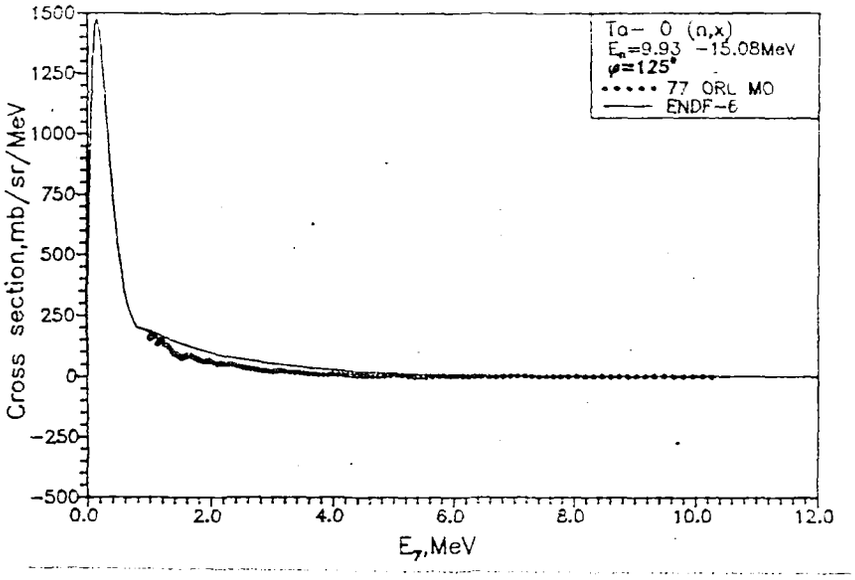
Ta- 0 (n,x)
E_n=9.93 -15.08MeV
φ=125°
77 ORL MO
ENDF-6
Cross section,mb/sr/MeV
E_γ,MeV

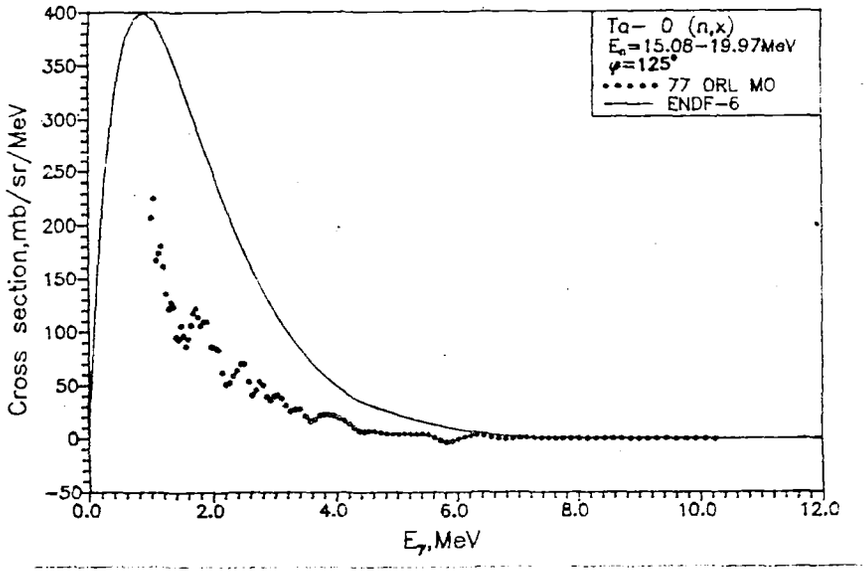
Ta- 0 (n,x)
E_n=15.08-19.97MeV
φ=125°
77 ORL MO
ENDF-6
Cross section,mb/sr/MeV
E_γ,MeV

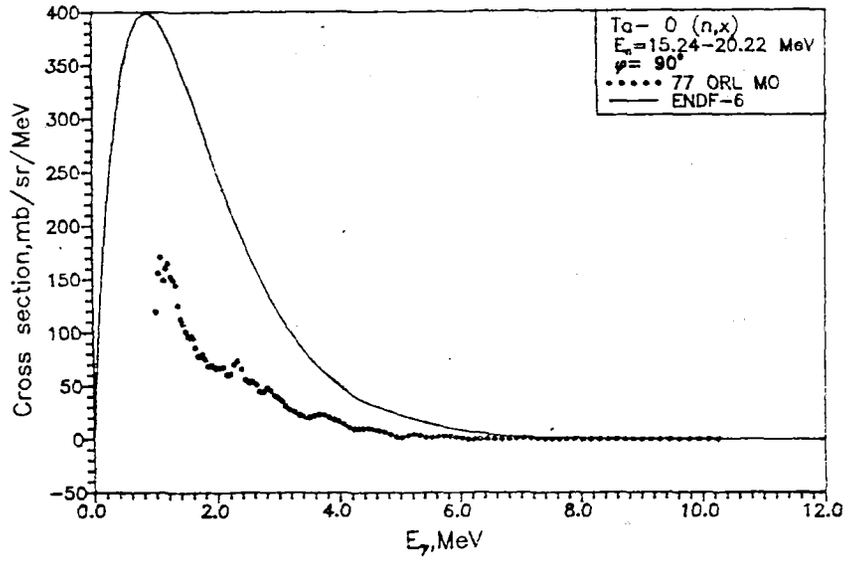
Ta- 0 (n,x)
E_n=15.24-20.22 MeV
φ= 90°
77 ORL MO
ENDF-6
Cross section,mb/sr/MeV
E_γ,MeV

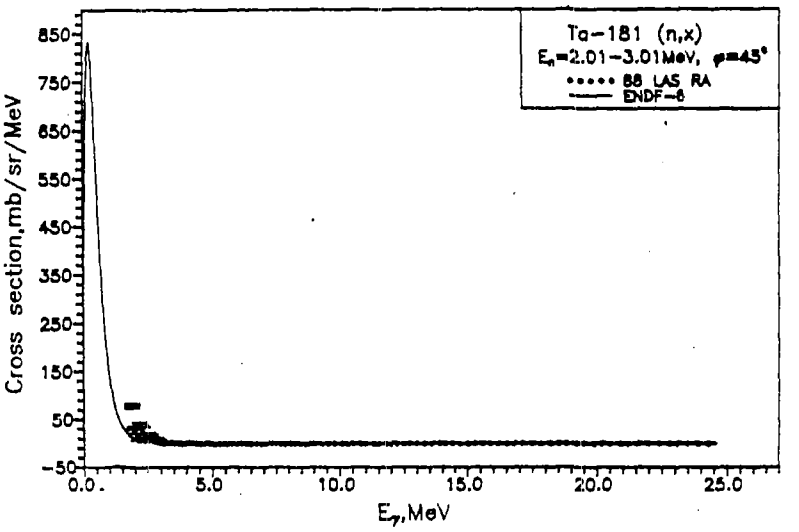
Ta-181 (n,x)
E_n=2.01-3.01MeV, φ=45°
88 LAS RA
ENDF-6
Cross section,mb/sr/MeV
E_γ,MeV

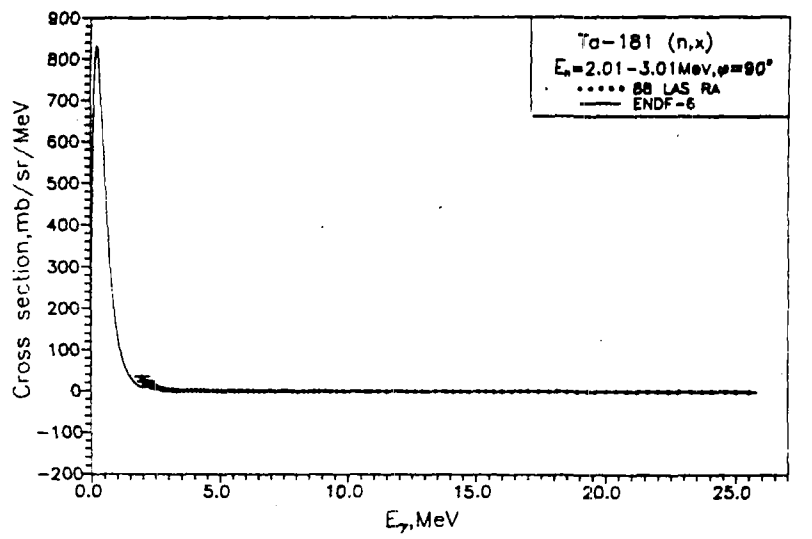
Ta-181 (n,x)
E_n=2.01-3.01MeV,φ=90°
88 LAS RA
ENDF-6
Cross section,mb/sr/MeV
E_γ,MeV

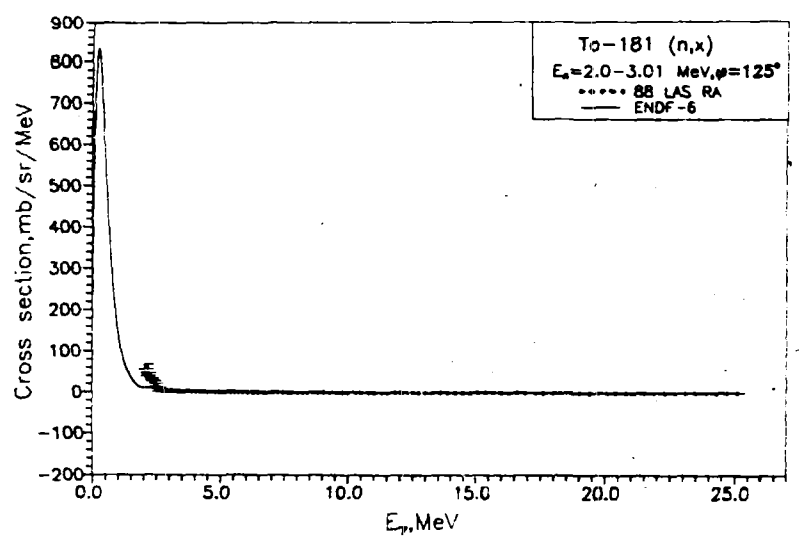
Ta-181 (n,x)
E_n=2.0-3.01 MeV,φ=125°
88 LAS RA
ENDF-6
Cross section,mb/sr/MeV
E_γ,MeV

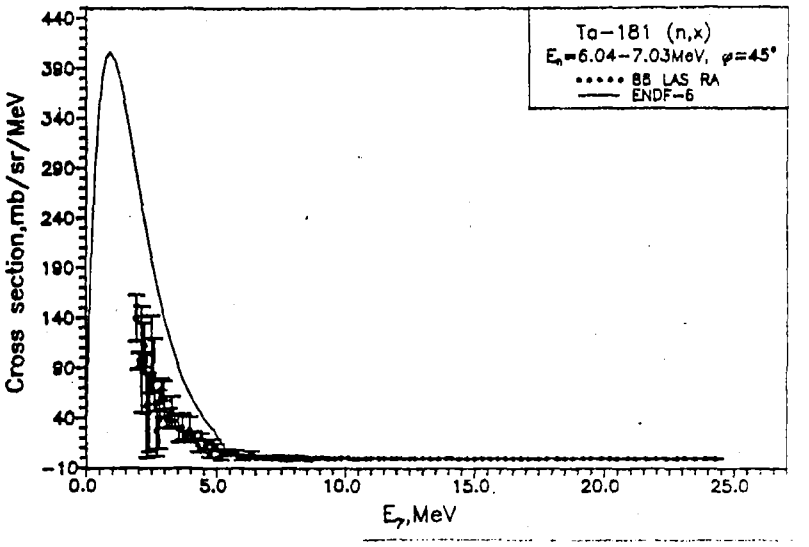
Ta-181 (n,x)
E_n=6.04-7.03MeV, φ=45°
88 LAS RA
ENDF-6
Cross section,mb/sr/MeV
E_γ,MeV

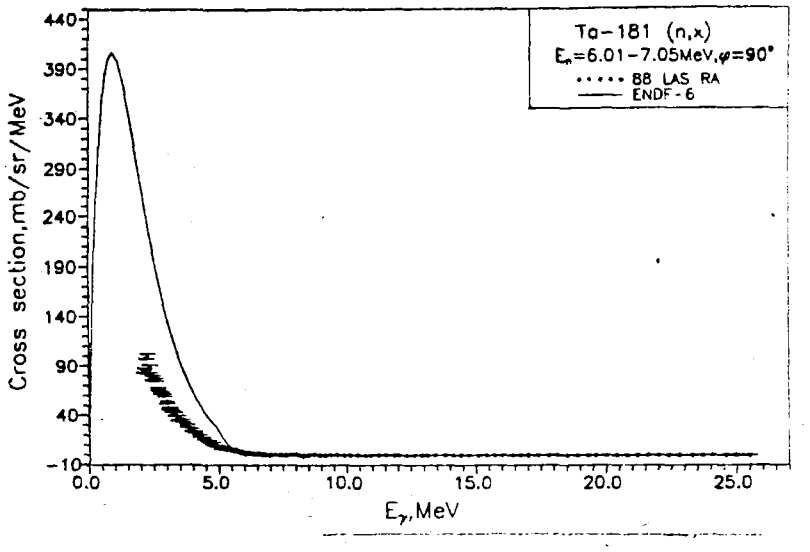
Ta-181 (n,x)
E_n=6.01-7.05MeV,φ=90°
88 LAS RA
ENDF-6
Cross section,mb/sr/MeV
E_γ,MeV

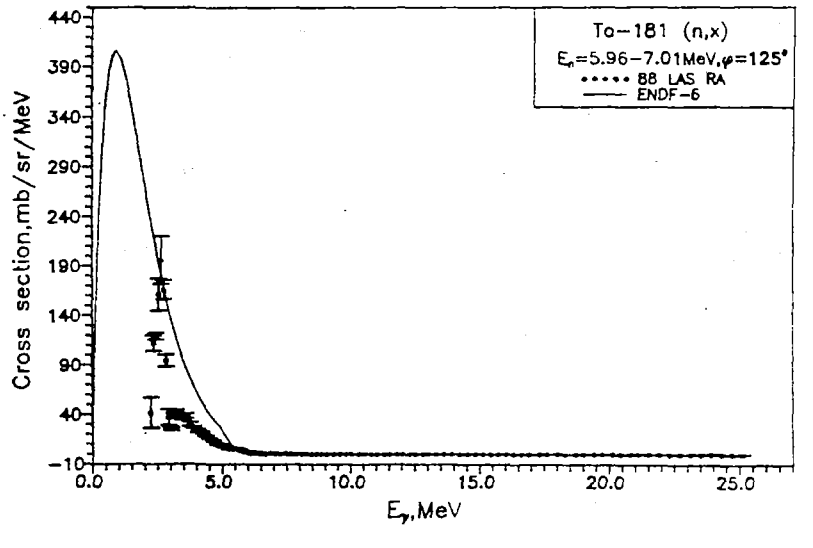
Ta-181 (n,x)
E_n=5.96-7.01MeV,φ=125°
88 LAS RA
ENDF-6
Cross section,mb/sr/MeV
E_γ,MeV

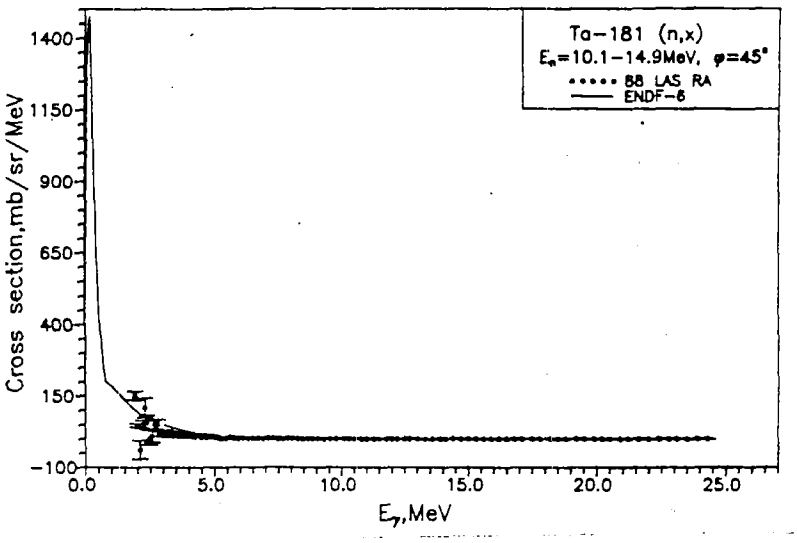
Ta−181 (n,x)
E_n=10.1−14.9MeV, φ=45°
88 LAS RA
ENDF−6
Cross section,mb/sr/MeV
1400
1150
900
650
400
150
−100
0.0
5.0
10.0
15.0
20.0
25.0
E_γ,MeV

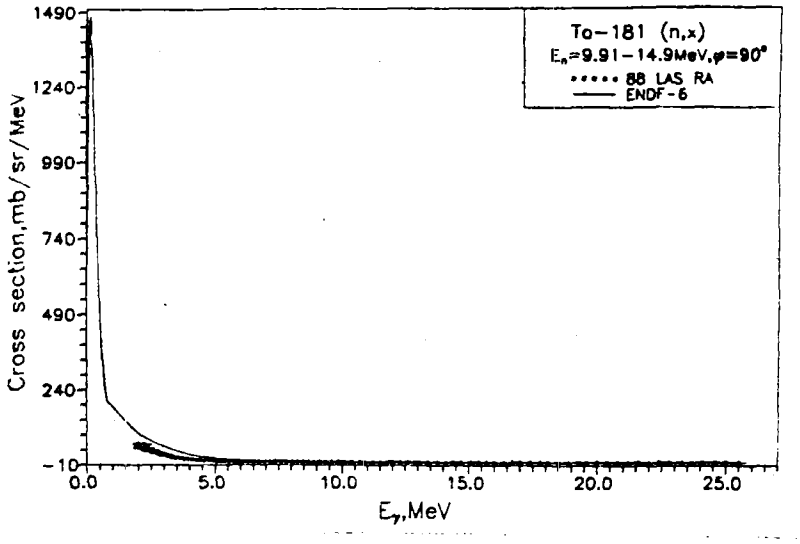
Ta−181 (n,x)
E_n=9.91−14.9MeV, φ=90°
88 LAS RA
ENDF−6
Cross section,mb/sr/MeV
1490
1240
990
740
490
240
−10
0.0
5.0
10.0
15.0
20.0
25.0
E_γ,MeV

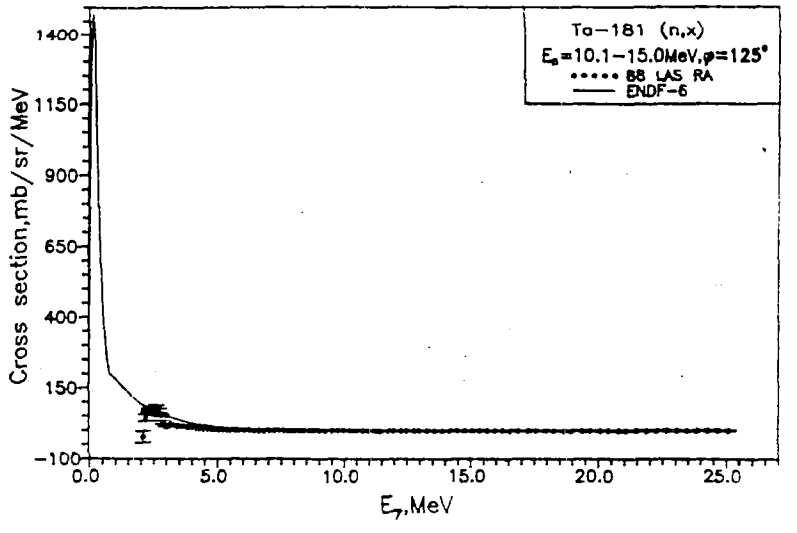
Ta−181 (n,x)
E_n=10.1−15.0MeV, φ=125°
88 LAS RA
ENDF−6
Cross section,mb/sr/MeV
1400
1150
900
650
400
150
−100
0.0
5.0
10.0
15.0
20.0
25.0
E_γ,MeV

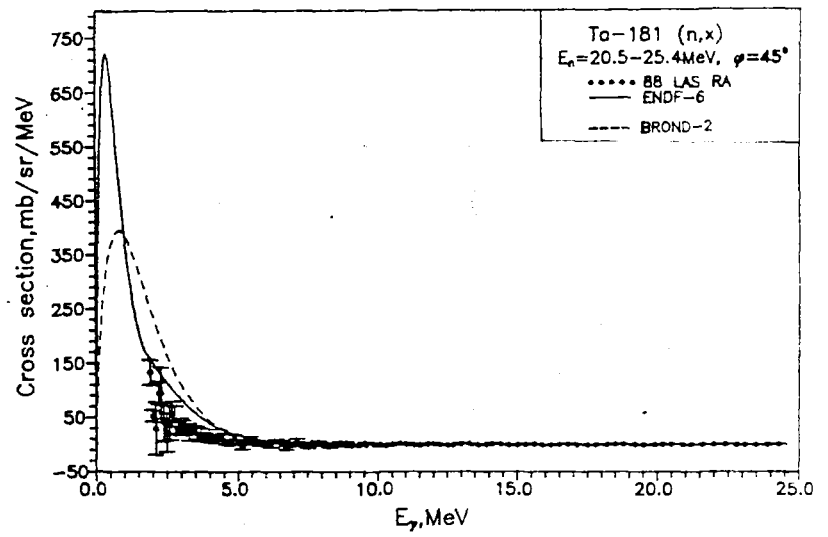
Ta-181 (n,x)
E_n=20.5-25.4MeV, φ=45°
88 LAS RA
ENDF-6
BROND-2
Cross section,mb/sr/MeV
E_γ,MeV

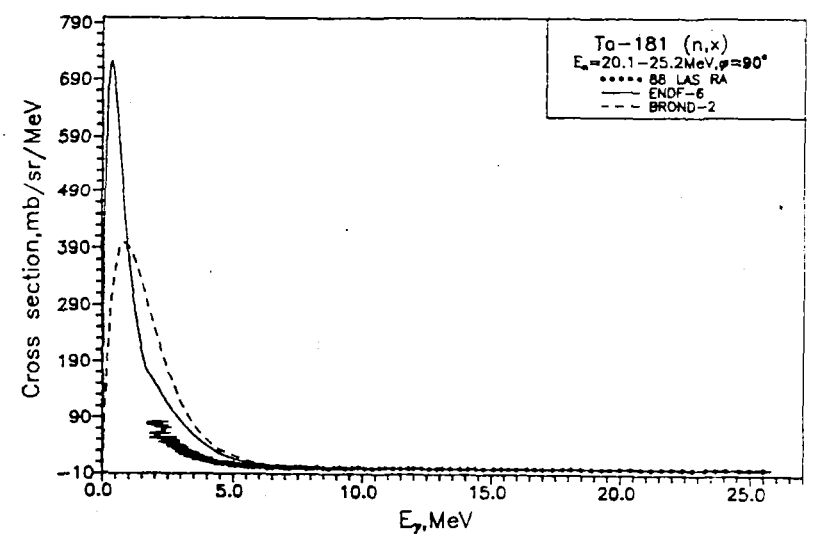
Ta-181 (n,x)
E_n=20.1-25.2MeV,φ=90°
88 LAS RA
ENDF-6
BROND-2
Cross section,mb/sr/MeV
E_γ,MeV

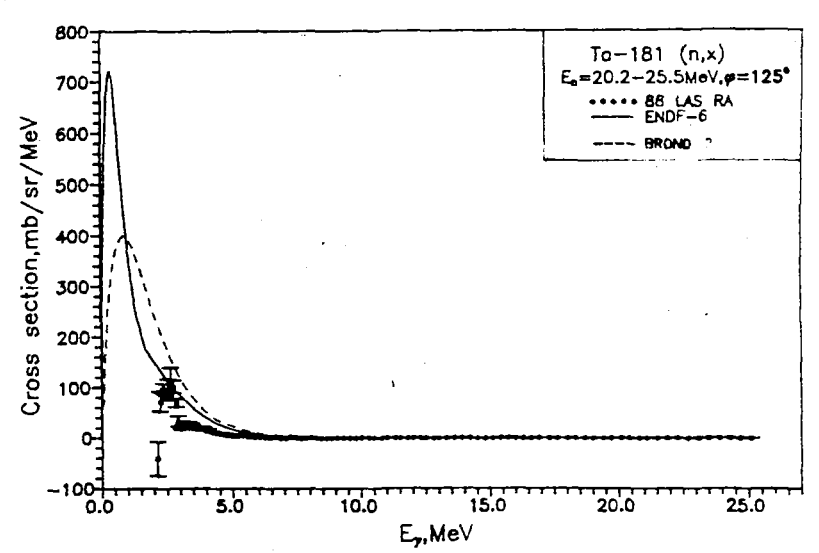
Ta-181 (n,x)
E_n=20.2-25.5MeV,φ=125°
88 LAS RA
ENDF-6
BROND
Cross section,mb/sr/MeV
E_γ,MeV

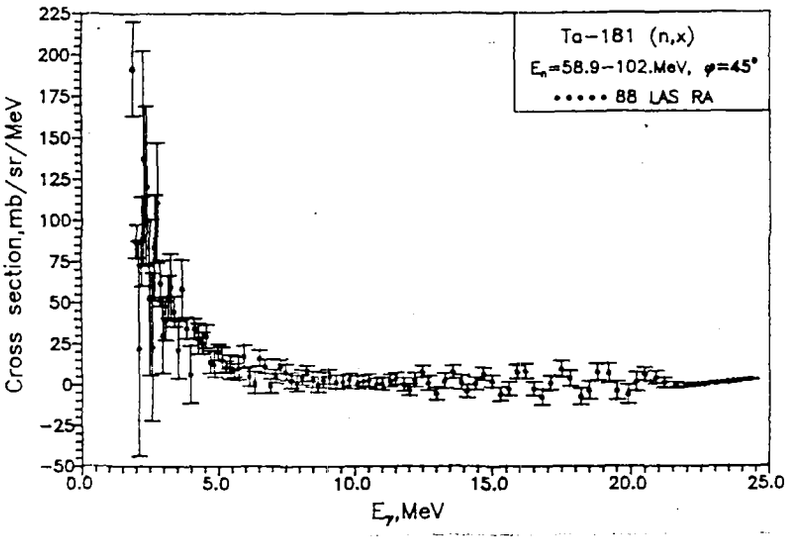
Ta-181 (n,x)
E_n=58.9-102.MeV, φ=45°
88 LAS RA
Cross section,mb/sr/MeV
E_γ,MeV

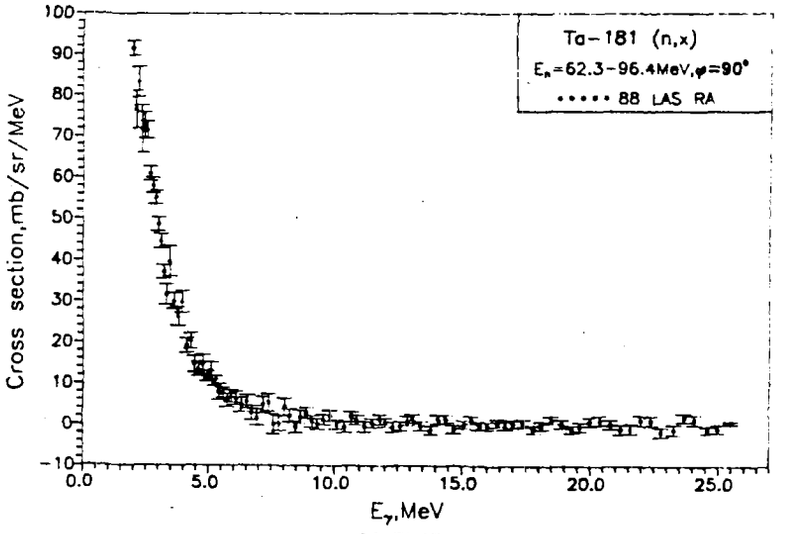
Ta-181 (n,x)
E_n=62.3-96.4MeV,φ=90°
88 LAS RA
Cross section,mb/sr/MeV
E_γ,MeV

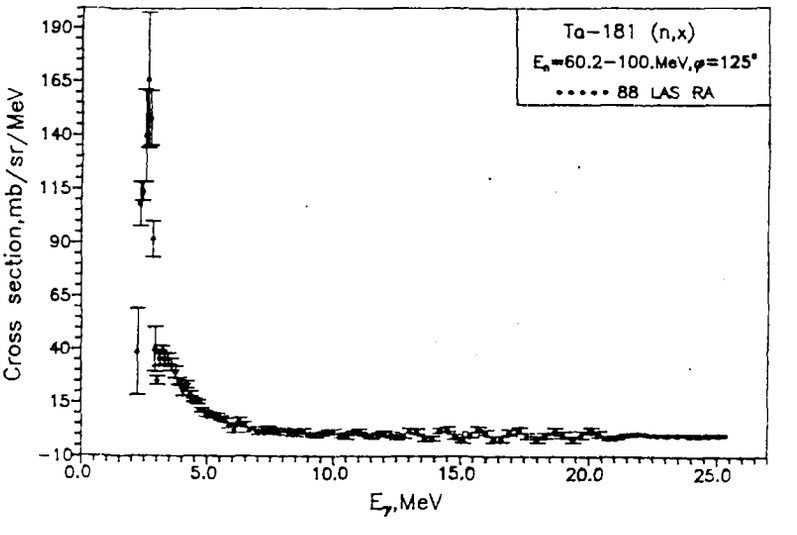
Ta-181 (n,x)
E_n=60.2-100.MeV,φ=125°
88 LAS RA
Cross section,mb/sr/MeV
E_γ,MeV

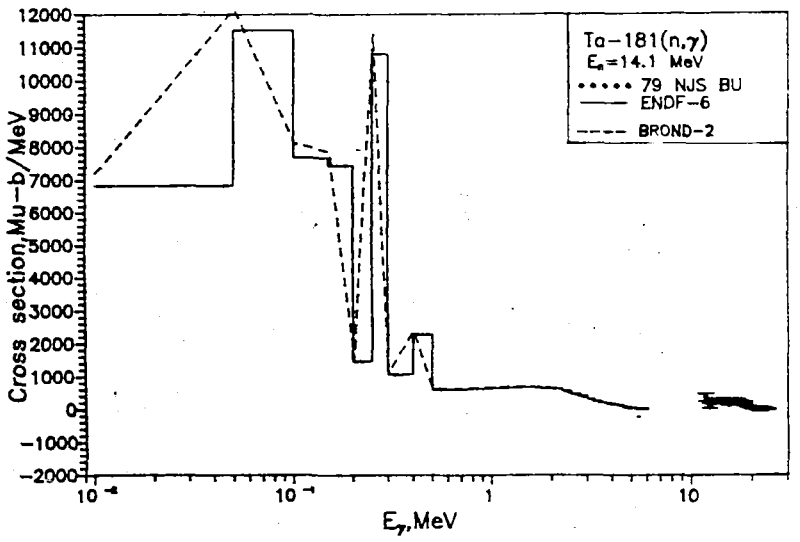
Ta-181(n,γ)
E_n=14.1 MeV
79 NJS BU
ENDF-6
BROND-2
Cross section,Mu-b/MeV
E_γ,MeV

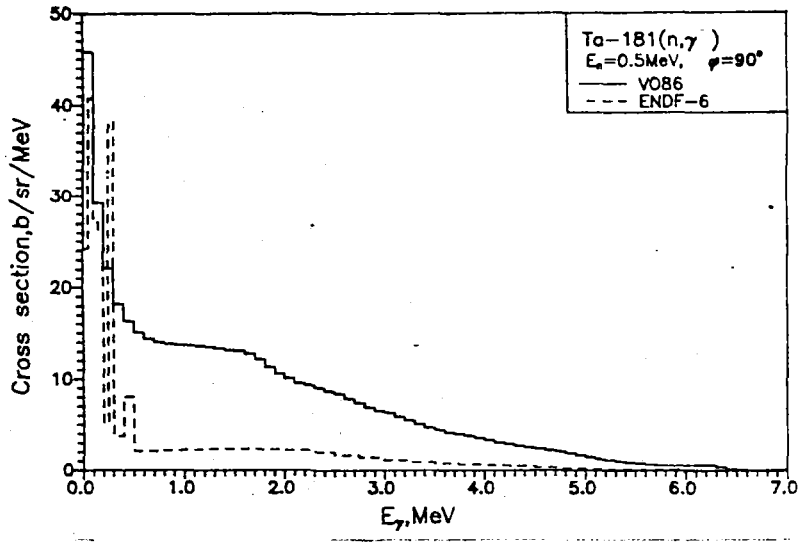
Ta-181(n,γ)
E_n=0.5MeV, φ=90°
V086
ENDF-6
Cross section,b/sr/MeV
E_γ,MeV

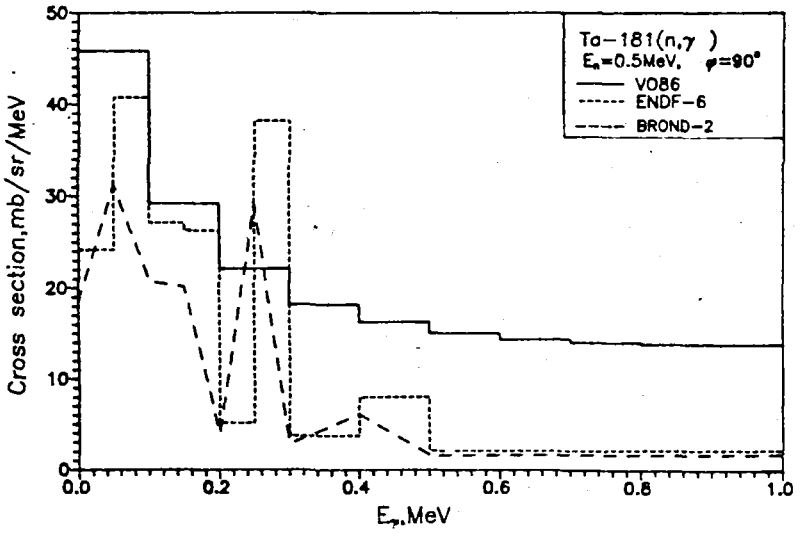
Ta-181(n,γ)
E_n=0.5MeV, φ=90°
V086
ENDF-6
BROND-2
Cross section,mb/sr/MeV
E_γ,MeV

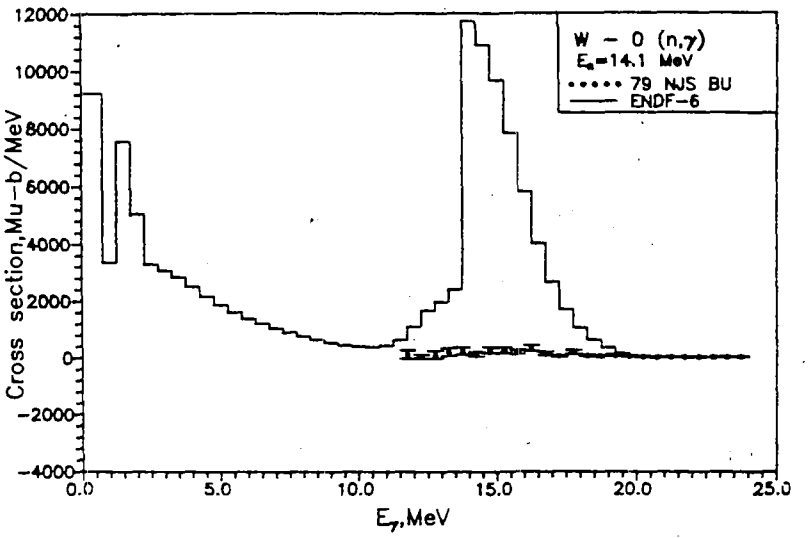
W - 0 (n,γ)
E_n=14.1 MeV
79 NJS BU
ENDF-6
Cross section,Mu-b/MeV
E_γ,MeV

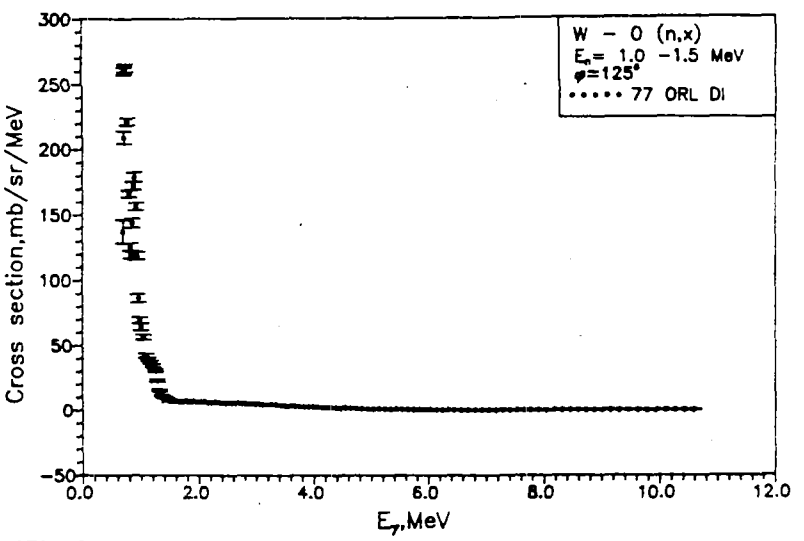
W - 0 (n,x)
E_n= 1.0 -1.5 MeV
φ=125°
77 ORL DI
Cross section,mb/sr/MeV
E_γ,MeV

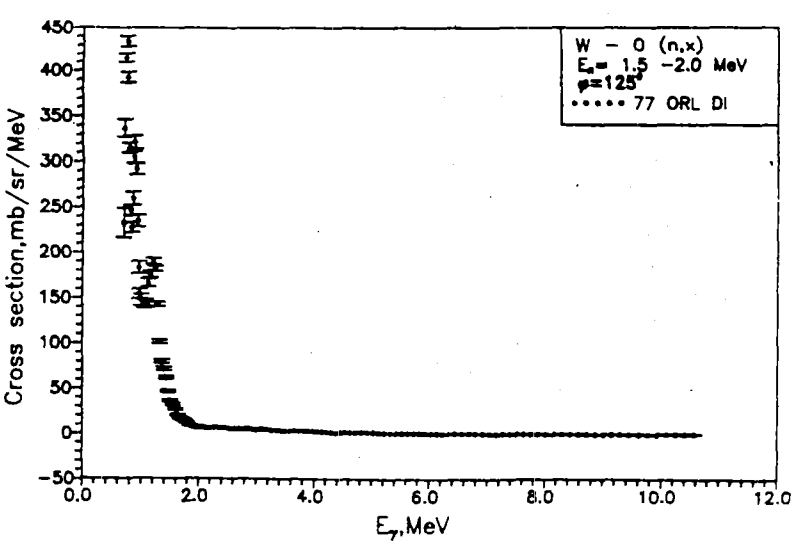
W - 0 (n,x)
E_n= 1.5 -2.0 MeV
φ=125°
77 ORL DI
Cross section,mb/sr/MeV
E_γ,MeV

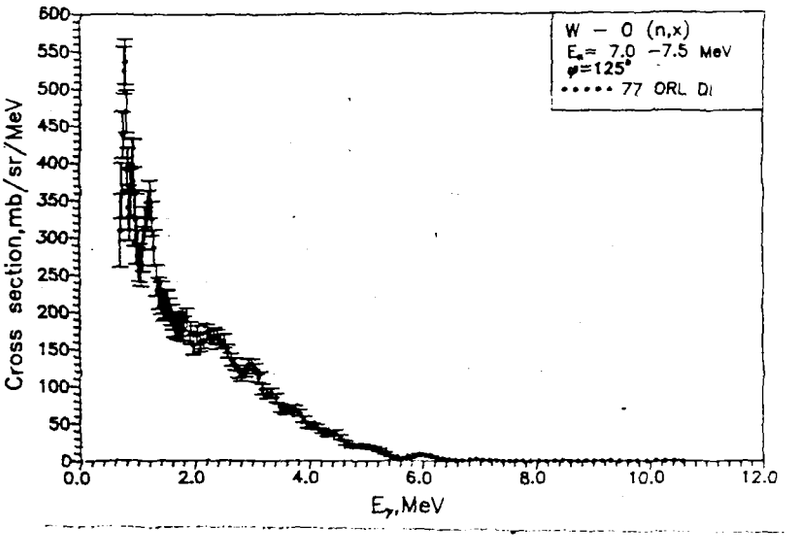
W – O (n,x)
E_n= 7.0 –7.5 MeV
φ=125°
••••• 77 ORL DI
Cross section,mb/sr/MeV
E_γ,MeV

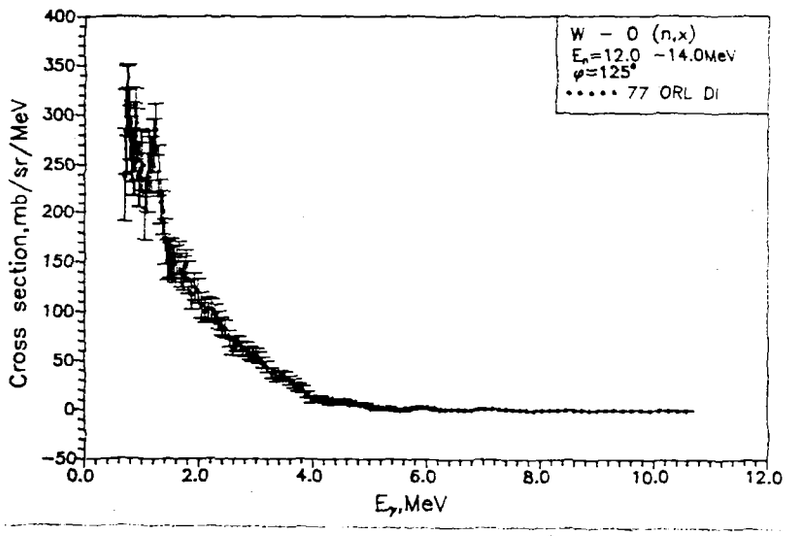
W – O (n,x)
E_n=12.0 –14.0MeV
φ=125°
••••• 77 ORL DI
Cross section,mb/sr/MeV
E_γ,MeV

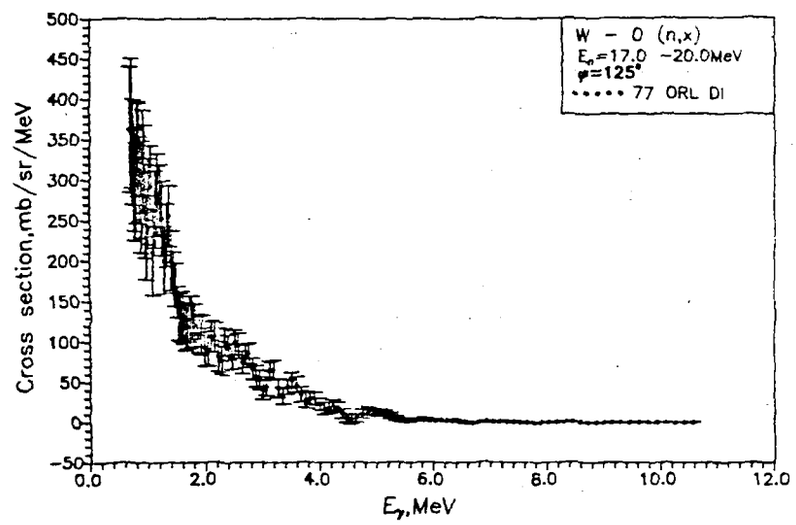
W – O (n,x)
E_n=17.0 –20.0MeV
φ=125°
••••• 77 ORL DI
Cross section,mb/sr/MeV
E_γ,MeV

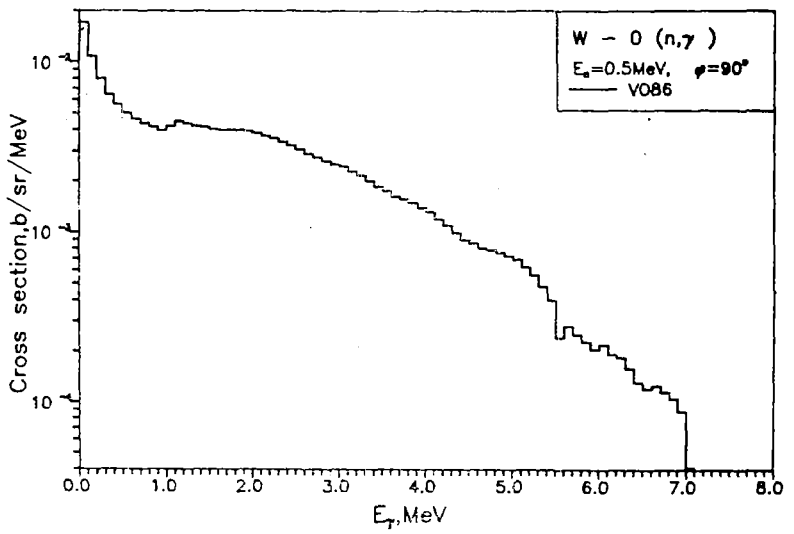
W - 0 (n,γ)
E_n=0.5MeV, φ=90°
V086
Cross section,b/sr/MeV
E_γ,MeV

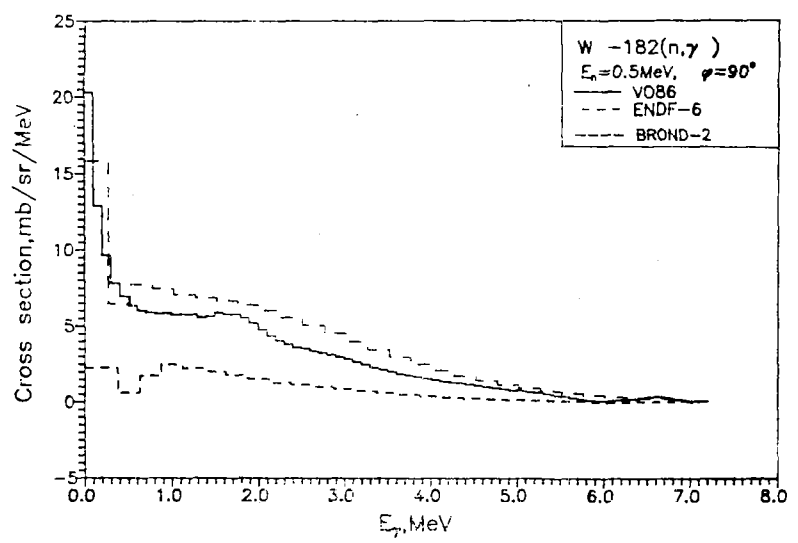
W -182(n,γ)
E_n=0.5MeV, φ=90°
V086
ENDF-6
BROND-2
Cross section,mb/sr/MeV
E_γ,MeV

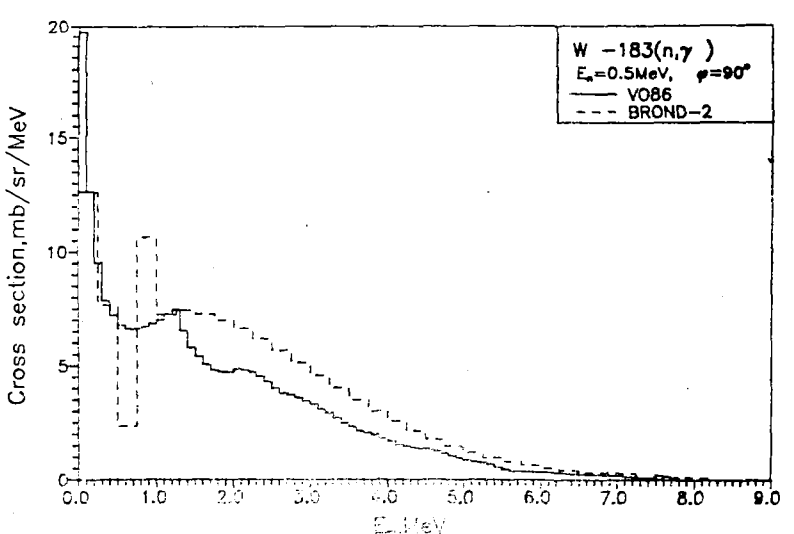
W -183(n,γ)
E_n=0.5MeV, φ=90°
V086
BROND-2
Cross section,mb/sr/MeV
E_γ,MeV

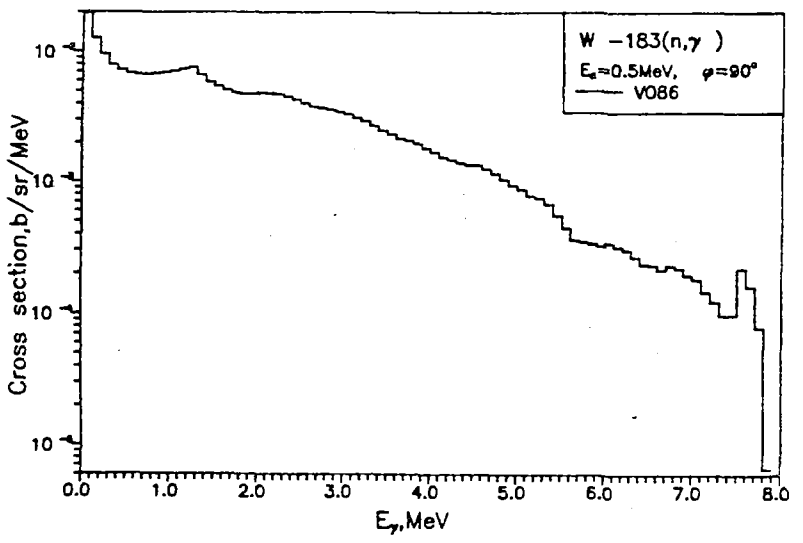
W −183(n,γ)
E=0.5MeV, φ=90°
V086
Cross section,b/sr/MeV
Eγ,MeV

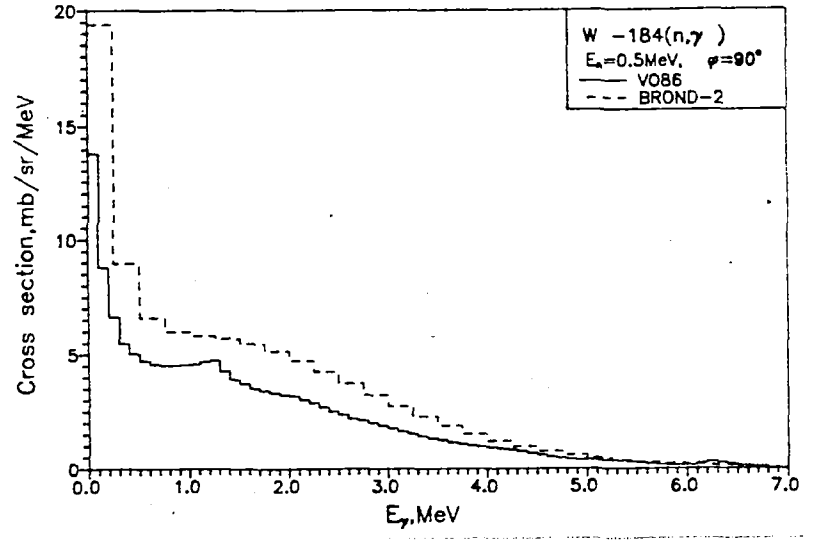
W −184(n,γ)
E=0.5MeV, φ=90°
V086
BROND−2
Cross section,mb/sr/MeV
Eγ,MeV

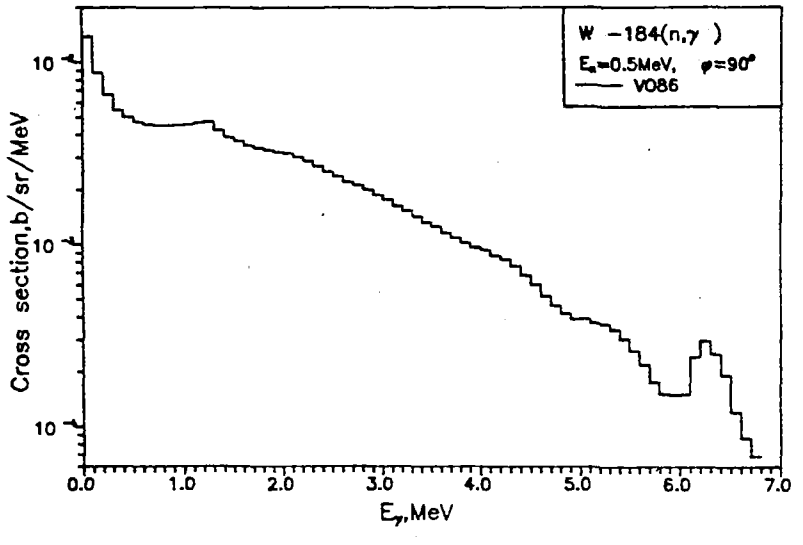
W −184(n,γ)
E=0.5MeV, φ=90°
V086
Cross section,b/sr/MeV
Eγ,MeV

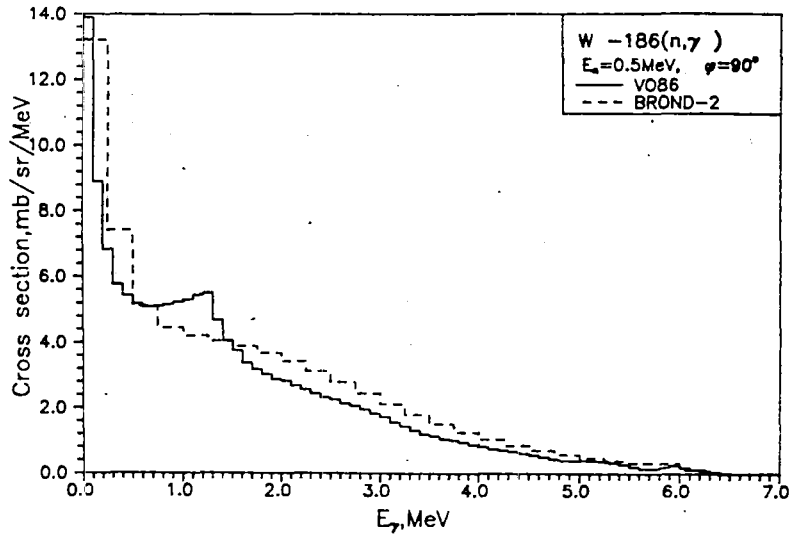
W −186(n,γ)
E=0.5MeV, φ=90°
V086
BROND−2
Cross section,mb/sr/MeV
E,MeV

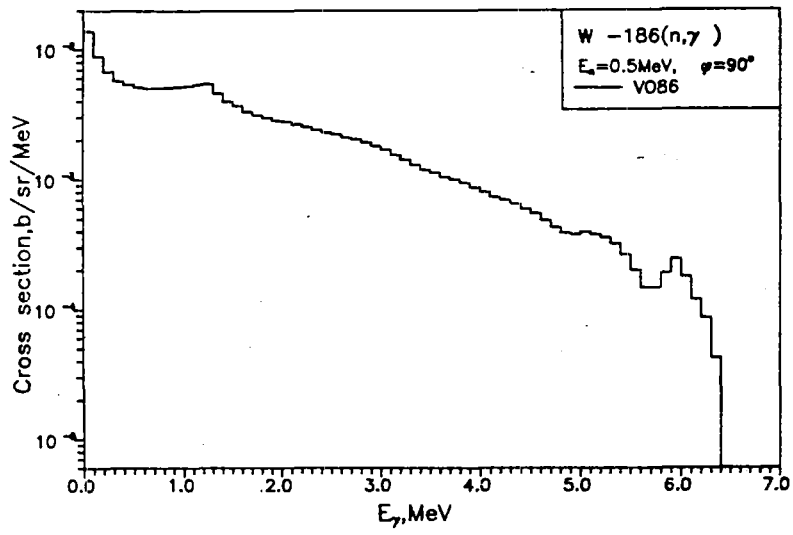
W −186(n,γ)
E=0.5MeV, φ=90°
V086
Cross section,b/sr/MeV
E,MeV

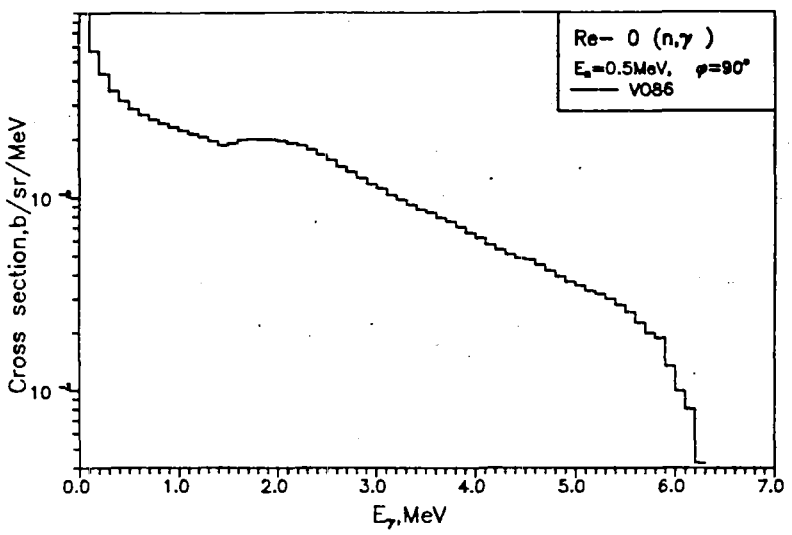
Re− 0 (n,γ)
E=0.5MeV, φ=90°
V086
Cross section,b/sr/MeV
E,MeV

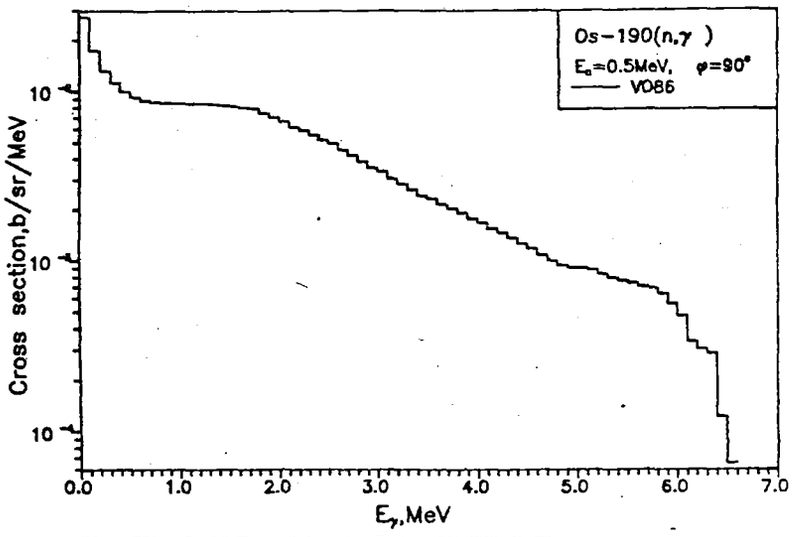
Os−190(n,γ)
E_n=0.5MeV, φ=90°
V086
Cross section,b/sr/MeV
E_γ,MeV

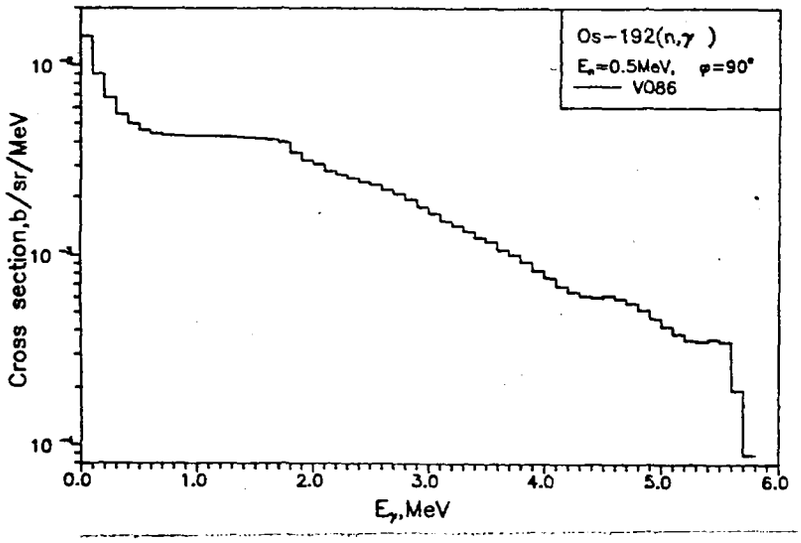
Os−192(n,γ)
E_n=0.5MeV, φ=90°
V086
Cross section,b/sr/MeV
E_γ,MeV

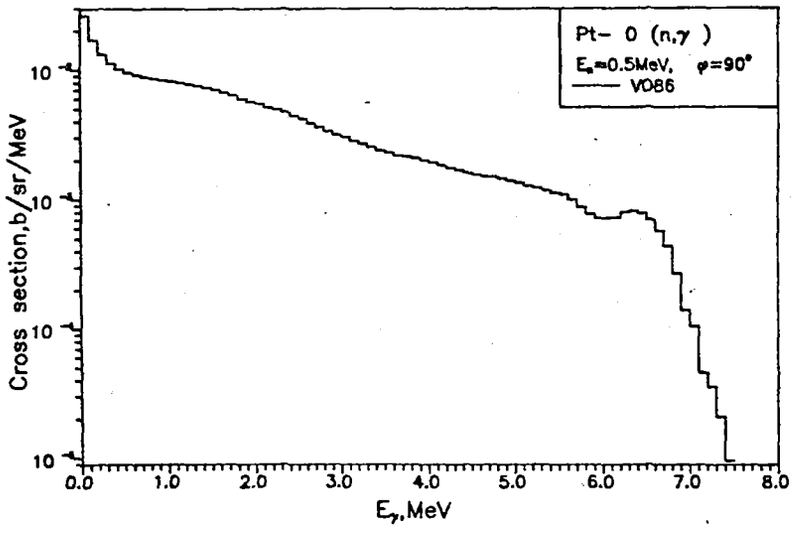
Pt− 0 (n,γ)
E_n=0.5MeV, φ=90°
V086
Cross section,b/sr/MeV
E_γ,MeV

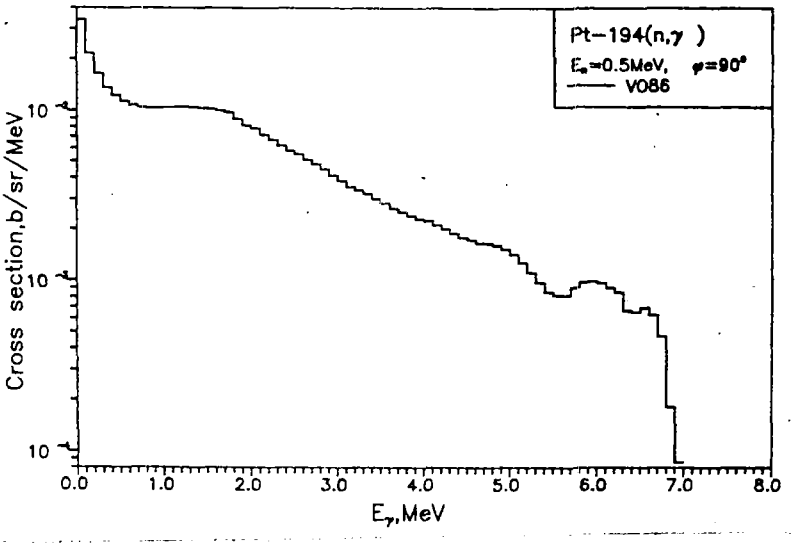
Pt−194(n,γ)
E=0.5MeV, φ=90°
V086
Cross section,b/sr/MeV
E,MeV

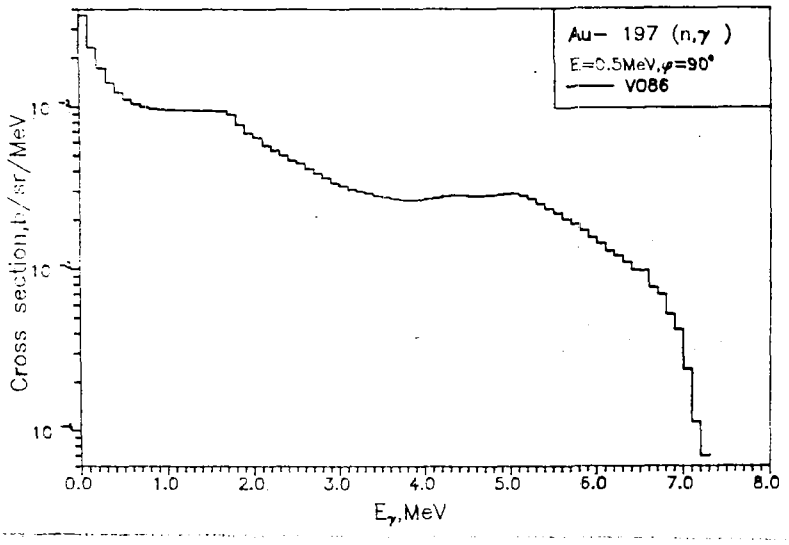
Au− 197 (n,γ)
E=0.5MeV,φ=90°
V086
Cross section,b/sr/MeV
E,MeV

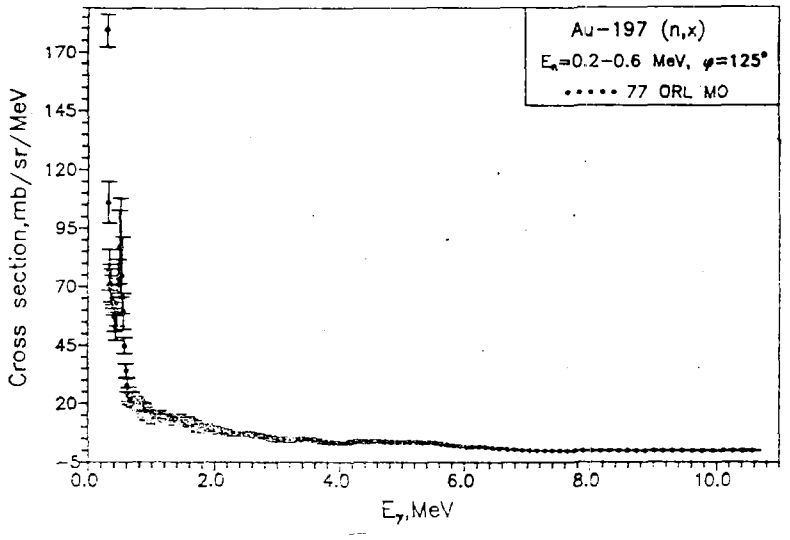
Au−197 (n,x)
E=0.2−0.6 MeV, φ=125°
77 ORL MO
Cross section,mb/sr/MeV
E,MeV

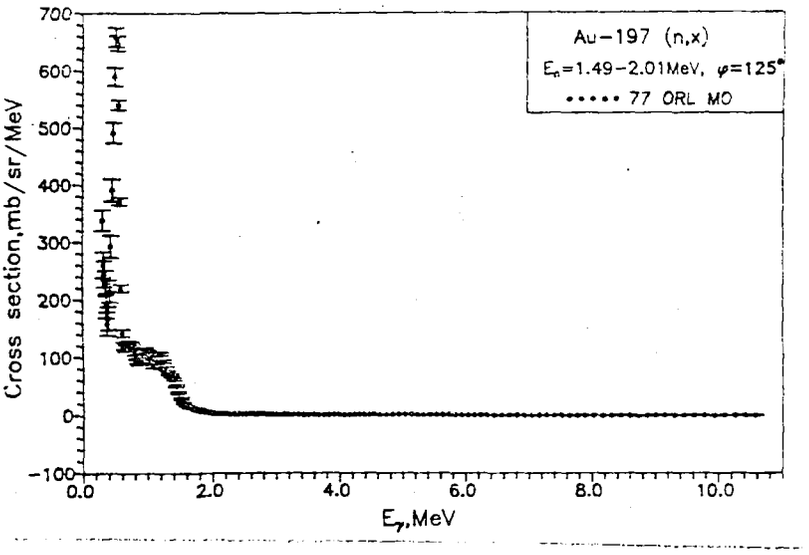
Au-197 (n,x)
E_n=1.49-2.01MeV, φ=125°
••••• 77 ORL MO
Cross section,mb/sr/MeV
E_γ,MeV

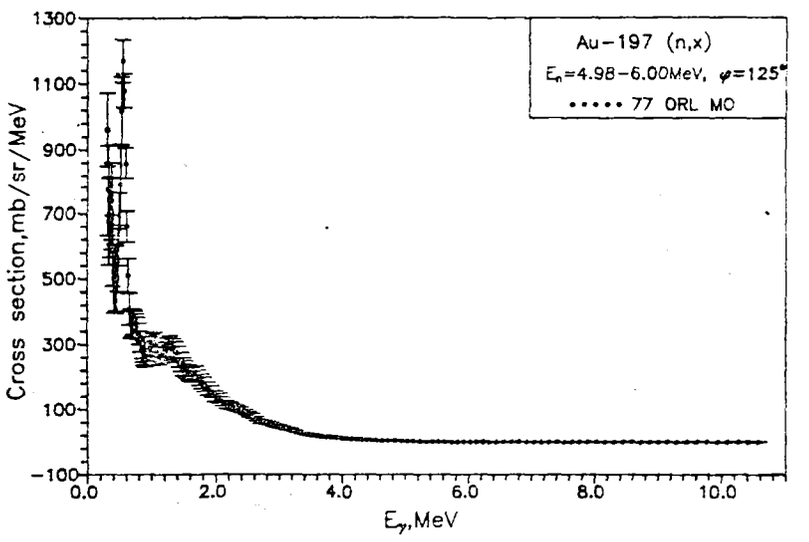
Au-197 (n,x)
E_n=4.98-6.00MeV, φ=125°
••••• 77 ORL MO
Cross section,mb/sr/MeV
E_γ,MeV

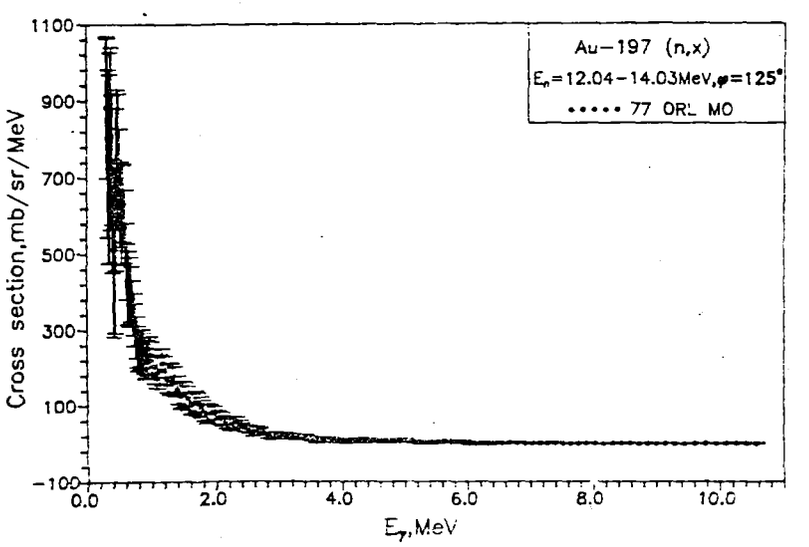
Au-197 (n,x)
E_n=12.04-14.03MeV, φ=125°
••••• 77 ORL MO
Cross section,mb/sr/MeV
E_γ,MeV

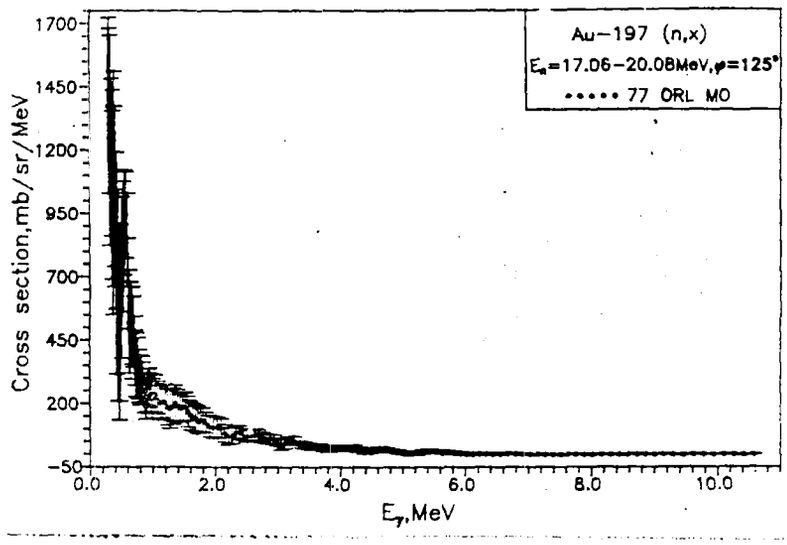
Au−197 (n,x)
E_n=17.06−20.08MeV,φ=125°
77 ORL MO
Cross section,mb/sr/MeV
E_γ,MeV

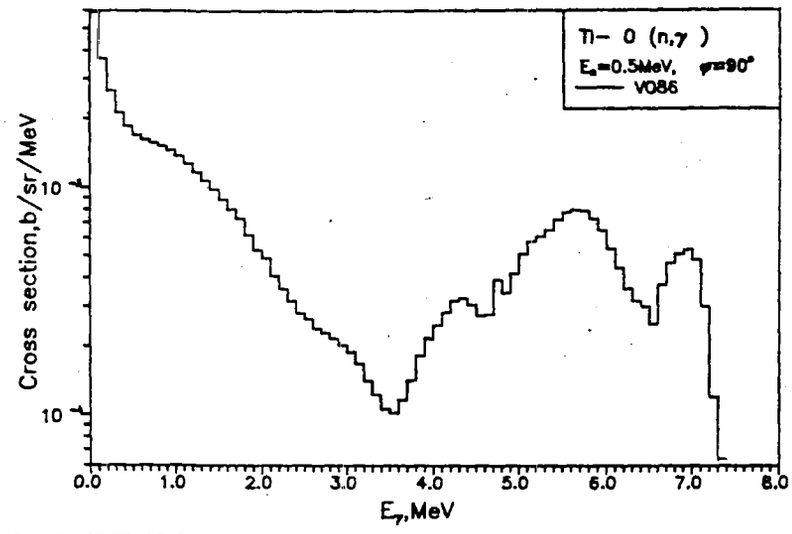
Tl− 0 (n,γ)
E_n=0.5MeV, φ=90°
V086
Cross section,b/sr/MeV
E_γ,MeV

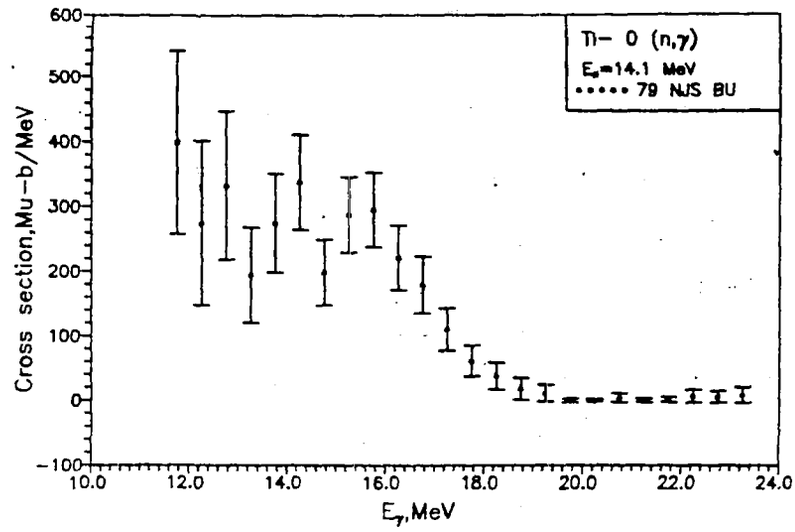
Tl− 0 (n,γ)
E_n=14.1 MeV
79 NJS BU
Cross section,Mu−b/MeV
E_γ,MeV

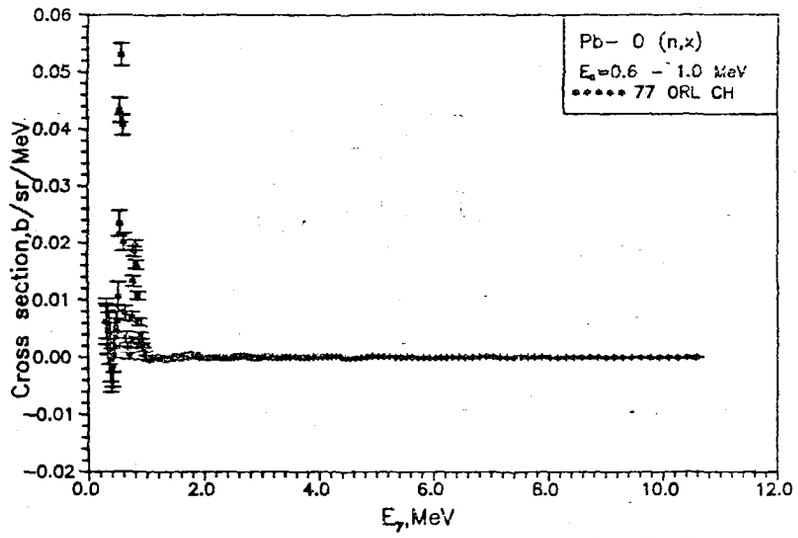
Pb– 0 (n,x)
E_n=0.6 – 1.0 MeV
77 ORL CH
Cross section,b/sr/MeV
E_γ,MeV

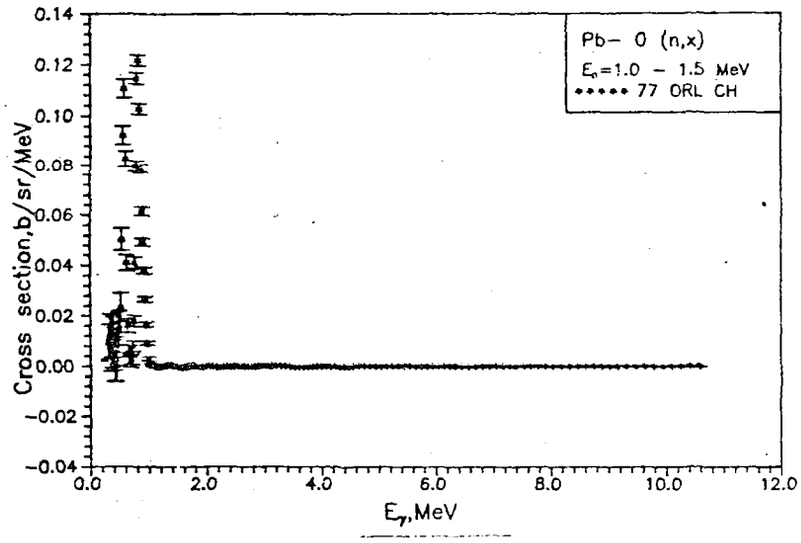
Pb– 0 (n,x)
E_n=1.0 – 1.5 MeV
77 ORL CH
Cross section,b/sr/MeV
E_γ,MeV

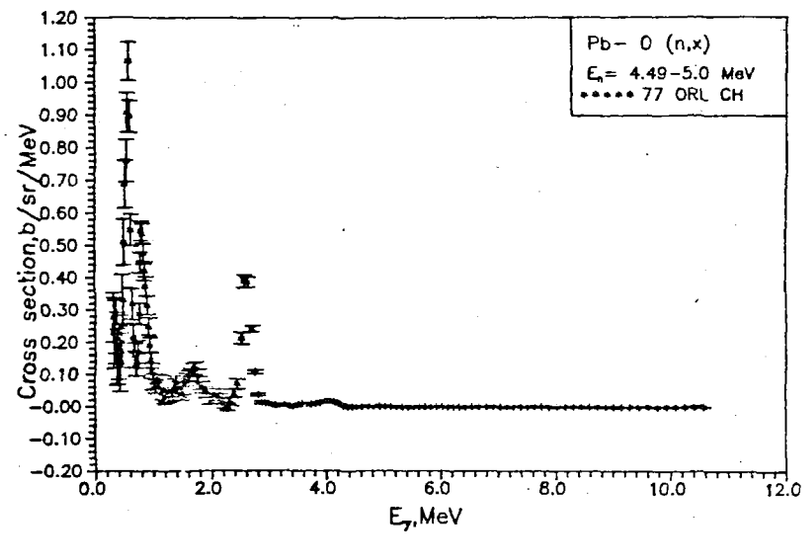
Pb– 0 (n,x)
E_n= 4.49–5.0 MeV
77 ORL CH
Cross section,b/sr/MeV
E_γ,MeV

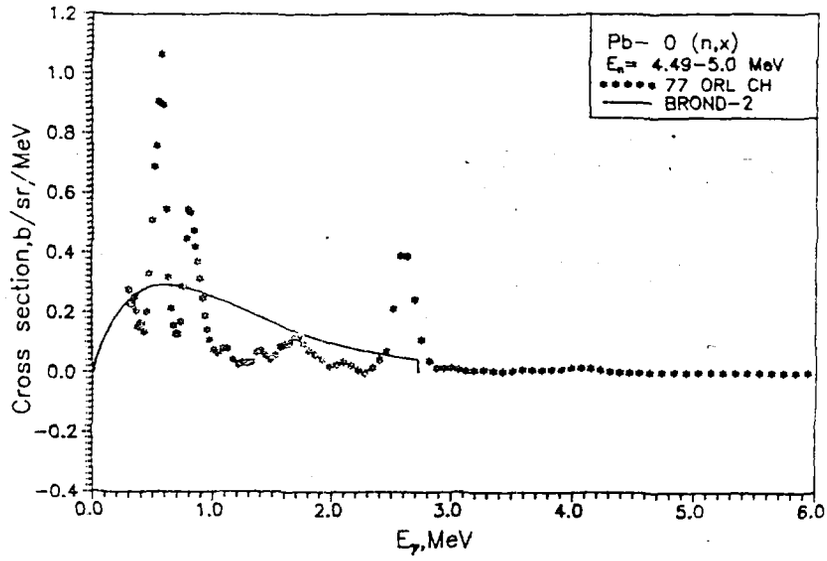
Pb- 0 (n,x)
E_n= 4.49-5.0 MeV
77 ORL CH
BROND-2
Cross section,b/sr/MeV
E_γ,MeV

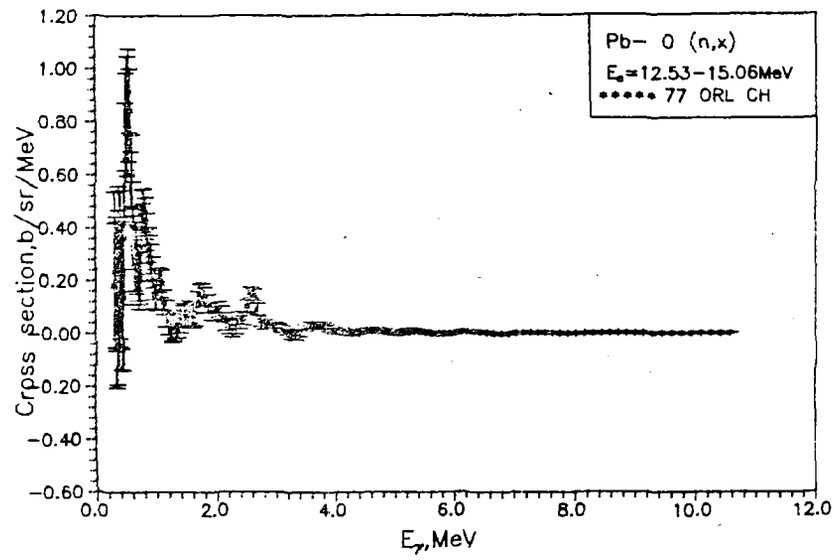
Pb- 0 (n,x)
E_n=12.53-15.06MeV
77 ORL CH
Crpss section,b/sr/MeV
E_γ,MeV

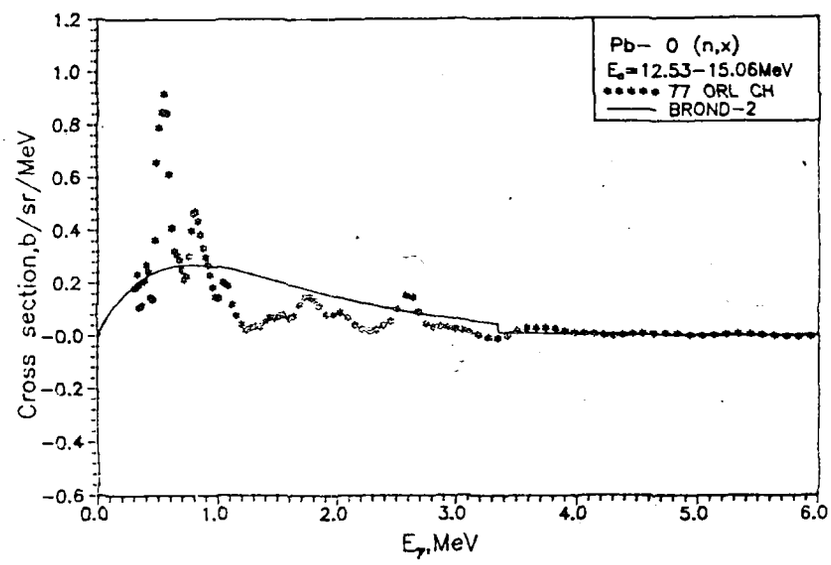
Pb- 0 (n,x)
E_n=12.53-15.06MeV
77 ORL CH
BROND-2
Cross section,b/sr/MeV
E_γ,MeV

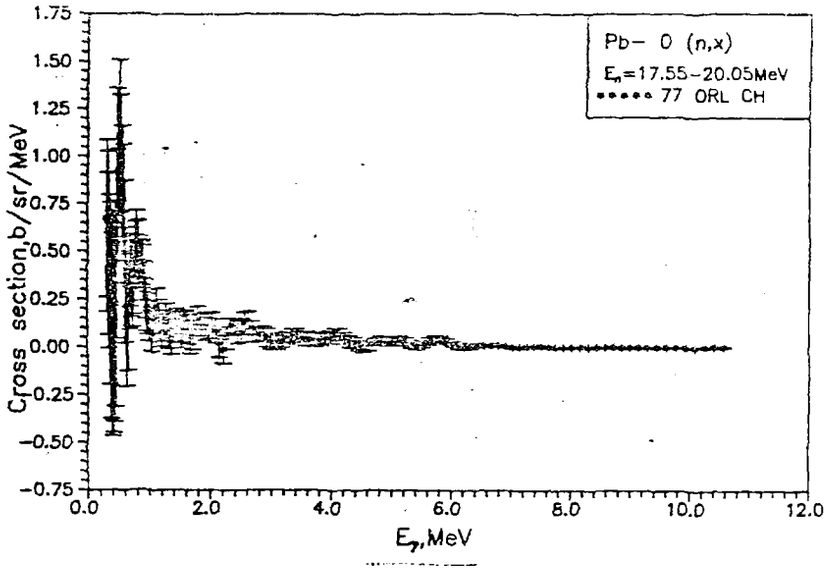
Pb- 0 (n,x)
E_n=17.55-20.05MeV
77 ORL CH
Cross section,b/sr/MeV
E_γ,MeV

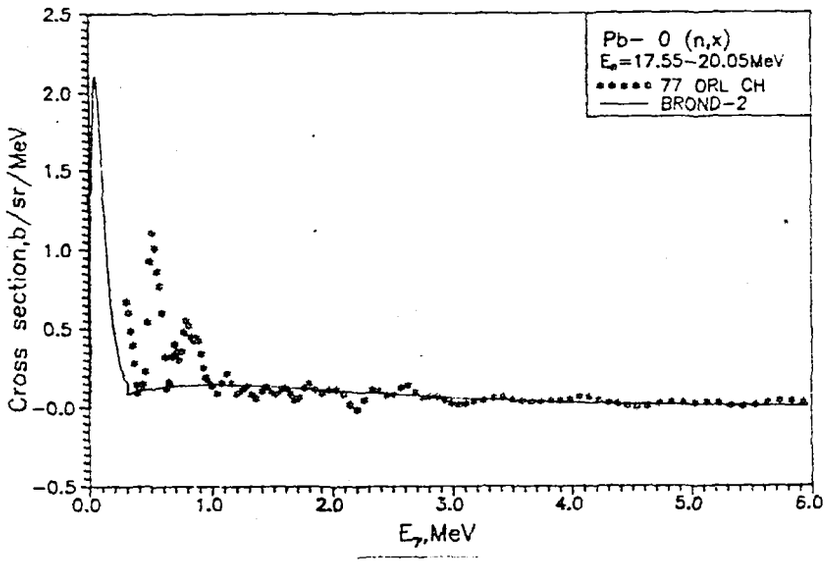
Pb- 0 (n,x)
E_n=17.55-20.05MeV
77 ORL CH
BROND-2
Cross section,b/sr/MeV
E_γ,MeV

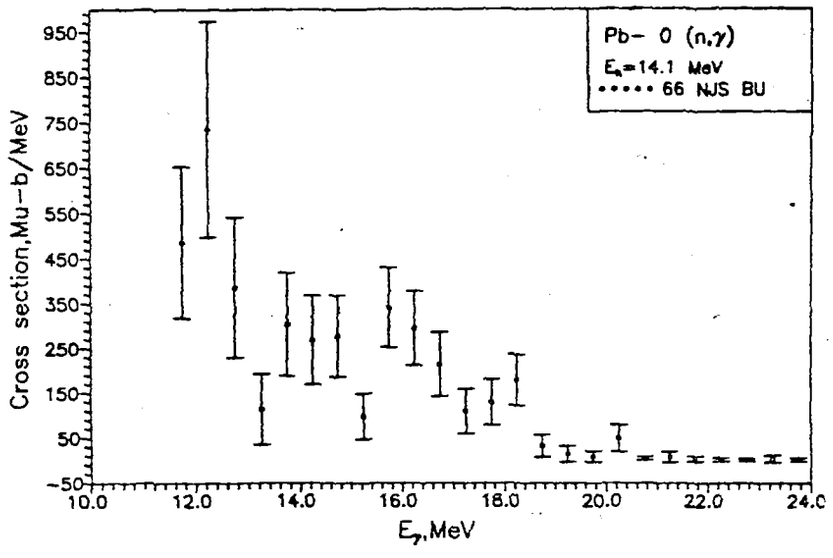
Pb- 0 (n,γ)
E_n=14.1 MeV
66 NJS BU
Cross section,Mu-b/MeV
E_γ,MeV

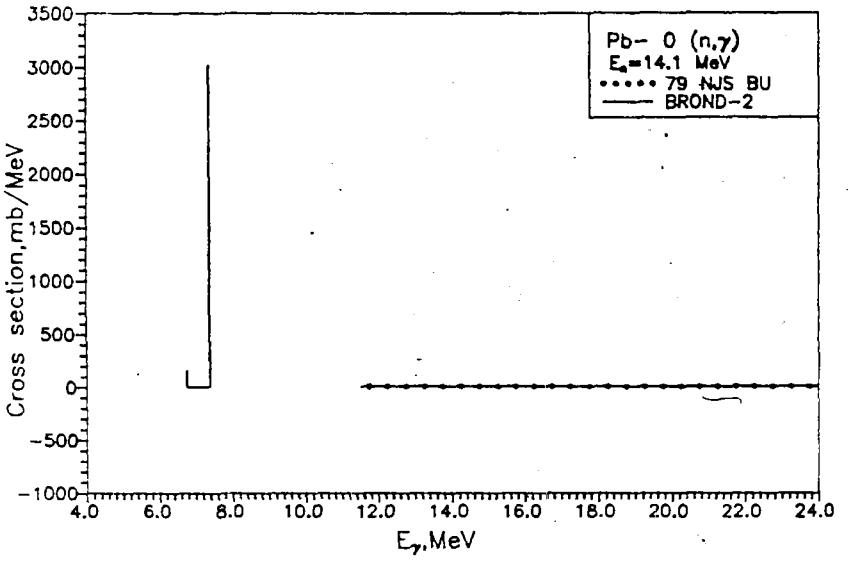
Pb- 0 (n,γ)
E_n=14.1 MeV
79 NJS BU
BROND-2
Cross section,mb/MeV
E_γ,MeV

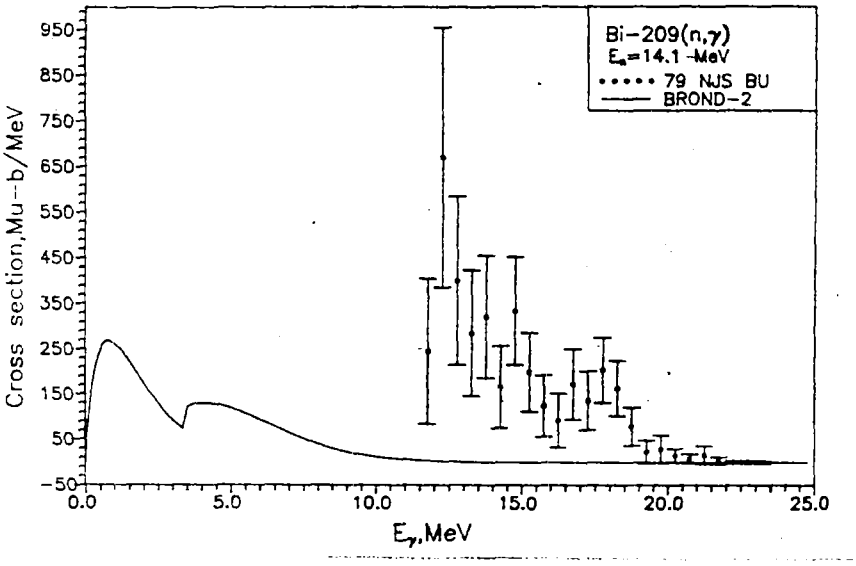
Bi-209(n,γ)
E_n=14.1 MeV
79 NJS BU
BROND-2
Cross section,Mu-b/MeV
E_γ,MeV

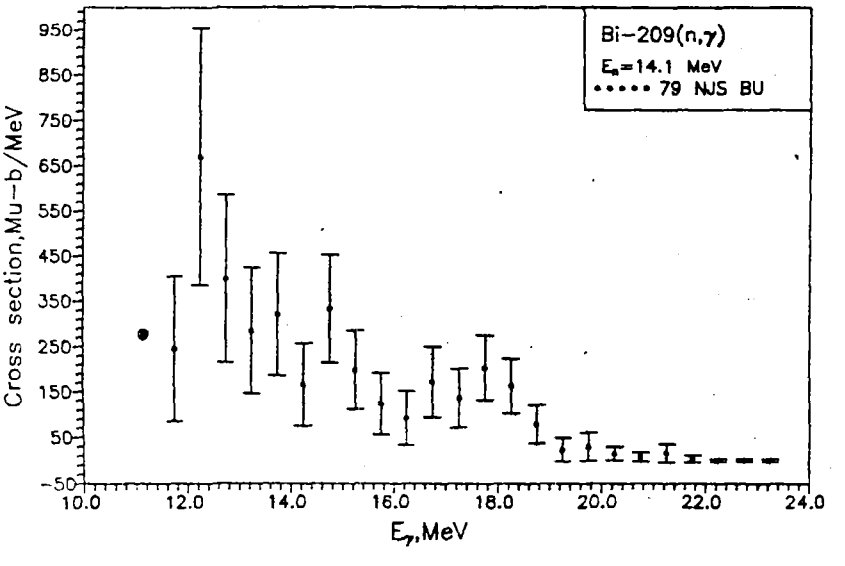
Bi-209(n,γ)
E_n=14.1 MeV
79 NJS BU
Cross section,Mu-b/MeV
E_γ,MeV

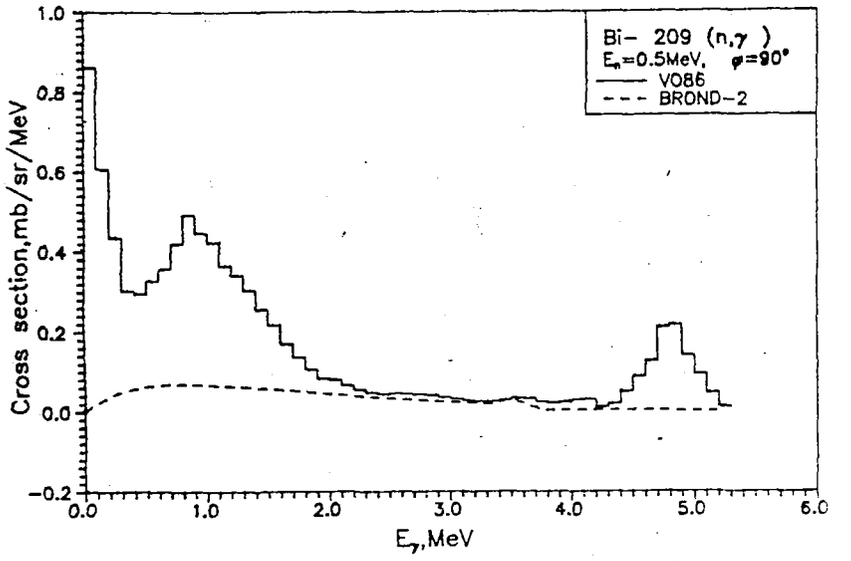
Bi- 209 (n,γ)
E_n=0.5MeV, φ=90°
V086
BROND-2
Cross section,mb/sr/MeV
E_γ,MeV

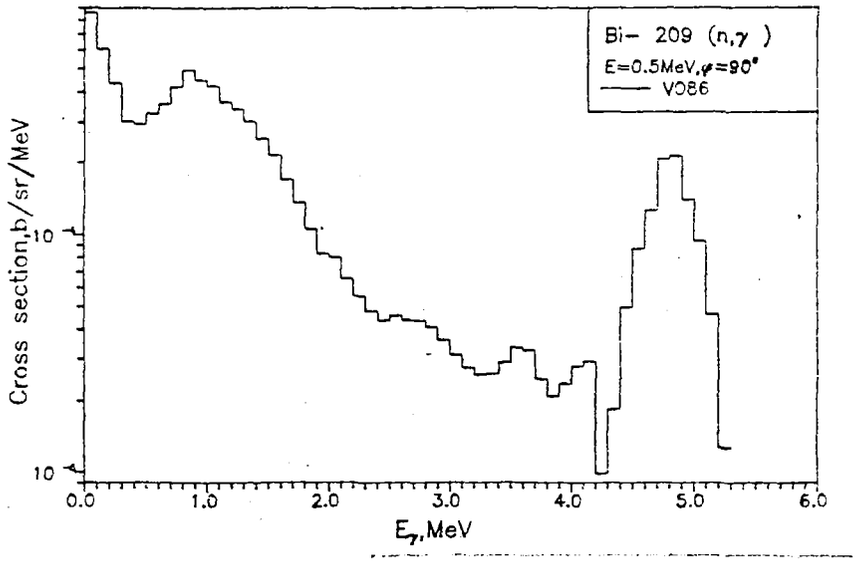
Bi- 209 (n,γ)
E=0.5MeV,φ=90°
V086
Cross section,b/sr/MeV
E_γ,MeV

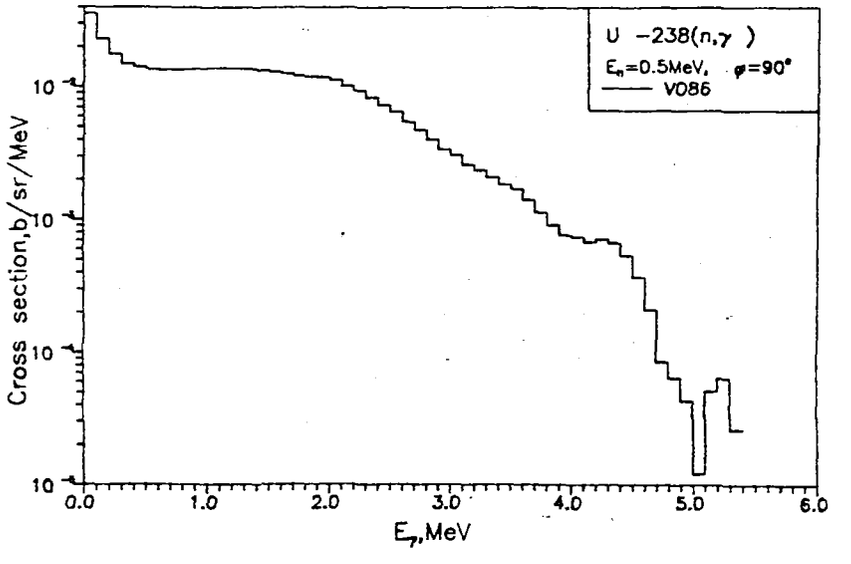
U -238(n,γ)
E_n=0.5MeV, φ=90°
V086
Cross section,b/sr/MeV
E_γ,MeV

PART 2.

GAMMA-RAY PRODUCTION CROSS-SECTIONS

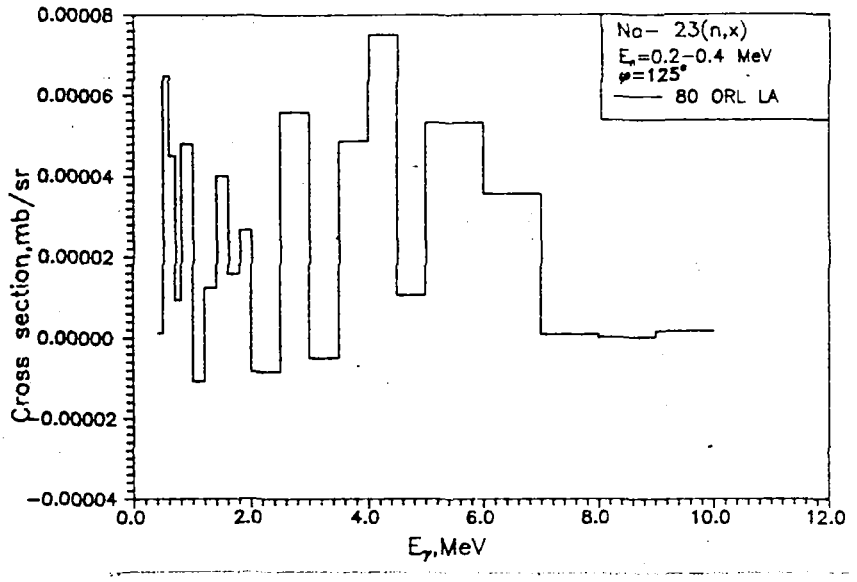
Na- 23(n,x)
E_n=0.2-0.4 MeV
φ=125°
80 ORL LA
Cross section,mb/sr
E_γ,MeV

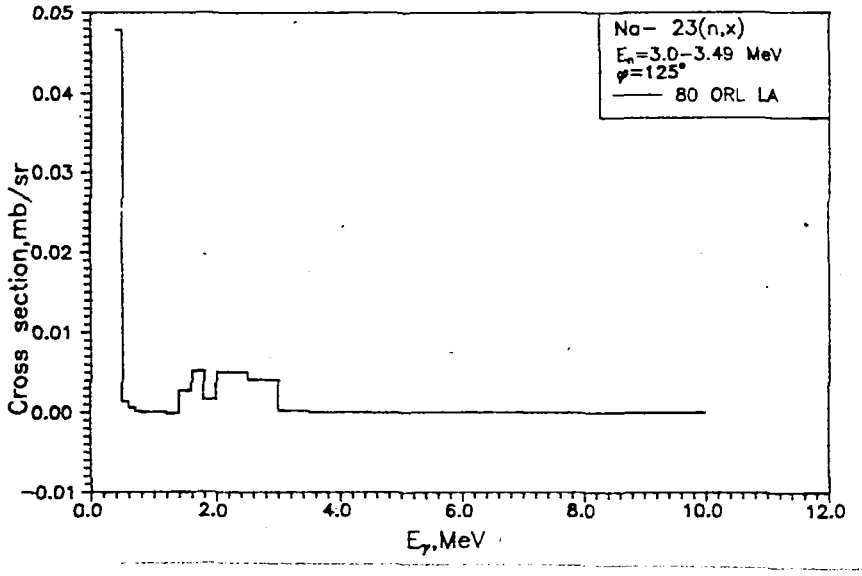
Na- 23(n,x)
E_n=3.0-3.49 MeV
φ=125°
80 ORL LA
Cross section,mb/sr
E_γ,MeV

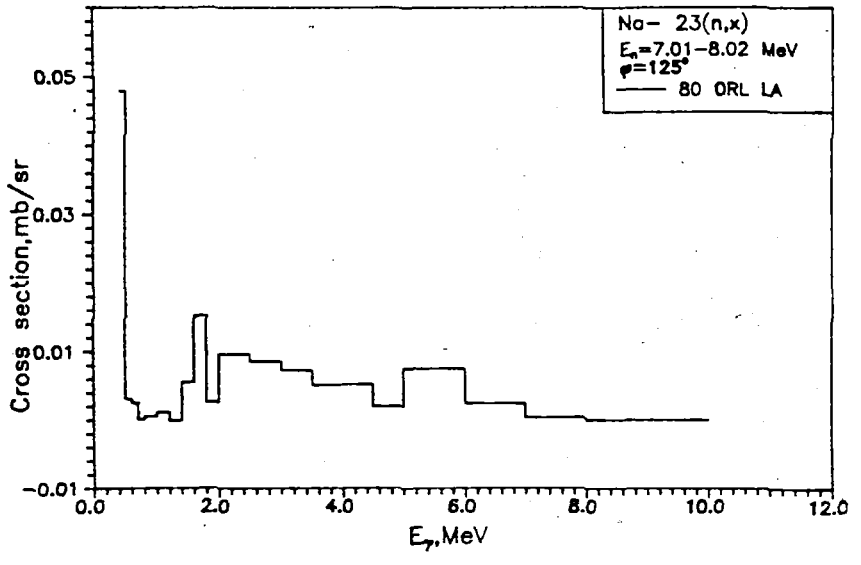
Na- 23(n,x)
E_n=7.01-8.02 MeV
φ=125°
80 ORL LA
Cross section,mb/sr
E_γ,MeV

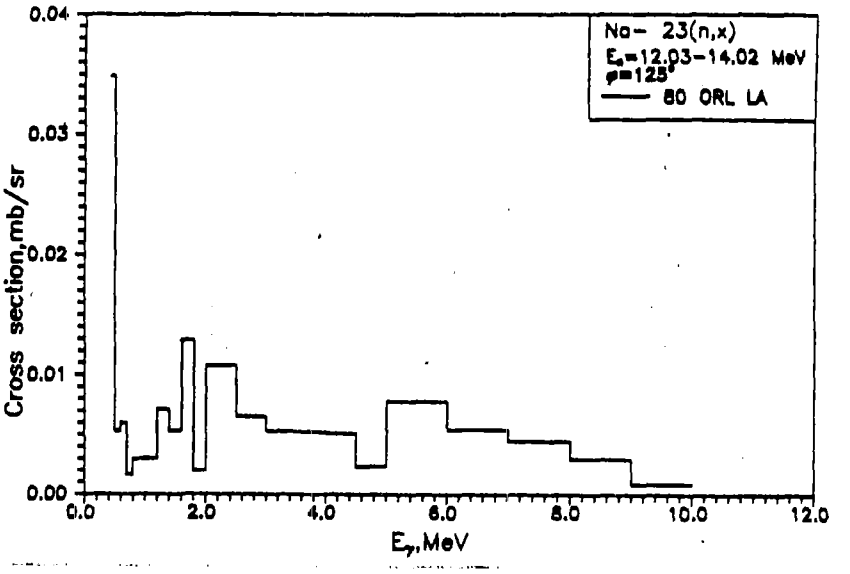
Na- 23(n,x)
E_n=12.03-14.02 MeV
φ=125°
80 ORL LA
Cross section,mb/sr
E_γ,MeV

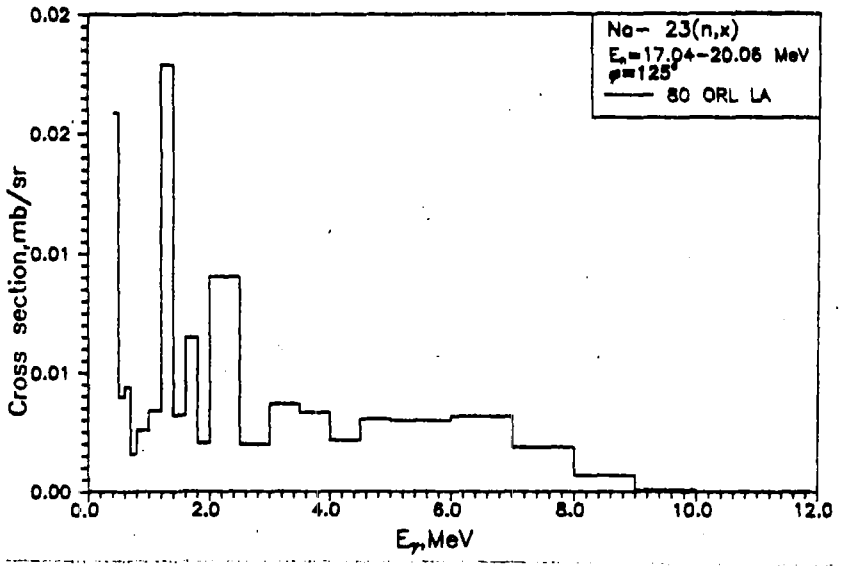
Na- 23(n,x)
E_n=17.04-20.06 MeV
φ=125°
80 ORL LA
Cross section,mb/sr
E_γ,MeV

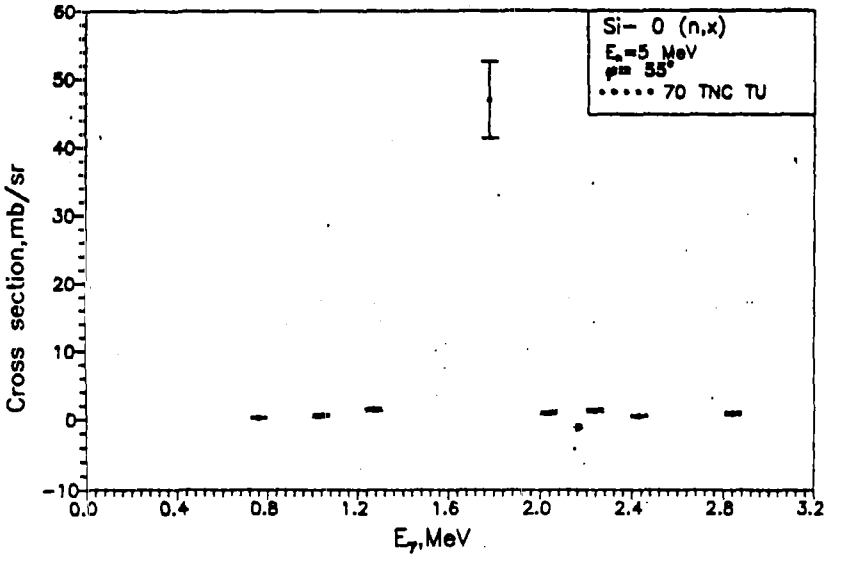
Si- 0 (n,x)
E_n=5 MeV
φ= 55°
70 TNC TU
Cross section,mb/sr
E_γ,MeV

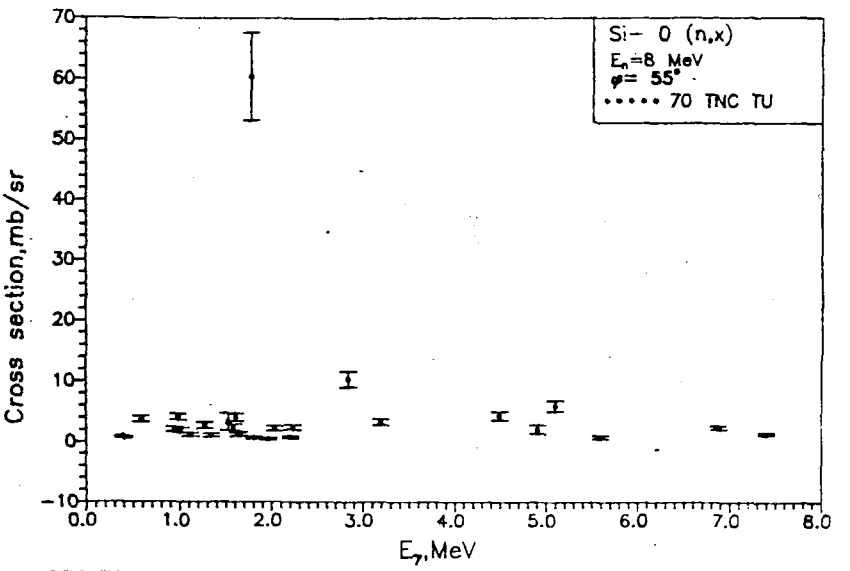
Si- 0 (n,x)
E_n=8 MeV
φ= 55°
••••• 70 TNC TU
Cross section,mb/sr
E_γ,MeV

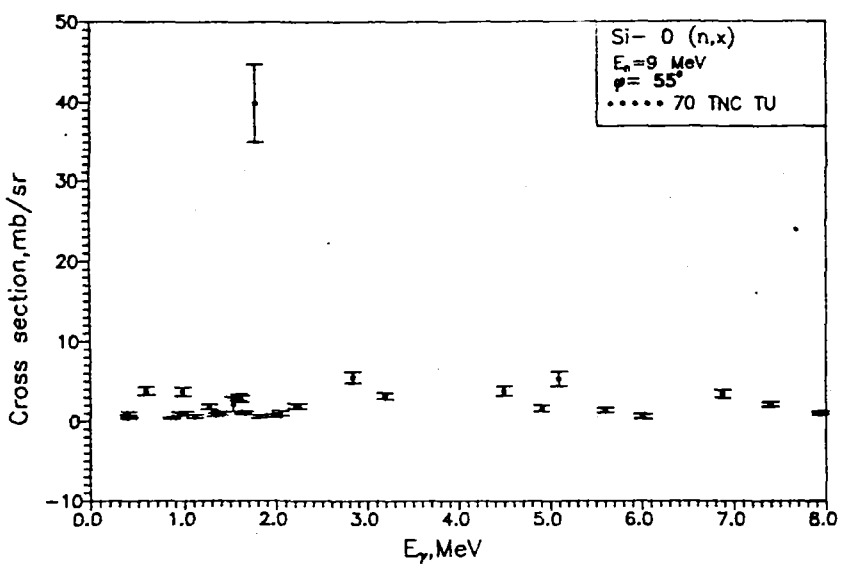
Si- 0 (n,x)
E_n=9 MeV
φ= 55°
••••• 70 TNC TU
Cross section,mb/sr
E_γ,MeV

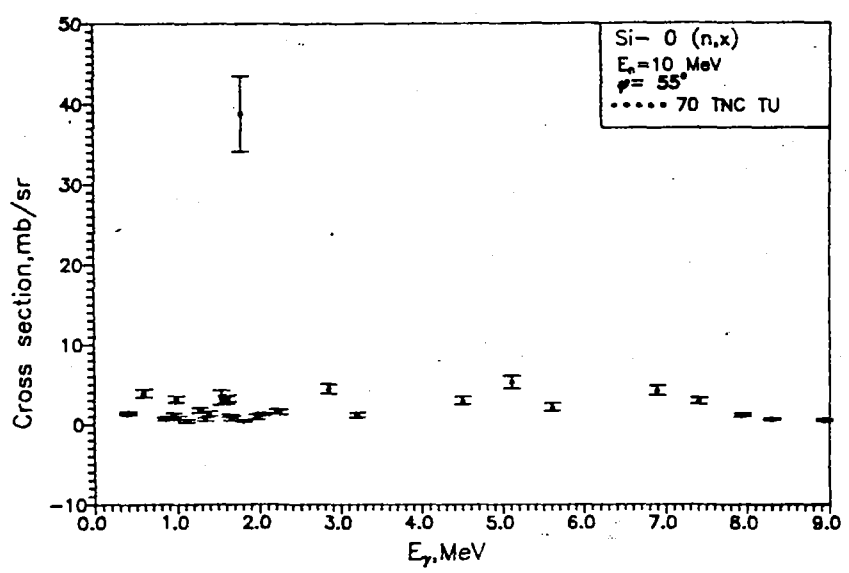
Si- 0 (n,x)
E_n=10 MeV
φ= 55°
••••• 70 TNC TU
Cross section,mb/sr
E_γ,MeV

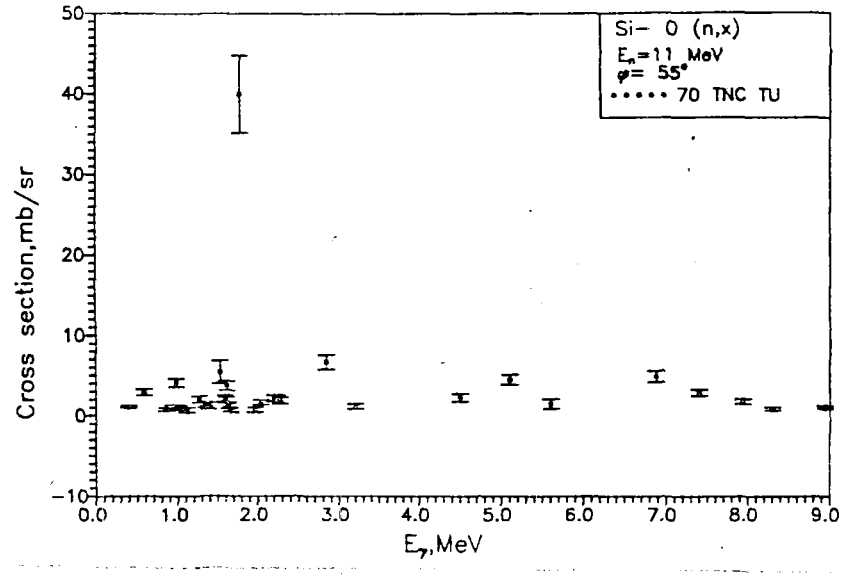
Si– 0 (n,x)
E_n=11 MeV
φ= 55°
70 TNC TU
Cross section,mb/sr
E_γ,MeV

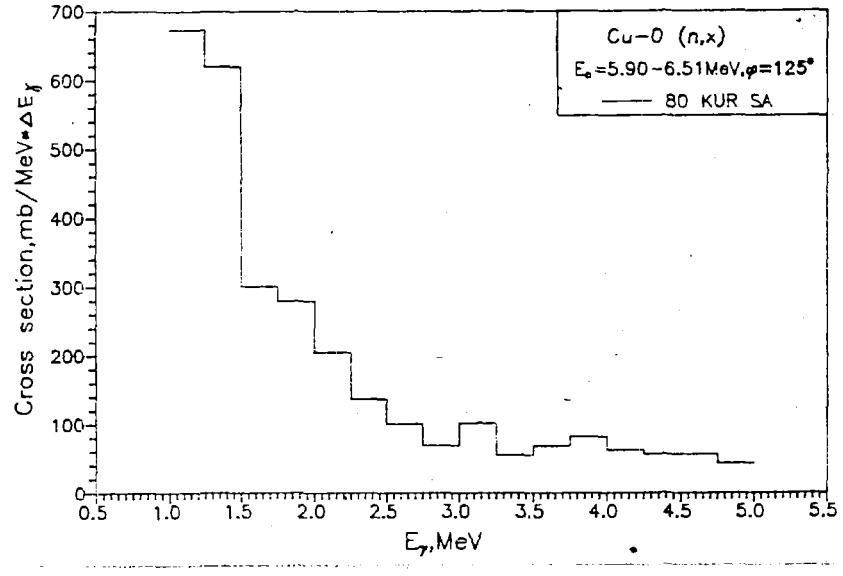
Cu–0 (n,x)
E_n=5.90–6.51MeV,φ=125°
80 KUR SA
Cross section,mb/MeV*ΔE_γ
E_γ,MeV

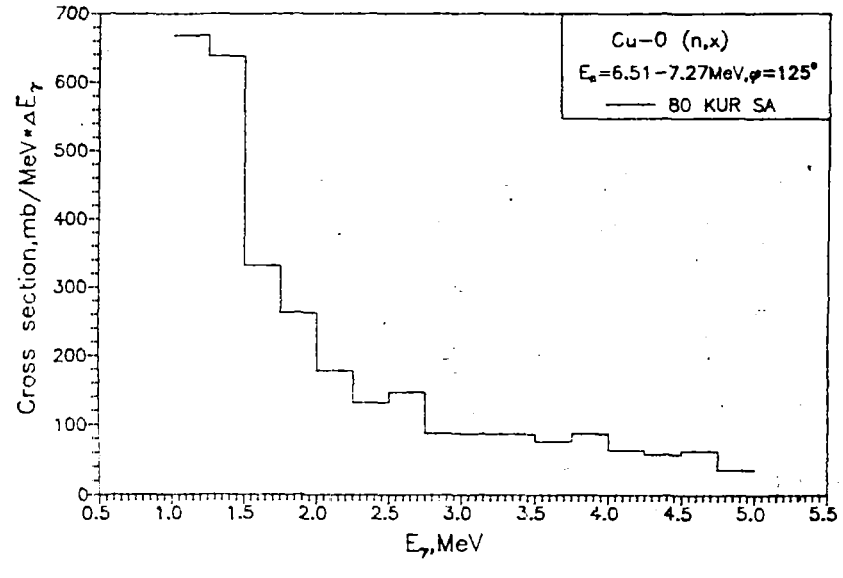
Cu–0 (n,x)
E_n=6.51–7.27MeV,φ=125°
80 KUR SA
Cross section,mb/MeV*ΔE_γ
E_γ,MeV

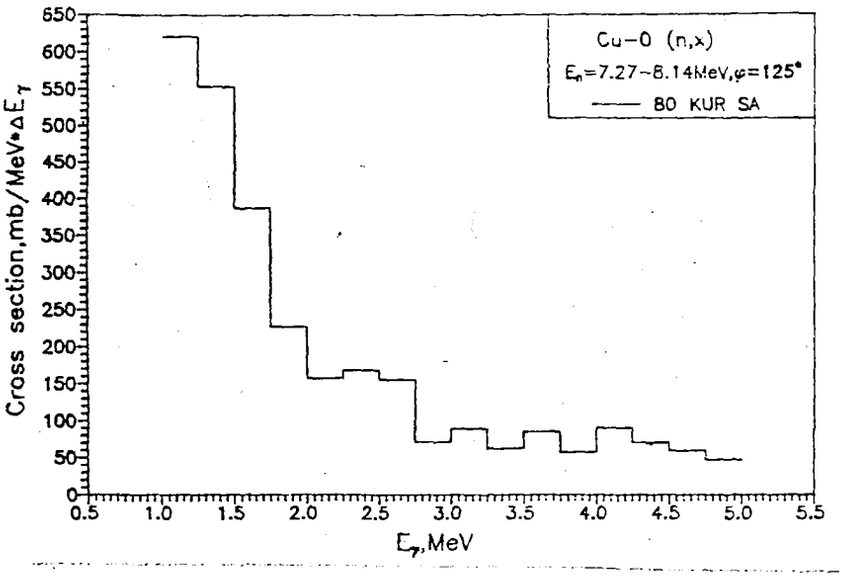
Cu-0 (n,x)
E_n=7.27-8.14MeV,φ=125°
80 KUR SA
Cross section,mb/MeV*ΔE$_\gamma$
E$_\gamma$,MeV

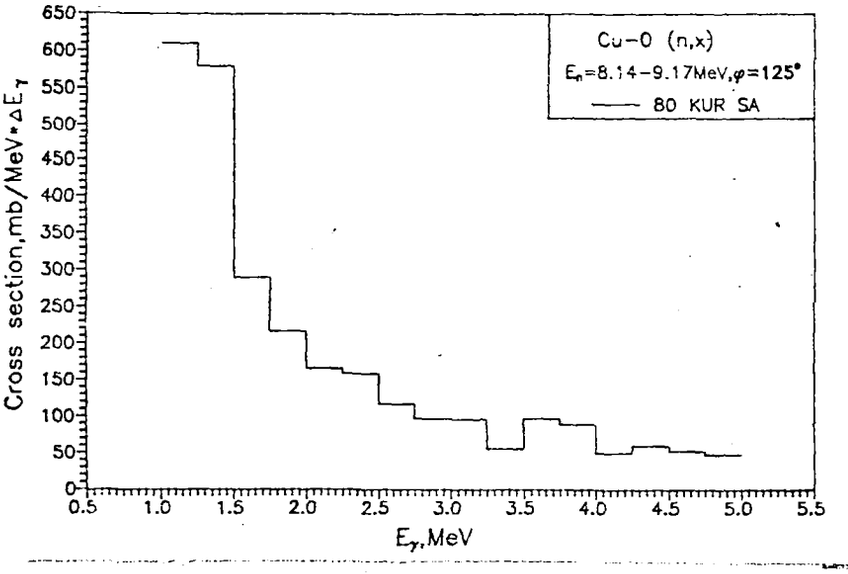
Cu-0 (n,x)
E_n=8.14-9.17MeV,φ=125°
80 KUR SA
Cross section,mb/MeV*ΔE$_\gamma$
E$_\gamma$,MeV

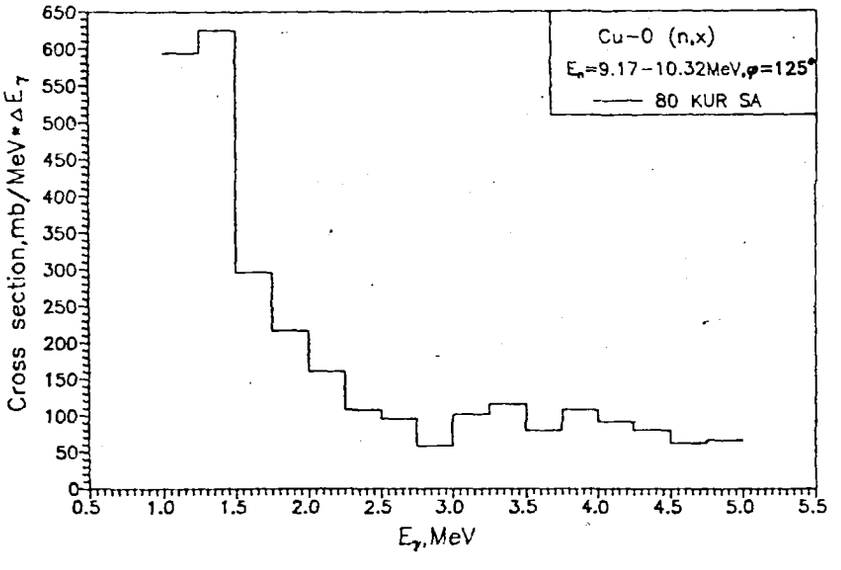
Cu-0 (n,x)
E_n=9.17-10.32MeV,φ=125°
80 KUR SA
Cross section,mb/MeV*ΔE$_\gamma$
E$_\gamma$,MeV

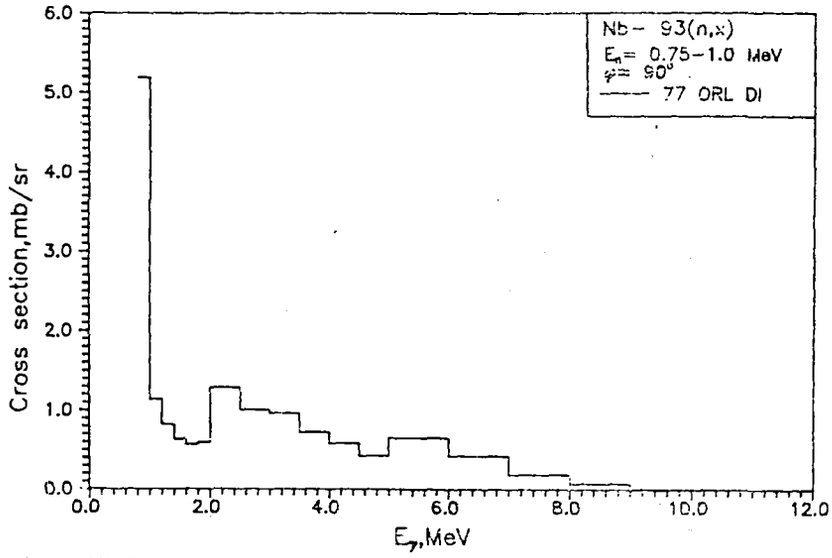
Nb- 93(n,x)
E_n= 0.75-1.0 MeV
φ= 90°
77 ORL DI
Cross section,mb/sr
E_γ,MeV

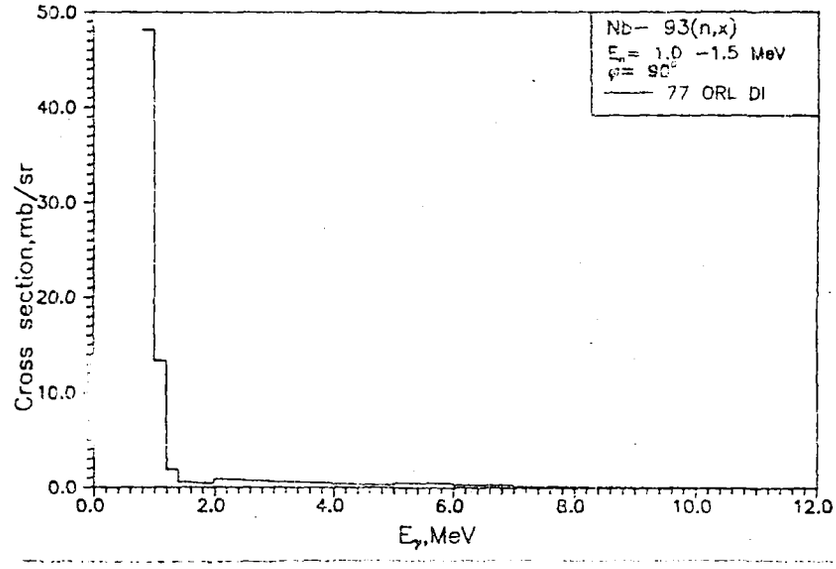
Nb- 93(n,x)
E_n= 1.0 -1.5 MeV
φ= 90°
77 ORL DI
Cross section,mb/sr
E_γ,MeV

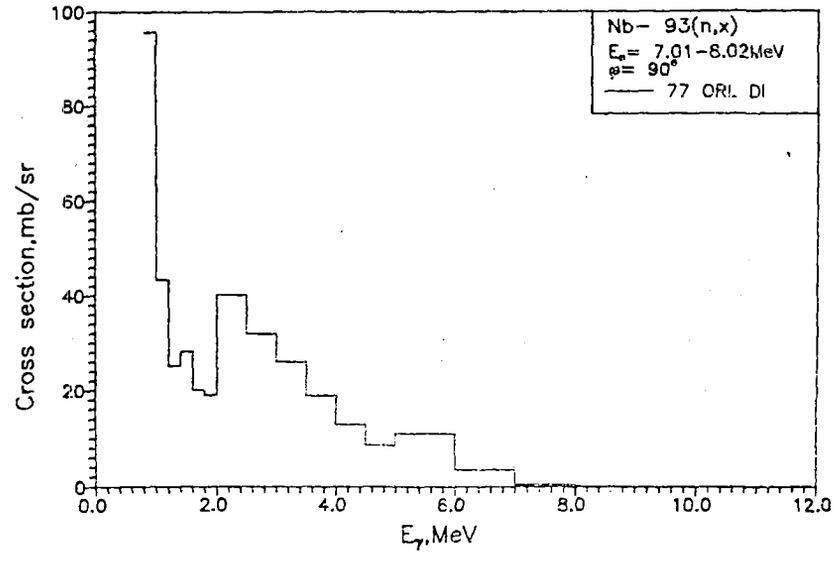
Nb- 93(n,x)
E_n= 7.01-8.02MeV
φ= 90°
77 ORL DI
Cross section,mb/sr
E_γ,MeV

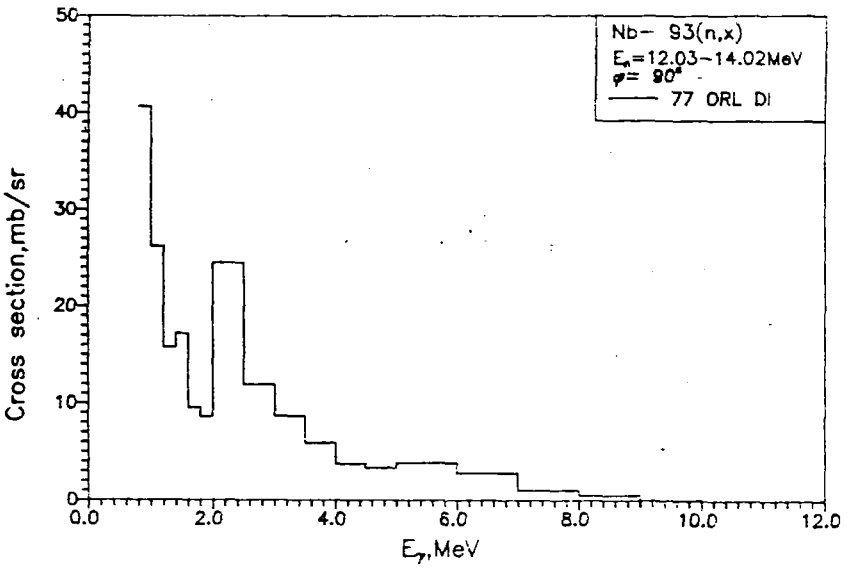
Nb- 93(n,x)
E_n=12.03-14.02MeV
φ= 90°
77 ORL DI
Cross section,mb/sr
E_γ,MeV

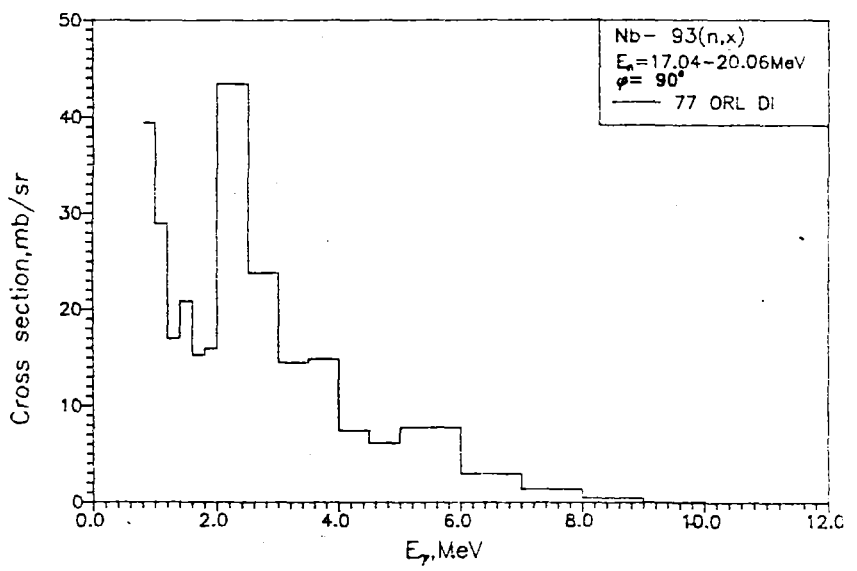
Nb- 93(n,x)
E_n=17.04-20.06MeV
φ= 90°
77 ORL DI
Cross section,mb/sr
E_γ,MeV

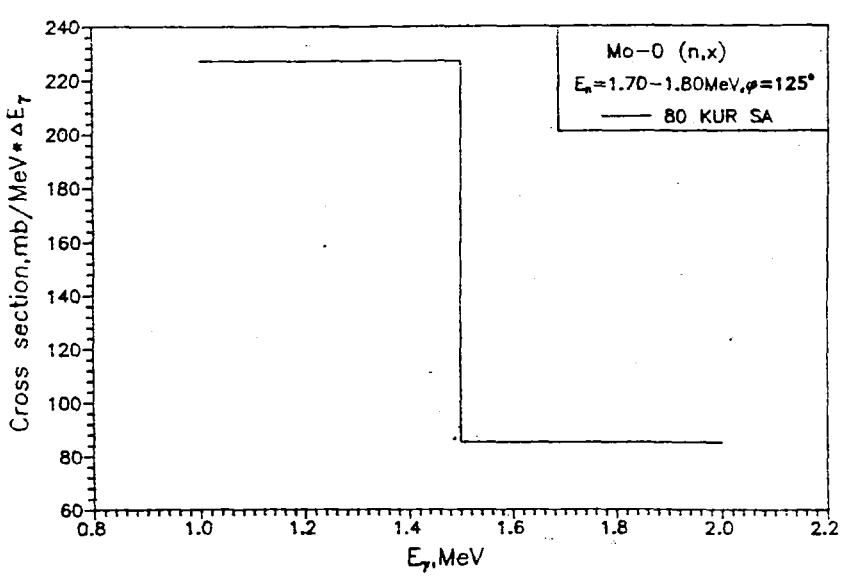
Mo-0 (n,x)
E_n=1.70-1.80MeV,φ=125°
80 KUR SA
Cross section,mb/MeV*ΔE$_\gamma$
E_γ,MeV

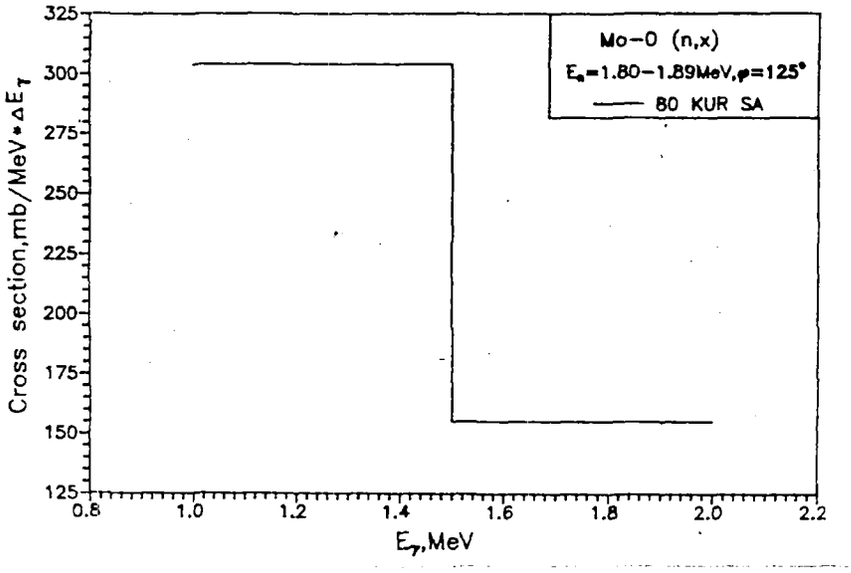
Mo-0 (n,x)
E_n=1.80-1.89MeV,φ=125°
80 KUR SA
Cross section,mb/MeV*ΔE$_\gamma$
E$_\gamma$,MeV

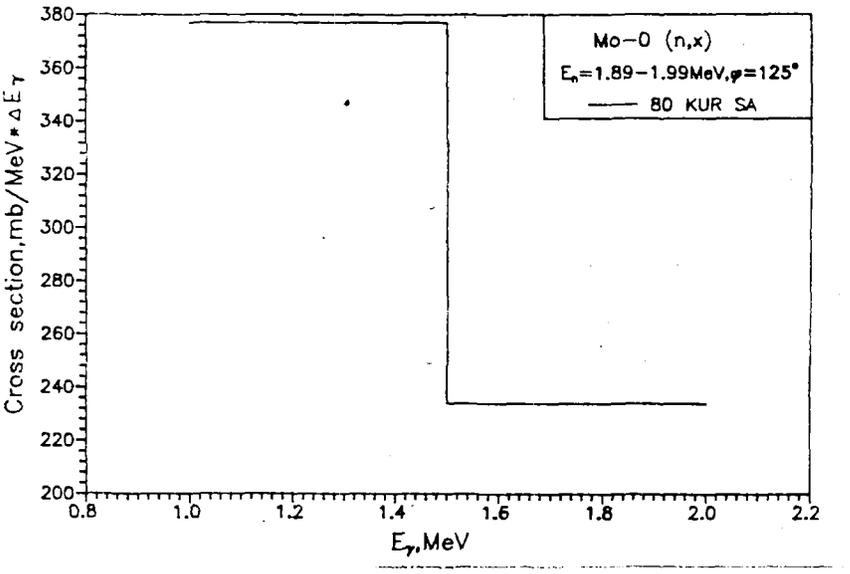
Mo-0 (n,x)
E_n=1.89-1.99MeV,φ=125°
80 KUR SA
Cross section,mb/MeV*ΔE$_\gamma$
E$_\gamma$,MeV

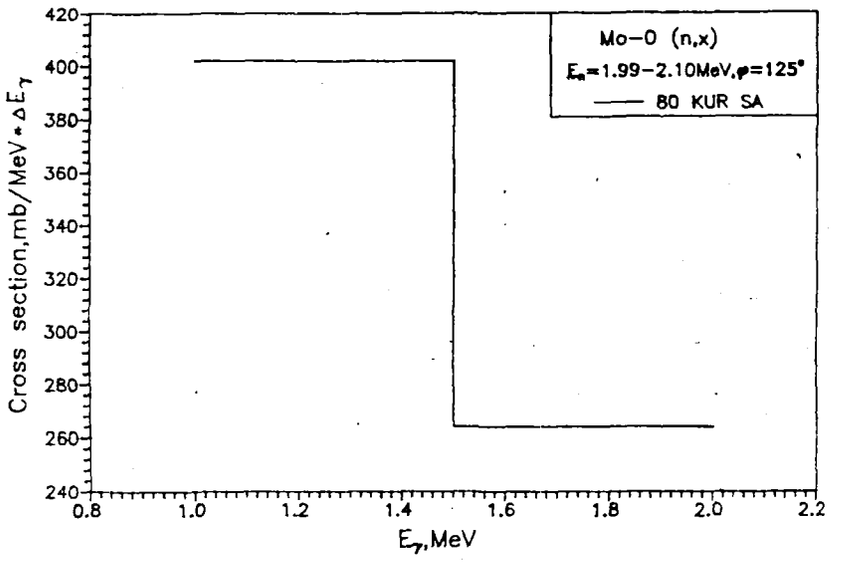
Mo-0 (n,x)
E_n=1.99-2.10MeV,φ=125°
80 KUR SA
Cross section,mb/MeV*ΔE$_\gamma$
E$_\gamma$,MeV

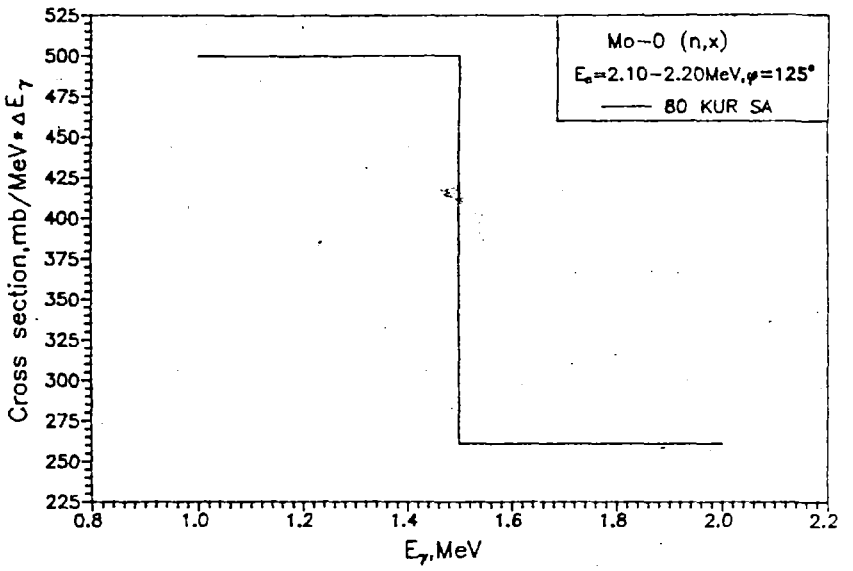
Mo-0 (n,x)
E_n=2.10-2.20MeV,φ=125°
80 KUR SA
Cross section,mb/MeV*ΔE$_\gamma$
E$_\gamma$,MeV

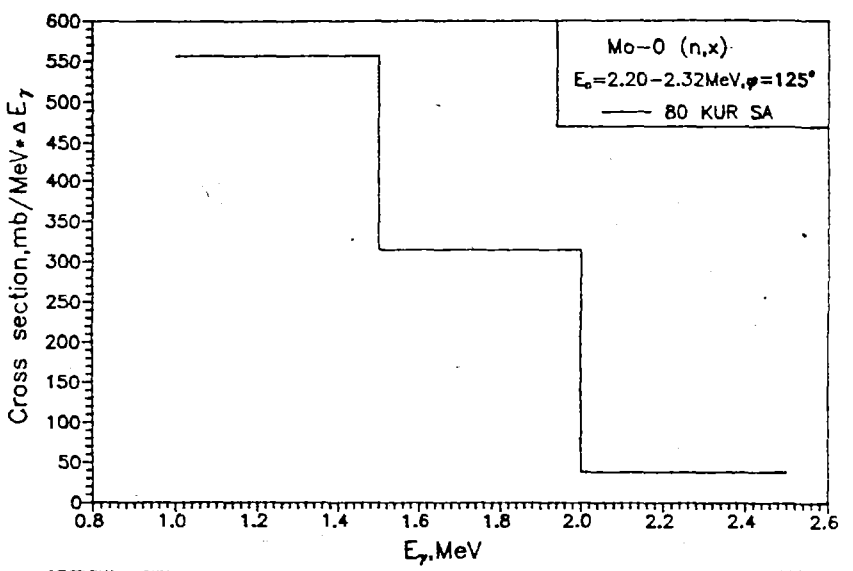
Mo-0 (n,x)
E_n=2.20-2.32MeV,φ=125°
80 KUR SA
Cross section,mb/MeV*ΔE$_\gamma$
E$_\gamma$,MeV

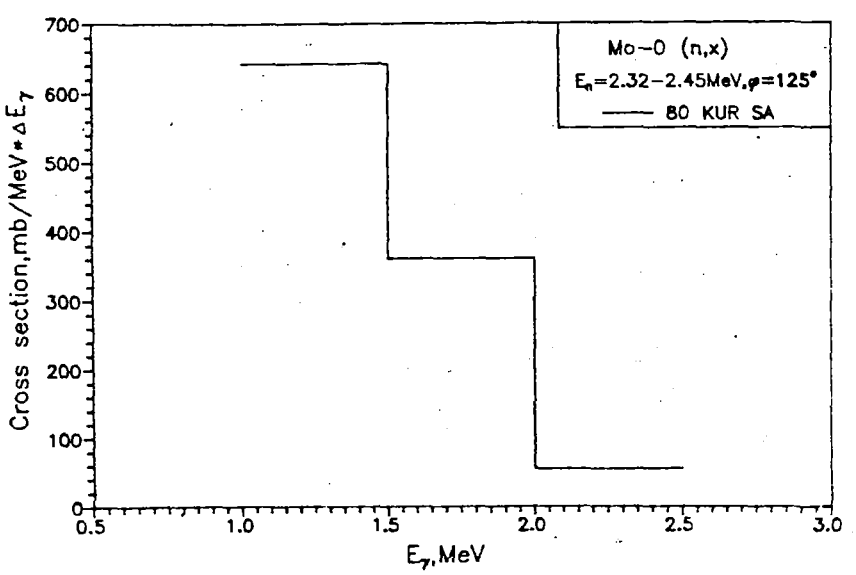
Mo-0 (n,x)
E_n=2.32-2.45MeV,φ=125°
80 KUR SA
Cross section,mb/MeV*ΔE$_\gamma$
E$_\gamma$,MeV

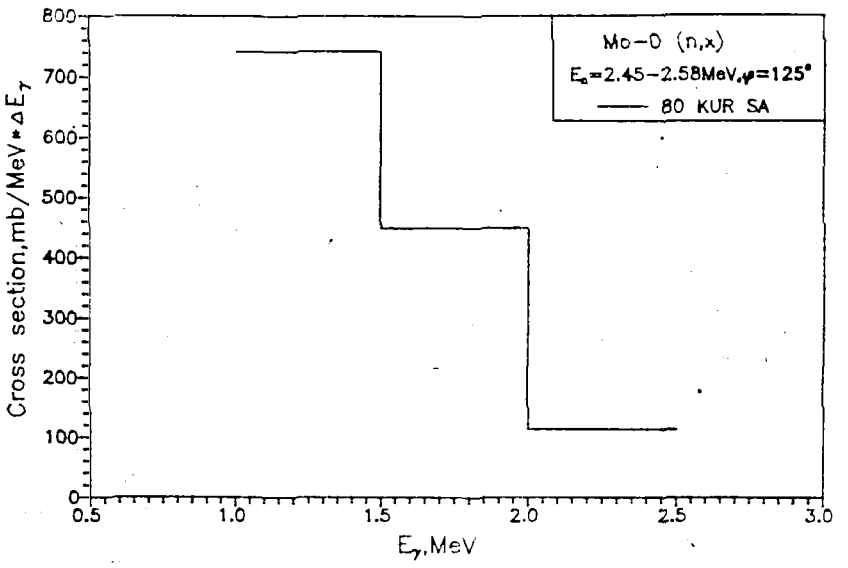
Mo-0 (n,x)
E_n=2.45-2.58MeV,φ=125°
80 KUR SA
Cross section,mb/MeV*ΔE$_\gamma$
E$_\gamma$,MeV

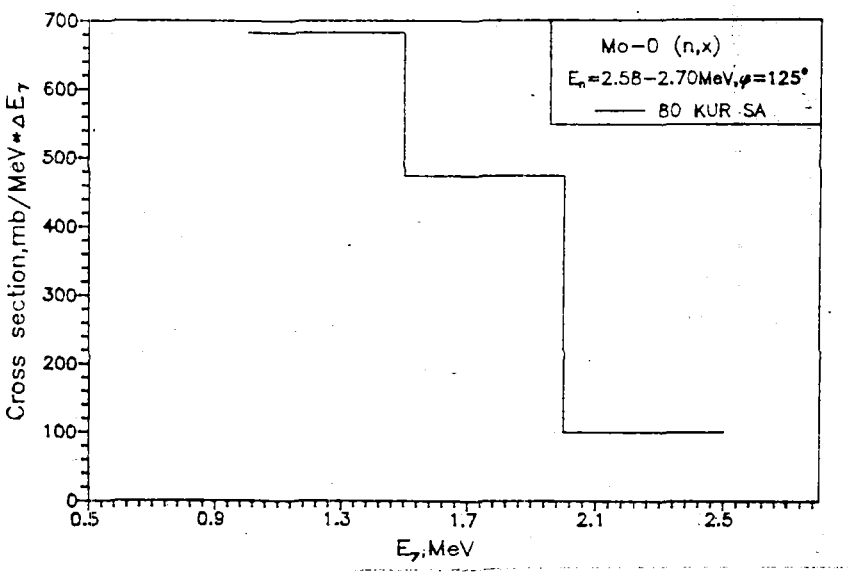
Mo-0 (n,x)
E_n=2.58-2.70MeV,φ=125°
80 KUR SA
Cross section,mb/MeV*ΔE$_\gamma$
E$_\gamma$,MeV

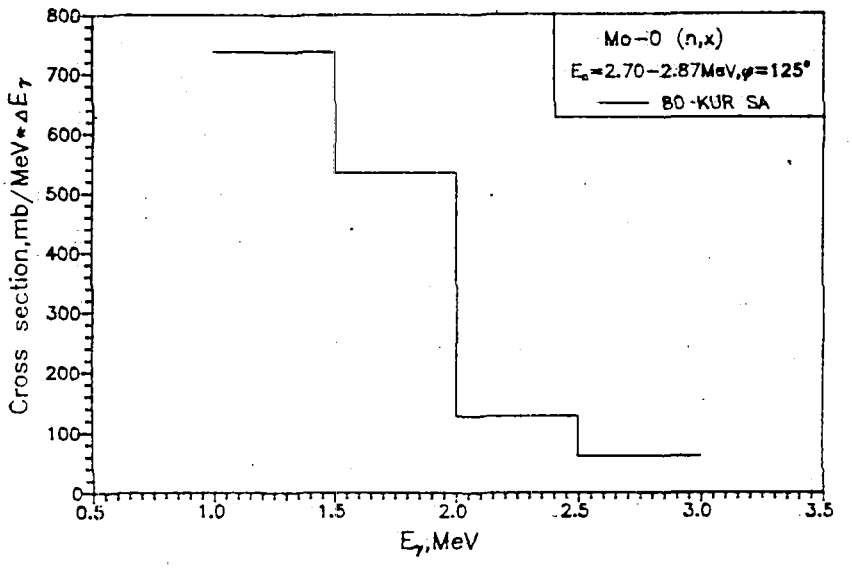
Mo-0 (n,x)
E_n=2.70-2.87MeV,φ=125°
80 KUR SA
Cross section,mb/MeV*ΔE$_\gamma$
E$_\gamma$,MeV

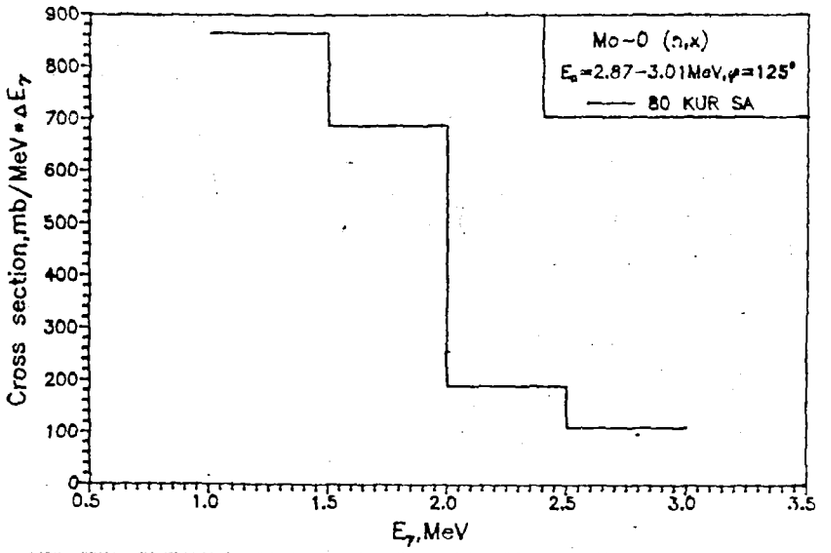
Mo-0 (n,x)
E_n=2.87-3.01MeV,φ=125°
80 KUR SA
Cross section,mb/MeV*ΔE$_\gamma$
E$_\gamma$,MeV

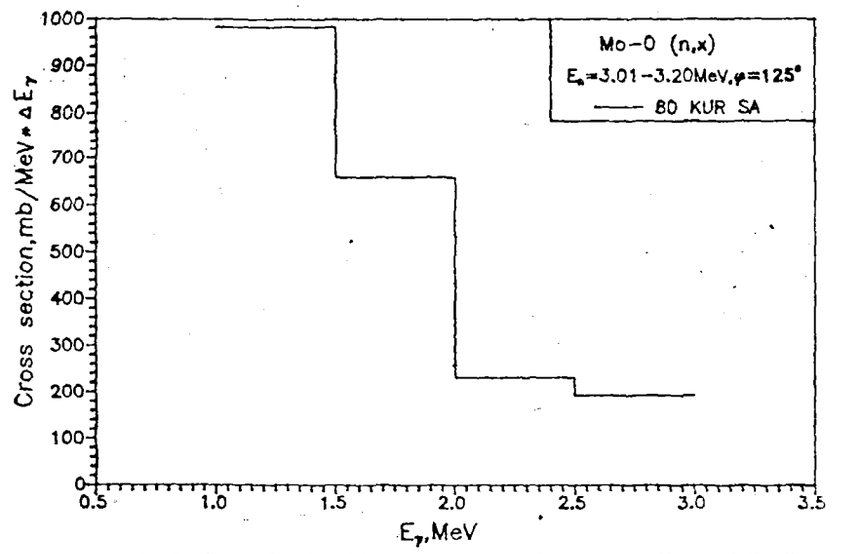
Mo-0 (n,x)
E_n=3.01-3.20MeV,φ=125°
80 KUR SA
Cross section,mb/MeV*ΔE$_\gamma$
E$_\gamma$,MeV

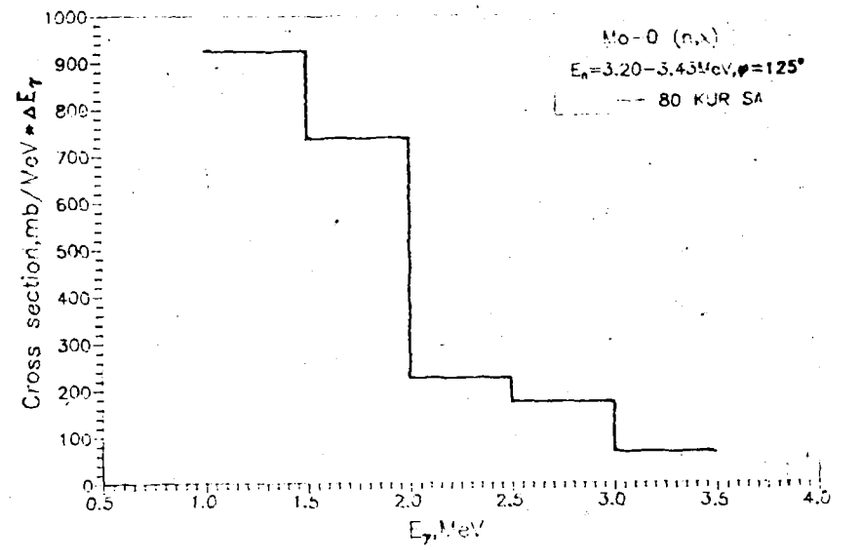
Mo-0 (n,x)
E_n=3.20-3.45MeV,φ=125°
80 KUR SA
Cross section,mb/MeV*ΔE$_\gamma$
E$_\gamma$,MeV

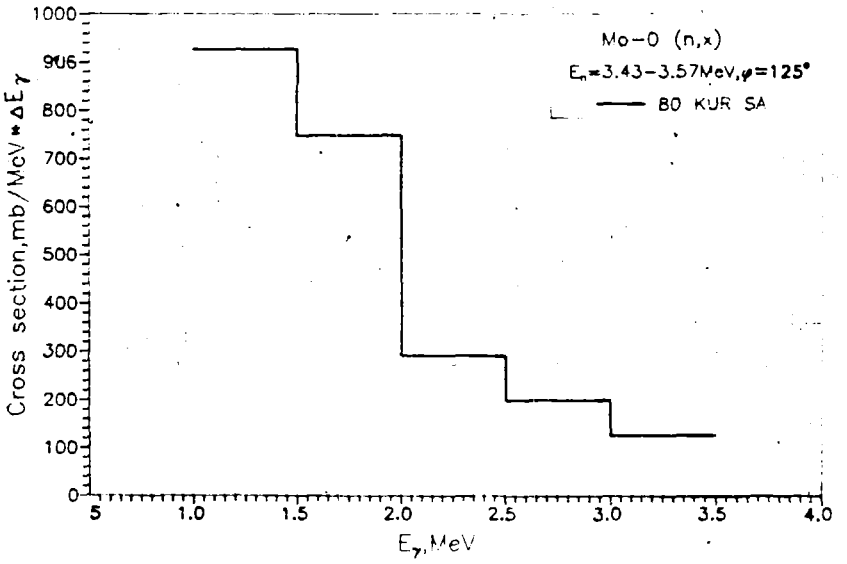
Mo-0 (n,x)
E_n=3.43-3.57MeV,φ=125°
80 KUR SA
Cross section,mb/MeV*ΔE$_\gamma$
E_γ,MeV

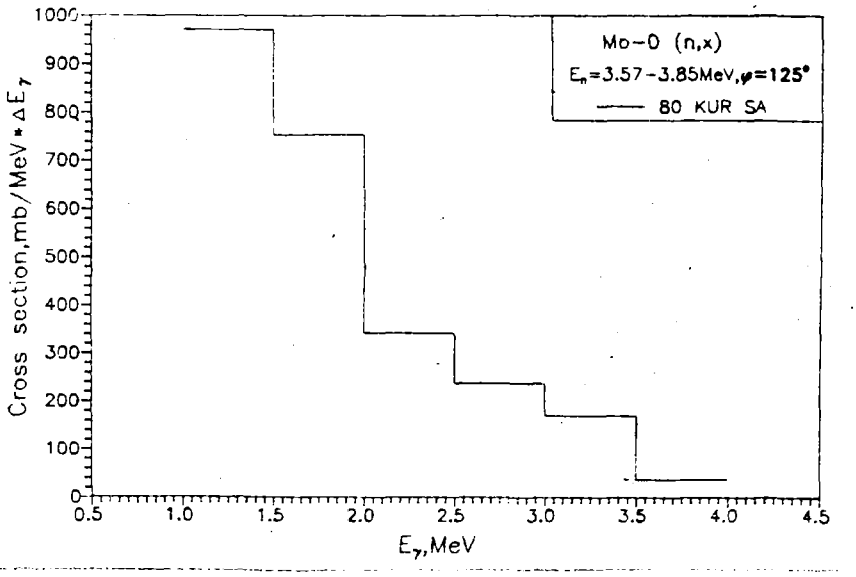
Mo-0 (n,x)
E_n=3.57-3.85MeV,φ=125°
80 KUR SA
Cross section,mb/MeV*ΔE$_\gamma$
E_γ,MeV

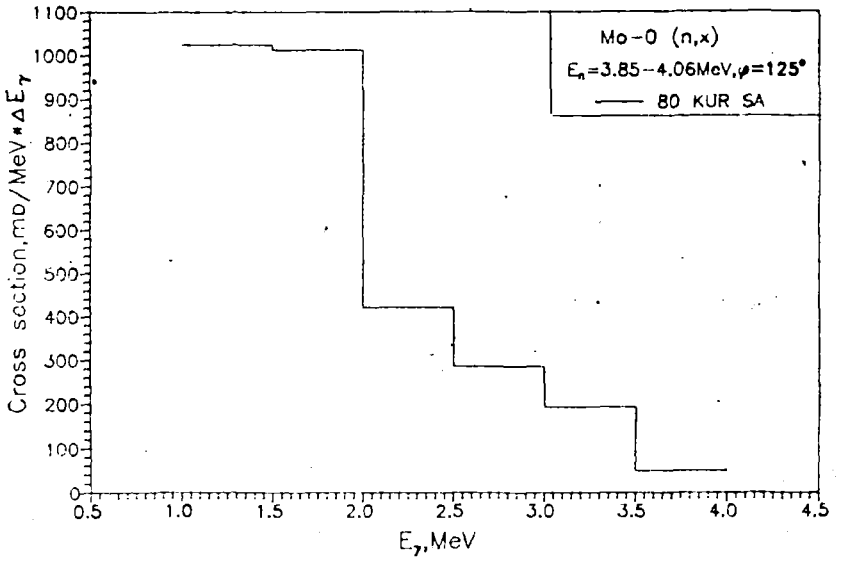
Mo-0 (n,x)
E_n=3.85-4.06MeV,φ=125°
80 KUR SA
Cross section,mb/MeV*ΔE$_\gamma$
E_γ,MeV

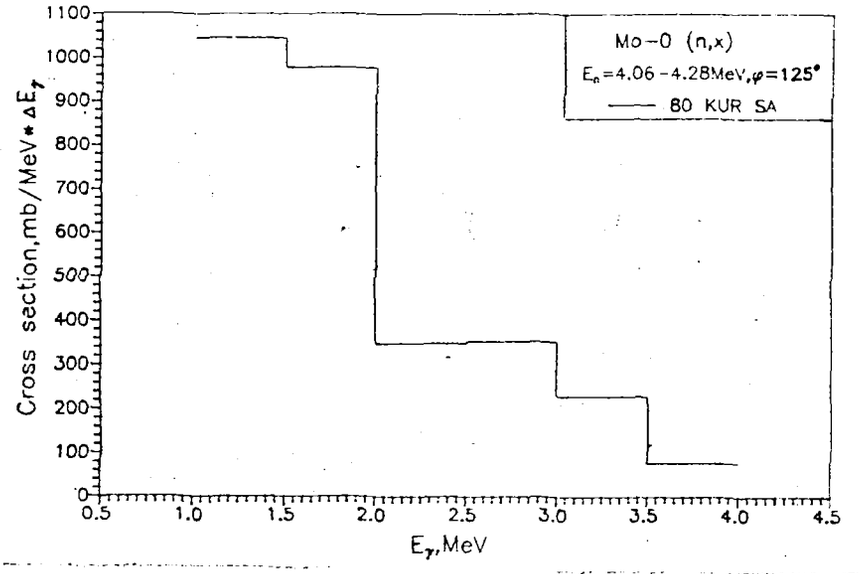
Mo-0 (n,x)
E_n=4.06-4.28MeV,φ=125°
80 KUR SA
Cross section,mb/MeV*ΔE$_\gamma$
E$_\gamma$,MeV

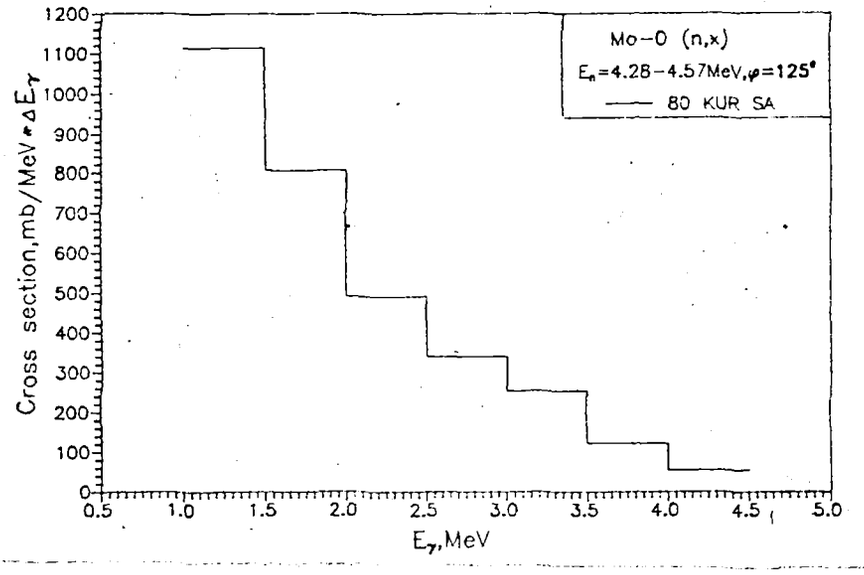
Mo-0 (n,x)
E_n=4.28-4.57MeV,φ=125°
80 KUR SA
Cross section,mb/MeV*ΔE$_\gamma$
E$_\gamma$,MeV

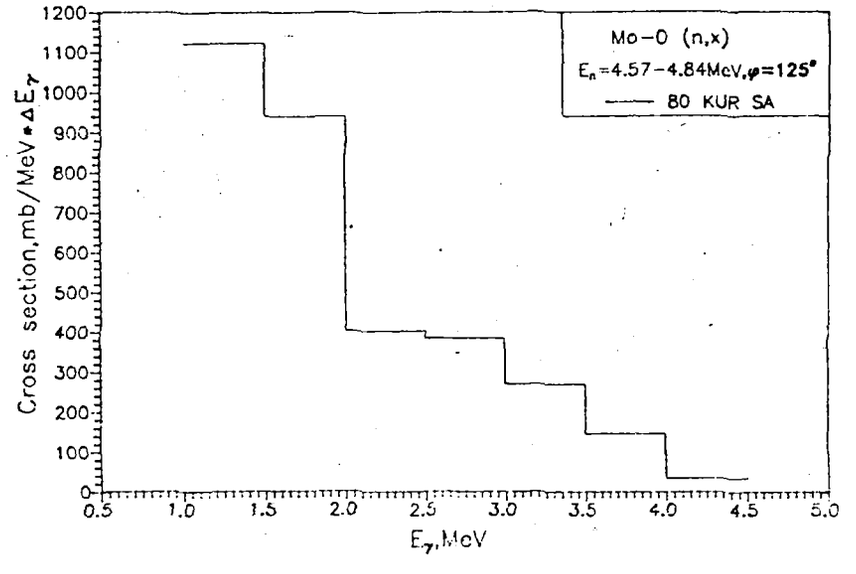
Mo-0 (n,x)
E_n=4.57-4.84MeV,φ=125°
80 KUR SA
Cross section,mb/MeV*ΔE$_\gamma$
E$_\gamma$,MeV

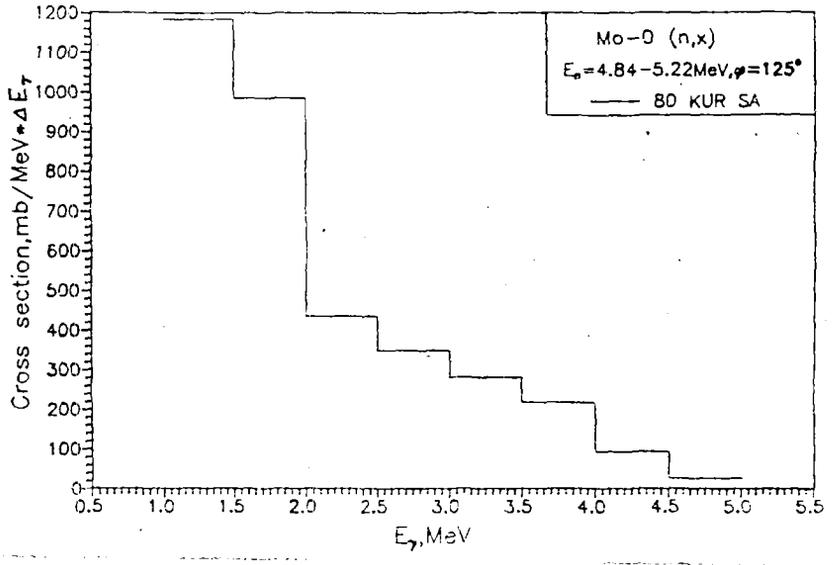
Mo-0 (n,x)
E_n=4.84-5.22MeV,φ=125°
80 KUR SA
Cross section,mb/MeV*ΔE$_\gamma$
E$_\gamma$,MeV

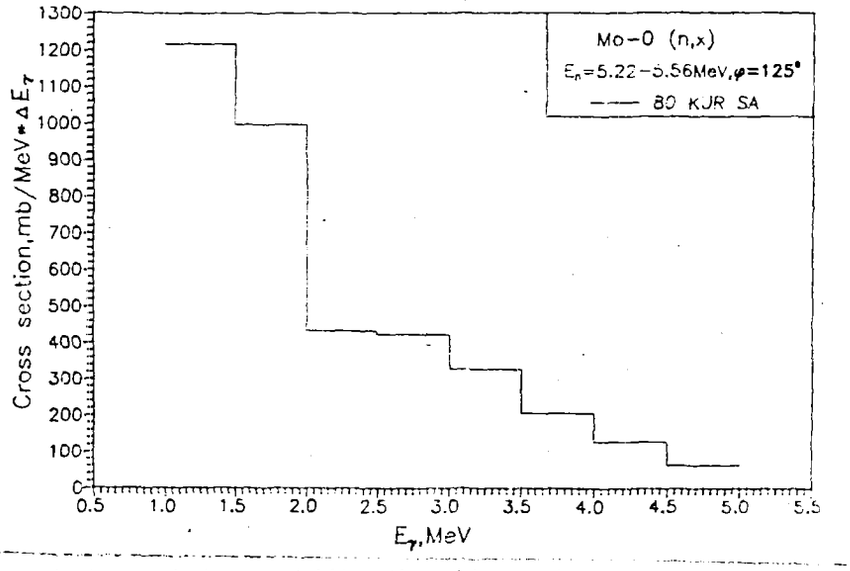
Mo-0 (n,x)
E_n=5.22-5.56MeV,φ=125°
80 KJR SA
Cross section,mb/MeV*ΔE$_\gamma$
E$_\gamma$,MeV

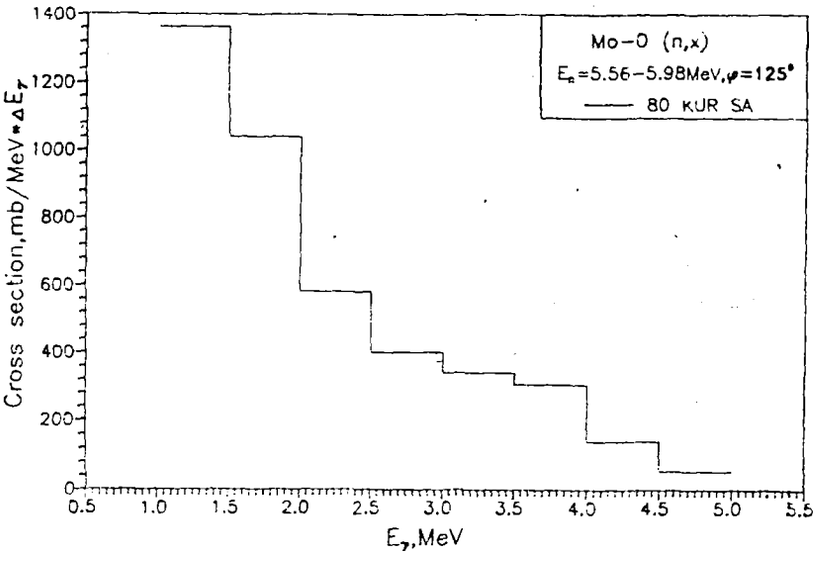
Mo-0 (n,x)
E_n=5.56-5.98MeV,φ=125°
80 KUR SA
Cross section,mb/MeV*ΔE$_\gamma$
E$_\gamma$,MeV

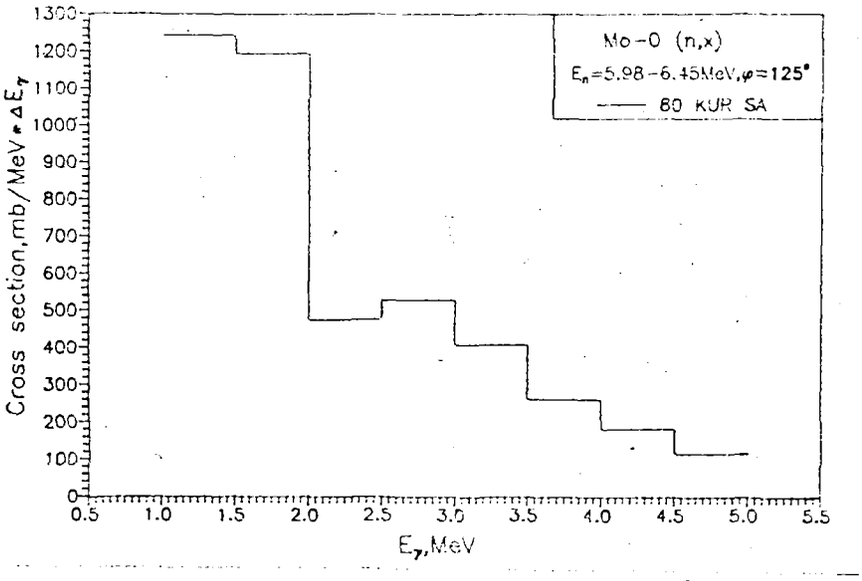
Mo-0 (n,x)
E_n=5.98-6.45MeV,φ=125°
80 KUR SA
Cross section,mb/MeV*ΔE$_\gamma$
E$_\gamma$,MeV

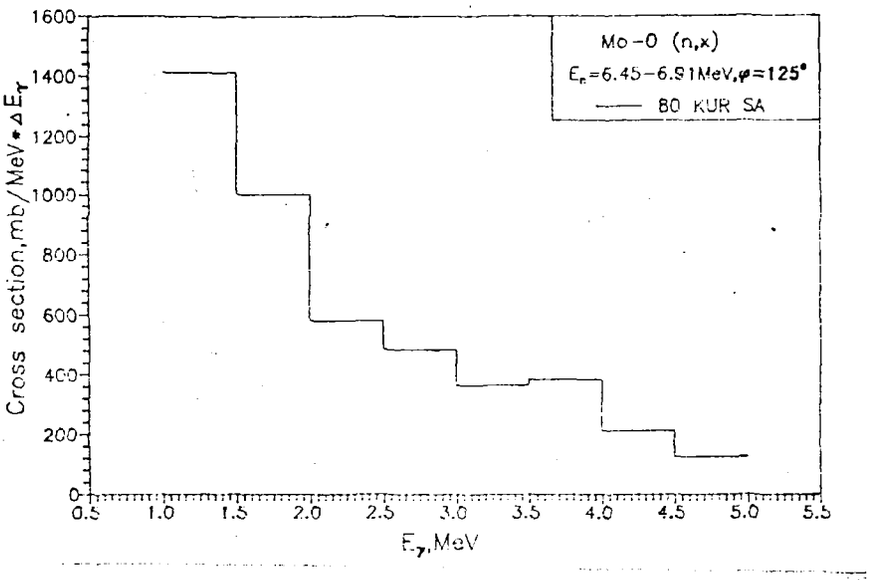
Mo-0 (n,x)
E_n=6.45-6.91MeV,φ=125°
80 KUR SA
Cross section,mb/MeV*ΔE$_\gamma$
E$_\gamma$,MeV

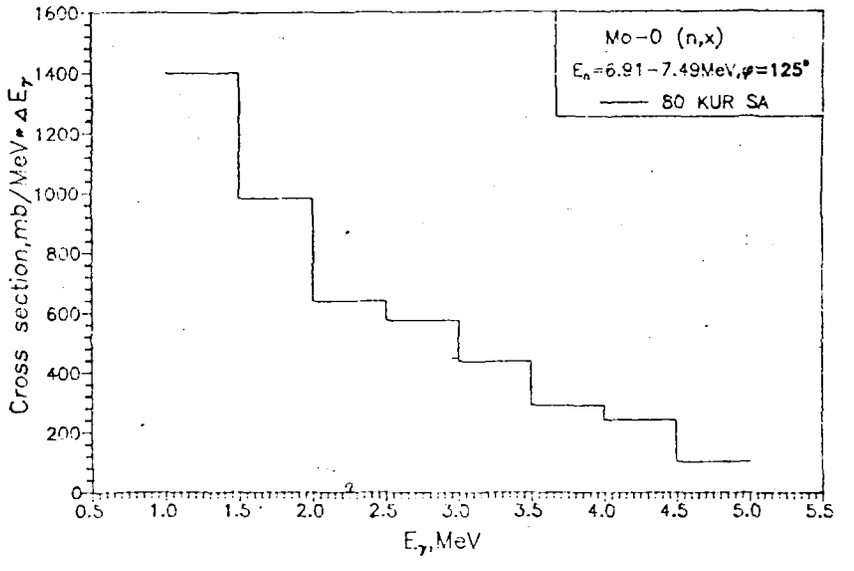
Mo-0 (n,x)
E_n=6.91-7.49MeV,φ=125°
80 KUR SA
Cross section,mb/MeV*ΔE$_\gamma$
E$_\gamma$,MeV

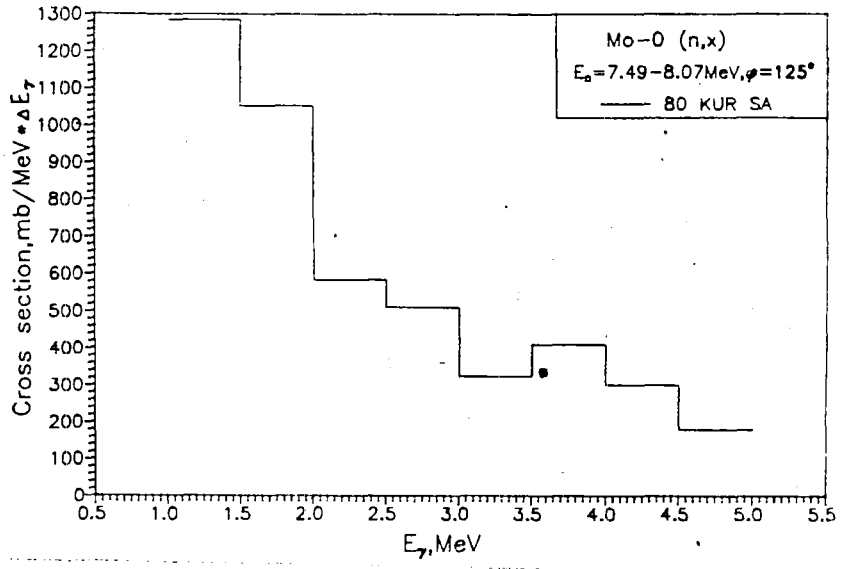
Mo-0 (n,x)
E_n=7.49-8.07MeV,φ=125°
80 KUR SA
Cross section,mb/MeV*ΔE$_\gamma$
E_γ,MeV

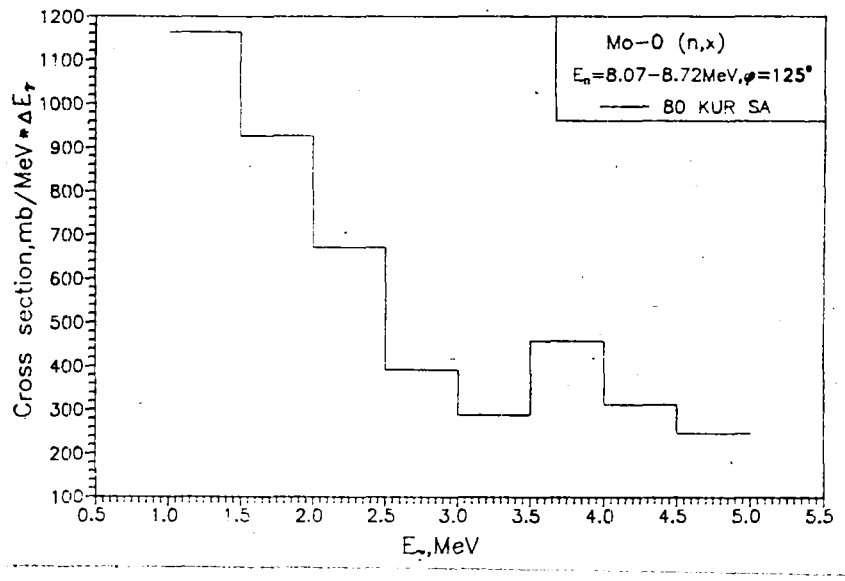
Mo-0 (n,x)
E_n=8.07-8.72MeV,φ=125°
80 KUR SA
Cross section,mb/MeV*ΔE$_\gamma$
E_γ,MeV

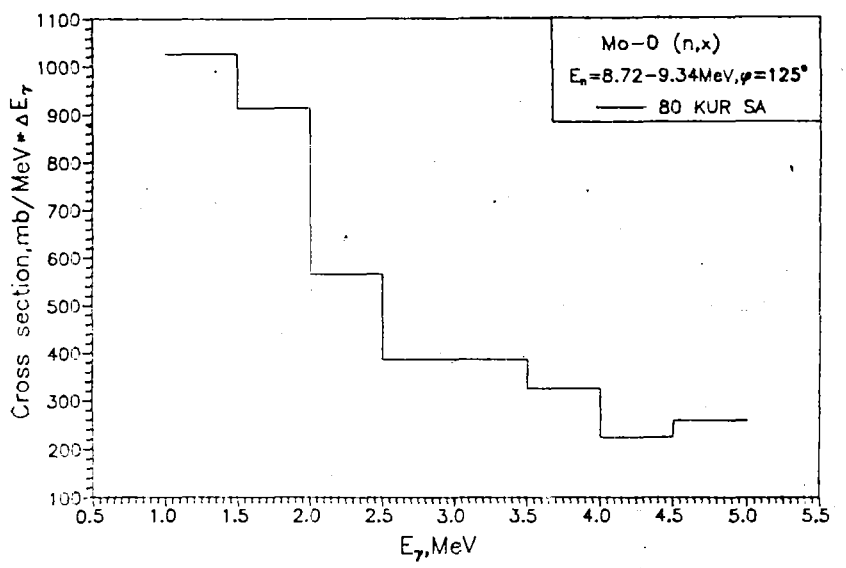
Mo-0 (n,x)
E_n=8.72-9.34MeV,φ=125°
80 KUR SA
Cross section,mb/MeV*ΔE$_\gamma$
E_γ,MeV

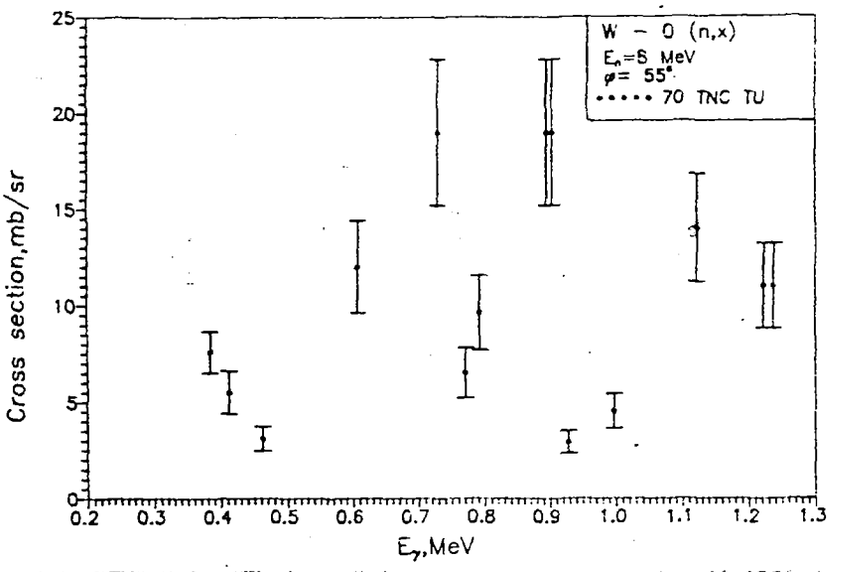
W - O (n,x)
E_n=8 MeV
φ= 55°
70 TNC TU
Cross section,mb/sr
E_γ,MeV

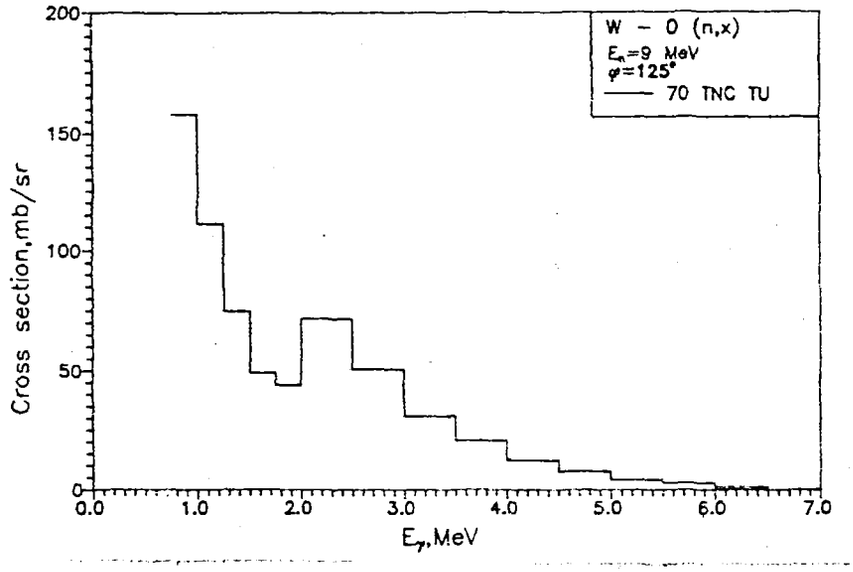
W - O (n,x)
E_n=9 MeV
φ=125°
70 TNC TU
Cross section,mb/sr
E_γ,MeV

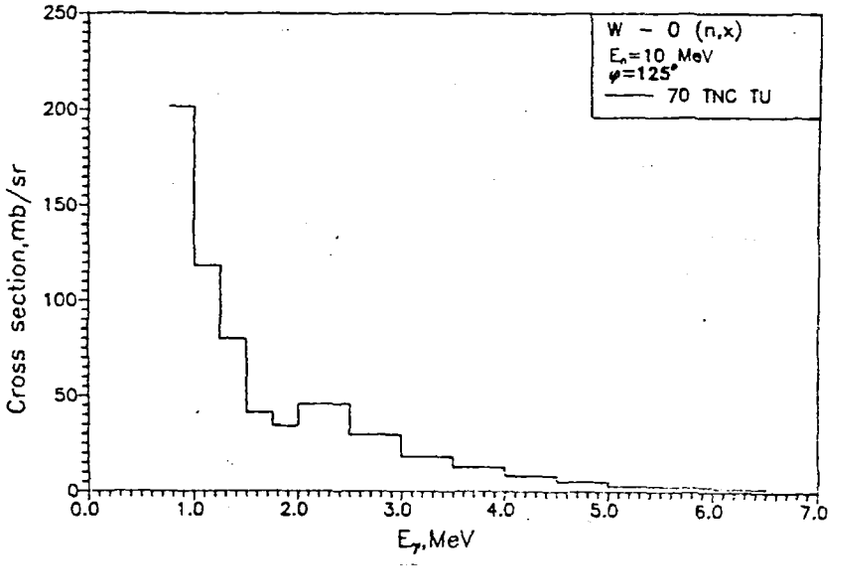
W - O (n,x)
E_n=10 MeV
φ=125°
70 TNC TU
Cross section,mb/sr
E_γ,MeV

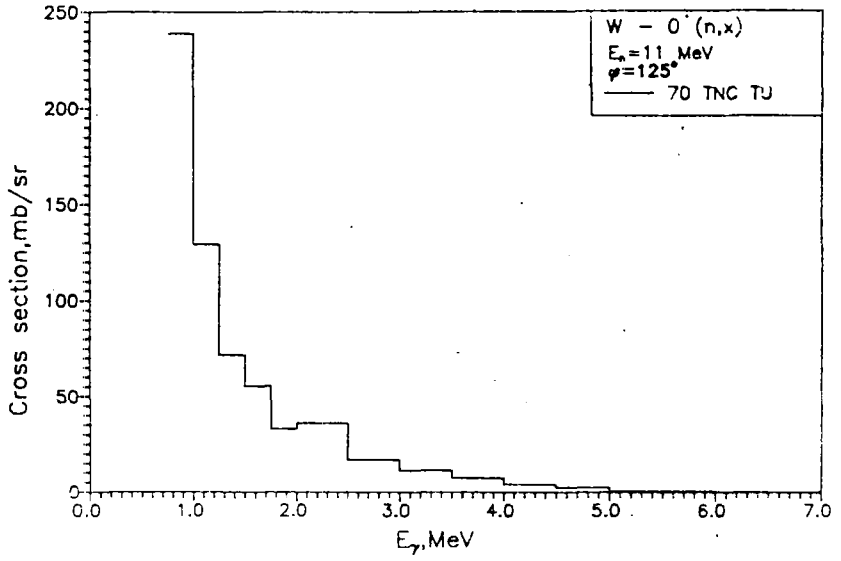
W - 0 (n,x)
E_n=11 MeV
φ=125°
70 TNC TU
Cross section,mb/sr
E_γ,MeV

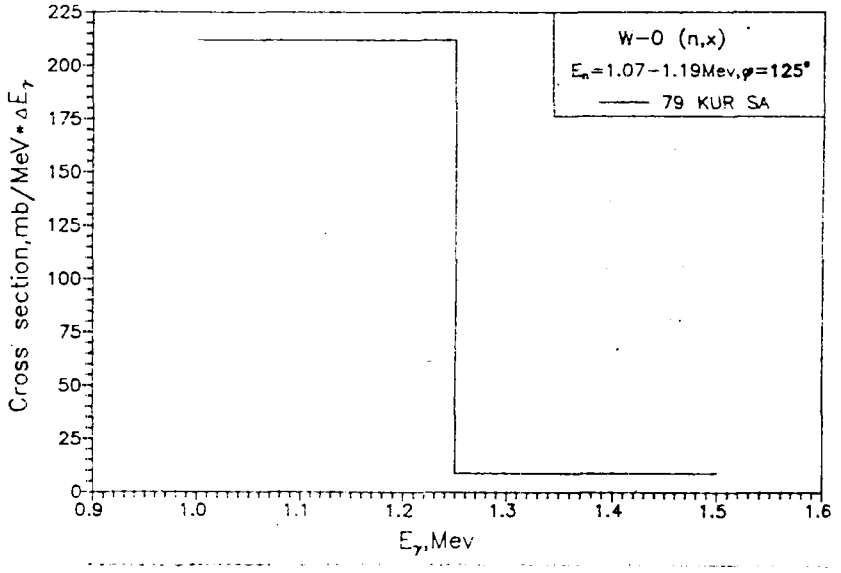
W-0 (n,x)
E_n=1.07-1.19Mev,φ=125°
79 KUR SA
Cross section,mb/MeV * ΔE_γ
E_γ,Mev

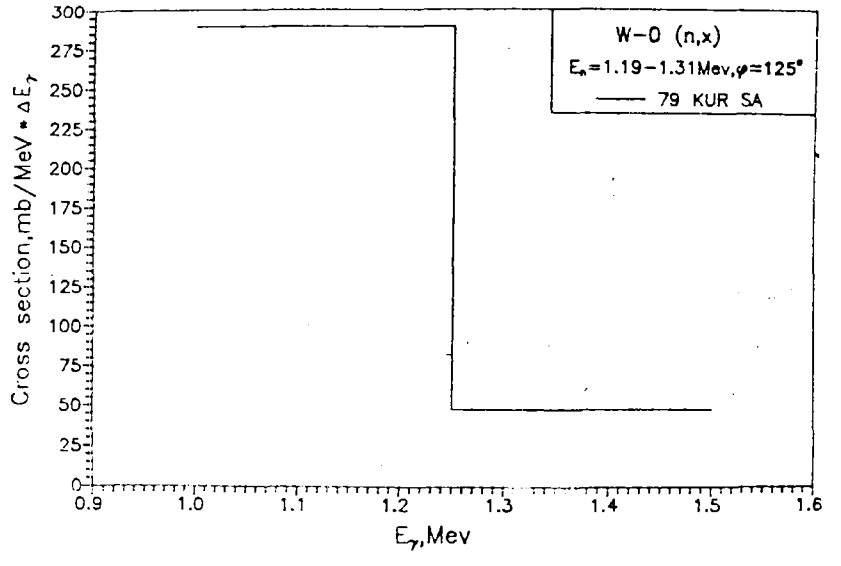
W-0 (n,x)
E_n=1.19-1.31Mev,φ=125°
79 KUR SA
Cross section,mb/MeV * ΔE_γ
E_γ,Mev

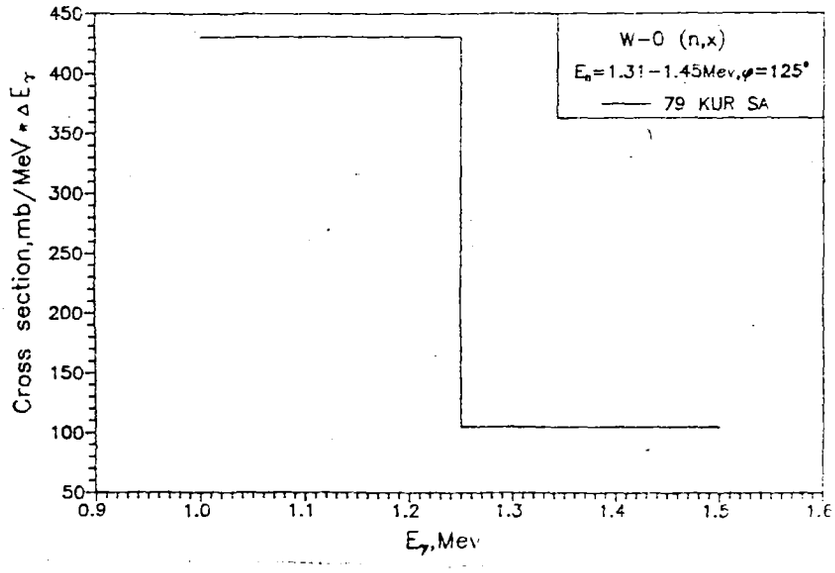
W-O (n,x)
E_n=1.31-1.45Mev,φ=125°
79 KUR SA
Cross section,mb/MeV*ΔE_γ
E_γ,Mev

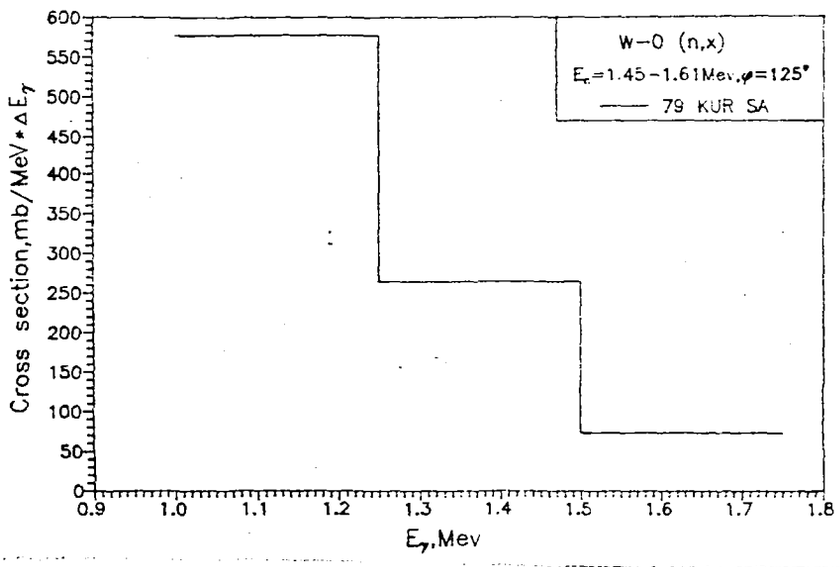
W-O (n,x)
E_n=1.45-1.61Mev,φ=125°
79 KUR SA
Cross section,mb/MeV*ΔE_γ
E_γ,Mev

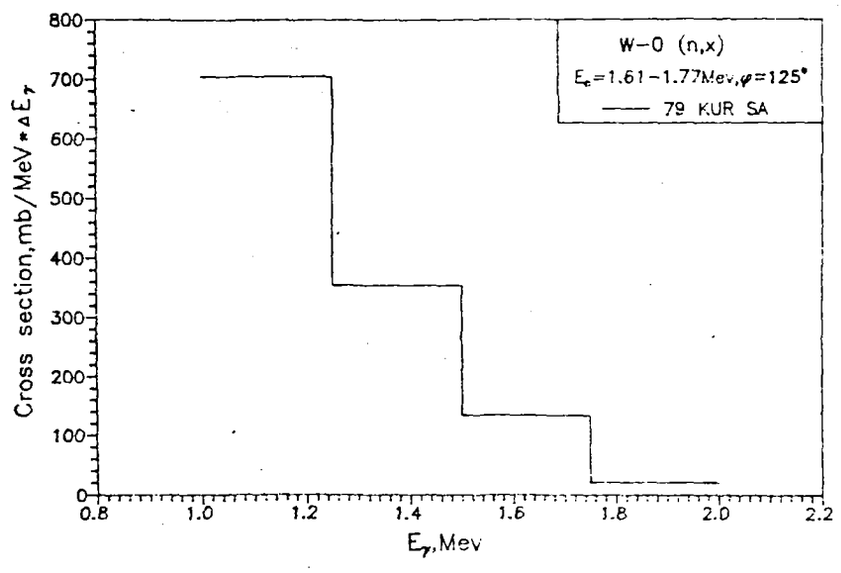
W-O (n,x)
E_n=1.61-1.77Mev,φ=125°
79 KUR SA
Cross section,mb/MeV*ΔE_γ
E_γ,Mev

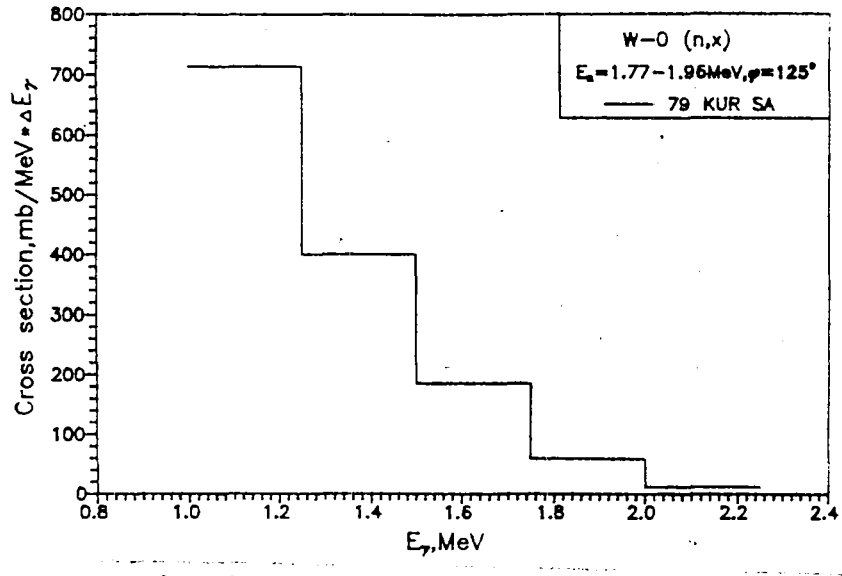
W-O (n,x)
E_n=1.77-1.96MeV,φ=125°
79 KUR SA
Cross section,mb/MeV*ΔE_γ
E_γ,MeV

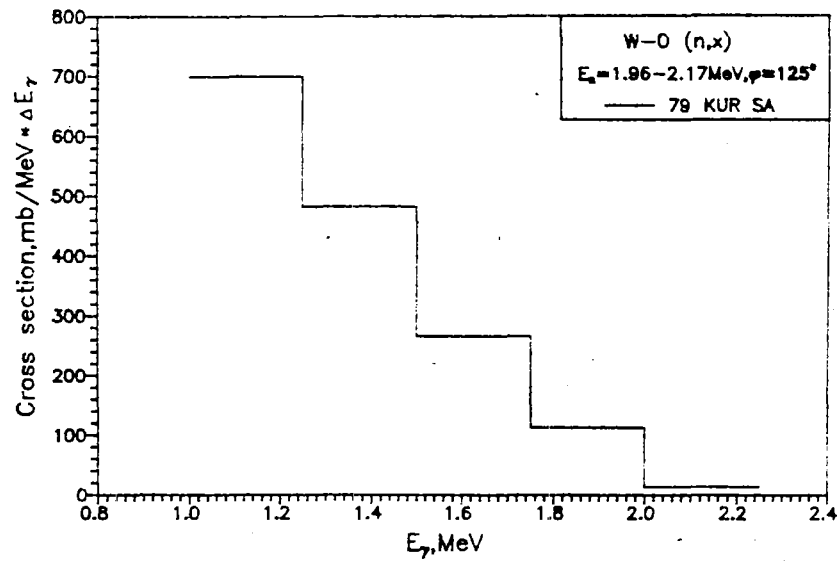
W-O (n,x)
E_n=1.96-2.17MeV,φ=125°
79 KUR SA
Cross section,mb/MeV*ΔE_γ
E_γ,MeV

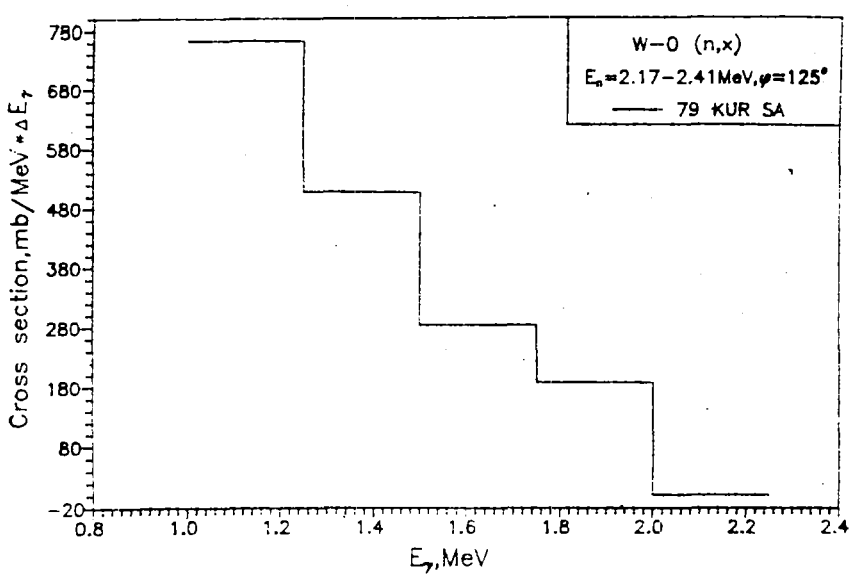
W-O (n,x)
E_n=2.17-2.41MeV,φ=125°
79 KUR SA
Cross section,mb/MeV*ΔE_γ
E_γ,MeV

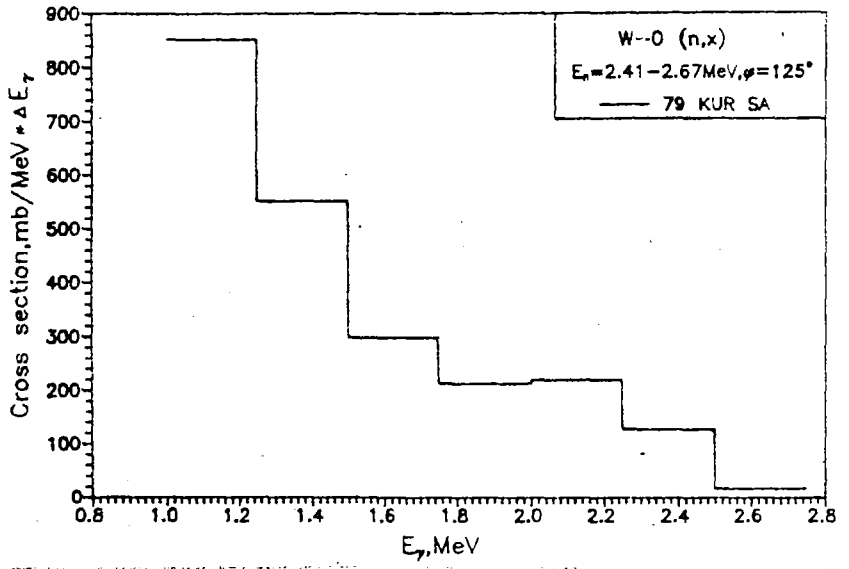
W--O (n,x)
E_n=2.41-2.67MeV,φ=125°
79 KUR SA
Cross section,mb/MeV*ΔE_γ
E_γ,MeV

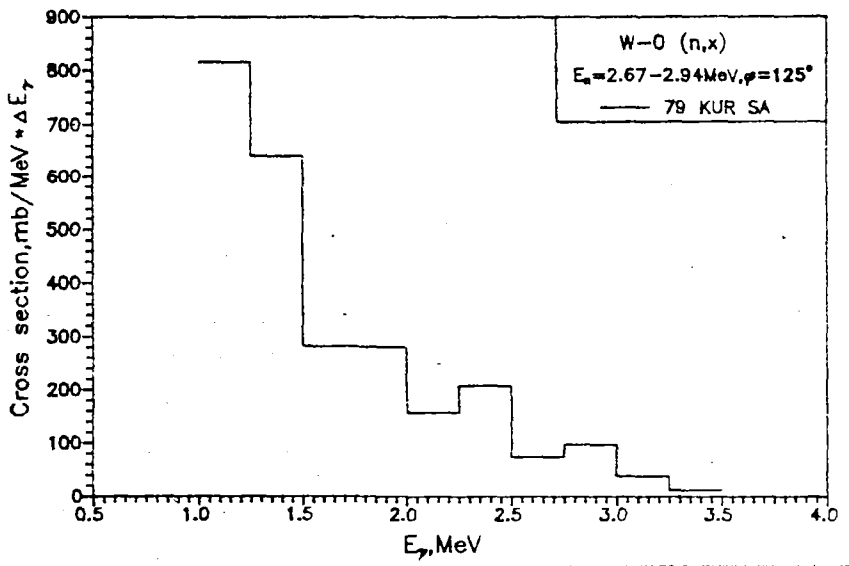
W-O (n,x)
E_n=2.67-2.94MeV,φ=125°
79 KUR SA
Cross section,mb/MeV*ΔE_γ
E_γ,MeV

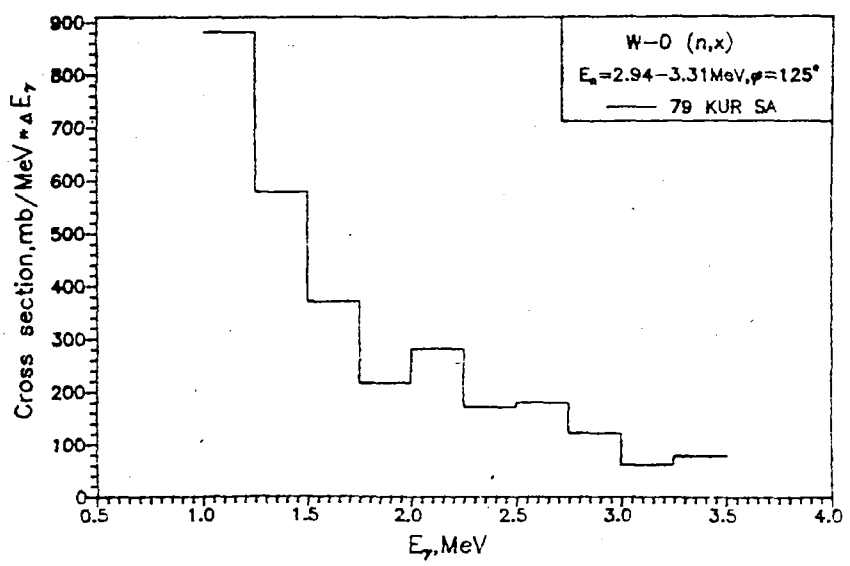
W-O (n,x)
E_n=2.94-3.31MeV,φ=125°
79 KUR SA
Cross section,mb/MeV*ΔE_γ
E_γ,MeV

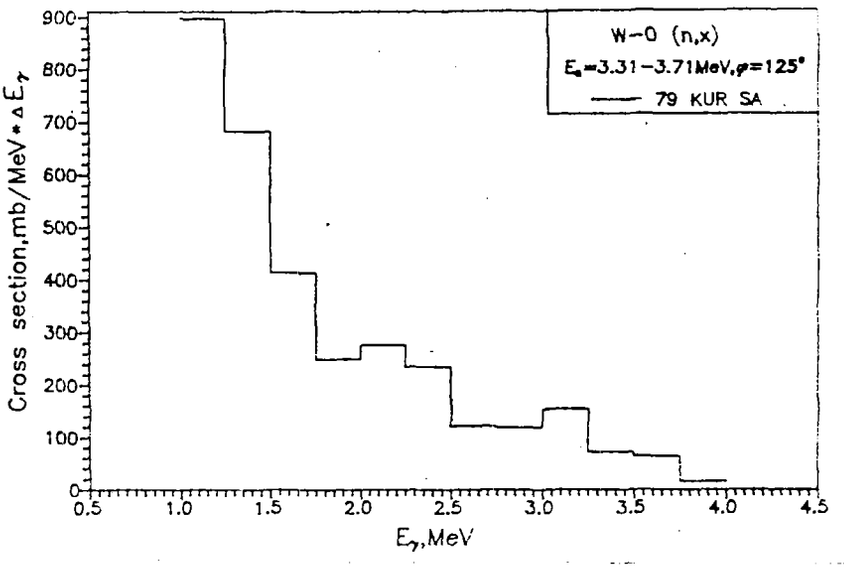
W-0 (n,x)
E_n=3.31-3.71MeV,φ=125°
79 KUR SA
Cross section,mb/MeV * Δ E_γ
E_γ,MeV

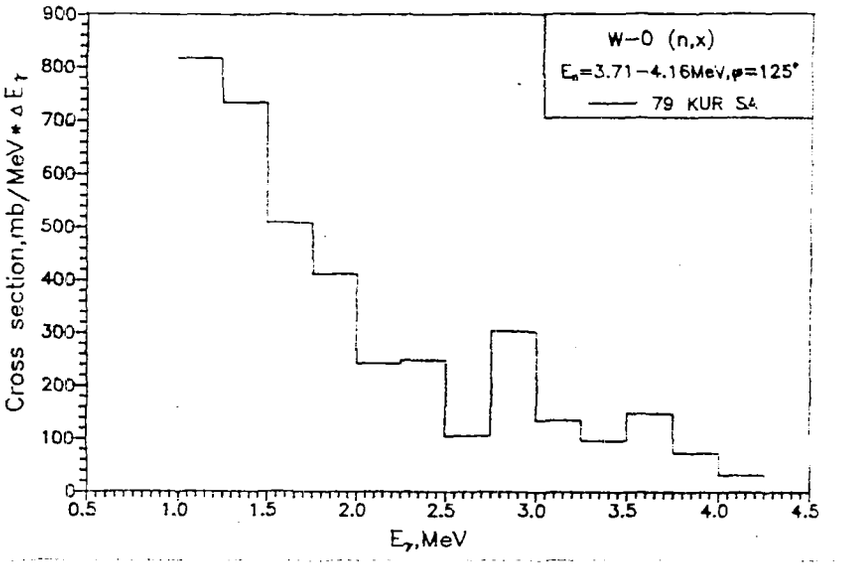
W-0 (n,x)
E_n=3.71-4.16MeV,φ=125°
79 KUR SA
Cross section,mb/MeV * Δ E_γ
E_γ,MeV

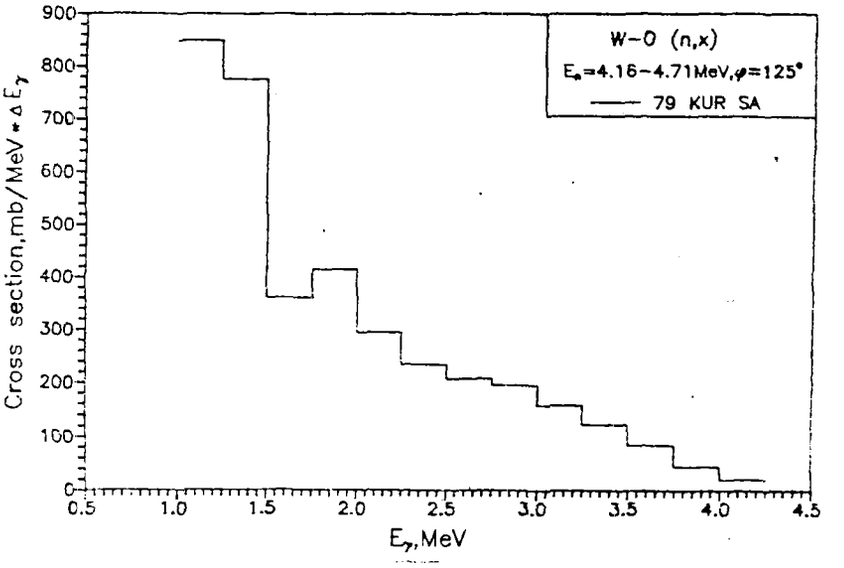
W-0 (n,x)
E_n=4.16-4.71MeV,φ=125°
79 KUR SA
Cross section,mb/MeV * Δ E_γ
E_γ,MeV

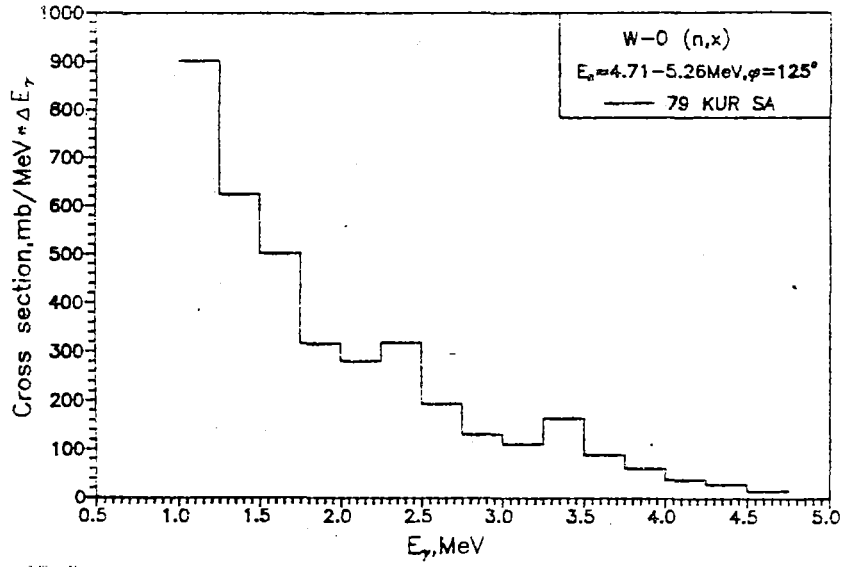
W-0 (n,x)
E_n=4.71-5.26MeV,φ=125°
79 KUR SA
Cross section,mb/MeV*ΔE_γ
E_γ,MeV

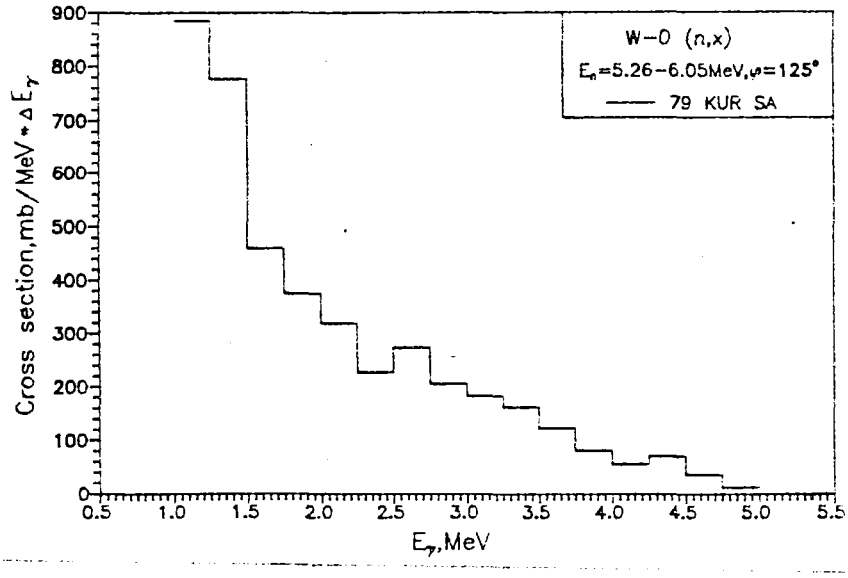
W-0 (n,x)
E_n=5.26-6.05MeV,φ=125°
79 KUR SA
Cross section,mb/MeV*ΔE_γ
E_γ,MeV

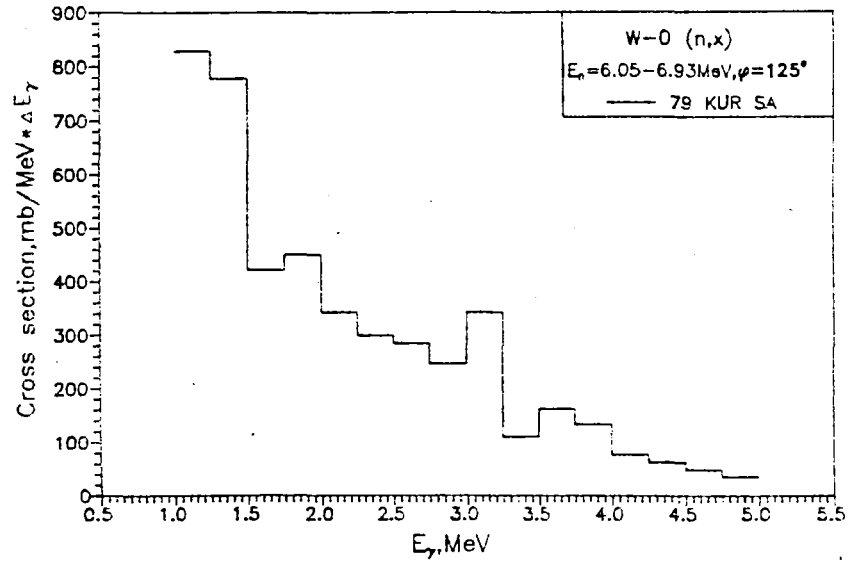
W-0 (n,x)
E_n=6.05-6.93MeV,φ=125°
79 KUR SA
Cross section,mb/MeV*ΔE_γ
E_γ,MeV

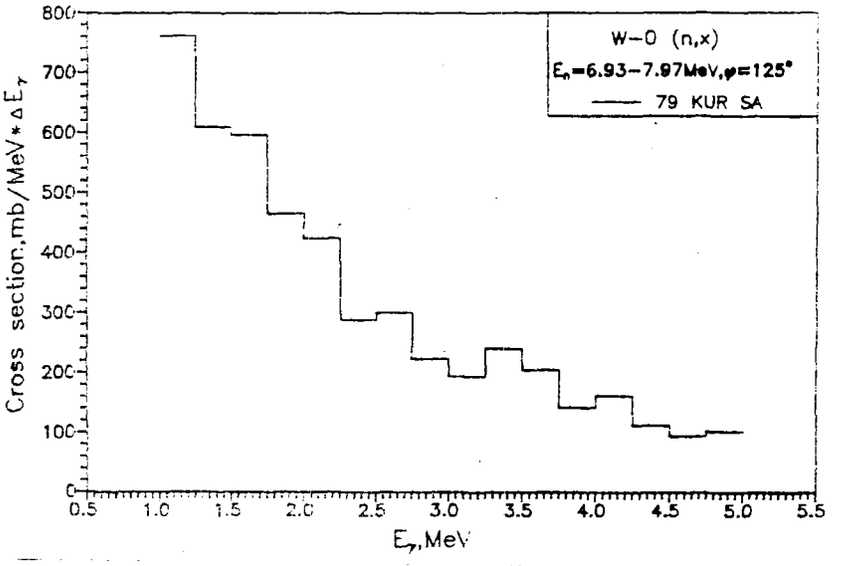
W-0 (n,x)
E_n=6.93-7.97MeV,φ=125°
79 KUR SA
Cross section,mb/MeV*ΔE$_\gamma$
E$_\gamma$,MeV

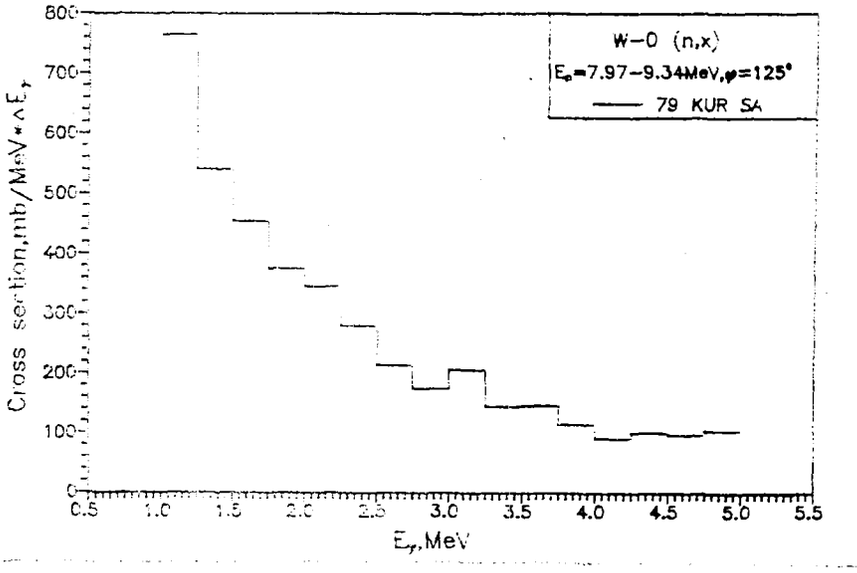
W-0 (n,x)
E_n=7.97-9.34MeV,φ=125°
79 KUR SA
Cross section,mb/MeV*ΔE$_\gamma$
E$_\gamma$,MeV

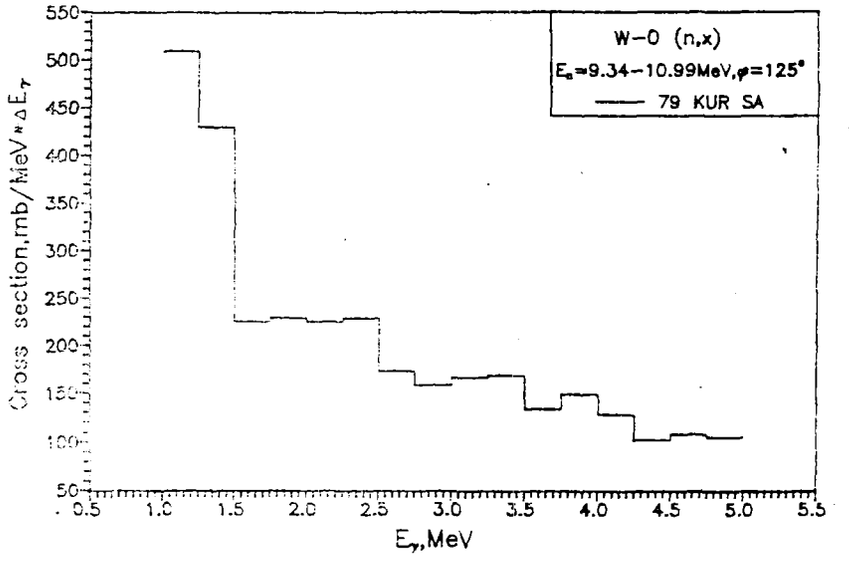
W-0 (n,x)
E_n=9.34-10.99MeV,φ=125°
79 KUR SA
Cross section,mb/MeV*ΔE$_\gamma$
E$_\gamma$,MeV

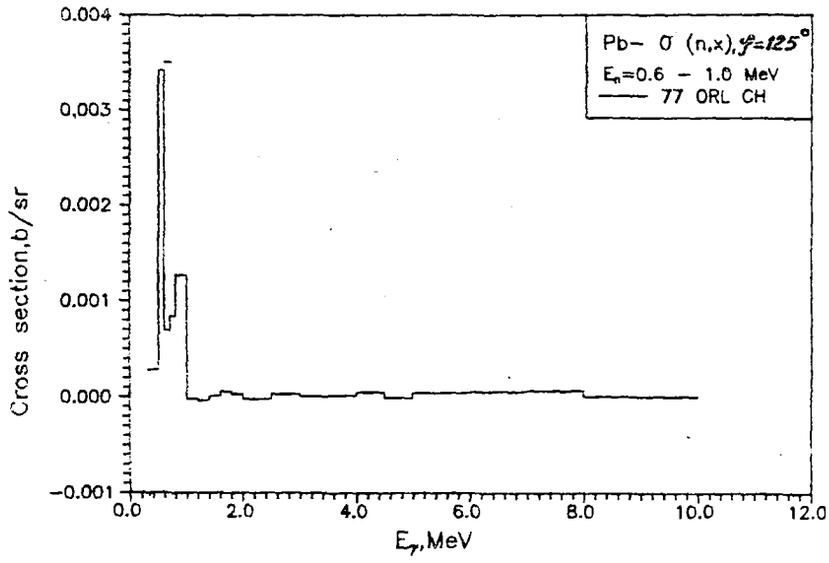
Pb- 0 (n,x), φ=125°
En=0.6 - 1.0 MeV
77 ORL CH
Cross section,b/sr
Eγ,MeV

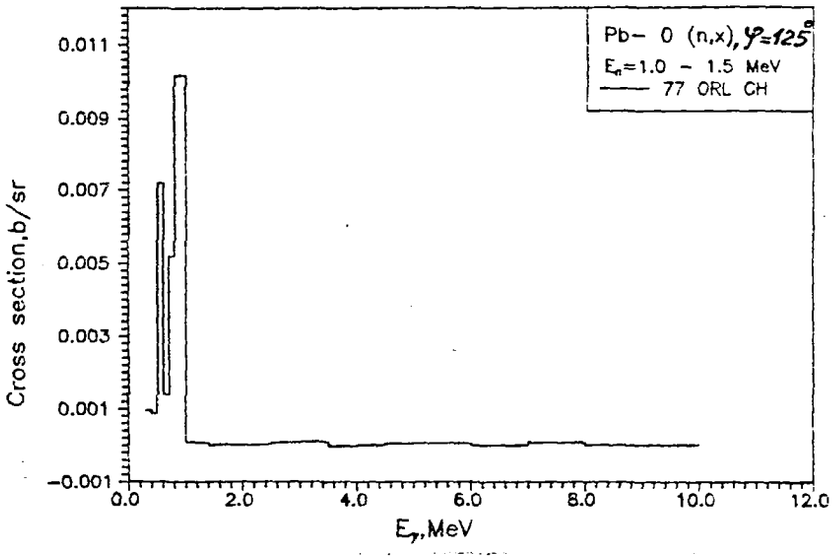
Pb- 0 (n,x), φ=125°
En=1.0 - 1.5 MeV
77 ORL CH
Cross section,b/sr
Eγ,MeV

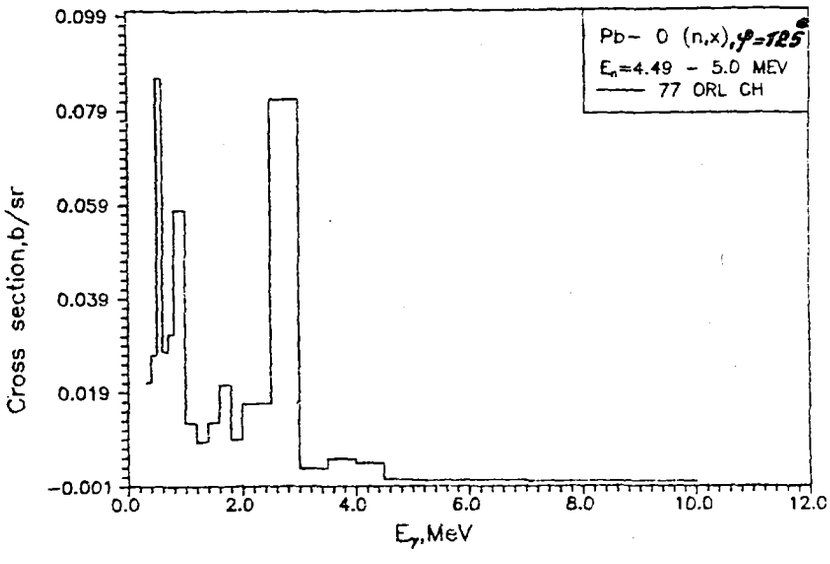
Pb- 0 (n,x), φ=125°
En=4.49 - 5.0 MEV
77 ORL CH
Cross section,b/sr
Eγ,MeV

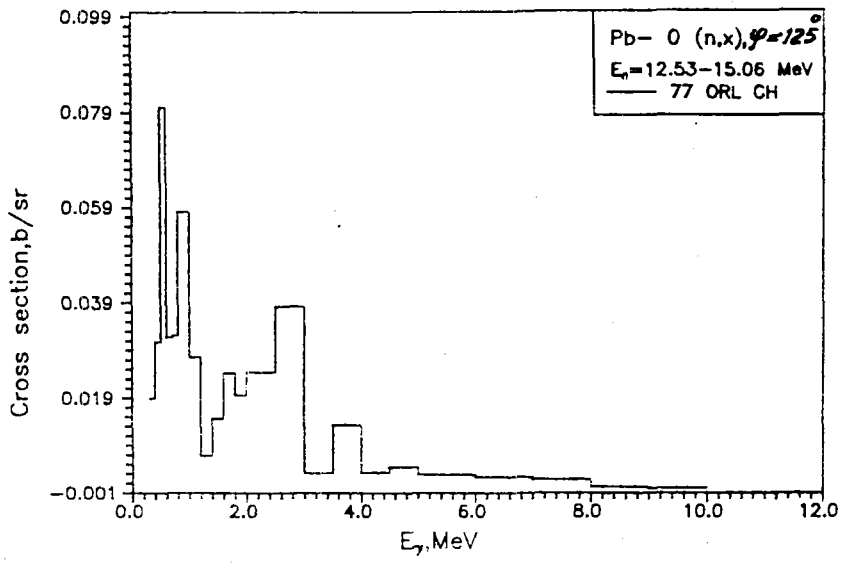
Pb– 0 (n,x), φ=125°
E_n=12.53–15.06 MeV
77 ORL CH
Cross section,b/sr
E_γ,MeV
0.099
0.079
0.059
0.039
0.019
–0.001
0.0
2.0
4.0
6.0
8.0
10.0
12.0

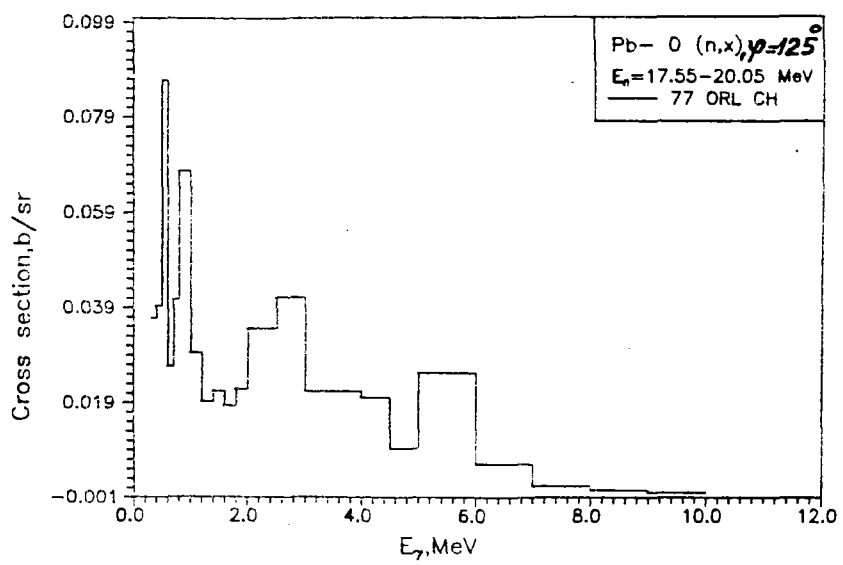
Pb– 0 (n,x), φ=125°
E_n=17.55–20.05 MeV
77 ORL CH
Cross section,b/sr
E_γ,MeV
0.099
0.079
0.059
0.039
0.019
–0.001
0.0
2.0
4.0
6.0
8.0
10.0
12.0

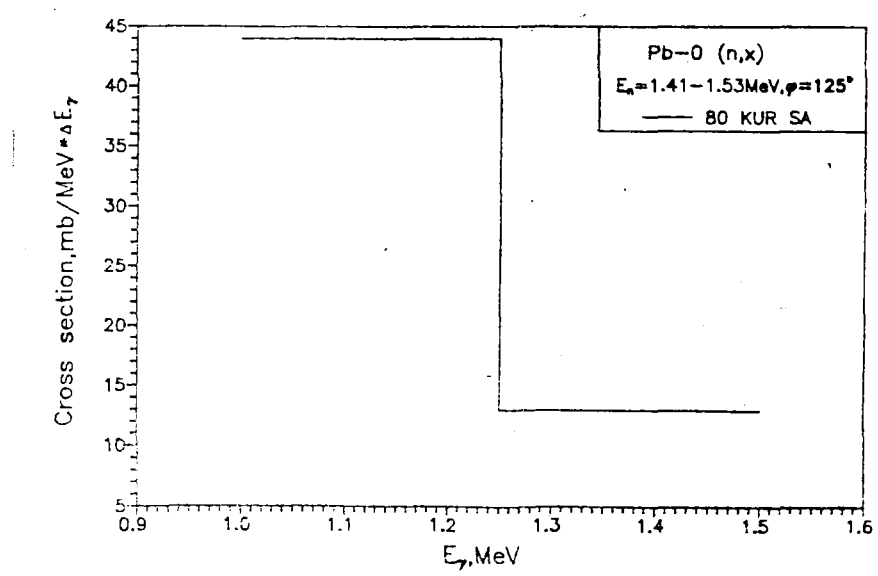
Pb–0 (n,x)
E_n=1.41–1.53MeV, φ=125°
80 KUR SA
Cross section,mb/MeV*ΔE_γ
E_γ,MeV
45
40
35
30
25
20
15
10
5
0.9
1.0
1.1
1.2
1.3
1.4
1.5
1.6

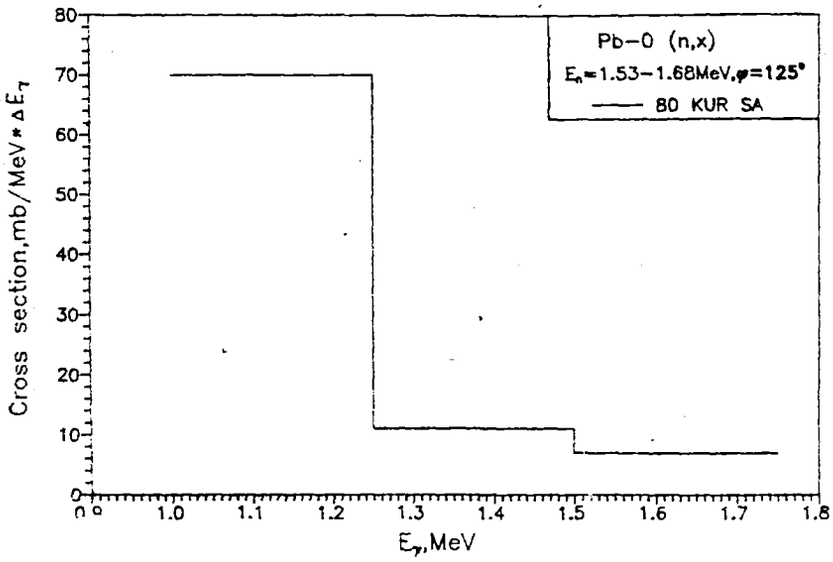
Pb–0 (n,x)
E_n=1.53–1.68MeV,φ=125°
80 KUR SA
Cross section,mb/MeV*ΔE_γ
E_γ,MeV

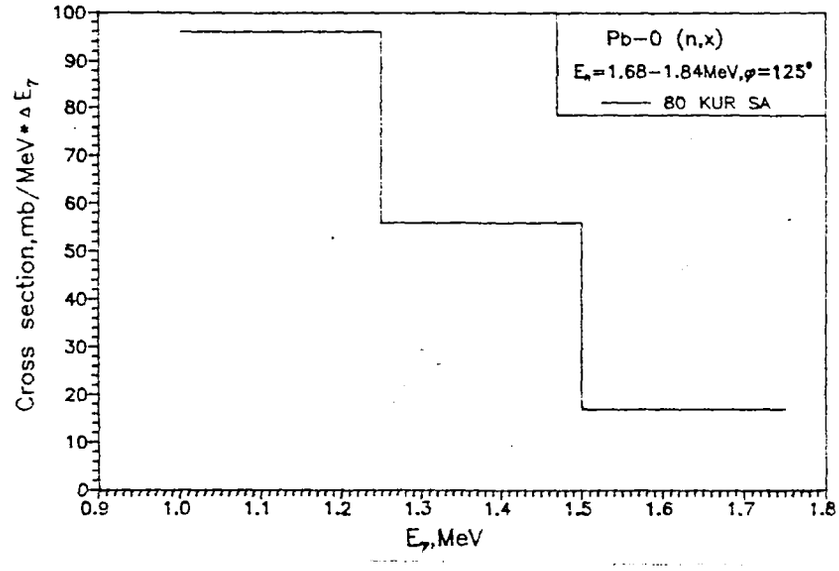
Pb–0 (n,x)
E_n=1.68–1.84MeV,φ=125°
80 KUR SA
Cross section,mb/MeV*ΔE_γ
E_γ,MeV

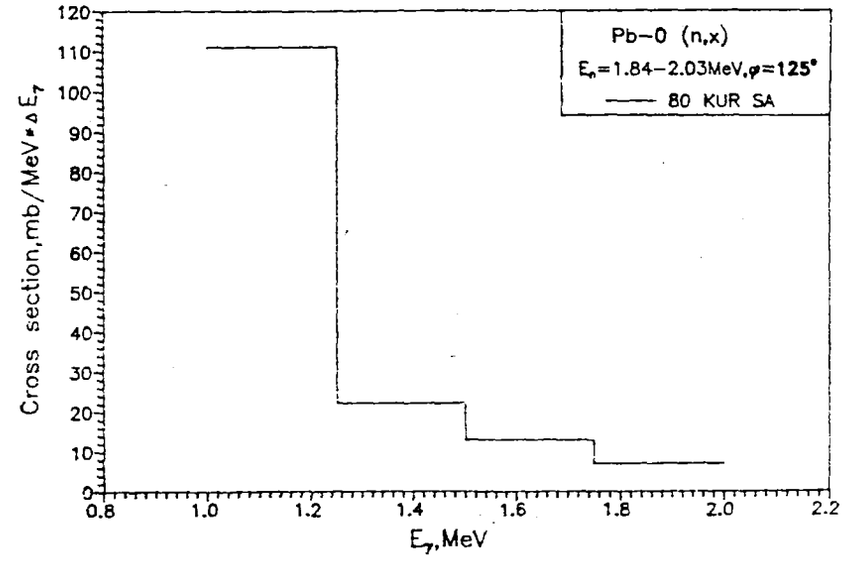
Pb–0 (n,x)
E_n=1.84–2.03MeV,φ=125°
80 KUR SA
Cross section,mb/MeV*ΔE_γ
E_γ,MeV

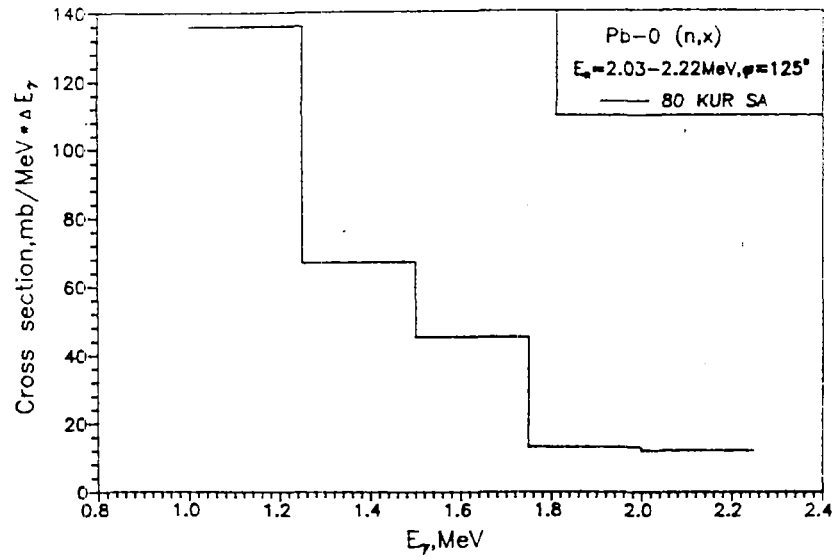
Pb-0 (n,x)
E_n=2.03-2.22MeV,φ=125°
80 KUR SA
Cross section,mb/MeV*ΔE_γ
E_γ,MeV

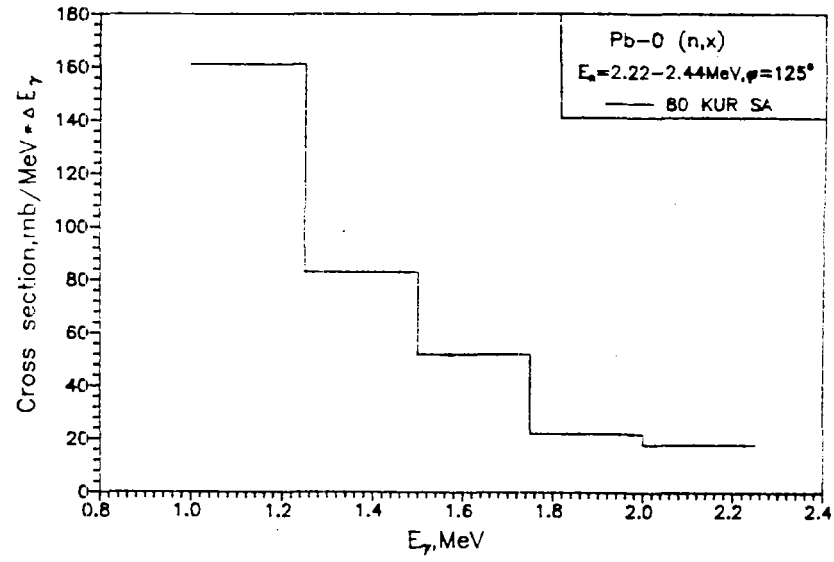
Pb-0 (n,x)
E_n=2.22-2.44MeV,φ=125°
80 KUR SA
Cross section,mb/MeV*ΔE_γ
E_γ,MeV

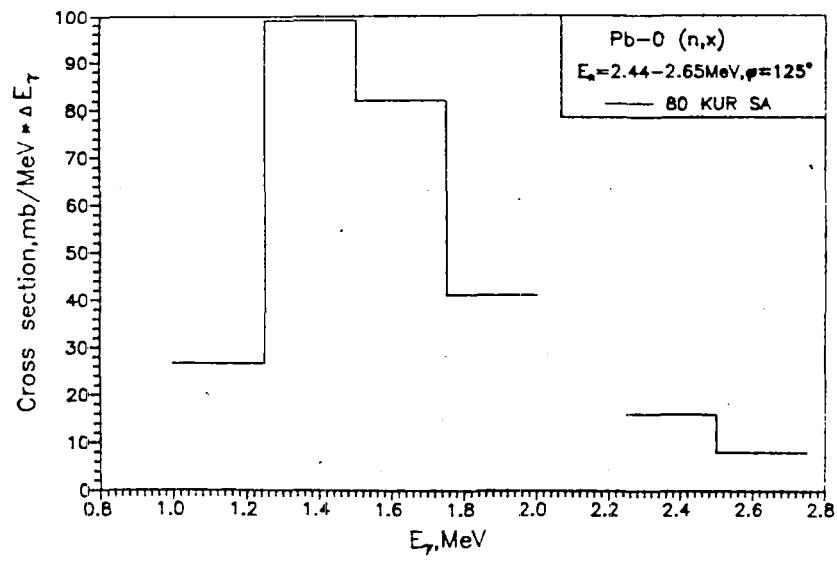
Pb-0 (n,x)
E_n=2.44-2.65MeV,φ=125°
80 KUR SA
Cross section,mb/MeV*ΔE_γ
E_γ,MeV

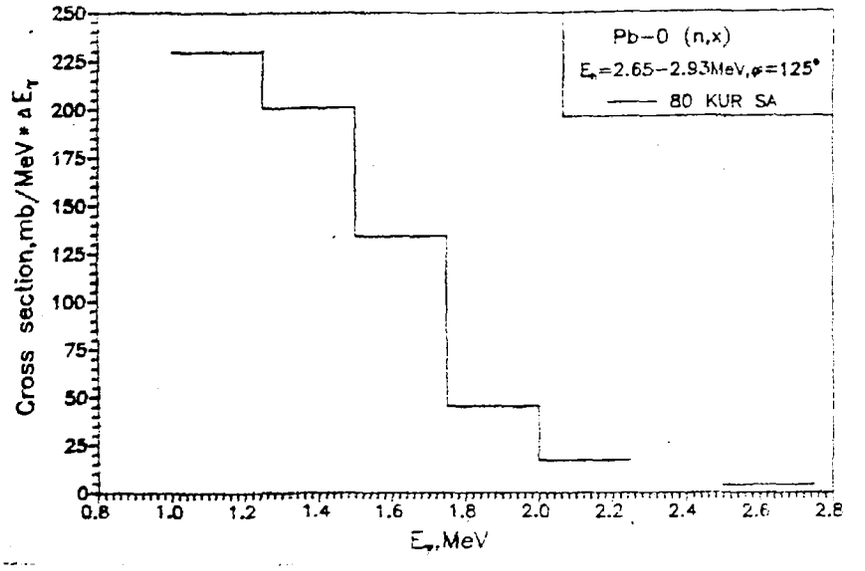
Pb–0 (n,x)
E_n=2.65–2.93MeV,φ=125°
80 KUR SA
Cross section,mb/MeV*ΔE_γ
E_γ,MeV

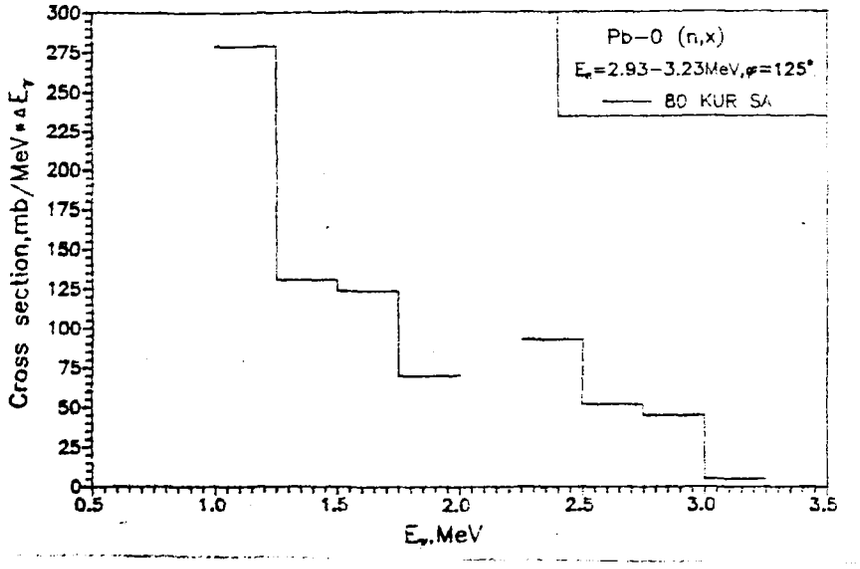
Pb–0 (n,x)
E_n=2.93–3.23MeV,φ=125°
80 KUR SA
Cross section,mb/MeV*ΔE_γ
E_γ,MeV

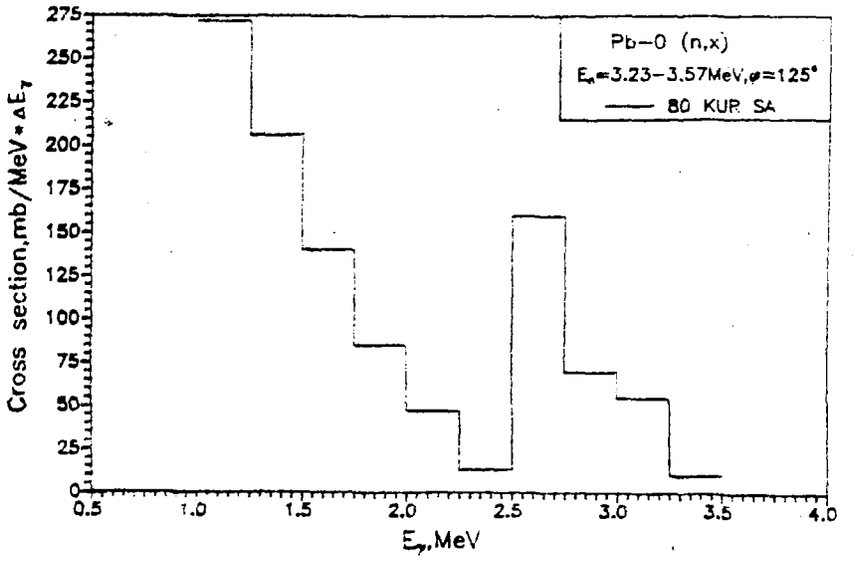
Pb–0 (n,x)
E_n=3.23–3.57MeV,φ=125°
80 KUR SA
Cross section,mb/MeV*ΔE_γ
E_γ,MeV

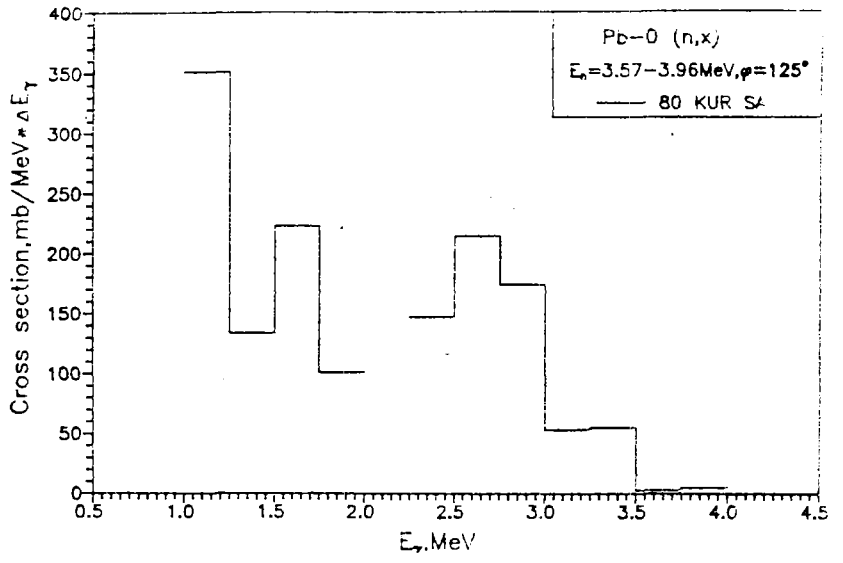
Pb-0 (n,x)
E_n=3.57-3.96MeV,φ=125°
80 KUR SA
Cross section,mb/MeV*ΔE_γ
E_γ,MeV

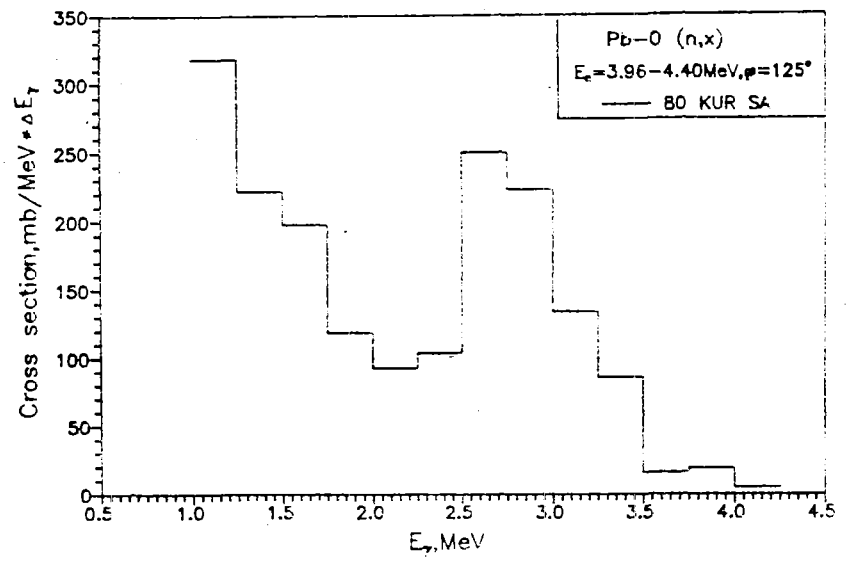
Pb-0 (n,x)
E_n=3.96-4.40MeV,φ=125°
80 KUR SA
Cross section,mb/MeV*ΔE_γ
E_γ,MeV

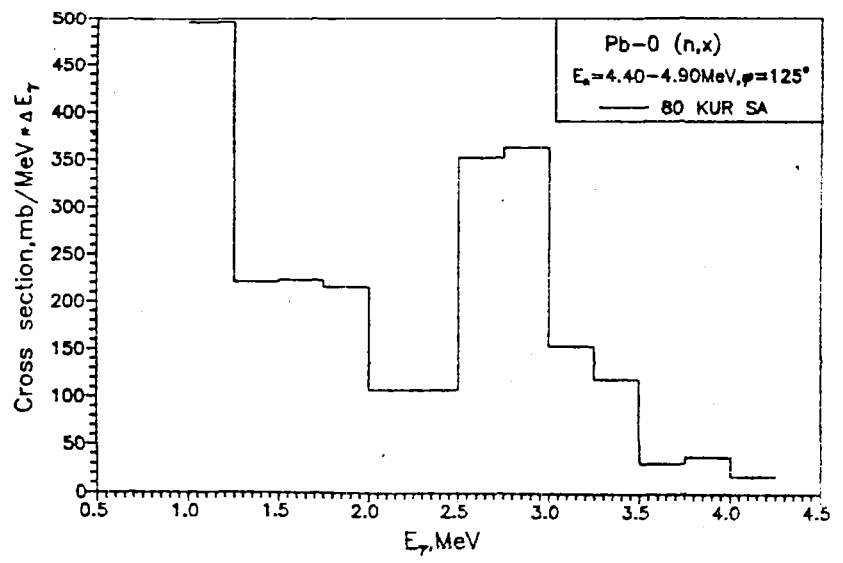
Pb-0 (n,x)
E_n=4.40-4.90MeV,φ=125°
80 KUR SA
Cross section,mb/MeV*ΔE_γ
E_γ,MeV

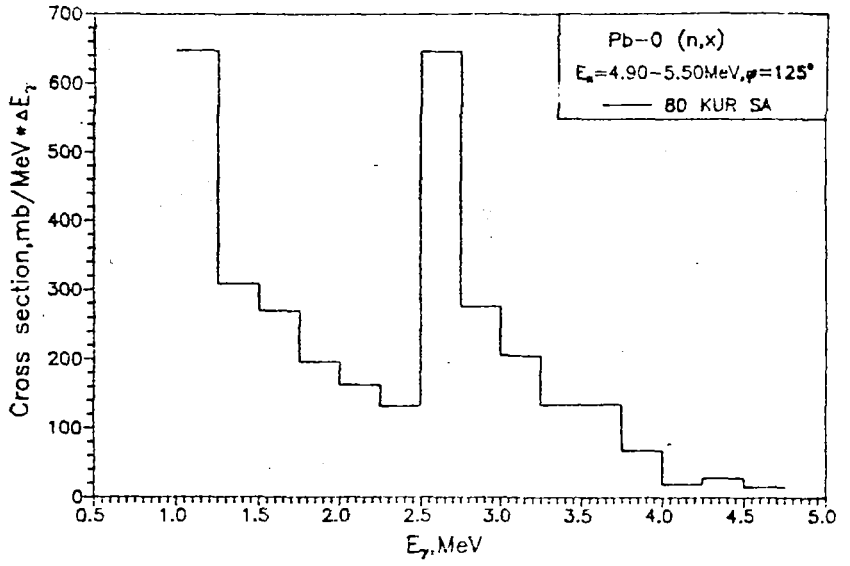
Pb-0 (n,x)
E_n=4.90-5.50MeV,φ=125°
80 KUR SA
Cross section,mb/MeV*ΔE$_\gamma$
E_γ,MeV

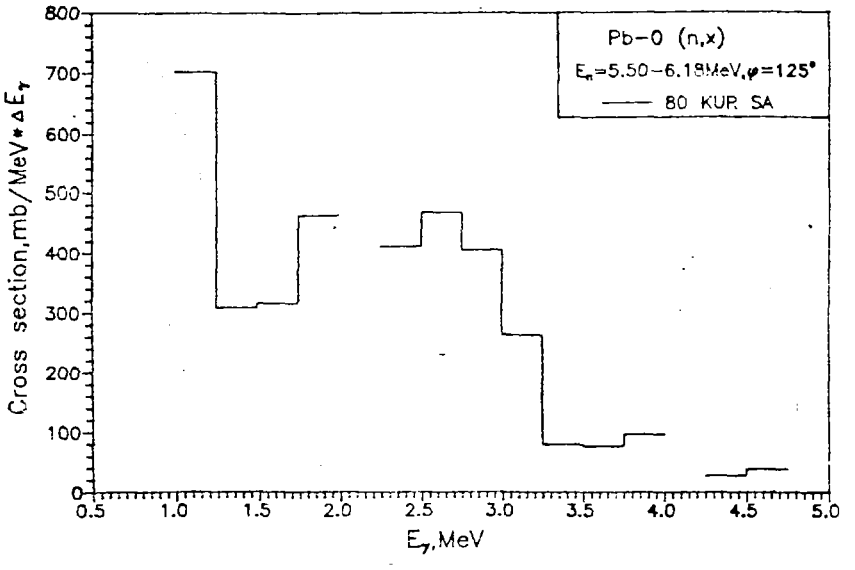
Pb-0 (n,x)
E_n=5.50-6.18MeV,φ=125°
80 KUR SA
Cross section,mb/MeV*ΔE$_\gamma$
E_γ,MeV

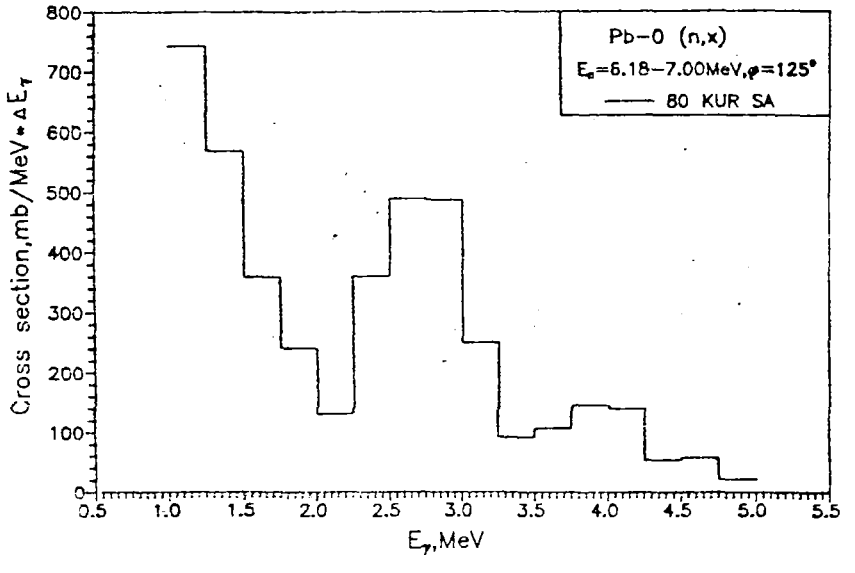
Pb-0 (n,x)
E_n=6.18-7.00MeV,φ=125°
80 KUR SA
Cross section,mb/MeV*ΔE$_\gamma$
E_γ,MeV

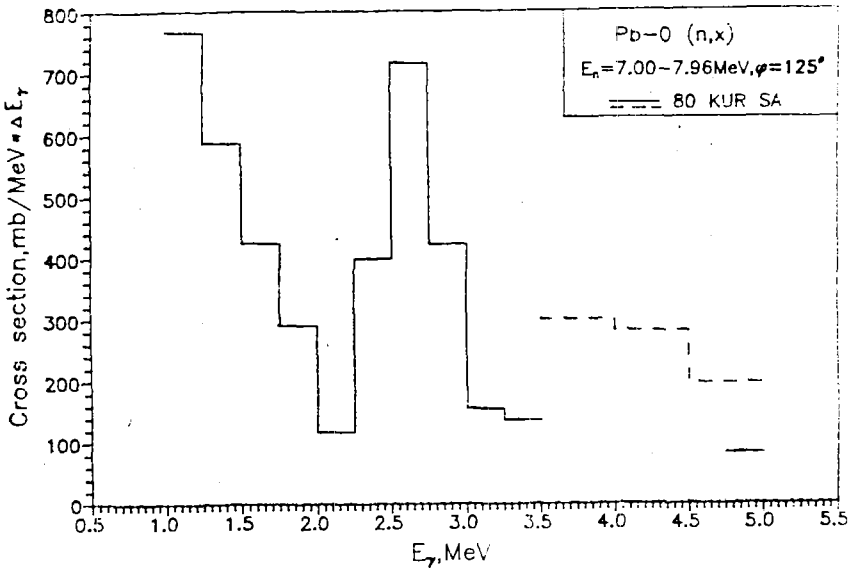
Pb-0 (n,x)
E_n=7.00-7.96MeV,φ=125°
80 KUR SA
Cross section,mb/MeV*ΔE$_\gamma$
E$_\gamma$,MeV

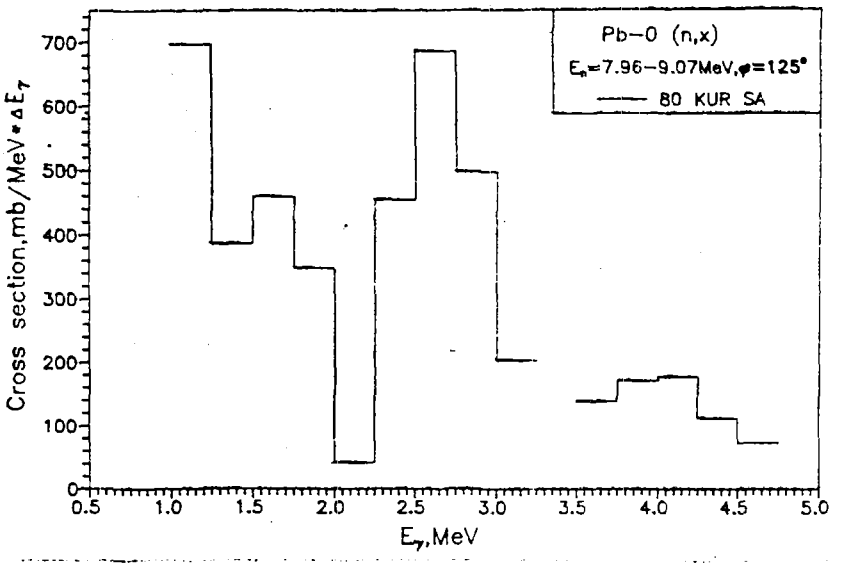
Pb-0 (n,x)
E_n=7.96-9.07MeV,φ=125°
80 KUR SA
Cross section,mb/MeV*ΔE$_\gamma$
E$_\gamma$,MeV

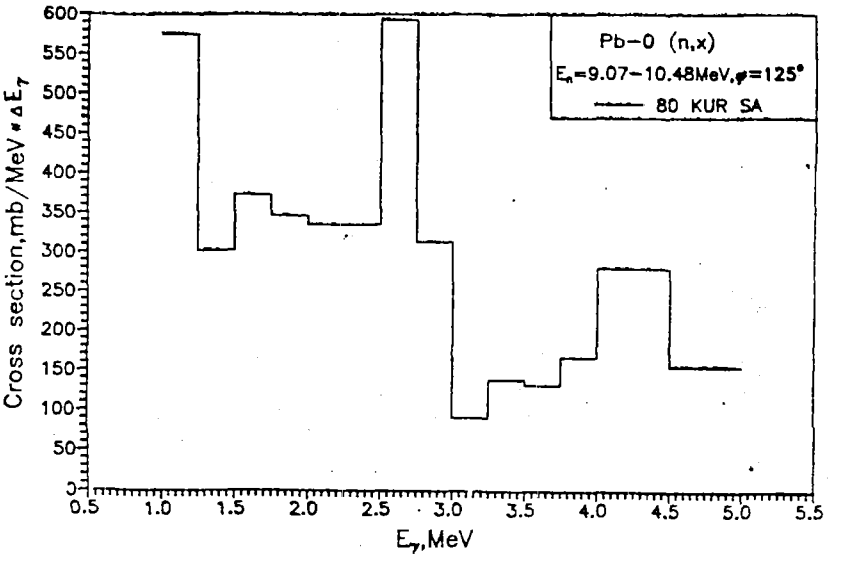
Pb-0 (n,x)
E_n=9.07-10.48MeV,φ=125°
80 KUR SA
Cross section,mb/MeV*ΔE$_\gamma$
E$_\gamma$,MeV

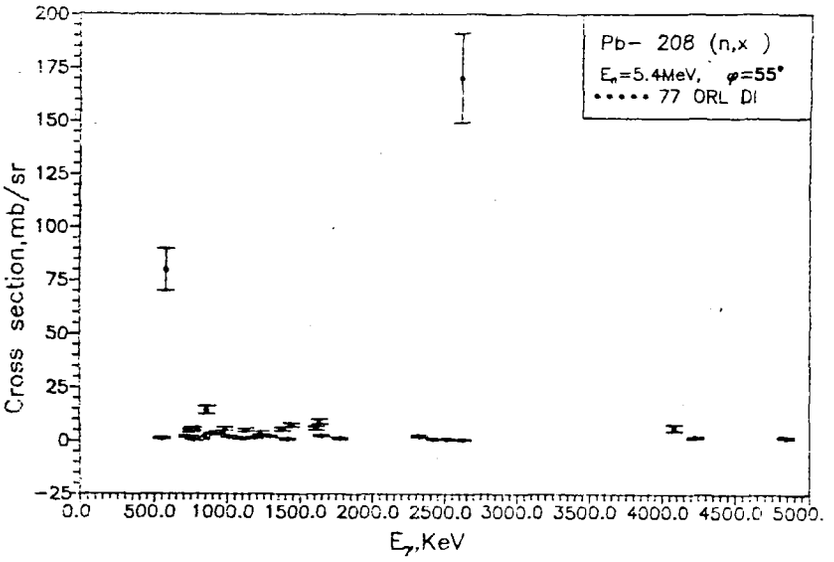
Pb– 208 (n,x)
E_n=5.4MeV, φ=55°
77 ORL DI
Cross section,mb/sr
E_γ,KeV

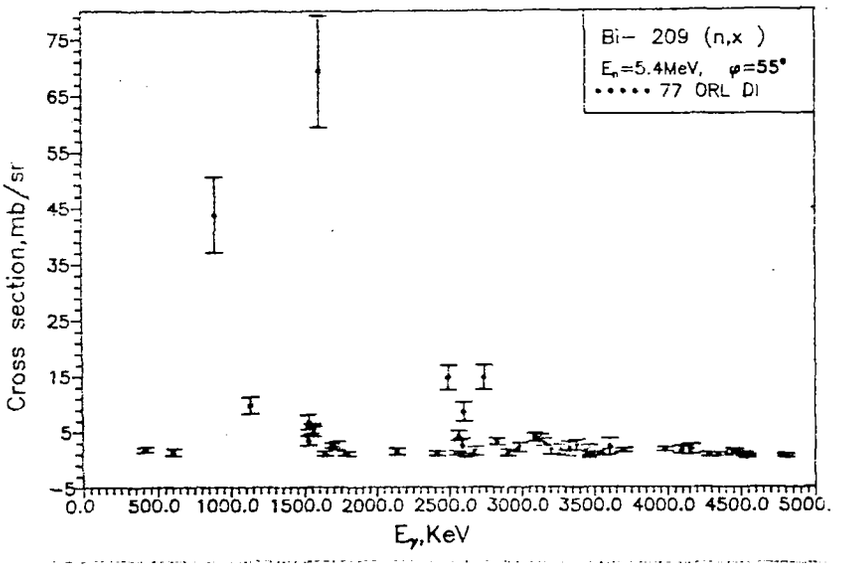
Bi– 209 (n,x)
E_n=5.4MeV, φ=55°
77 ORL DI
Cross section,mb/sr
E_γ,KeV

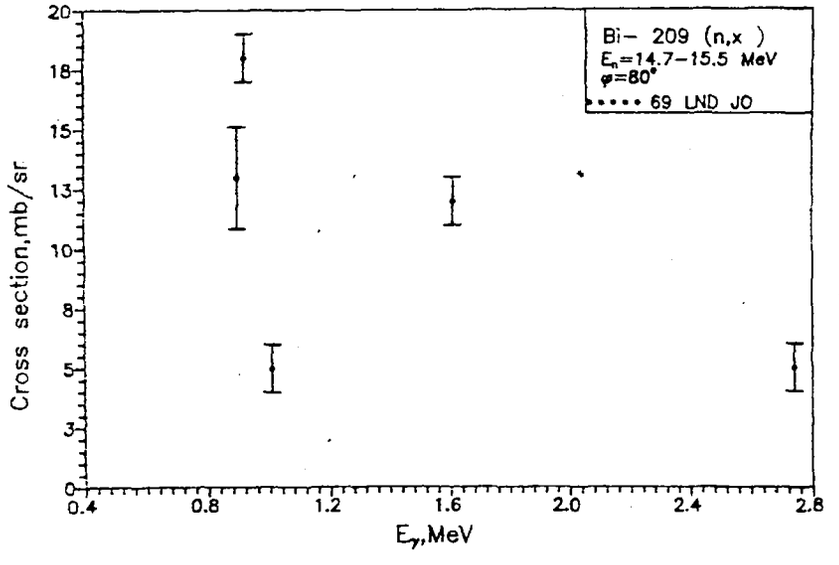
Bi– 209 (n,x)
E_n=14.7–15.5 MeV
φ=80°
69 LND JO
Cross section,mb/sr
E_γ,MeV

Nuclear Data Section
International Atomic Energy Agency
P.O. Box 100
A-1400 Vienna
Austria

e-mail, INTERNET: SERVICES@IAEAND.IAEA.OR.AT
e-mail, BITNET: RNDS@IAEA1
fax: (43-1) 20607
cable: INATOM VIENNA
telex: 1-12645 atom a
telephone: (43-1) 2060-21710

online: TELNET or FTP: IAEAND.IAEA.OR.AT
username: IAEANDS for interactive Nuclear Data Information System
username: NDSOPEN for FTP file transfer